

This is a repository copy of *Highly efficient NHC-iridium-catalyzed β -methylation of alcohols with methanol at low catalyst loadings*.

White Rose Research Online URL for this paper:

<https://eprints.whiterose.ac.uk/id/eprint/175979/>

Version: Accepted Version

Article:

Lu, Zeye, Zheng, Qingshu, Zeng, Guangkuo et al. (3 more authors) (2021) Highly efficient NHC-iridium-catalyzed β -methylation of alcohols with methanol at low catalyst loadings. *Science China Chemistry*. pp. 1361-1366. ISSN: 1674-7291

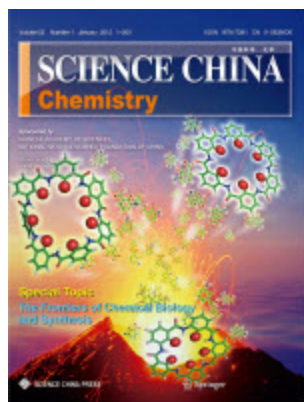
<https://doi.org/10.1007/s11426-021-1017-0>

Reuse

Items deposited in White Rose Research Online are protected by copyright, with all rights reserved unless indicated otherwise. They may be downloaded and/or printed for private study, or other acts as permitted by national copyright laws. The publisher or other rights holders may allow further reproduction and re-use of the full text version. This is indicated by the licence information on the White Rose Research Online record for the item.

Takedown

If you consider content in White Rose Research Online to be in breach of UK law, please notify us by emailing eprints@whiterose.ac.uk including the URL of the record and the reason for the withdrawal request.



Highly Efficient NHC-Iridium-Catalyzed β -Methylation of Alcohols with Methanol at Low Catalyst Loadings

Journal:	SCIENCE CHINA Chemistry
Manuscript ID	SCC-2021-0251.R1
Manuscript Type:	Article
Date Submitted by the Author:	n/a
Complete List of Authors:	Lu, Zeye; Fudan University, Department of Chemistry Zheng, Qingshu; Fudan University, Department of Chemistry Zeng, Guangkuo; Fudan University, Department of Chemistry Kuang, Yunyan; Fudan University, Department of Chemistry Clark, James; University of York, Department of Chemistry Tu, Tao; Fudan University, Department of Chemistry
Keywords:	hydrogen-borrowing, ligand effect, iridium, N-heterocyclic carbene, methylation
Speciality:	Organic Chemistry
Note: The following files were submitted by the author for peer review, but cannot be converted to PDF. You must view these files (e.g. movies) online.	
Table1.cdx Table2.cdx Table3.cdx	

SCHOLARONE™
Manuscripts

Highly Efficient NHC-Iridium-Catalyzed β -Methylation of Alcohols with Methanol at Low Catalyst Loadings

Zeye Lu,¹ Qingshu Zheng,¹ Guangkuo Zeng,¹ Yunyan Kuang,¹ James H. Clark,⁴ and Tao Tu^{1,2,3*}

¹Shanghai Key Laboratory of Molecular Catalysis and Innovative Materials, Department of Chemistry, Fudan University, 2005 Songhu Road, Shanghai 200438, China.

²State Key Laboratory of Organometallic Chemistry, Shanghai Institute of Organic Chemistry, Chinese Academy of Sciences, Shanghai 200032, China.

³Green Catalysis Center and College of Chemistry, Zhengzhou University, Zhengzhou 450001, China.

⁴Green Chemistry Centre of Excellence, University of York, York YO 105DD, UK.

*Corresponding Author: (email: taotu@fudan.edu.cn)

Abstract: The methylation of alcohols is of great importance since a broad number of bioactive and pharmaceutical alcohols contain methyl groups. Here, a highly efficient β -methylation of primary and secondary alcohols with methanol has been achieved by using bis-*N*-heterocyclic carbene iridium (bis-NHC-Ir) complexes. Broad substrate scope and up to quantitative yields were achieved at low catalyst loadings with only hydrogen and water as by-products. The protocol was readily extended to the β -alkylation of alcohols with several primary alcohols. Control experiments, along with DFT calculations and crystallographic studies revealed that ligand effect is critical for their excellent catalytic performance, shedding light on more challenging Guerbet reactions with simple alcohols.

hydrogen-borrowing, ligand effect, iridium, *N*-heterocyclic carbene, methylation

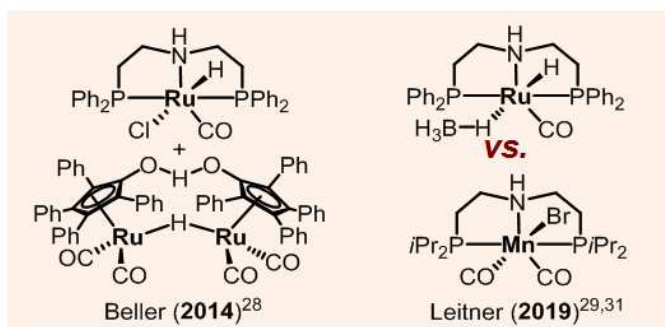
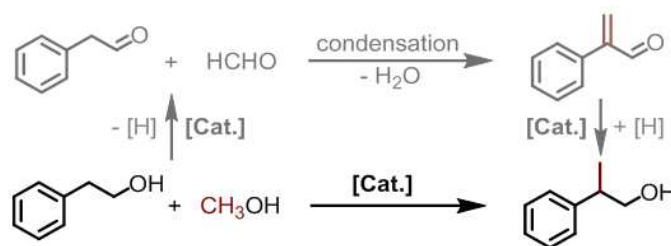
1 Introduction

The alkylation of alcohols constitutes one of the most crucial C-C bond forming reactions [1-6]. Among them, the methylation of alcohols is of great importance since a broad number of bioactive and pharmaceutical alcohols contain methyl groups [7-10]. In contrast with conventional methylation reagents such as sensitive Grignard reagents, toxic methyl iodide and methyl sulfate [11-12], methylation with inexpensive methanol via a hydrogen-borrowing pathway [13-19] is considered as one of the most promising and sustainable approaches [20-25]. Due to its high energy consumption for the dehydrogenation of methanol [26-27], the first example of selective β -methylation of 2-arylethanol was realized by Beller and coworkers by combining two distinct Ru-complexes (Ru-MACHO and Shvo catalysts (Figure 1a) [28]. Subsequently, Leitner and coworkers realized the identical transformations by using a single Ru catalyst (Ru-MACHO-BH₄) with up to 84% yield [29-30]. Furthermore, the Leitner and Kempe groups simultaneously accomplished the methylations using earth-abundant manganese analogues as catalysts with better yields (up to 92%) [31-32]. Interestingly, as aforementioned, current best results for this challenging transformation were achieved by catalysts containing earth-abundant metals rather than the generally more active noble metals, both at high catalyst loadings. This surprising outcome encouraged us to get insight into this topic.

The plausible mechanism on the β -methylation of alcohols involves the dehydrogenation of methanol and its coupling partner to the corresponding formaldehyde and aldehyde/ketone, respectively. Followed by cross-aldol

condensation of two different aldehydes or between ketone and aldehyde, and the desired methylation product is then formed after re-hydrogenation (Figure 1a). This multi-step cascade transformation is obviously challenging for a single catalyst to realize dehydrogenation and hydrogenation simultaneously. Another issue worth to mention is that the aldol-condensation step is generally considered as a base-mediated transformation and high energy is usually required [33]. Therefore, how to design highly efficient bi-/multi-functional catalysts to low the energy for the cascade steps is the key issue.

a) Previous work: with catalysts bearing phosphine ligands



b) This work: by using bis-NHC-Iridium complexes

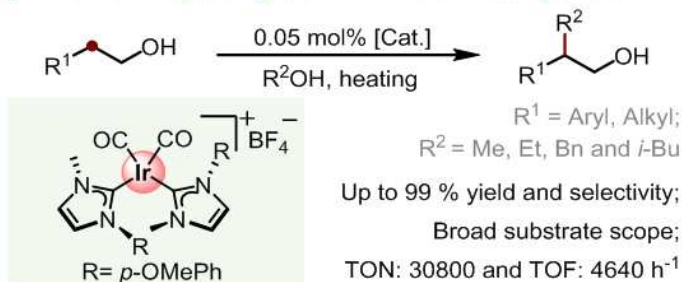


Figure 1 Represented β -methylation of alcohols.

Robust *N*-heterocyclic carbenes (NHCs) with strong σ -donating and weak π -accepting properties can be utilized to design highly efficient bifunctional catalysts [34-39]. Recently, we also found NHC-Ir complexes exhibited very high catalytic activity towards various multi-step transformations [40-44]. Furthermore, to the best of our knowledge, there is no example on homogeneous Ir-catalyzed β -methylation of alcohols, especially with NHC ligands. Herein, by using newly designed bis-NHC-Ir complexes, we realized excellent selectivity and yields (both > 99%) towards the β -methylation of diverse alcohols at low catalyst loading (0.05 mol%, Figure 1b). Broad substrate scopes with primary and secondary alcohols were achieved, and the protocol was readily extended to the β -alkylation of alcohols, further highlighting the applicability of the bis-NHC-Ir complexes.

Initially, in light of the excellent performance of NHC-Ir complexes [45-46], the β -methylation of 2-phenyl ethanol (**1**) was selected as a model reaction to test our hypothesis. After optimization, a good yield of methylated product (**3**, 74%, Figure 2) could be achieved by using 0.05 mol% mono-NHC-Ir complexes **4a**, derived from *N,N'*-dimethylimidazolium iodide [47], with 2 equiv. *t*BuONa in 1 mL methanol at 140 °C for 24 hours. An increased yield (84%, Figure 2) was observed with its *N*-phenyl substituted analogue **4b** under the otherwise identical reaction conditions. In consideration that the number of NHC-ligands may benefit their catalytic activity [43], bis-NHC-Ir complexes **5a-d** were then applied (Figure S5). Although inferior outcomes were obtained for the known bis-NHC-Ir complexes **5a** and **5b** with two methyl groups (56% and 57%, respectively), excellent yields were achieved with our

10

14

2 Experimental

General procedure for bis-NHC-Ir-catalyzed β -methylation of primary alcohols. To a sealed tube (35 mL) equipped with a stir bar, Ir-NHC catalyst **5d** (0.05 mol%), methanol (1 mL), ^tBuONa (2 mmol) and primary alcohol (1 mmol) was added under nitrogen atmosphere. The solution was heated at 140 °C for 24 h. 1,3,5-Trimethoxybenzene was added as an internal standard, and sent for NMR measurement. Pure products were obtained by column chromatography over silica gel using ethyl acetate/petroleum ether mixture as eluent.

General procedure for bis-NHC-Ir-catalyzed β -methylation of secondary alcohols. To a sealed tube (35 mL) equipped with a stir bar, Ir-NHC catalyst **5d** (0.1 mol%) methanol (1 mL), ^tBuONa (3 mmol) and primary alcohol (1 mmol) was added under nitrogen atmosphere. The solution was heated at 140 °C for 24 h. 1,3,5-Trimethoxybenzene was added as an internal standard, and sent for NMR measurement. Pure products were obtained by column chromatography over silica gel using ethyl acetate/petroleum ether mixture as eluent.

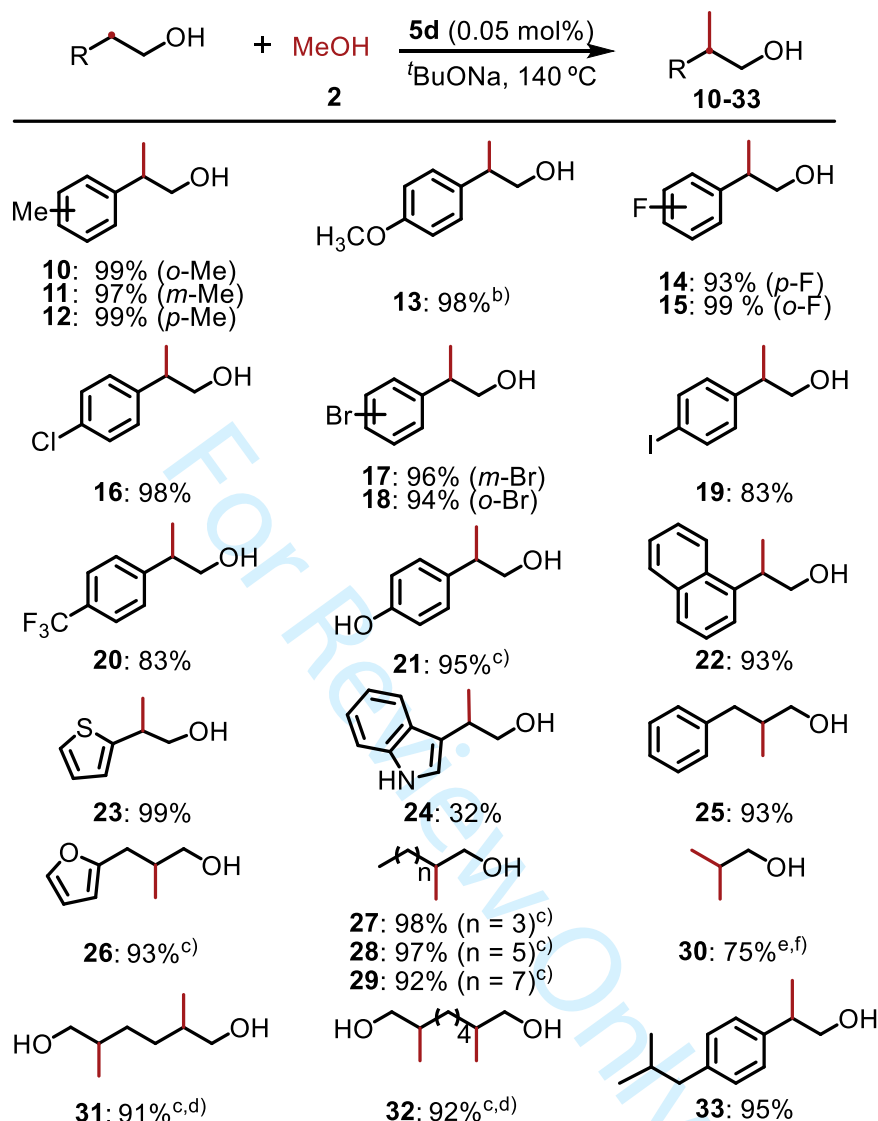
More experimental details and characterizations are available in the Supporting Information.

3 Results and discussion

After optimization of the reaction conditions and catalyst screening, the substrate scope of primary alcohols was then investigated (Table 1). In the presence of 0.05 mol% bis-NHC-Ir **5d**, good to excellent yields of corresponding methylated products

(**10–33**) were obtained with high selectivity. In the case of aryl ethanol, both electron-donating (**10–13**) and electron-withdrawing (**14–18**) substituents proved to be compatible and almost quantitative yields were observed. The position of substituent hardly affects the methylation results, excellent yields were attained with *ortho*-, *meta*-, and *para*-methylphenyl ethanol (97%–99% for **10–12**). Halogenated substrates were also well compatible (93–99%, **14–18**). A slight inferior yield (83%) was achieved with the iodo-analogue (**19**). Electron-withdrawing trifluoromethyl group gave a good yield of 83% (**20**) though nitro- and cyano- analogues were hardly converted to desired products under the optimal reaction conditions. To our delight, unprotected hydroxyl group was also well tolerated, and a yield of 95% was attained (**21**). Additionally, bulky and heterocyclic substrates containing S, N atoms were also suitable (**22–24**). Remarkably, this protocol was readily extended to the syntheses of drug precursors. For instance, the ibuprofen precursor **33** could be accessed in 95% yield under the standard reaction conditions and in 90% yield even on gram-scale experiment. And the precursor **33** could be easily converted to ibuprofen by selective dehydrogenation using our developed self-supported ruthenium catalyst (Scheme S1) [44].

Table 1 Substrate scope of various primary alcohols ^{a)}



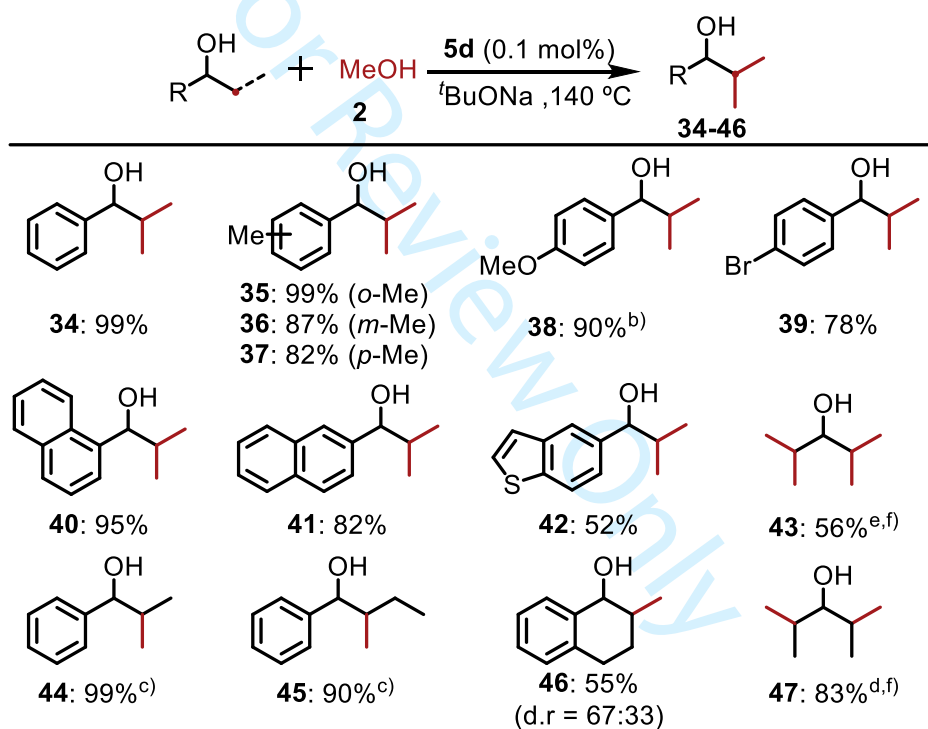
- a) Reaction carried out with bis-NHC-Ir **5d** (0.05 mol%), primary alcohol **1** (1 mmol) and ^tBuONa (2 mmol) in 1 mL methanol at 140 °C under N₂ atmosphere for 24 h, yields are determined by ¹H NMR analysis with 1,3,5-trimethoxybenzene as an internal standard. b) Using mesitylene as an internal standard. c) With ^tBuONa (3 mmol). d) With **5d** (0.1 mol%). e) With **5d** (0.2 mol%) and ^tBuONa (6 mmol) at 150 °C for 24 h. f) Yields are determined by GC-MS with mesitylene as an internal standard.

Encouraged by the results from aryl ethanols, the methylation of aliphatic alcohols was then investigated. 3-Phenyl-1-propanol (**25**) was obtained in 93% yield under otherwise identical reaction conditions. Excellent yield of 3-furanpropanol (93%, **26**) was also gained with 3 equivalents of base. Other long-chain alkyl primary alcohols also resulted in excellent to quantitative yields (92-98% for **27-29**). In the case of simple short chain alcohol like ethanol, di- β -methylation product *iso*-butanol was produced with a yield of 75% (**30**). Pleasingly, the protocol is readily extended to the β -methylation of diols. Octanediol and hexanediol were conveniently converted into dimethyl products **31** (91%) and **32** (92%), respectively. These results were obviously better than other known catalytic systems [29].

With the excellent outcomes from primary alcohols, less active secondary alcohols were then studied by our newly developed protocol (Table 2). By slightly increasing the catalyst loading to 0.1 mol% and the base to 3 equiv., quantitative yield of dimethylated product **34** was observed with 2-phenyl ethanol. Electron-donating substituents including methyl and methoxyl barely hampered the dimethylation process, and the corresponding products **35**, **36**, **37** and **38** were attained in good to excellent yields (82-99%). Due to the incomplete hydrogenation of the ketone intermediate, only a 78% yield was achieved with *para*-bromo-phenyl ethan-1-ol (**39**). Bulky naphthalene substrates resulted in 1- and 2-isomers **40** and **41** in yields of 95% and 82%, respectively. This suggests that bulkiness hardly hampered the methylation process. When the heterocyclic substrate 1-(benzo[*b*]thiophen-5-yl) ethan-1-ol was studied, a moderate yield was obtained (**42**, 52%). Probably due to its low boiling

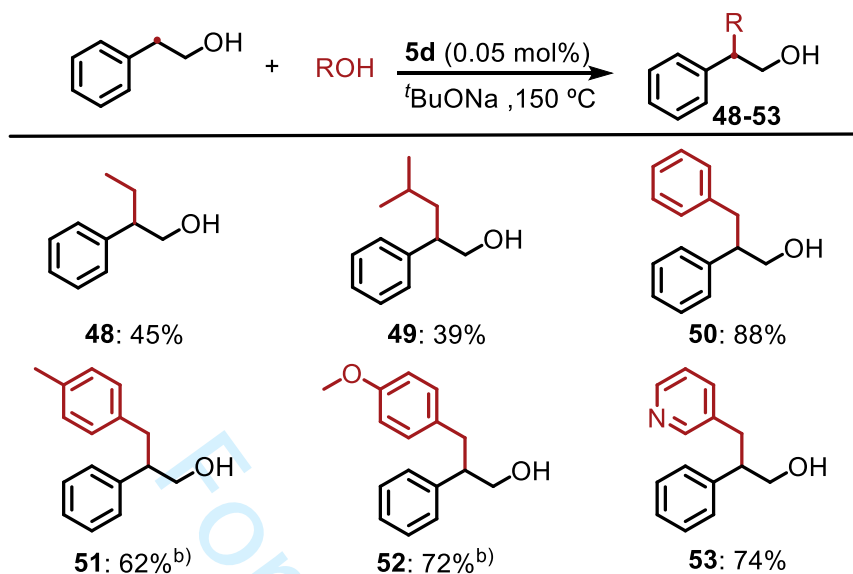
points, the aliphatic secondary alcohol, isopropyl alcohol, afforded slightly low yield of the methylated products (**43**, 56%). For the β -substituted substrates, quantitative yields were obtained with 1-phenylpropanol (**44**) while a 90% yield was observed its analogue with a longer carbon chain (**45**). Cyclic tetrahydro-1-naphthol (**46**) was converted into the methylated products in 55% yield, and acyclic 3-amyl alcohol gave the **47** in 83% yield by slightly increasing the amount of base.

Table 2 Substrate scope of various secondary alcohols ^{a)}



a) With bis-NHC-Ir **5d** (0.1 mol%), secondary alcohol **1** (1 mmol) and ^tBuONa (3 mmol) in 1 mL methanol at 140 °C under N₂ atmosphere for 24 h, yields are determined by ¹H NMR analysis with 1,3,5-trimethoxybenzene as an internal standard. b) Using mesitylene as an internal standard. c) With **5d** (0.05 mol%), ^tBuONa (2 mmol). d) With ^tBuONa (6 mmol). e) With **5d** (0.2 mol%), ^tBuONa (12 mmol). f) Yields are determined by GC-MS with mesitylene as an internal standard.

Table 3 Alkylation of 2-phenylethanol with diverse primary alcohols ^{a)}



a) With **5d** (0.05 mol%), 2-phenyl ethanol **1** (1 mmol) and $t\text{BuONa}$ (3 mmol) in 1 mL primary alcohol at 150 °C under N_2 atmosphere for 24 h, yields are determined by ^1H NMR analysis with 1,3,5-trimethoxybenzene as an internal standard. b) Add 5 mmol primary alcohol and use 1.5 mL *p*-xylene as solvent.

Inspired by the excellent results obtained in the β -methylation of diverse alcohols with methanol, more general β -alkylation with other primary alcohols instead of methanol were investigated (Table 3). Although possible side-products are unavoidable due to the possible Guerbet reaction [48-49], 45% and 39% yield of β -alkylated products (**48** and **49**) could be still be achieved when ethanol or *iso*-butanol were applied instead of methanol at 150 °C. **Delightedly, all selected benzyl alcohols and even heterocyclic analogues were also suitable alkylation**

reagents. Good to excellent yields were observed for these substrates (62%-88%, **50-53**), further indicating the applicability of the protocol.

Crystals suitable for single-crystal X-ray diffraction were obtained by slow evaporation of the dichloromethane solution of bis-NHC-Ir complexes **5c** or **5d**. Combining the crystal data of complex **5a** in the previous study [37], the possible ligand effects on catalytic performance were then explored. As depicted in Figure 3a, when the methyl substitutes on NHC ligands was replaced by phenyl groups, the Cco-Ir bonds were slightly increased (1.874 Å vs 1.882 Å for **5a** vs **5c**), consequently the CO ligands could be much more easily dissociated, leaving a vacant position for the later transformation. An unsymmetric crystal structure was observed with complex **5d**, in which the lengths of two Cco-Ir bonds were slightly different (1.884 Å and 1.888 Å) but both are longer than those observed in complexes **5a** and **5c** (Figure 3a), highlighting that one of CO ligands might be more easily dissociated from the Ir center and facilitating the initial step of dehydrogenation of alcohols. Furthermore, the percent buried volumes (% V_{bur}) and steric maps of complexes **5a**, **5c** and **5d** were calculated by SambVca 2.1 (Figure 3b) [50-52]. As we expected, the steric bulkiness of complexes **5c** and **5d** (% V_{bur} = 51.6% and 51.1%) are much hindered than that of analogue **5a** (% V_{bur} = 47.9%), which might be another key issue to affect catalytic performance along with the electronic effect of NHC ligands.

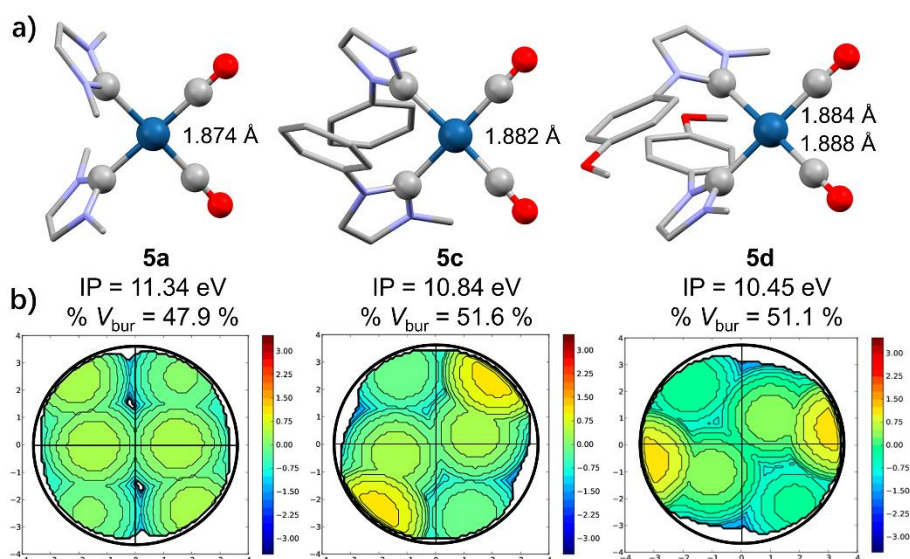


Figure 3 a) Crystal structures of complexes **5a**, **5c** and **5d**, and the corresponding C_{CO}-Ir bond lengths (Colour code: Ir, cyan; O, red; N, blue; C grey. Hydrogens are omitted for clarity). b) Percent buried volumes and steric maps of complexes **5a**, **5c** and **5d**.

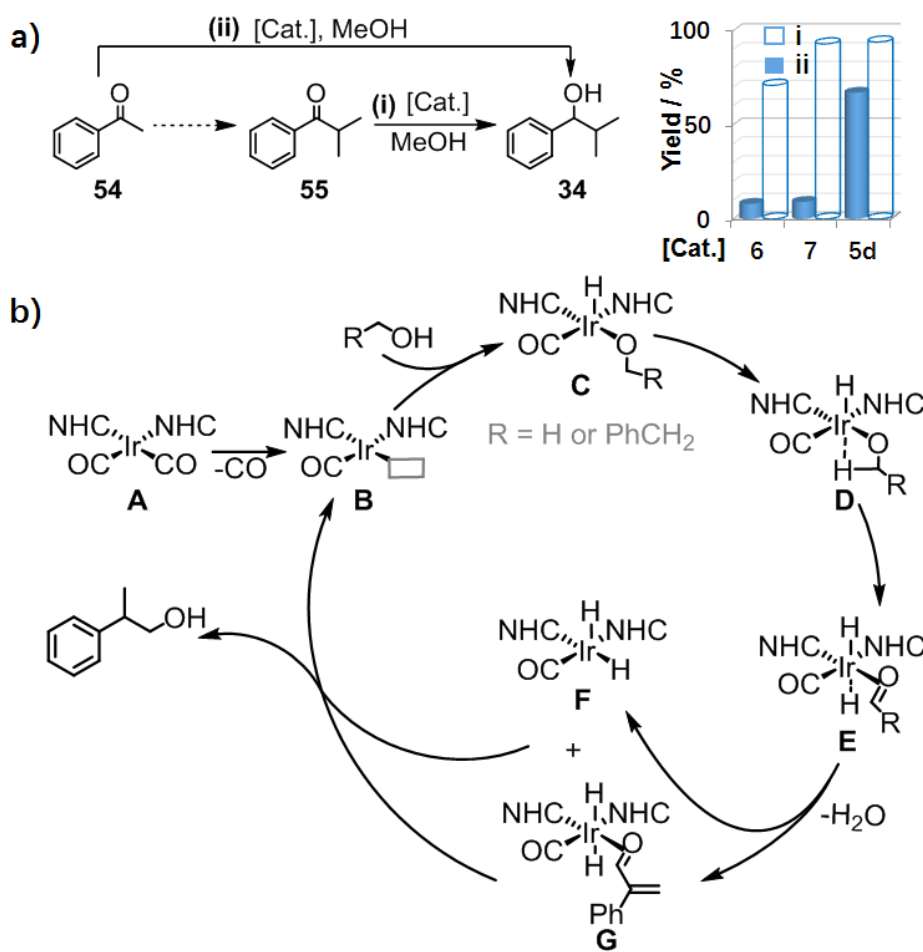
In order to further understand these observations from the crystal structures, density functional theory (DFT) calculations were performed to elucidate the electronic nature of the iridium carbonyl complexes bearing different types of NHC ligands. The calculations indicated that the ionization potentials (IP, in eV) of Ir centers [43] follow the sequence of **5a** (11.34 eV) > **5c** (10.84 eV) > **5d** (10.45 eV). The lower IP of the iridium centers in complexes **5c** and **5d** with N-aryl substituents than that in complex **5a** implied that the generation of active Ir(III)-H species from NHC-Ir (I) after dehydrogenation is more feasible [42]. Recalling the strong *trans*-effect [53] observed in the crystal structure of complex **5d**, the ready dissociation of one CO ligand may facilitate the first dehydrogenation step. Therefore, the yields of product **3** were

increased along with the trend of **5a** < **5c** < **5d** (Figure 2), highlighting the crucial role of the ligand effect during the β -methylation process.

Further control experiments were carried out to study the reaction mechanism. Initially, the possible radical or nanoparticles reaction pathways were excluded by TEMPO (2,2,6,6-tetramethyl-1-piperidinyloxy) or mercury tests (Scheme S3, eq. i, ii) respectively [54]. The reaction profile revealed that more than half of the substrates were consumed within 1.5 h in the presence of 0.05 mol% **5d**, reflecting the high catalytic activity of **5d** (Figure S17). Surprisingly, no possible aldehyde or olefin unsaturated intermediates were detected, implying that the base-mediated aldol condensation coupling after dehydrogenation of phenylethanol and methanol was extremely fast. Secondly, when acetophenone (**54**) or di-methylated-ketone (**55**) was applied as a substrate, 67% or 94% of the di-methylated product **34** was obtained (Scheme S2, i, ii) under otherwise standard conditions, indicating both of them were possible intermediates. Notably, other viable catalysts **6-9** exhibited much lower yields than **5d** in the former transformation (Figure 4a, ii, and Scheme S2) but with similarly high catalytic activity in the latter conversion (Figure 4a, i, and Scheme S2), implying the high efficiency of **5d** accelerated the C-C bond formation step of acetophenone to di-methylated-ketone via aldol-condensation, which was usually considered as a base-mediated process with high energy requirement without catalyst assisting [33]. This observation was also in agreement with recently reports with DFT calculations [42, 55].

Finally, upon using deuterated methanol in the β -methylation of acetophenone (**54**), above 90% of hydrogens at all possible positions were replaced by deuteriums (Scheme S3, eq. iii), indicating methanol was the hydrogen resource and a hydrogen-borrowing mechanism is involved [14-19]. When 2-phenylethanol was used instead of acetophenone, the proportion of **nondeuterated** alcohol protons increased to about 20% (Scheme S3, eq. iv), suggesting the alcohol substrate like **aryl ethanol** is also a hydrogen source. The kinetic isotope effect (KIE) experiment at the first two hours by using methanol or deuterated methanol gave out a k_H/k_D value of 2.26, indicating the dehydrogenation of methanol is the rate-determining step (Figure S18) [56-57].

Based on these control experiments and previous reports [28,31], a plausible mechanism was proposed in Figure 4b. Initially, CO dissociates from bis-NHC-Ir complex **A** to form species **B** with a free coordination site. Two different alcohols are readily dehydrogenated into their corresponding ketones/aldehydes simultaneously by **B** to generate Ir-hydride species **C**, **D** and **E**, subsequently. Along with bis-NHC-Ir-H₂ species **F** formation, α,β -unsaturated aldehyde coordinated iridium-dihydride species **G** was then produced after the aldol-condensation **under the basic conditions**. The unsaturated aldehyde intermediates are reduced in situ by the dihydride species to give out the final methylation product and regenerate the active bis-NHC-Ir species **B** to complete the catalytic cycles.



4 Conclusions

In conclusion, a highly efficient and selective β -methylation of primary and secondary alcohols with methanol as a clean C1 source was realized by using novel bis-NHC-Ir complexes at low catalyst loadings. The protocol was readily extended to β -alkylation of alcohols with other primary alkyl alcohols. Crystallographic and computational studies revealed the crucial ligand effects on the catalytic efficiency. A detailed mechanistic study indicated besides hydrogen-borrowing processes, the high

1 efficiency of the newly developed bis-NHC-Ir catalysts was attributed to their
2 superior activity in the challenging C-C bond formation step. Our protocol not only
3 revealed the ligand effect is pivotal for this challenging transformation but also pave
4 the way to more challenging Guerbet reactions.

6 **Acknowledgements** Financial support from the National Key R&D Program of China (No.
7 2016YFA0202902), the National Natural Science Foundation of China (Nos. 21871059,
8 21861132002 and 21572036) and the Department of Chemistry at Fudan University is
9 gratefully acknowledged.

10 **Conflicts of interest** The authors declare that they have no conflict of interest.

11 **Supporting information** The supporting information is available online at
12 <http://chem.scichina.com> and <http://link.springer.com/journal/11426>. The supporting
13 materials are published as submitted, without typesetting or editing. The responsibility for
14 scientific accuracy and content remains entirely with the authors.

- 1
2
3
4 1 1 Zimmerman JB, Anastas PT, Erythropel HC, Leitner W. *Science*, 2020, 367: 397-400
5
6 2 2 Zetzsche LE, Narayan ARH. *Nat Rev Chem*, 2020, 4: 334-346
7
8 3 3 Crabtree RH. *Chem Rev*, 2017, 117: 9228-9246
9
10 4 4 Ravelli D, Protti S, Fagnoni M. *Chem Rev*, 2016, 116: 9850-9913
11
12 5 5 Brahmachari G. *RSC Adv*, 2016, 6: 64676-64725
13
14 6 6 Gunanathan C, Milstein D. *Science*, 2013, 341: 1229712
15
16 7 7 Leitner W, Klankermayer J, Pischinger P, Pitsch H, Kohse-Hoinghaus H. *Angew Chem*
17
18 8 *Int Ed*, 2017, 56: 5412-5452
19
20 9 8 Natte K, Neumann H, Beller M, Jagadeesh RV. *Angew Chem Int Ed*, 2017, 56:
21
22 10 6384-6394
23
24 11 9 Schonherr H, Cernak T. *Angew Chem Int Ed*, 2013, 52: 12256-12267
25
26 12 10 Barreiro EJ, Kummerle EA, Fraga CA. *Chem Rev*, 2011, 111: 5215-5246
27
28 13 11 Chen YT. *Chem Eur J*, 2019, 25: 3405-3439
29
30 14 12 Szekeley G, Amores de Sousa MG, Gil M, Ferreira FC, Heggie W. *Chem Rev*, 2015, 115:
31
32 15 8182-8229
33
34 16 13 Wang K, Zhang L, Tang WJ, Sun HM, Xue D, Lei M, Xiao JL, Wang C. *Angew Chem*
35
36 17 *Int Ed*, 2020, 59: 11408-11415
37
38 18 14 He ZH, Liu HZ, Qian QL, Lu L, Guo WW, Zhang LJ, Han BX. *Sci China Chem*, 2017,
39
40 19 60: 927-933
41
42 20 15 Ng TW, Liao G, Lau KK, Pan HJ, Zhao Y. *Angew Chem Int Ed*, 2020, 59: 11384-11389
43
44 21 16 Irrgang T, Kempe R. *Chem Rev*, 2019, 119: 2524-2549
45
46 22 17 Chakraborty S, Daw P, David YB, Milstein D. *ACS Catal*, 2018, 8: 10300-10305
47
48
49
50
51
52
53
54
55
56
57
58
59
60

- 1
2
3
4 1 18 Peña-López M, Piehl P, Elangovan S, Neumann H, Beller M. *Angew Chem Int Ed*, 2016,
5
6 55: 14967-14971
7
8
9 3 19 Watson AJ, Williams MJ. *Science*, 2010, 329: 635-636
10
11
12 4 20 Lan XB, Ye ZR, Liu JH, Huang M, Shao YX, Cai X, Liu Y, Ke ZF. *ChemSusChem*,
13
14 2020, 13: 2557-2563
15
16
17 6 21 Bettoni L, Gaillard S, Renaud JL. *Org Lett*, 2019, 21: 8404-8408
18
19
20 7 22 Polidano K, Williams MJ, Morrill LC. *ACS Catal*, 2019, 9: 8575-8580
21
22 8 23 Polidano K, Allen BDW, Williams MJ, Morrill LC. *ACS Catal*, 2018, 8: 6440-6445
23
24
25 9 24 Lan XB, Ye ZR, Huang M, Liu JH, Liu Y, Ke ZF. *Org Lett*, 2019, 21: 8065-8070
26
27
28 10 25 Shen D, Poole DL, Shotton CC, Kornahrens AF, Healy MP, Donohoe TJ. *Angew Chem*
29
30 11 *Int Ed*, 2015, 54: 1642-1645
31
32
33 12 26 Lin WH, Chang HF. *Catal Today*, 2004, 97: 181-188
34
35
36 13 27 Qian M, Liauw MA, Emig G. *Appl Catal A-Gen*, 2003, 238: 211-222.
37
38
39 14 28 Li Y, Li HQ, Junge H, Beller M. *Chem Commun*, 2014, 50: 14991-14994
40
41
42 15 29 Kaithal A, Schmitz M, Hölscher M, Leitner W. *ChemCatChem*, 2019, 11: 5287-5291
43
44
45 16 30 Wesselbaum S, Stein TV, Klankermayer J, Leitner W. *Angew Chem Int Ed*, 2012, 51:
46
47 7499-7502
48
49 18 31 Kaithal A, Bonn P, Holscher M, Leitner W. *Angew Chem Int Ed*, 2020, 59: 215-220
50
51
52 19 32 Schlagbauer M, Kallmeier F, Irrgang T, Kempe R. *Angew Chem Int Ed*, 2020, 59:
53
54 20 1485-1490
55
56
57 21 33 Kaithal A, Schmitz M, Hoscher M, Leitner W. *ChemCatChem*, 2020, 12: 781-787
58
59
60 22 34 Chen KQ, Sheng H, Liu Q, Shao PL, Chen XY. *Sci China Chem*, 2021, 64: 7-16

- 1
2
3
4 1 35 Campos J, Sharninghausen LS, Crabtree RH, Balcells D. *Angew Chem Int Ed*, 2014, 53:
5
6 2 12808-12811
7
8
9 3 36 Hopkinson MN, Richter C, Schedler M, Glorius F. *Nature*, 2014, 510: 485-496
10
11 4 37 Sharninghausen LS, Campos J, Manas MG, Crabtree RH. *Nat Commun*, 2014, 5: 5084
12
13
14 5 38 Gonzalez SD, Marion N, Nolan SP. *Chem Rev*, 2009, 109: 3612-3676
15
16
17 6 39 Chen JA, Huang Y. *Sci China Chem*, 2016, 59: 251-254
18
19
20 7 40 Wu JJ, Shen LY, Duan S, Chen ZN, Zheng QS, Liu YQ, Sun ZM, Clark JH, Xu X, Tu T.
21
22 8 *Angew Chem Int Ed*, 2020, 59: 13871-13878
23
24
25 9 41 Wang JQ, Wu JJ, Chen ZN, Wen DH, Chen JB, Zheng QS, Xu X, Tu T. *J Catal*, 2020,
26
27 10 389: 337-344
28
29
30 11 42 Wu JJ, Shen LY, Chen ZN, Zheng QS, Xu X, Tu T. *Angew Chem Int Ed*, 2020, 59:
31
32 12 10421-10425
33
34
35 13 43 Chen JB, Wu JJ, Tu T. *ACS Sustain Chem Eng*, 2017, 5: 11744-11751
36
37
38 14 44 Sun ZM, Liu YQ, Chen JB, Huang CY, Tu T. *ACS Catal*, 2015, 5: 6573-6578
39
40
41 15 45 Iglesias M, Oro LA. *Chem Soc Rev*, 2018, 47: 2772-2808
42
43
44 16 46 Manas MG, Campos J, Sharninghausen LS, Lin E, Crabtree RH. *Green Chem*, 2015, 17:
45
46 17 594-600
47
48
49 18 47 Dobereiner GE, Nova A, Schley ND, Hazari N, Miller SJ, Eisenstein O, Crabtree RH. *J*
50
51 19 *Am Chem Soc*, 2011, 133: 7547-7562
52
53
54 20 48 Fu SM, Shao ZH, Wang YJ, Liu Q. *J Am Chem Soc*, 2017, 139: 11941-11948
55
56
57 21 49 Xie YJ, David Y, Shimon LJ, Milstein D. *J Am Chem Soc*, 2016, 138: 9077-9080
58
59
60

- 1
2
3
4 1 50 Falivene L, Cao Z, Petta A, Serra L, Poater A, Oliva R, Scarano V, Cavallo L. *Nat Chem*,
5
6 2 2019, 11: 872
7
8
9 3 51 Clavier H, Nolan SP. *Chem Commun*, 2010, 46: 841-861
10
11
12 4 52 Poater A, Cosenza B, Correa A, Giudice S, Ragone F, Scarano V, Cavallo L. *Eur J Inorg*
13
14 5 *Chem*, 2009, 1759-1766
15
16
17 6 53 Tu T, Zhou YG, Hou XL, Dai LX, Dong XC, Yu XH, Sun J. *Organometallics*, 2003, 22:
18
19 7 1255-1265
20
21
22 8 54 Crabtree RH. *Chem Rev*, 2012, 112: 1536-1554.
23
24
25 9 55 Jimenez MV, Tornos J. Modrego FJ, Torrente JJ, Oro LA. *Chem Eur J*, 2015, 21:
26
27 10 17877-17889
28
29
30 11 56 Vellakkaran M, Singh K, Banerjee D. *ACS Catal*, 2017, 7: 8152-8158
31
32
33 12 57 Simmons EM, Hartwig JF. *Angew Chem Int Ed*, 2012, 51: 3066-3072
34
35 13
36
37
38
39
40
41
42
43
44
45
46
47
48
49
50
51
52
53
54
55
56
57
58
59
60

Supporting Information

Highly Efficient NHC-Iridium-Catalyzed β -Methylation of Alcohols with Methanol at Low Catalyst Loadings

Zeye Lu,¹ Qingshu Zheng,¹ Guangkuo Zeng,¹ Yunyan Kuang,¹ James H. Clark,⁴ & Tao Tu^{1,2,3*}

¹*Shanghai Key Laboratory of Molecular Catalysis and Innovative Materials, Department of Chemistry, Fudan University, 2005 Songhu Road, Shanghai 200438, China.*

²*State Key Laboratory of Organometallic Chemistry, Shanghai Institute of Organic Chemistry, Chinese Academy of Sciences, Shanghai 200032, China.*

³*Green Catalysis Center and College of Chemistry, Zhengzhou University, Zhengzhou 450001, China.*

⁴*Green Chemistry Centre of Excellence, University of York, York YO 105DD, UK.*

*Corresponding Author: (Email: taotu@fudan.edu.cn)

Table of Contents

1. General	S3
2. Syntheses of NHC-Iridium complexes	S4
3. NMR spectra of imidazolium salts and catalysts.....	S7
3.1 NMR spectra of imidazolium salts L3-L4	S7
3.2 NMR spectra of iridium complexes 5c-5d	S10
4. High resolution mass spectrometry of iridium complex 5d	S13
5. Crystal structures of iridium complexes 5c and 5d	S14
6. β -Methylation of primary and secondary alcohols with methanol	S25
6.1 Optimization of reaction conditions	S25
6.2 Procedure of TON and TOF of β -methylation with methanol	S26
6.3 General procedure for β -methylation of primary alcohols with methanol	S26
6.4 Preparation of ibuprofen from precursor 33 using self-supported Ru catalyst.....	S33
6.5 General procedure for β -methylation of secondary alcohols with methanol.....	S34
6.6 General procedure for β -alkylation of 2-phenyl ethanol with primary alcohols	S38
7. Control experiments.....	S40
7.1 Procedure for β -methylation of 2-arylethanol with TEMPO.....	S40
7.2 Procedure for β -methylation of 2-arylethanol with Hg	S40
7.3 Reaction profile for β -methylation of 2-arylethanol.....	S40
7.4 Procedure for β -methylation of acetophenone with methanol.....	S41
7.5 Procedure for hydrogen transfer of di-methylated-ketone with methanol.....	S41
7.6 Procedure for β -methylation of acetophenone with CD ₃ OD	S42
7.7 Procedure for β -methylation of 2-arylethanol with CD ₃ OD.....	S42
7.8 Procedure for KIE experiment of β -methylation with CH ₃ OH or CD ₃ OD.	S43
8. ¹ H NMR spectra of reaction mixtures after β -methylation of alcohols	S44
9. NMR spectra of isolated products	S45
References.....	S87

1. General

All commercial reagents were used directly without further purification, unless otherwise stated. All reaction sealed tubes (35 mL) were purchased from Beijing Synthware Glass. CDCl_3 , D_2O and $\text{DMSO-}d_6$ were purchased from Cambridge Isotope Laboratories. ^1H , ^{13}C , and ^{19}F spectra were recorded on Bruker 400 DRX spectrometers at room temperature. The chemical shifts (δ) for ^1H NMR are given in parts per million (ppm) referenced to the residual proton signal of the deuterated solvent (CHCl_3 at δ 7.26 ppm, $\text{DMSO-}d_6$ at δ 2.50 ppm, D_2O at δ 4.79 ppm); coupling constants are expressed in hertz (Hz). ^{13}C NMR spectra were referenced to the carbon signal of CDCl_3 (77.0 ppm) or $\text{DMSO-}d_6$ (39.5 ppm). The following abbreviations are used to describe NMR signals: s = singlet, d = doublet, t = triplet, m = multiplet, q = quartet. ESI-TOF-MS spectra were recorded on a Bruker micrOTOF II instrument. Single-crystal X-ray diffraction data for iridium complexes were collected at 173 K on a Bruker D8 VENTURE microfocus X-ray source system. GC-MS spectra were recorded on Agilent technologies 7890A GC system and 5975C inert MSD with Triple-Axis Detector. High resolution mass spectra (HR-MS) were acquired using a Q-Exactive Focus Hybrid Quadrupole-Orbitrap Mass Spectrometer (Thermo Fisher) equipped with a Dionex Ultimate 3000 HPLC system (Thermo Fisher).

GC method: The instrument was set to an injection volume of 1 μL , an inlet split ratio of 100:1, and inlet and detector temperatures of 250 and 280 $^\circ\text{C}$. The temperature program used for all of the analyses is as follows: 40 $^\circ\text{C}$, 3 min; 5 $^\circ\text{C}/\text{min}$ to 95 $^\circ\text{C}$. Response factor for all of the necessary compounds with respect to standard benzene was calculated from the average of three independent GC runs.

Computational methods: The percent buried volumes (% V_{bur}) and steric maps of complexes **5a**, **5c** and **5d** were calculated by SambVca 2.1^{S1-S2} at <https://www.molnac.unisa.it/OMtools/sambvca2.1/index.html>.

For the geometry optimization, the quantum calculations were performed by using generalized gradient approximation functional and the correction of the D3 version of

Grimme's empirical dispersion with Becke-Johnson damping (PBED3(BJ)).^{S3-S5} The all-electron basis sets of 6-31+G(d,p)^{S6} and the Stuttgart/Dresden effective-core potential (SDD)^{S7-S9} were used for main group elements and Ir atom, respectively. Analytical frequencies were calculated in order to confirm that a local minimum has no imaginary frequency. Charge analyses were performed using the APT schemes.^{S10} All calculations were carried out using the Gaussian 16 program.^{S11}

2. Syntheses of NHC-Iridium complexes

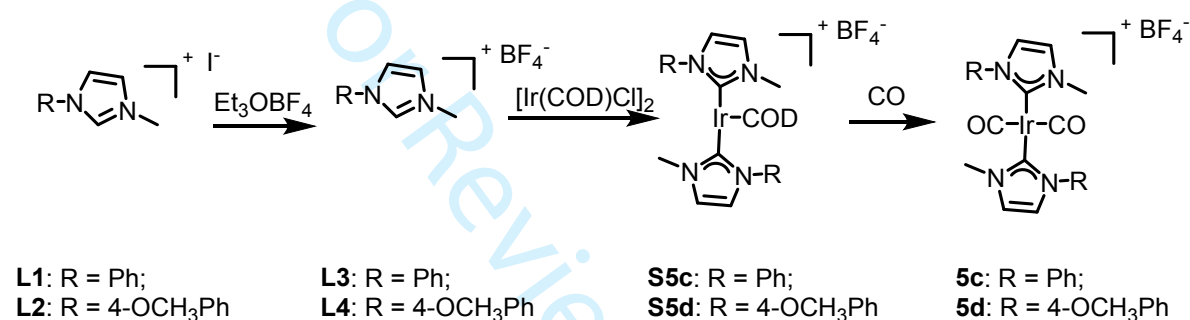


Figure S1. Syntheses of NHC-Ir complexes.

The NHC-Ir complexes **4a-4b**, **5a-5b** was synthesized according to previously reported procedures.^{S12-S14}

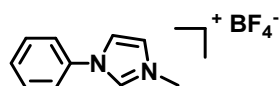
Syntheses of compounds L3-L4: Iodized salt (**L1** or **L2**, 10 mmol)^{S15} was added into 100 mL DCM and stir at room temperature until completely dissolved. Then Et_3OBF_4 (3.9 g, 20 mmol) was added to the solution and stirring for 16 h at room temperature. After the reaction, 100 mL methanol was added for another 1 h stirring. The reaction mixture was then concentrated and recrystallized with ether to afford the formation of white solid.

Syntheses of compounds S5c-S5d: $[\text{Ir}(\text{COD})\text{Cl}]_2$ (201 mg, 0.3 mmol) was dissolved in 10 mL dry EtOH and added to a 50 mL Schlenk tube with a magnetic stir bar. Then NaH (28 mg, 1.2 mmol) was added to the solution and then after stirring of 1 h,

imidazole tetrafluoroborate salt (**S5c** or **S5d**) (2 mmol) was added. The reaction mixture was stirred for 24 h at room temperature. The obtained mixture was directly used for the following CO exchange without purification.

Syntheses of compounds 5c-5d: **S5c** or **S5d** in 15 mL dry DCM, CO (g) was bubbled through the solution at room temperature for 4 h. Solvent was evaporated and pure products were obtained by column chromatography over silica gel using DCM/methanol (100:1) mixture as eluent. The solid was further washed with Et₂O and dried to obtain complex **5c** or **5d** as a bright yellow solid (60 % for two steps).

L3:



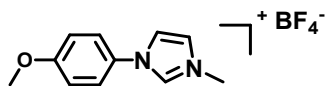
¹H NMR (400 MHz, DMSO-*d*₆, 298 K) δ = 9.70 (s, 1H, imidazole-H), 8.27 (d, 1H, *J* = 1.5 Hz, ArCH), 7.93 (s, 1H, ArCH), 7.76 (d, 2H, *J* = 8.0 Hz, ArCH), 7.67 (dd, 2H, *J* = 10.4, 5.0 Hz, ArCH), 7.55-7.62 (m, 1H, ArCH), 3.95 (s, 3H, CH₃) ppm.

¹³C NMR (101 MHz, DMSO-*d*₆, 298 K) δ = 135.9, 134.8, 130.3, 129.8, 124.5, 121.9, 121.0, 36.1 ppm.

¹⁹F NMR (376 MHz, DMSO-*d*₆, 298 K) δ = 148.28 ppm.

HRMS (ESI), *m/z*: [M-BF₄]⁺ calculated for C₁₀H₁₁N₂: 159.0922, found: 159.0912.

L4:



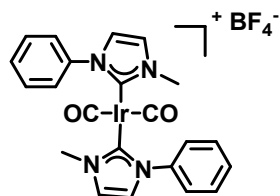
¹H NMR (400 MHz, DMSO-*d*₆, 298 K) δ = 9.61 (s, 1H, imidazole-H), 8.19 (t, 1H, *J* = 1.8 Hz, ArCH), 7.90 (t, 1H, *J* = 1.8 Hz, ArCH), 7.63-7.71 (m, 2H, ArCH), 7.17-7.22 (m, 2H, ArCH), 3.92 (s, 3H, OCH₃), 3.84 (s, 3H, CH₃) ppm.

¹³C NMR (101 MHz, DMSO-*d*₆, 298 K) δ = 160.0, 135.8, 127.9, 124.2, 123.5, 121.3, 115.2, 55.8, 36.1 ppm.

¹⁹F NMR (376 MHz, DMSO-*d*₆, 298 K) δ = 148.24 ppm.

HRMS (ESI), m/z : $[M-BF_4]^+$ calculated for $C_{11}H_{13}N_2O$: 189.1028, found 189.1020.

5c:



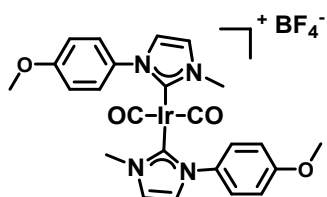
1H NMR (400 MHz, $DMSO-d_6$, 298 K) δ = 7.45-7.56 (m, 4H, ArCH), 7.24-7.36 (m, 3H, ArCH), 3.23 (s, 3H, CH_3) ppm.

^{13}C NMR (101 MHz, $DMSO-d_6$, 298 K) δ = 180.1, 166.9, 138.7, 129.5, 129.0, 125.0, 124.2, 123.5, 38.1 ppm.

^{19}F NMR (376 MHz, $DMSO-d_6$, 298 K) δ = 148.30 ppm.

HRMS (ESI), m/z : $[M-BF_4]^+$ calculated for $C_{22}H_{20}IrN_4O_2$: 565.1215, found 565.1215.

5d:



1H NMR (400 MHz, $DMSO-d_6$, 298 K) δ = 7.47 (d, 1H, J = 1.7 Hz, ArCH), 7.40 (d, 1H, J = 1.3 Hz, ArCH), 7.15 (d, 2H, J = 8.7 Hz, ArCH), 6.95-7.01 (m, 2H, ArCH), 3.84 (s, 3H, OCH_3), 3.26 (s, 3H, CH_3) ppm.

^{13}C NMR (101 MHz, $DMSO-d_6$, 298 K) δ = 180.2, 166.8, 159.5, 131.7, 126.3, 124.2, 123.7, 114.4, 55.7, 37.8 ppm.

^{19}F NMR (376 MHz, $DMSO-d_6$, 298 K) δ = 148.31 ppm.

HRMS (ESI), m/z : $[M-BF_4]^+$ calculated for $C_{24}H_{24}IrN_4O_4$: 625.1422, found 625.1437.

3. NMR spectra of imidazolium salts and catalysts

3.1 NMR spectra of imidazolium salts L3-L4

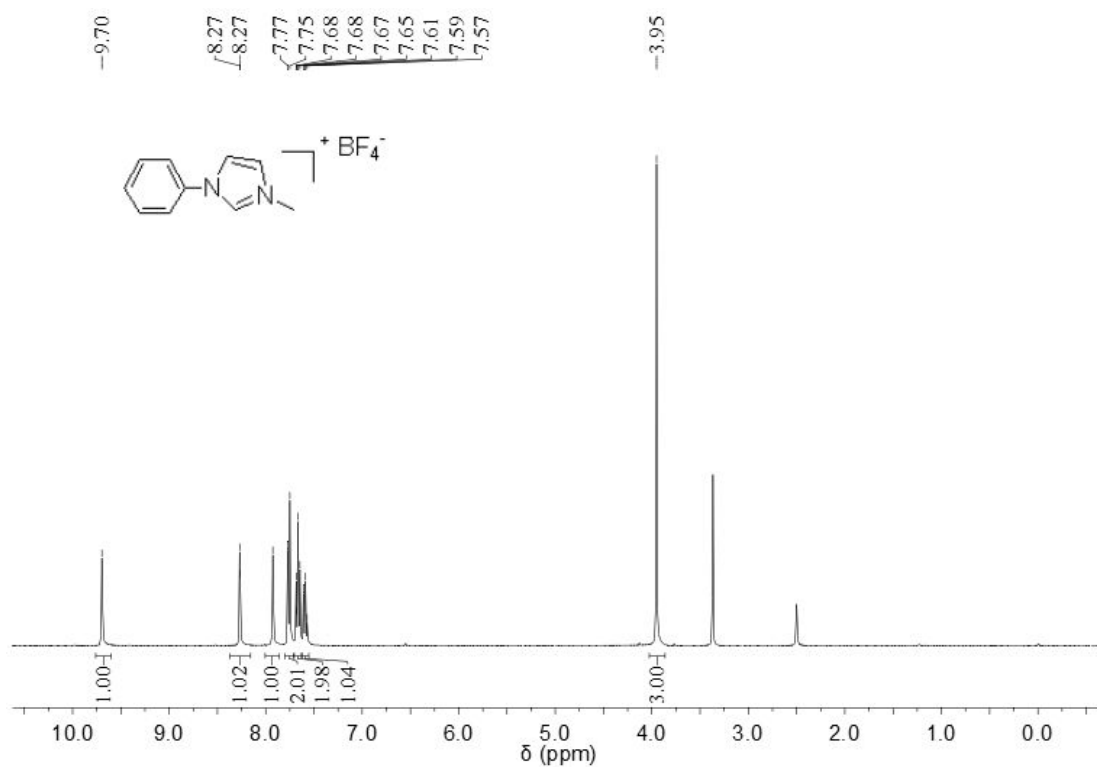


Figure S2. ^1H NMR (400 MHz, $\text{DMSO}-d_6$, 298 K) spectrum of L3.

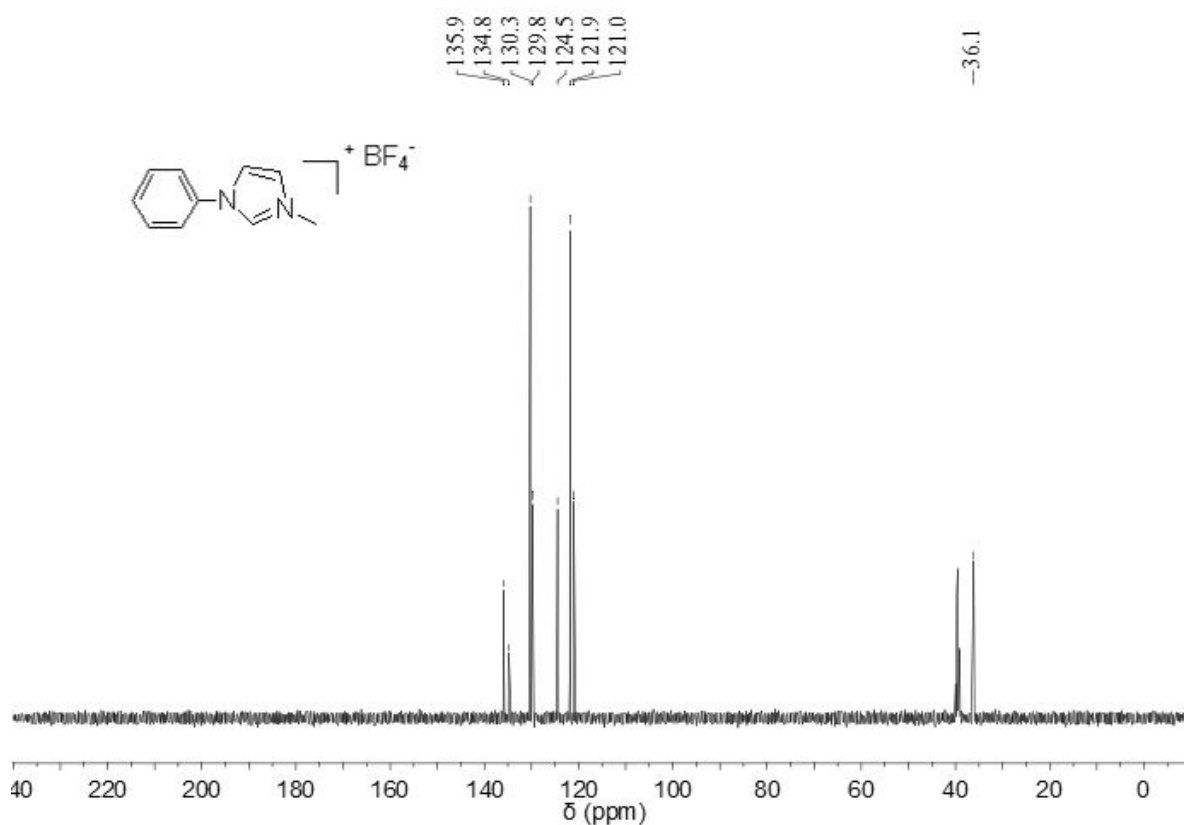


Figure S3. ¹³C NMR (101 MHz, DMSO-*d*₆, 298 K) spectrum of L3.

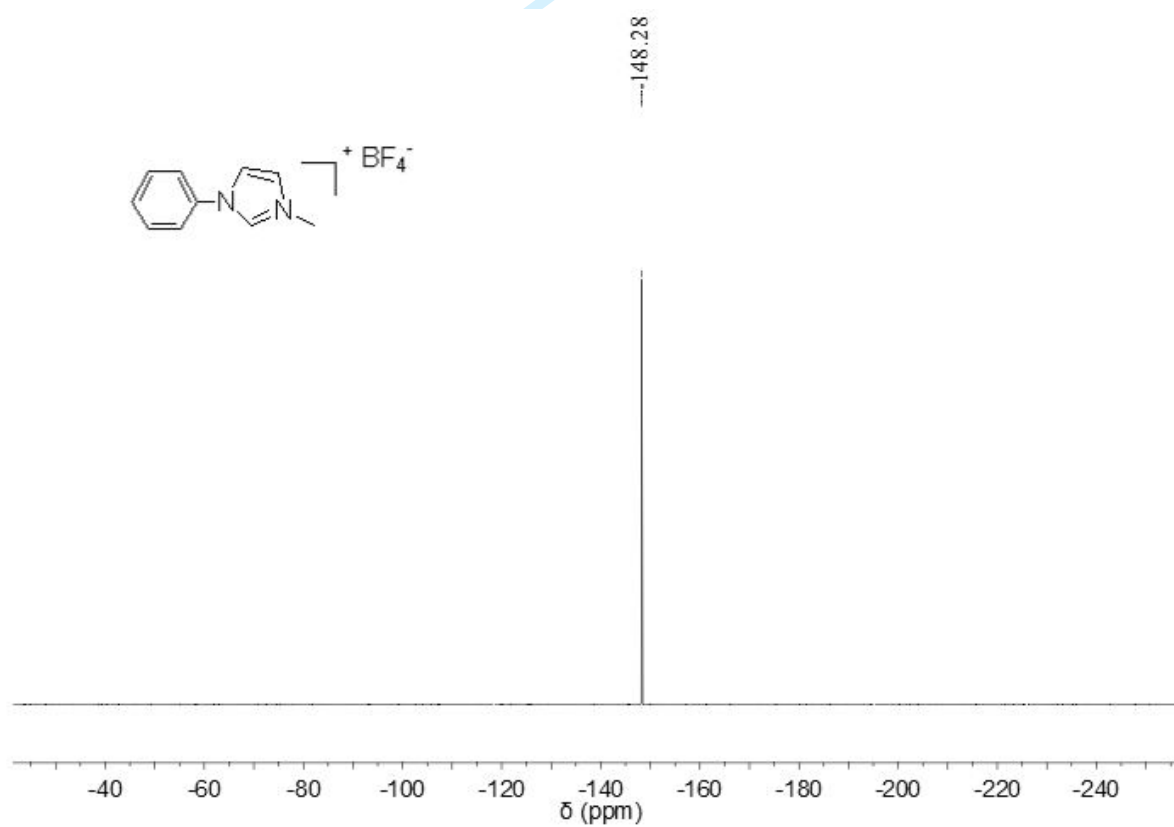


Figure S4. ¹⁹F NMR (376 MHz, DMSO-*d*₆, 298 K) spectrum of L3.

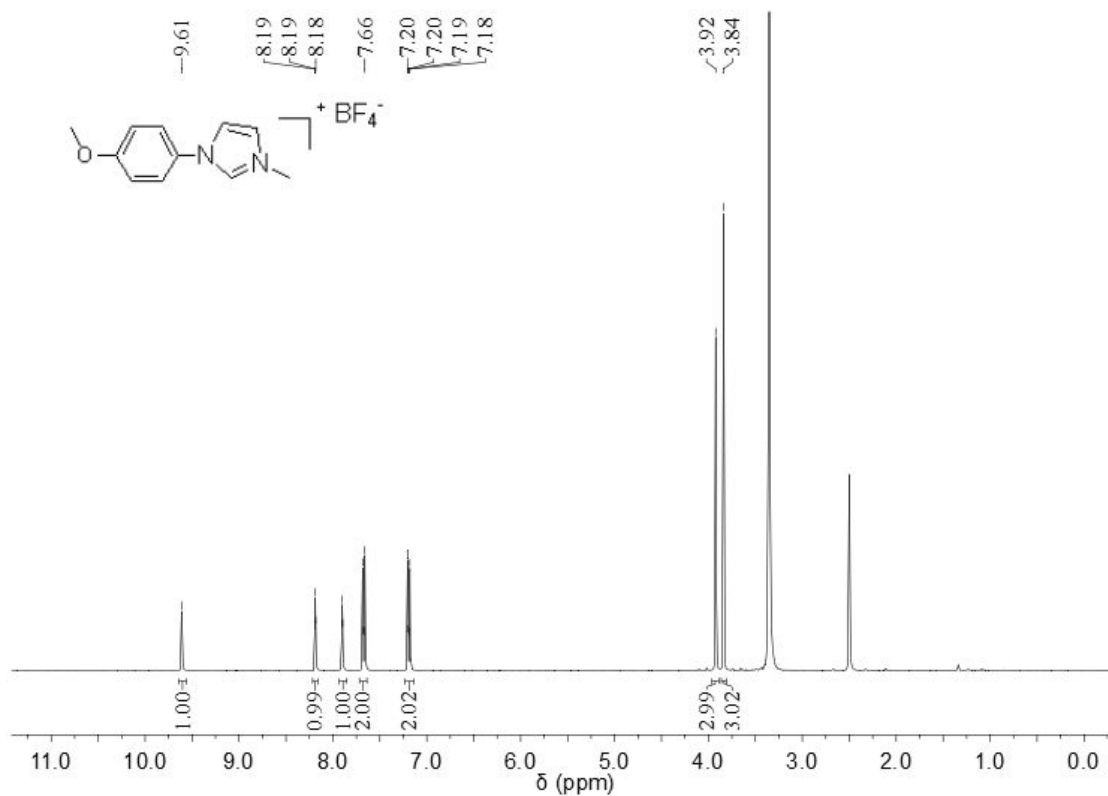


Figure S5. ¹H NMR (400 MHz, DMSO-*d*₆, 298 K) spectrum of L4.

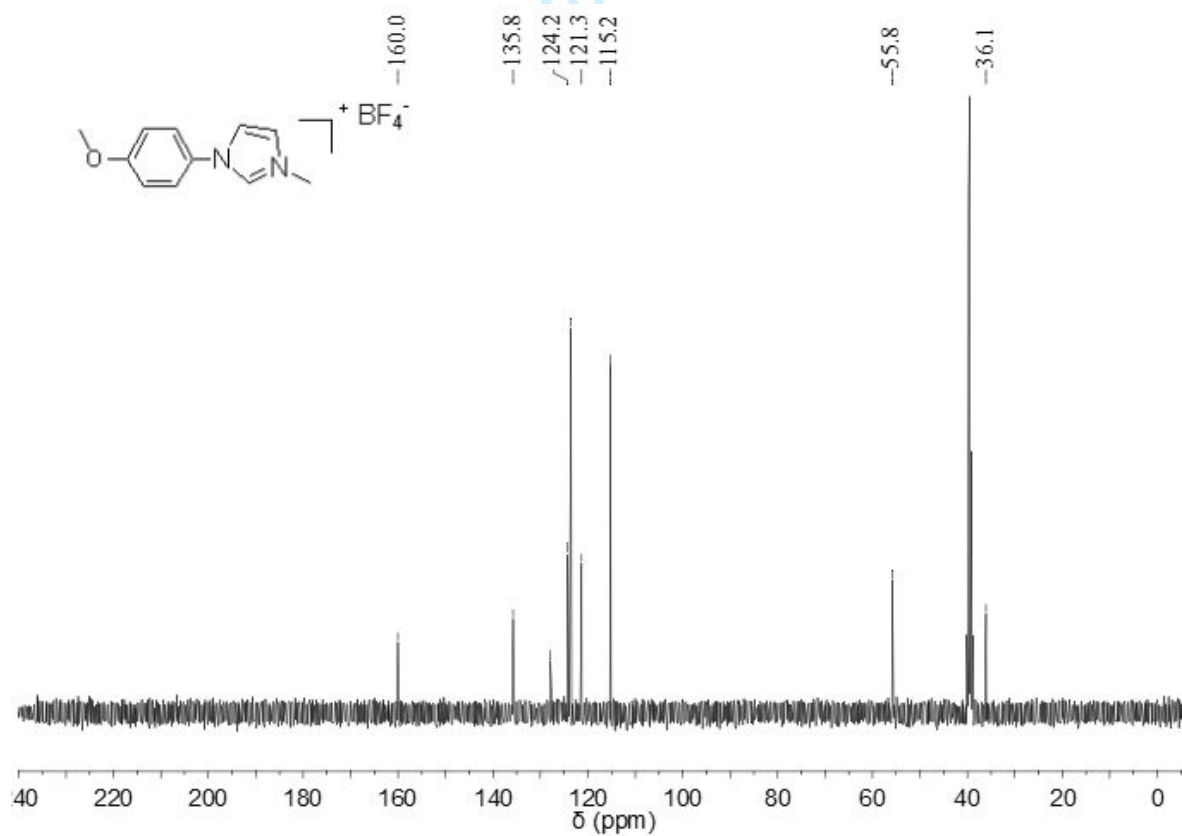


Figure S6. ¹³C NMR (101 MHz, DMSO-*d*₆, 298 K) spectrum of L4.

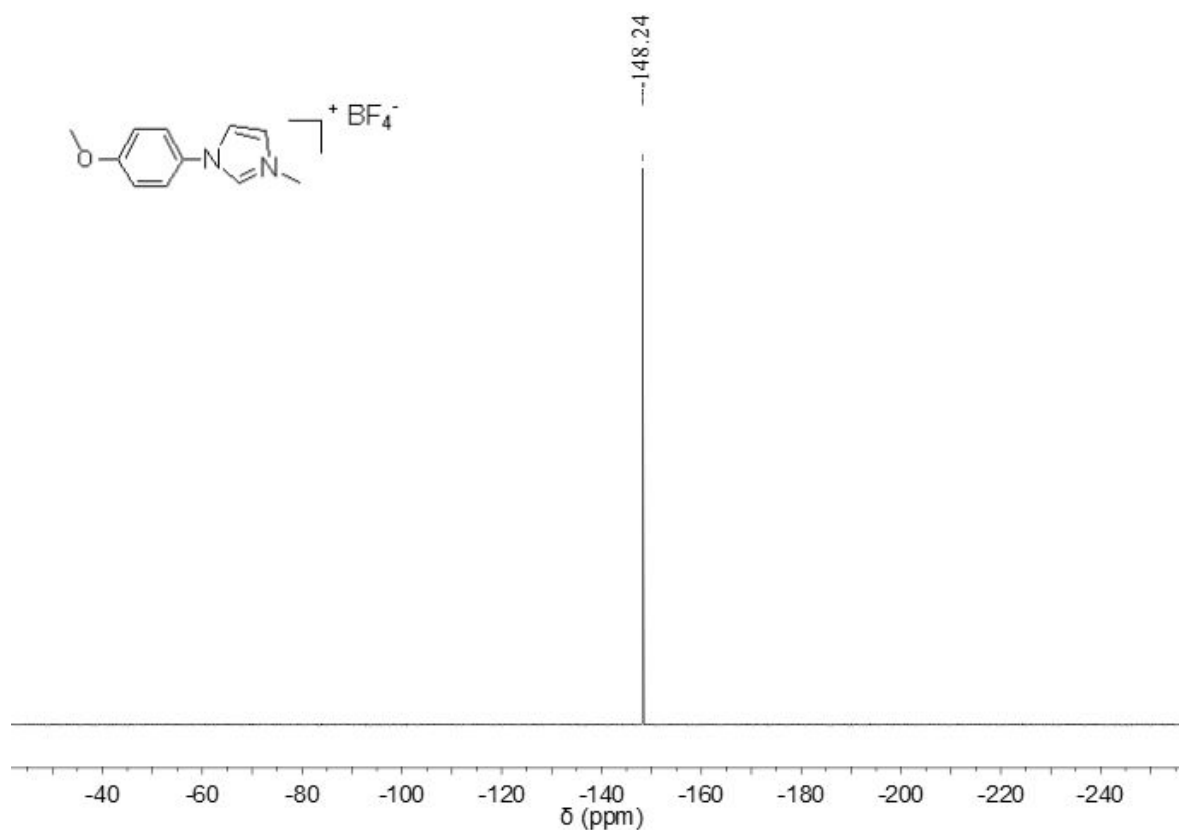


Figure S7. ^{19}F NMR (376 MHz, $\text{DMSO-}d_6$, 298 K) spectrum of **L4**.

3.2 NMR spectra of iridium complexes **5c-5d**

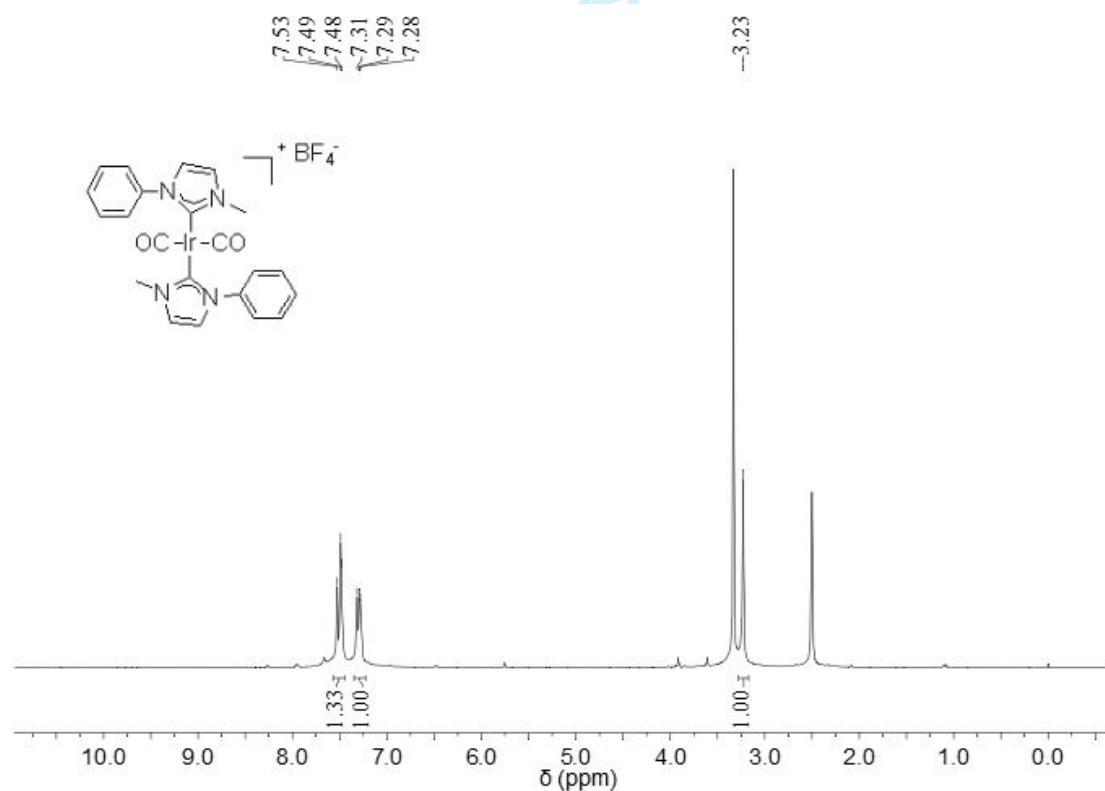


Figure S8. ^1H NMR (400 MHz, $\text{DMSO-}d_6$, 298 K) spectrum of **5c**.

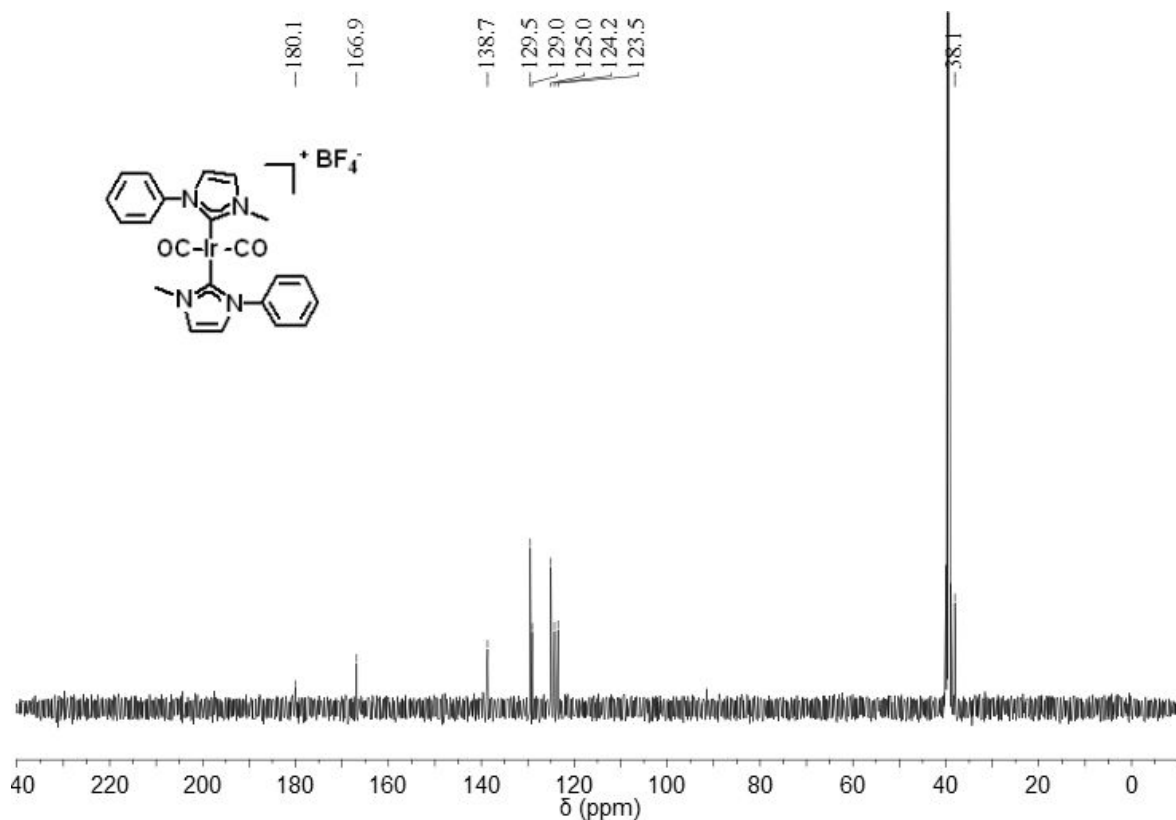


Figure S9. ¹³C NMR (101 MHz, DMSO-*d*₆, 298 K) spectrum of **5c**.

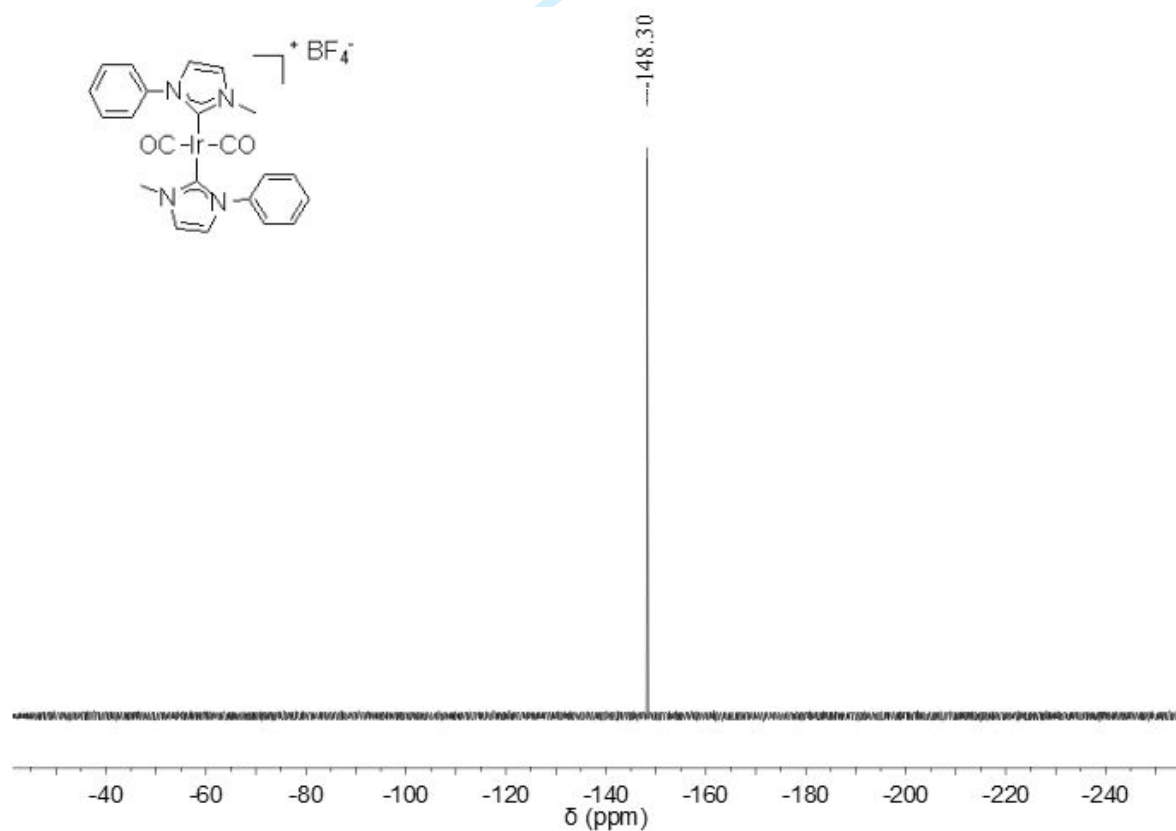


Figure S10. ¹⁹F NMR (376 MHz, DMSO-*d*₆, 298 K) spectrum of **5c**.

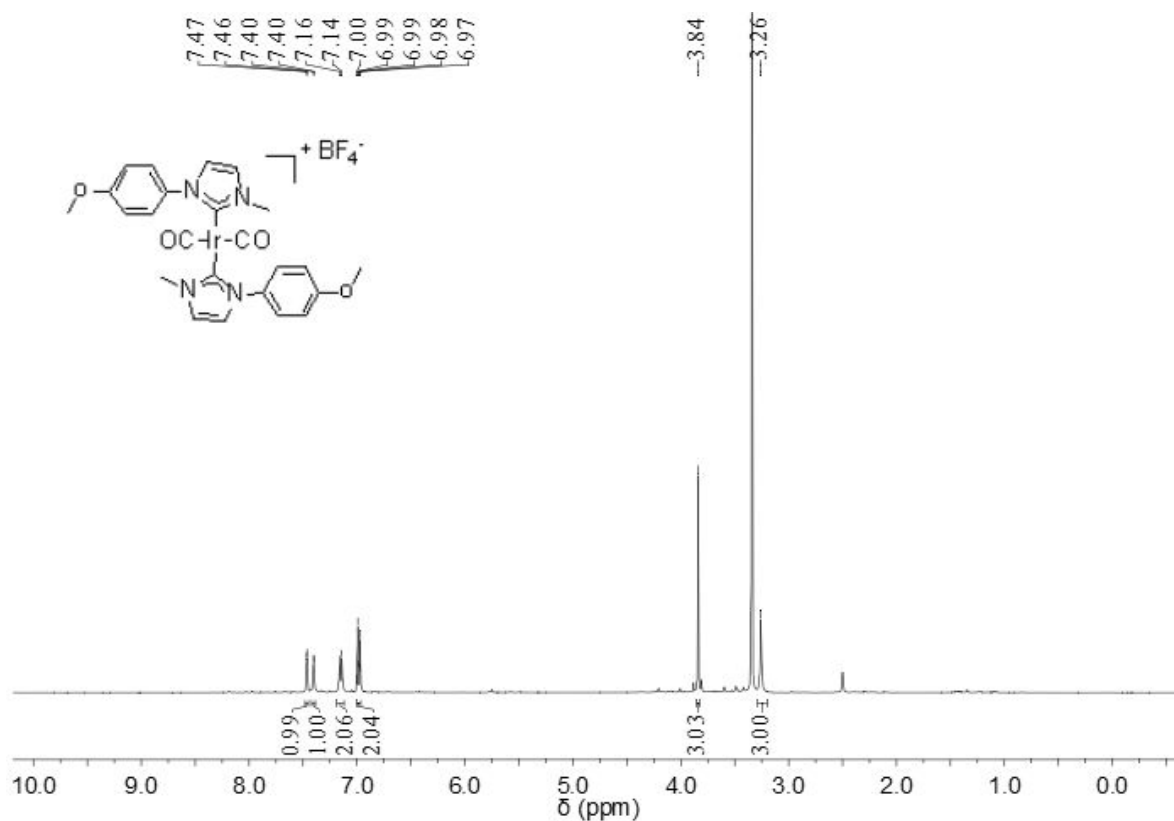


Figure S11. ^1H NMR (400 MHz, $\text{DMSO}-d_6$, 298 K) spectrum of **5d**.

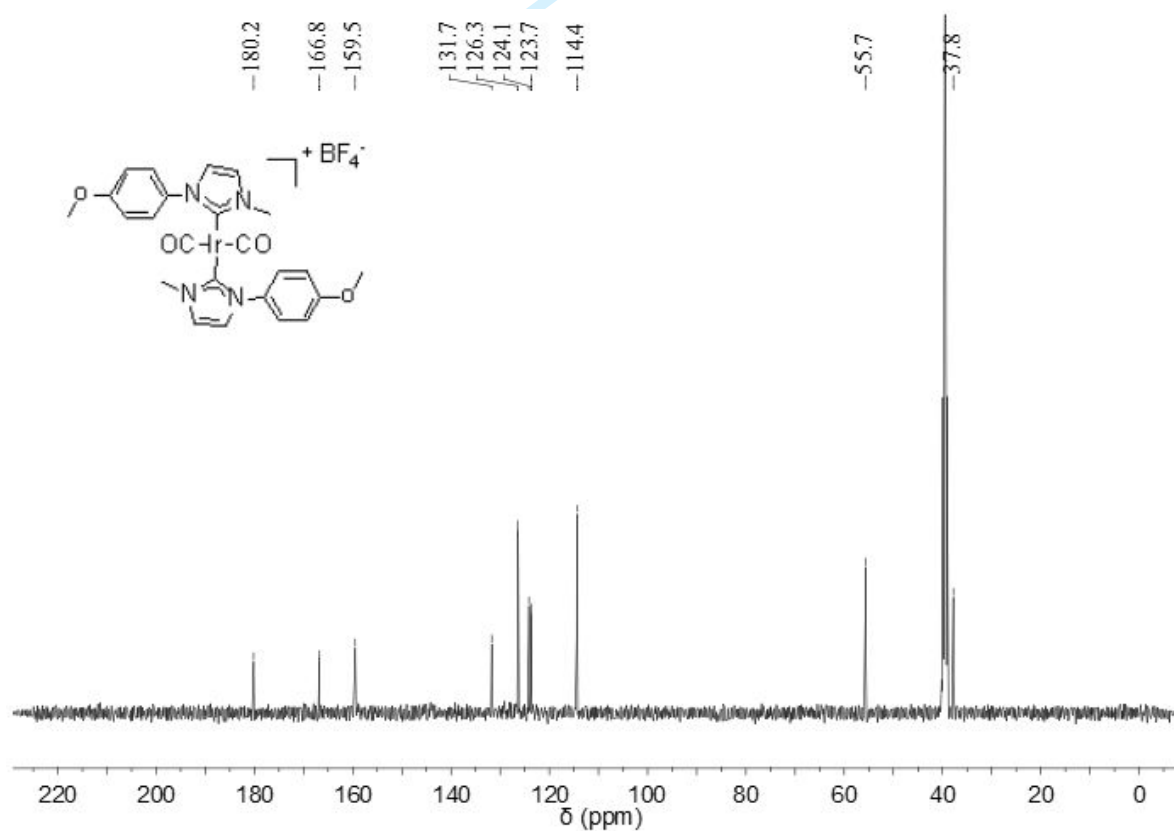


Figure S12. ^{13}C NMR (101 MHz, $\text{DMSO}-d_6$, 298 K) spectrum of **5d**.

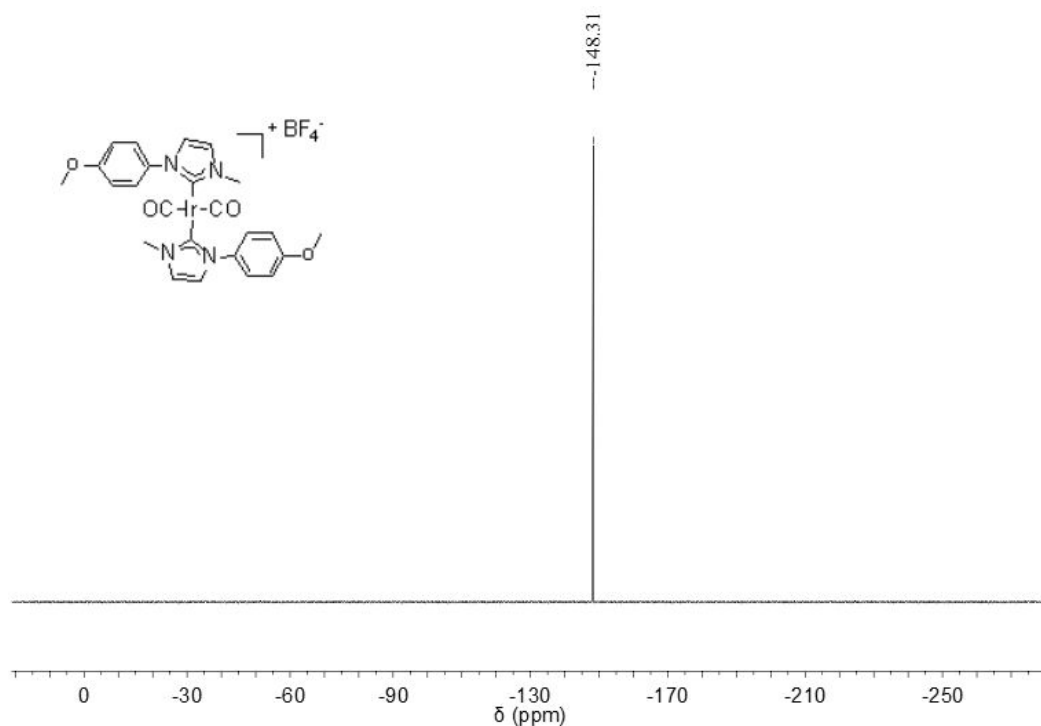


Figure S13. ^{19}F NMR (376 MHz, $\text{DMSO}-d_6$, 298 K) spectrum of **5d**.

4. High resolution mass spectrometry of iridium complex **5d**

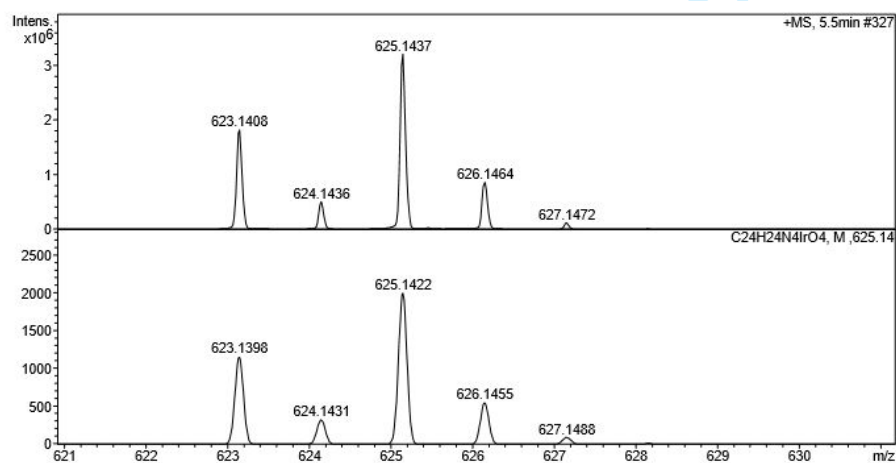
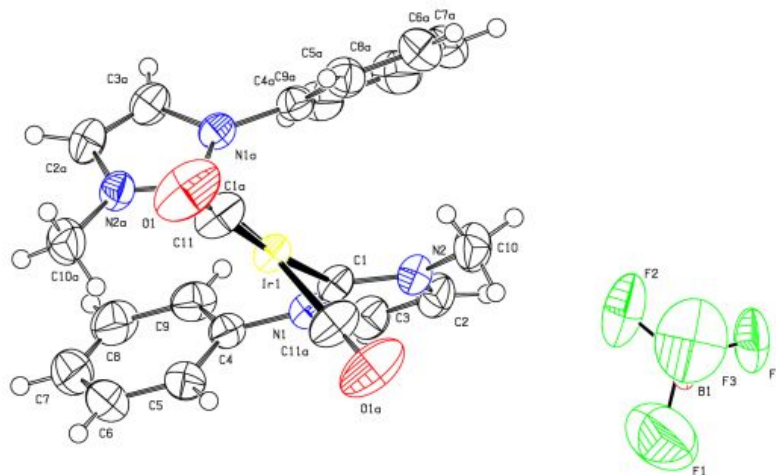


Figure S14. High resolution mass spectrometry of iridium complex **5d**

Yellow block crystals suitable for single-crystal X-ray diffractions were obtained by slow evaporation of their dichloromethane solutions.



S14

Table S1 Crystal data and structure refinement for Ir complex **5c**.

Identification code	5c
Empirical formula	C ₂₂ H ₂₀ B F ₄ Ir N ₄ O ₂
Formula weight	651.43
Temperature	293(2) K
Wavelength	1.34138 Å
Crystal system	Monoclinic
Space group	C2/c
Unit cell dimensions	a = 15.2636(15) Å $\alpha = 90^\circ$. b = 13.1155(13) Å $\beta = 119.206(2)^\circ$. c = 13.685(2) Å $\gamma = 90^\circ$.
Volume	2391.3(5) Å ³
Z	4
Density (calculated)	1.809 mg/m ³
Absorption coefficient	7.501 mm ⁻¹
F(000)	1256
Crystal size	0.120 x 0.100 x 0.080 mm ³
Theta range for data collection	5.778 to 59.495°.
Index ranges	-19 ≤ h ≤ 19, -16 ≤ k ≤ 16, -17 ≤ l ≤ 17
Reflections collected	14873
Independent reflections	2653 [R(int) = 0.0425]
Completeness to theta = 53.594°	99.9 %
Absorption correction	Semi-empirical from equivalents
Max. and min. transmission	0.581 and 0.462
Refinement method	Full-matrix least-squares on F ²
Data / restraints / parameters	2653 / 28 / 179
Goodness-of-fit on F ²	1.058
Final R indices [I > 2σ(I)]	R1 = 0.0252, wR2 = 0.0718
R indices (all data)	R1 = 0.0257, wR2 = 0.0726
Extinction coefficient	0.00038(7)
Largest diff. peak and hole	0.859 and -0.643 e.Å ⁻³

Table S2 Bond lengths [Å] and angles [°] for Ir complex **5c**.

Ir(1)-C(11)#1	1.882(4)
Ir(1)-C(11)	1.882(4)
Ir(1)-C(1)	2.080(3)
Ir(1)-C(1)#1	2.080(3)
B(1)-B(1)#2	0.38(3)
B(1)-F(4)#2	1.22(3)
B(1)-F(3)#2	1.270(12)
B(1)-F(3)	1.371(12)
B(1)-F(1)	1.372(17)
B(1)-F(4)	1.379(16)
B(1)-F(2)	1.386(16)
B(1)-F(2)#2	1.40(3)
B(1)-F(1)#2	1.74(2)
F(1)-F(3)#2	1.648(18)
F(2)-F(4)#2	0.55(2)
F(3)-F(3)#2	0.80(3)
N(1)-C(1)	1.358(4)
N(1)-C(3)	1.385(4)
N(1)-C(4)	1.430(4)
N(2)-C(1)	1.351(4)
N(2)-C(2)	1.383(4)
N(2)-C(10)	1.464(4)
O(1)-C(11)	1.138(5)
C(2)-C(3)	1.338(5)
C(2)-H(2)	0.9300
C(3)-H(3)	0.9300
C(4)-C(9)	1.385(4)
C(4)-C(5)	1.389(4)
C(5)-C(6)	1.385(5)
C(5)-H(5)	0.9300
C(6)-C(7)	1.379(6)
C(6)-H(6)	0.9300
C(7)-C(8)	1.381(6)
C(7)-H(7)	0.9300
C(8)-C(9)	1.402(5)
C(8)-H(8)	0.9300

C(9)-H(9)	0.9300
C(10)-H(10A)	0.9600
C(10)-H(10B)	0.9600
C(10)-H(10C)	0.9600
C(11)#1-Ir(1)-C(11)	91.6(2)
C(11)#1-Ir(1)-C(1)	90.43(17)
C(11)-Ir(1)-C(1)	173.99(14)
C(11)#1-Ir(1)-C(1)#1	173.99(14)
C(11)-Ir(1)-C(1)#1	90.43(17)
C(1)-Ir(1)-C(1)#1	88.11(15)
B(1)#2-B(1)-F(4)#2	107(7)
B(1)#2-B(1)-F(3)#2	97.5(16)
F(4)#2-B(1)-F(3)#2	125(2)
B(1)#2-B(1)-F(3)	66.7(14)
F(4)#2-B(1)-F(3)	117(2)
F(3)#2-B(1)-F(3)	35.2(13)
B(1)#2-B(1)-F(1)	164(8)
F(4)#2-B(1)-F(1)	87.8(13)
F(3)#2-B(1)-F(1)	77.1(13)
F(3)-B(1)-F(1)	111.3(11)
B(1)#2-B(1)-F(4)	58(6)
F(4)#2-B(1)-F(4)	121.5(15)
F(3)#2-B(1)-F(4)	113.2(19)
F(3)-B(1)-F(4)	106.9(17)
F(1)-B(1)-F(4)	110.6(15)
B(1)#2-B(1)-F(2)	84(6)
F(4)#2-B(1)-F(2)	23.1(11)
F(3)#2-B(1)-F(2)	135(2)
F(3)-B(1)-F(2)	112.1(19)
F(1)-B(1)-F(2)	109.9(14)
F(4)-B(1)-F(2)	105.9(9)
B(1)#2-B(1)-F(2)#2	80(6)
F(4)#2-B(1)-F(2)#2	114.5(7)
F(3)#2-B(1)-F(2)#2	118(2)
F(3)-B(1)-F(2)#2	124.4(19)
F(1)-B(1)-F(2)#2	89.5(15)
F(4)-B(1)-F(2)#2	22.6(10)

F(2)-B(1)-F(2)#2	107.2(17)
B(1)#2-B(1)-F(1)#2	12(6)
F(4)#2-B(1)-F(1)#2	98.2(16)
F(3)#2-B(1)-F(1)#2	96.4(12)
F(3)-B(1)-F(1)#2	62.7(10)
F(1)-B(1)-F(1)#2	173.0(13)
F(4)-B(1)-F(1)#2	69.4(10)
F(2)-B(1)-F(1)#2	76.4(13)
F(2)#2-B(1)-F(1)#2	91.4(13)
B(1)-F(1)-F(3)#2	48.7(6)
B(1)-F(1)-B(1)#2	3.3(17)
F(3)#2-F(1)-B(1)#2	47.7(6)
F(4)#2-F(2)-B(1)	61(3)
F(4)#2-F(2)-B(1)#2	77(3)
B(1)-F(2)-B(1)#2	15.6(14)
F(3)#2-F(3)-B(1)#2	79.3(11)
F(3)#2-F(3)-B(1)	65.5(10)
B(1)#2-F(3)-B(1)	15.8(14)
F(3)#2-F(3)-F(1)#2	131.8(15)
B(1)#2-F(3)-F(1)#2	54.2(9)
B(1)-F(3)-F(1)#2	69.6(9)
F(2)#2-F(4)-B(1)#2	96(3)
F(2)#2-F(4)-B(1)	81(3)
B(1)#2-F(4)-B(1)	15.2(16)
C(1)-N(1)-C(3)	110.8(3)
C(1)-N(1)-C(4)	126.2(3)
C(3)-N(1)-C(4)	123.0(2)
C(1)-N(2)-C(2)	110.9(2)
C(1)-N(2)-C(10)	126.2(3)
C(2)-N(2)-C(10)	122.9(3)
N(2)-C(1)-N(1)	104.5(2)
N(2)-C(1)-Ir(1)	126.6(2)
N(1)-C(1)-Ir(1)	128.7(2)
C(3)-C(2)-N(2)	107.1(3)
C(3)-C(2)-H(2)	126.5
N(2)-C(2)-H(2)	126.5
C(2)-C(3)-N(1)	106.7(3)
C(2)-C(3)-H(3)	126.6

1
2
3
4
5
6
7
8
9
10
11
12
13
14
15
16
17
18
19
20
21
22
23
24
25
26
27
28
29
30
31
32
33
34
35
36
37
38
39
40
41
42
43
44
45
46
47
48
49
50
51
52
53
54
55
56
57
58
59
60

N(1)-C(3)-H(3)	126.6
C(9)-C(4)-C(5)	121.4(3)
C(9)-C(4)-N(1)	118.6(3)
C(5)-C(4)-N(1)	120.0(3)
C(6)-C(5)-C(4)	119.1(3)
C(6)-C(5)-H(5)	120.4
C(4)-C(5)-H(5)	120.4
C(7)-C(6)-C(5)	120.5(4)
C(7)-C(6)-H(6)	119.7
C(5)-C(6)-H(6)	119.7
C(6)-C(7)-C(8)	120.0(3)
C(6)-C(7)-H(7)	120.0
C(8)-C(7)-H(7)	120.0
C(7)-C(8)-C(9)	120.7(3)
C(7)-C(8)-H(8)	119.6
C(9)-C(8)-H(8)	119.6
C(4)-C(9)-C(8)	118.2(3)
C(4)-C(9)-H(9)	120.9
C(8)-C(9)-H(9)	120.9
N(2)-C(10)-H(10A)	109.5
N(2)-C(10)-H(10B)	109.5
H(10A)-C(10)-H(10B)	109.5
N(2)-C(10)-H(10C)	109.5
H(10A)-C(10)-H(10C)	109.5
H(10B)-C(10)-H(10C)	109.5
O(1)-C(11)-Ir(1)	178.0(4)

Table S3 Crystal data and structure refinement for Ir complex **5d**.

Identification code	5d	
Empirical formula	C ₂₄ H ₂₄ B F ₄ Ir N ₄ O ₄	
Formula weight	711.48	
Temperature	173(2) K	
Wavelength	1.34138 Å	
Crystal system	Orthorhombic	
Space group	Pbca	
Unit cell dimensions	a = 16.1278(10) Å	□ α = 90°.
	b = 12.7211(8) Å	□ β = 90°.
	c = 25.0778(16) Å	□ γ = 90°.
Volume	5145.0(6) Å ³	
Z	8	
Density (calculated)	1.837 mg/m ³	
Absorption coefficient	7.051 mm ⁻¹	
F(000)	2768	
Crystal size	0.260 x 0.200 x 0.150 mm ³	
Theta range for data collection	3.066 to 58.995°.	
Index ranges	-20 ≤ h ≤ 20, -16 ≤ k ≤ 16, -32 ≤ l ≤ 32	
Reflections collected	80819	
Independent reflections	5612 [R(int) = 0.0469]	
Completeness to theta = 53.594°	99.7 %	
Absorption correction	Semi-empirical from equivalents	
Max. and min. transmission	0.752 and 0.536	
Refinement method	Full-matrix least-squares on F ²	
Data / restraints / parameters	5612 / 0 / 347	
Goodness-of-fit on F ²	1.236	
Final R indices [I > 2σ(I)]	R1 = 0.0327, wR2 = 0.0727	
R indices (all data)	R1 = 0.0330, wR2 = 0.0728	
Extinction coefficient	n/a	
Largest diff. peak and hole	1.185 and -1.485 e.Å ⁻³	

Table S4 Bond lengths [Å] and angles [°] for Ir complex **5d**.

Ir(1)-C(24)	1.884(5)
Ir(1)-C(23)	1.888(5)
Ir(1)-C(12)	2.081(4)
Ir(1)-C(1)	2.086(4)
B(1)-F(4)	1.369(6)
B(1)-F(2)	1.375(6)
B(1)-F(3)	1.379(7)
B(1)-F(1)	1.393(7)
N(1)-C(1)	1.353(5)
N(1)-C(3)	1.390(5)
N(1)-C(4)	1.435(5)
N(2)-C(1)	1.359(5)
N(2)-C(2)	1.374(5)
N(2)-C(11)	1.461(5)
N(3)-C(12)	1.353(5)
N(3)-C(14)	1.388(5)
N(3)-C(15)	1.446(5)
N(4)-C(12)	1.354(5)
N(4)-C(13)	1.378(5)
N(4)-C(22)	1.457(5)
O(1)-C(7)	1.364(5)
O(1)-C(10)	1.431(6)
O(2)-C(18)	1.368(5)
O(2)-C(21)	1.445(6)
O(3)-C(23)	1.132(6)
O(4)-C(24)	1.136(6)
C(2)-C(3)	1.350(6)
C(2)-H(2)	0.9500
C(3)-H(3)	0.9500
C(4)-C(5)	1.384(5)
C(4)-C(9)	1.398(5)
C(5)-C(6)	1.384(5)
C(5)-H(5)	0.9500
C(6)-C(7)	1.397(6)
C(6)-H(6)	0.9500
C(7)-C(8)	1.390(6)

C(8)-C(9)	1.370(6)
C(8)-H(8)	0.9500
C(9)-H(9)	0.9500
C(10)-H(10A)	0.9800
C(10)-H(10B)	0.9800
C(10)-H(10C)	0.9800
C(11)-H(11A)	0.9800
C(11)-H(11B)	0.9800
C(11)-H(11C)	0.9800
C(13)-C(14)	1.349(6)
C(13)-H(13)	0.9500
C(14)-H(14)	0.9500
C(15)-C(20)	1.377(5)
C(15)-C(16)	1.390(6)
C(16)-C(17)	1.386(6)
C(16)-H(16)	0.9500
C(17)-C(18)	1.388(6)
C(17)-H(17)	0.9500
C(18)-C(19)	1.385(6)
C(19)-C(20)	1.400(5)
C(19)-H(19)	0.9500
C(20)-H(20)	0.9500
C(21)-H(21A)	0.9800
C(21)-H(21B)	0.9800
C(21)-H(21C)	0.9800
C(22)-H(22A)	0.9800
C(22)-H(22B)	0.9800
C(22)-H(22C)	0.9800
C(24)-Ir(1)-C(23)	89.49(19)
C(24)-Ir(1)-C(12)	179.29(19)
C(23)-Ir(1)-C(12)	90.75(17)
C(24)-Ir(1)-C(1)	91.87(17)
C(23)-Ir(1)-C(1)	178.02(17)
C(12)-Ir(1)-C(1)	87.90(15)
F(4)-B(1)-F(2)	111.0(4)
F(4)-B(1)-F(3)	109.3(5)
F(2)-B(1)-F(3)	109.1(5)

1		
2		
3		
4	F(4)-B(1)-F(1)	110.3(5)
5	F(2)-B(1)-F(1)	109.1(4)
6	F(3)-B(1)-F(1)	107.9(4)
7		
8	C(1)-N(1)-C(3)	111.1(3)
9	C(1)-N(1)-C(4)	127.1(3)
10		
11	C(3)-N(1)-C(4)	121.7(3)
12	C(1)-N(2)-C(2)	110.8(3)
13		
14	C(1)-N(2)-C(11)	125.4(4)
15	C(2)-N(2)-C(11)	123.8(3)
16		
17	C(12)-N(3)-C(14)	111.3(3)
18	C(12)-N(3)-C(15)	126.1(3)
19		
20	C(14)-N(3)-C(15)	122.6(3)
21	C(12)-N(4)-C(13)	110.8(3)
22		
23	C(12)-N(4)-C(22)	125.9(4)
24	C(13)-N(4)-C(22)	123.3(3)
25		
26	C(7)-O(1)-C(10)	116.8(4)
27	C(18)-O(2)-C(21)	117.5(3)
28		
29	N(1)-C(1)-N(2)	104.6(3)
30	N(1)-C(1)-Ir(1)	128.3(3)
31		
32	N(2)-C(1)-Ir(1)	127.1(3)
33	C(3)-C(2)-N(2)	107.4(4)
34	C(3)-C(2)-H(2)	126.3
35		
36	N(2)-C(2)-H(2)	126.3
37		
38	C(2)-C(3)-N(1)	106.1(4)
39	C(2)-C(3)-H(3)	127.0
40		
41	N(1)-C(3)-H(3)	127.0
42	C(5)-C(4)-C(9)	120.2(4)
43	C(5)-C(4)-N(1)	121.2(3)
44		
45	C(9)-C(4)-N(1)	118.6(3)
46		
47	C(6)-C(5)-C(4)	120.3(4)
48	C(6)-C(5)-H(5)	119.8
49		
50	C(4)-C(5)-H(5)	119.8
51	C(5)-C(6)-C(7)	119.4(4)
52	C(5)-C(6)-H(6)	120.3
53		
54	C(7)-C(6)-H(6)	120.3
55		
56	O(1)-C(7)-C(8)	115.6(4)
57	O(1)-C(7)-C(6)	124.6(4)
58		
59	C(8)-C(7)-C(6)	119.8(4)
60		

C(9)-C(8)-C(7)	120.8(4)
C(9)-C(8)-H(8)	119.6
C(7)-C(8)-H(8)	119.6
C(8)-C(9)-C(4)	119.5(4)
C(8)-C(9)-H(9)	120.3
C(4)-C(9)-H(9)	120.3
O(1)-C(10)-H(10A)	109.5
O(1)-C(10)-H(10B)	109.5
H(10A)-C(10)-H(10B)	109.5
O(1)-C(10)-H(10C)	109.5
H(10A)-C(10)-H(10C)	109.5
H(10B)-C(10)-H(10C)	109.5
N(2)-C(11)-H(11A)	109.5
N(2)-C(11)-H(11B)	109.5
H(11A)-C(11)-H(11B)	109.5
N(2)-C(11)-H(11C)	109.5
H(11A)-C(11)-H(11C)	109.5
H(11B)-C(11)-H(11C)	109.5
N(3)-C(12)-N(4)	104.5(3)
N(3)-C(12)-Ir(1)	127.9(3)
N(4)-C(12)-Ir(1)	127.5(3)
C(14)-C(13)-N(4)	107.4(4)
C(14)-C(13)-H(13)	126.3
N(4)-C(13)-H(13)	126.3
C(13)-C(14)-N(3)	105.9(4)
C(13)-C(14)-H(14)	127.0
N(3)-C(14)-H(14)	127.0
C(20)-C(15)-C(16)	121.0(4)
C(20)-C(15)-N(3)	120.4(3)
C(16)-C(15)-N(3)	118.6(3)
C(17)-C(16)-C(15)	119.5(4)
C(17)-C(16)-H(16)	120.2
C(15)-C(16)-H(16)	120.2
C(16)-C(17)-C(18)	119.8(4)
C(16)-C(17)-H(17)	120.1
C(18)-C(17)-H(17)	120.1
O(2)-C(18)-C(19)	124.2(4)
O(2)-C(18)-C(17)	115.1(4)

1
2
3
4
5
6
7
8
9
10
11
12
13
14
15
16
17
18
19
20
21
22
23
24
25
26
27
28
29
30
31
32
33
34
35
36
37
38
39
40
41
42
43
44
45
46
47
48
49
50
51
52
53
54
55
56
57
58
59
60

C(19)-C(18)-C(17)	120.7(4)
C(18)-C(19)-C(20)	119.4(4)
C(18)-C(19)-H(19)	120.3
C(20)-C(19)-H(19)	120.3
C(15)-C(20)-C(19)	119.5(4)
C(15)-C(20)-H(20)	120.2
C(19)-C(20)-H(20)	120.2
O(2)-C(21)-H(21A)	109.5
O(2)-C(21)-H(21B)	109.5
H(21A)-C(21)-H(21B)	109.5
O(2)-C(21)-H(21C)	109.5
H(21A)-C(21)-H(21C)	109.5
H(21B)-C(21)-H(21C)	109.5
N(4)-C(22)-H(22A)	109.5
N(4)-C(22)-H(22B)	109.5
H(22A)-C(22)-H(22B)	109.5
N(4)-C(22)-H(22C)	109.5
H(22A)-C(22)-H(22C)	109.5
H(22B)-C(22)-H(22C)	109.5
O(3)-C(23)-Ir(1)	178.9(5)
O(4)-C(24)-Ir(1)	177.3(4)

6. β -Methylation of primary and secondary alcohols with methanol

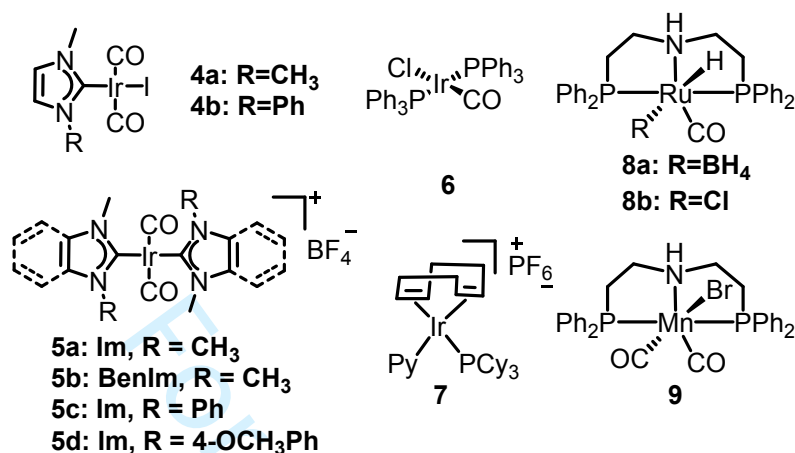
6.1 Optimization of reaction conditions

Table S5. Optimization of reaction conditions^a



Entry	Cat. (eq.)	Base (eq.)	Yield%
1	4a (0.05)	^t BuONa (2)	74
2	4b (0.05)	^t BuONa (2)	84
3	5a (0.05)	^t BuONa (2)	56
4	5b (0.05)	^t BuONa (2)	57
5	5c (0.05)	^t BuONa (2)	98
6	5d (0.05)	^t BuONa (2)	99
7	5c (0.01)	^t BuONa (2)	59
8	5d (0.01)	^t BuONa (2)	67
9	6 (0.05)	^t BuONa (2)	33
10	7 (0.05)	^t BuONa (2)	10
11	8a (0.05)	^t BuONa (2)	25
12	8b (0.05)	^t BuONa (2)	40
13	9 (0.05)	^t BuONa (2)	64
14	5d (0.05)	Cs ₂ CO ₃ (2)	92
15	5d (0.05)	^t BuOK (2)	90
16	5d (0.05)	^t BuONa (2)	99
17	5d (0.05)	^t BuONa (1.2)	73
18	5d (0.05)	-	0
19	-	^t BuONa (2)	0

^a Reactions were carried out with 2-phenyl ethanol (**1**, 1 mmol), catalyst (0.01- 0.05 mol%), base (1-2 equiv.) and MeOH (1 mL) at 140 °C under N₂ atmosphere for 24 hours and yields were determined by ¹H NMR analysis using mesitoxylene as an internal standard.



6.2 Procedure for TON and TOF of β -methylation with methanol

To a sealed tube (120 mL) equipped with a stir bar, Ir-NHC catalyst **5d** (0.001 mol%), methanol (5 mL), ^tBuONa (10 mmol) and 2-phenyl ethanol (610 mg, 5 mmol) were added under nitrogen atmosphere. The solution was heated at 200 °C for 96 h. After cooling to room temperature, mesitoxylene was added as an internal standard, and sent for NMR measurement. The methylated product was obtained in 30.8% yield, giving a TON of 30800.

To a sealed tube (35 mL) equipped with a stir bar, Ir-NHC catalyst **5d** (0.005 mol%), methanol (1 mL), ^tBuONa (2 mmol) and 2-phenyl ethanol (122 mg, 1 mmol) were added under nitrogen atmosphere. The solution was heated at 200 °C for 1 h. After cooling to room temperature, mesitoxylene was added as an internal standard, and sent for NMR measurement. The methylated product was obtained in 23.3% yield, giving a TOF of 4640 h⁻¹.

6.3 General procedure for β -methylation of primary alcohols with methanol

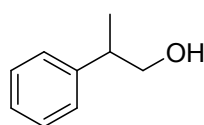
To a sealed tube (35 mL) equipped with a stir bar, Ir-NHC catalyst **5d** (0.05 mol%), methanol (1 mL), ^tBuONa (2 mmol) and primary alcohol (1 mmol) were added under

nitrogen atmosphere. The solution was heated at 140 °C for 24 h. After cooling to room temperature, mesitoxylene was added as an internal standard, and sent for NMR measurement.

Pure products were obtained by column chromatography over silica gel using ethyl acetate/petroleum ether mixture as eluent.

Yield of substrate **30** was determined by GC-MS without isolated because of its low boiling point.

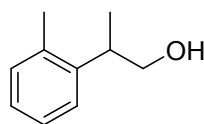
2-phenylpropan-1-ol (3) ^{S16}



¹H NMR (400 MHz, CDCl₃, 298 K) δ = 7.30-7.38 (m, 2H, ArCH), 7.21-7.28 (m, 3H, ArCH), 3.69 (d, 2H, J = 6.8 Hz, CH₂), 2.90-3.01 (m, 1H, CH), 1.29 (d, 3H, J = 7.0 Hz, CH₃) ppm.

¹³C NMR (101 MHz, CDCl₃, 298 K) δ = 143.8, 128.7, 127.6, 126.8, 68.8, 42.5, 17.7 ppm.

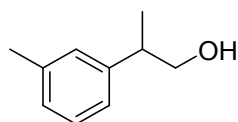
2-(o-tolyl)propan-1-ol (10) ^{S16}



¹H NMR (400 MHz, CDCl₃, 298 K) δ = 7.18-7.23 (m, 2H, ArCH), 7.10-7.17 (m, 2H, ArCH), 3.66-3.80 (m, 2H, CH₂), 3.22-3.32 (m, 1H, CH), 2.37 (s, 3H, CH₃), 1.34-1.44 (m, 1H, OH), 1.25 (d, 3H, J = 7.0 Hz, CH₃) ppm.

¹³C NMR (101 MHz, CDCl₃, 298 K) δ = 142.0, 136.6, 130.8, 126.6, 126.5, 125.6, 68.2, 37.4, 19.8, 17.7 ppm.

2-(m-tolyl)propan-1-ol (11) ^{S16}

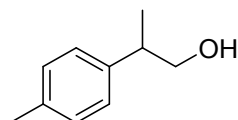


¹H NMR (400 MHz, CDCl₃, 298 K) δ = 7.19-7.25 (m, 1H, ArCH), 7.01-7.09 (m, 3H, ArCH), 3.70 (d, 2H, J = 6.7 Hz, CH₂), 2.85- 2.98 (m, 1H, CH), 2.36 (s, 3H, CH₃), 1.33-1.47 (m, 1H, OH), 1.27 (d, 3H, J = 7.0 Hz, CH₃) ppm.

¹³C NMR (101 MHz, CDCl₃, 298 K) δ = 143.6, 138.2, 128.6, 128.3, 127.5, 124.5,

68.7, 42.4, 21.5, 17.6 ppm.

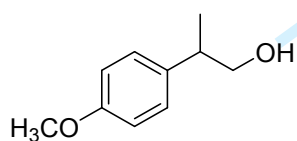
2-(p-tolyl)propan-1-ol (12)^{S17}



¹H NMR (400 MHz, CDCl₃, 298 K) δ = 7.15 (s, 4H, ArCH), 3.68 (d, 2H, J = 6.1 Hz, CH₂), 2.87- 2.97 (m, 1H, CH), 2.34 (s, 3H, CH₃), 1.36-1.46 (m, 1H, OH), 1.27 (d, 3H, J = 7.0 Hz, CH₃) ppm.

¹³C NMR (101 MHz, CDCl₃, 298 K) δ = 140.8, 136.4, 129.5, 127.6, 69.0, 42.3, 21.2, 17.9 ppm.

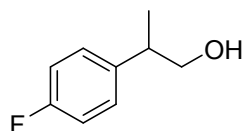
2-(4-methoxyphenyl)propan-1-ol (13)^{S16}



¹H NMR (400 MHz, CDCl₃, 298 K) δ = 7.16 (d, 2H, J = 8.7 Hz, ArCH), 6.88 (d, 2H, J = 8.7 Hz, ArCH), 3.80 (s, 3H, OCH₃), 3.61-3.72 (m, 2H, CH₂), 2.85-2.96 (m, 1H, CH), 1.28-1.35 (m, 1H, OH), 1.25 (d, 3H, J = 7.0 Hz, CH₃) ppm.

¹³C NMR (101 MHz, CDCl₃, 298 K) δ = 158.3, 135.6, 128.4, 114.0, 126.5, 68.8, 55.2, 41.5, 17.7 ppm.

2-(4-fluorophenyl)propan-1-ol (14)^{S16}

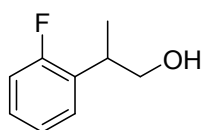


¹H NMR (400 MHz, CDCl₃, 298 K) δ = 7.15-7.24 (m, 2H, ArCH), 6.96-7.05 (m, 2H, ArCH), 3.64-3.74 (m, 2H, CH₂), 2.95 (dd, 1H, J = 13.8 and 6.9 Hz, CH), 1.26 (d, 3H, J = 7.0 Hz, CH₃) ppm.

¹³C NMR (101 MHz, CDCl₃, 298 K) δ = 162.8 (J = 245.2 Hz), 139.3 (J = 3.2 Hz), 128.9 (J = 7.9 Hz), 115.4 (J = 21.1 Hz), 68.6, 41.7, 17.7 ppm.

¹⁹F NMR (376 MHz, CDCl₃, 298 K) δ = 116.58 ppm.

2-(2-fluorophenyl)propan-1-ol (15)^{S18}



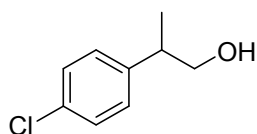
¹H NMR (400 MHz, CDCl₃, 298 K) δ = 7.17-7.29 (m, 2H, ArCH), 7.08-7.15 (m, 1H, ArCH), 7.00-7.07 (m, 1H, ArCH), 3.68-3.84 (m, 2H, CH₂), 3.25-3.37 (m, 1H, CH), 1.41 (t, 1H, J = 6.0 Hz, OH), 1.30

(d, 3H, $J = 7.0$ Hz, CH₃) ppm.

¹³C NMR (101 MHz, CDCl₃, 298 K) $\delta = 162.4$ ($J = 246.0$ Hz), 130.61 ($J = 14.5$ Hz), 128.6 ($J = 5.2$ Hz), 128.1 ($J = 8.4$ Hz), 124.3 ($J = 3.5$ Hz), 115.7 ($J = 22.9$ Hz), 67.4 ($J = 1.2$ Hz), 35.7, 16.7 ppm.

¹⁹F NMR (376 MHz, CDCl₃, 298 K) $\delta = 118.40$ ppm.

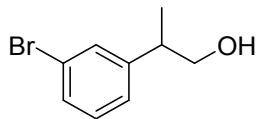
2-(4-chlorophenyl)propan-1-ol (16) ^{S16}



¹H NMR (400 MHz, CDCl₃, 298 K) $\delta = 7.27$ -7.33 (m, 2H, ArCH), 7.15-7.21 (m, 2H, ArCH), 3.64-3.74 (m, 2H, CH₂), 2.88-2.98 (m, 1H, CH), 1.28-1.35 (m, 1H, OH), 1.26 (d, 3H, $J = 7.0$ Hz, CH₃) ppm.

¹³C NMR (101 MHz, CDCl₃, 298 K) $\delta = 142.2$, 132.3, 128.8, 128.7, 68.5, 41.8, 17.5 ppm.

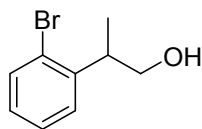
2-(3-bromophenyl)propan-1-ol (17) ^{S19}



¹H NMR (400 MHz, CDCl₃, 298 K) $\delta = 7.35$ -7.42 (m, 2H, ArCH), 7.15-7.23 (m, 2H, ArCH), 3.70 (d, 2H, $J = 6.3$ Hz, CH₂), 2.93 (dd, 1H, $J = 13.8$ and 6.9 Hz, CH), 1.30-1.40 (m, 1H, OH), 1.27 (d, 3H, $J = 7.0$ Hz, CH₃) ppm.

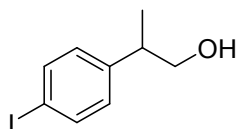
¹³C NMR (101 MHz, CDCl₃, 298 K) $\delta = 146.5$, 130.8, 130.4, 130.0, 126.4, 123.0, 68.6, 42.5, 17.7 ppm.

2-(2-bromophenyl)propan-1-ol (18) ^{S20}



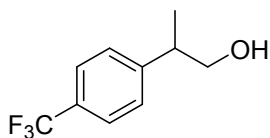
¹H NMR (400 MHz, CDCl₃, 298 K) $\delta = 7.35$ -7.42 (m, 2H, ArCH), 7.15-7.23 (m, 2H, ArCH), 3.70 (d, 2H, $J = 6.3$ Hz, CH₂), 2.93 (dd, 1H, $J = 13.8$ and 6.9 Hz, CH), 1.35-1.45 (m, 1H, OH), 1.27 (d, 3H, $J = 7.0$ Hz, CH₃) ppm.

¹³C NMR (101 MHz, CDCl₃, 298 K) $\delta = 142.6$, 133.1, 128.0, 127.7, 127.6, 125.2, 67.3, 40.7, 17.0 ppm.

2-(4-iodophenyl)propan-1-ol (19)^{S21}

¹H NMR (400 MHz, CDCl₃, 298 K) δ = 7.62-7.68 (m, 2H, ArCH), 6.96-7.04 (m, 2H, ArCH), 3.62-3.74 (m, 2H, CH₂), 2.90 (dd, 1H, J = 13.8, 6.9 Hz, CH), 1.29-1.36 (m, 1H, OH), 1.25 (d, 3H, J = 7.0 Hz, CH₃) ppm.

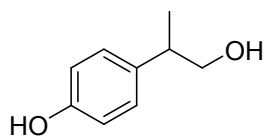
¹³C NMR (101 MHz, CDCl₃, 298 K) δ = 143.5, 143.4, 137.6, 129.5, 113.0, 91.8, 68.4, 42.0, 17.4 ppm.

2-(4-trifluoromethylphenyl)propan-1-ol (20)^{S16}

¹H NMR (400 MHz, CDCl₃, 298 K) δ = 7.59 (d, 2H, J = 8.1 Hz, ArCH), 7.36 (d, 2H, J = 8.1 Hz, ArCH), 3.74 (d, 2H, J = 6.8 Hz, CH₂), 3.03 (dd, 1H, J = 13.8 and 6.9 Hz, CH), 1.35-1.46 (m, 1H, OH), 1.30 (d, 3H, J = 7.0 Hz, CH₃) ppm.

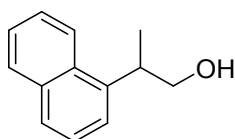
¹³C NMR (101 MHz, CDCl₃, 298 K) δ = 148.0, 129.1 (J = 32.5 Hz), 127.8, 125.5 (J = 3.5 Hz), 122.9, 68.3, 42.3, 17.4 ppm.

¹⁹F NMR (376 MHz, CDCl₃, 298 K) δ = 62.43 ppm.

2-(4-hydroxyphenyl)propan-1-ol (21)^{S22}

¹H NMR (400 MHz, D₂O, 298 K) δ = 7.22 (d, 2H, J = 8.3 Hz, ArCH), 6.90 (d, 2H, J = 8.3 Hz, ArCH), 3.67 (d, 2H, J = 6.9 Hz, CH₂), 2.84-2.96 (m, 1H, CH), 1.21 (d, 3H, J = 7.0 Hz, CH₃) ppm.

¹³C NMR (101 MHz, D₂O, 298 K) δ = 153.8, 136.3, 128.6, 115.3, 67.5, 40.6, 17.2 ppm.

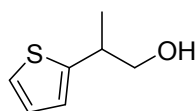
2-(naphthalen-1-yl)ethan-1-ol (22)^{S16}

¹H NMR (400 MHz, CDCl₃, 298 K) δ = 8.16 (d, 1H, J = 8.4 Hz, ArCH), 7.84-7.92 (m, 1H, ArCH), 7.76 (d, 1H, J = 8.0 Hz,

ArCH), 8.37-7.59 (m, 4H, ArCH), 3.93-3.99 (m, 2H, CH₂), 3.88 (dd, 1H, *J* = 9.4 and 4.2 Hz, CH), 1.29-1.36 (m, 1H, OH), 1.45 (d, 3H, *J* = 6.7 Hz, CH₃) ppm.

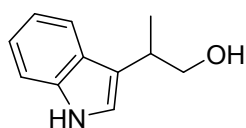
¹³C NMR (101 MHz, CDCl₃, 298 K) δ = 139.7, 134.2, 132.1, 129.1, 127.2, 126.2, 125.7, 123.2, 68.3, 36.5, 18.0 ppm.

For Review Only

2-(thiophen-2-yl)propan-1-ol (23)^{S17}

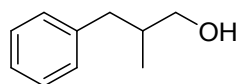
¹H NMR (400 MHz, CDCl₃, 298 K) δ = 7.19 (dd, 1H, J = 5.1 and 1.1 Hz, ArCH), 6.97 (dd, 1H, J = 5.1 and 3.5 Hz, ArCH), 6.88-6.92 (m, 1H, ArCH), 3.62-3.78 (m, 2H, CH₂), 3.17-3.33 (m, 1H, CH), 1.47-1.56 (m, 1H, OH), 1.36 (d, 3H, J = 7.0 Hz, CH₃) ppm.

¹³C NMR (101 MHz, CDCl₃, 298 K) δ = 147.5, 127.0, 124.0, 123.7, 69.1, 38.3, 18.7 ppm.

2-(1H-indol-3-yl)propan-1-ol (24)^{S16}

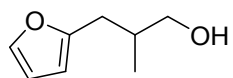
¹H NMR (400 MHz, CDCl₃, 298 K) δ = 8.05 (s, 1H, NH), 7.67 (d, 1H, J = 8.0 Hz, ArCH), 7.38 (d, 1H, J = 8.0 Hz, ArCH), 7.18-7.25 (m, 1H, ArCH), 7.10-7.17 (m, 1H, ArCH), 7.07 (d, 1H, J = 2.4 Hz, ArCH), 3.77-3.89 (m, 2H, CH₂), 3.27-3.37 (m, 1H, CH), 1.41 (d, 3H, J = 7.0 Hz, CH₃), 1.35-1.40 (m, 1H, OH) ppm.

¹³C NMR (101 MHz, CDCl₃, 298 K) δ = 136.6, 126.7, 122.2, 121.2, 119.4, 119.2, 118.0, 111.2, 67.9, 33.9, 17.2 ppm.

2-methyl-3-phenylpropan-1-ol (25)^{S17}

¹H NMR (400 MHz, CDCl₃, 298 K) δ = 7.24-7.33 (m, 1H, ArCH), 7.13-7.23 (m, 3H, ArCH), 3.42-3.58 (m, 2H, CH₂), 2.76 (dd, 1H, J = 13.4 and 6.3 Hz, CH₂), 2.42 (dd, 1H, J = 13.4 and 8.1 Hz, CH₂), 1.87-2.01 (m, 1H, CH), 1.39 (s, 1H, OH), 0.92 (d, 3H, J = 6.7 Hz, CH₃) ppm.

¹³C NMR (101 MHz, CDCl₃, 298 K) δ = 140.6, 129.1, 128.2, 125.9, 67.6, 39.7, 37.7, 16.4 ppm.

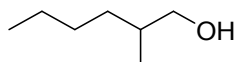
3-(furan-2-yl)-2-methylpropan-1-ol (26)^{S23}

¹H NMR (400 MHz, CDCl₃, 298 K) δ = 7.31 (d, 1H, J = 1.2 Hz, ArCH), 6.28 (dd, 1H, J = 2.8 and 2.0 Hz, ArCH), 6.02 (d, 1H, J = 2.6 Hz, ArCH), 3.50 (d, 2H, J = 5.5 Hz, CH₂), 2.73 (dd, 1H, J = 14.9 and 6.2 Hz,

CH₂), 2.55 (dd, 1H, J = 14.9 and 7.3 Hz, CH₂), 1.97- 2.09 (m, 1H, CH), 1.46-1.73 (br, 1H, OH), 0.95 (d, 3H, J = 6.8 Hz, CH₃) ppm.

¹³C NMR (101 MHz, CDCl₃, 298 K) δ = 154.7, 141.2, 110.3, 106.3, 67.6, 35.6, 31.7, 16.6 ppm.

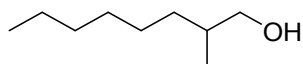
2-methylhexan-1-ol (27)^{S17}



¹H NMR (400 MHz CDCl₃, 298 K) δ = 3.50 (dd, 1H, J = 10.4 and 5.8 Hz, CH₂), 3.41 (dd, 1H, J = 10.5 and 6.6 Hz, CH₂), 1.54-1.67 (m, 1H, CH), 1.18-1.45 (m, 6H, CH₂), 1.04-1.16 (m, 1H, OH), 0.77-0.94 (m, 6H, CH₃) ppm.

¹³C NMR (101 MHz, CDCl₃, 298 K) δ = 68.6, 35.9, 33.0, 29.3, 23.1, 16.7, 14.2 ppm.

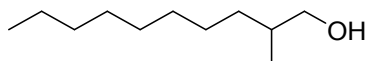
2-methyloctan-1-ol (28)^{S17}



¹H NMR (400 MHz, CDCl₃, 298 K) δ = 3.47-3.55 (m, 1H, CH₂), 3.37-3.46 (m, 1H, CH₂), 1.56- 1.67 (m, 1H, CH), 1.19-1.47 (m, 10H, CH₂), 1.05-1.18 (m, 1H, OH), 0.84-0.95 (m, 6H, CH₃) ppm.

¹³C NMR (101 MHz, CDCl₃, 298 K) δ = 68.4, 35.8, 33.2, 31.8, 29.6, 26.9, 22.6, 16.6, 14.1 ppm.

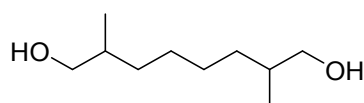
2-methyldecan-1-ol (29)^{S17}



¹H NMR (400 MHz, CDCl₃, 298 K) δ = 3.46-3.56 (m, 1H, CH₂), 3.37-3.45 (m, 1H, CH₂), 1.53- 1.66 (m, 1H, CH), 1.17-1.46 (m, 14H, CH₂), 1.02-1.16 (m, 1H, OH), 0.83-0.95 (m, 6H, CH₃) ppm.

¹³C NMR (101 MHz, CDCl₃, 298 K) δ = 68.4, 35.8, 33.2, 31.9, 30.0, 29.3, 27.0, 22.7, 16.6, 14.1 ppm.

2,7-dimethyloctane-1,8-diol (31)^{S17}

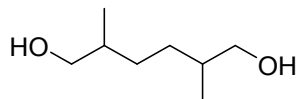


¹H NMR (400 MHz, CDCl₃, 298 K) δ = 3.47-3.55 (m, 2H, CH₂), 3.37-3.46 (m, 2H, CH₂), 1.56- 1.67 (m, 2H,

CH), 1.19-1.47 (m, 8H, CH₂), 1.05-1.18 (m, 2H, OH), 0.84-0.95 (m, 6H, CH₃) ppm.

¹³C NMR (101 MHz, CDCl₃, 298 K) δ = 68.4, 68.3, 35.7, 33.0, 27.2, 27.2, 16.6, 16.5 ppm.

2,5-dimethylhexane-1,6-diol (**32**)^{S17}

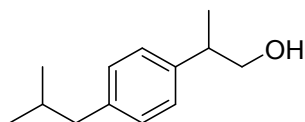


¹H NMR (400 MHz, CDCl₃, 298 K) δ = 3.38-3.58 (m, 4H, CH₂), 1.53-1.67 (m, 4H, CH₂), 1.35-1.54 (m, 2H, CH),

1.06-1.22 (m, 2H, OH), 0.87-0.96 (m, 6H, CH₃) ppm.

¹³C NMR (101 MHz, CDCl₃, 298 K) δ = 68.1, 68.0, 35.3, 35.9, 30.2, 30.2, 16.7, 16.5 ppm.

2-(*p*-isobutyl)propan-1-ol (**33**)^{S17}



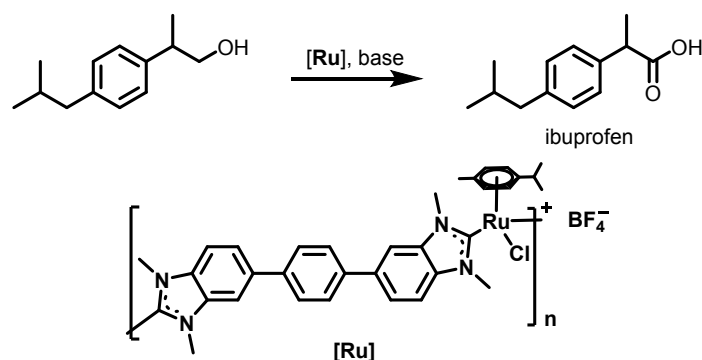
¹H NMR (400 MHz, CDCl₃, 298 K) δ = 7.07-7.17 (m, 4H, ArCH), 3.64-3.73 (m, 2H, CH₂), 2.86-3.00 (m, 1H, CH),

2.93 (d, 2H, *J* = 7.0 Hz, CH₂), 1.79- 1.92 (m, 1H, CH), 1.30-1.39 (m, 1H, OH), 1.27 (d, 3H, *J* = 7.0 Hz, CH₃), 0.91 (d, 6H, *J* = 6.6 Hz, CH₃) ppm.

¹³C NMR (101 MHz, CDCl₃, 298 K) δ = 140.7, 140.1, 129.4, 127.2, 68.8, 45.1, 42.0, 30.20, 22.4, 17.6 ppm.

6.4 Preparation of ibuprofen from precursor **33** using self-supported Ru catalyst

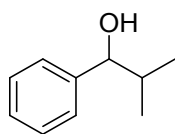
To a sealed tube (15 mL) equipped with a stir bar, self-supported **Ru** catalyst^[24] (0.5 mol%), KOH (4 mmol), ibuprofen precursor **33** (1 mmol) and toluene (1 mL) were added under nitrogen atmosphere at 140 °C for 24 h. The product was obtained in a yield of 34%.

Scheme S1 Preparation of ibuprofen from precursor **33****6.5 General procedure for β -methylation of secondary alcohols with methanol**

To a sealed tube (35 mL) equipped with a stir bar, Ir-NHC catalyst **5d** (0.1 mol%), methanol (1 mL), t BuONa (3 mmol) and secondary alcohol (1 mmol) were added under nitrogen atmosphere. The solution was heated at 140 °C for 24 h. After cooling to room temperature, mesitoxylene was added as an internal standard, and sent for NMR measurement.

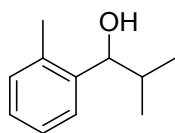
Pure products were obtained by column chromatography over silica gel using ethyl acetate/petroleum ether mixture as eluent.

Yield of substrate **43** and **47** was determined by GC-MS without isolated because of its low boiling point.

2-methyl-1-phenylpropan-1-ol (34) ^{S17}

^1H NMR (400 MHz, CDCl_3 , 298 K) δ = 7.24-7.38 (m, 5H, ArCH), 4.37 (dd, 1H, J = 6.9 and 3.2 Hz, CH), 1.91- 2.02 (m, 1H, CH), 1.82 (d, 1H, J = 3.2 Hz, OH), 1.01 (d, 3H, J = 6.8 Hz, CH_3), 0.80 (d, 3H, J = 6.8 Hz, CH_3) ppm.

^{13}C NMR (101 MHz, CDCl_3 , 298 K) δ = 143.6, 128.2, 127.4, 126.5, 80.0, 35.2, 19.0, 18.2 ppm.

2-methyl-1-(*o*-tolyl)propan-1-ol (35) ^{S17}

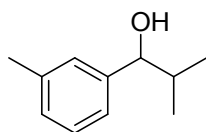
^1H NMR (400 MHz, CDCl_3 , 298 K) δ = 7.39-7.47 (m, 1H, ArCH),

S36

7.09-7.25 (m, 3H, ArCH), 4.32 (d, 1H, $J = 6.9$ Hz, CH), 2.35 (s, 3H, CH₃), 1.89- 2.01 (m, 1H, CH), 1.71-1.80 (m, 1H, OH), 1.01 (d, 3H, $J = 6.8$ Hz, CH₃), 0.79 (d, 3H, $J = 6.8$ Hz, CH₃) ppm.

¹³C NMR (101 MHz, CDCl₃, 298 K) $\delta = 142.1, 135.0, 130.3, 127.0, 126.0, 126.0, 75.7, 34.5, 19.4, 17.8$ ppm.

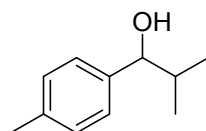
2-methyl-1-(*m*-tolyl)propan-1-ol (36) ^{S25}



¹H NMR (400 MHz, CDCl₃, 298 K) $\delta = 7.23$ (t, 1H, $J = 7.5$ Hz, ArCH), 7.10 (dd, 3H, $J = 14.3$ and 7.5 Hz, ArCH), 4.32 (dd, 1H, $J = 6.7$ and 2.5 Hz, CH), 2.36 (s, 3H, CH₃), 1.87-2.03 (m, 1H, CH), 1.83-1.80 (m, 1H, OH), 1.01 (d, 3H, $J = 6.8$ Hz, CH₃), 0.80 (d, 3H, $J = 6.8$ Hz, CH₃) ppm.

¹³C NMR (101 MHz, CDCl₃, 298 K) $\delta = 143.8, 137.9, 128.3, 128.2, 127.4, 123.8, 80.2, 35.3, 21.6, 19.2, 18.4$ ppm.

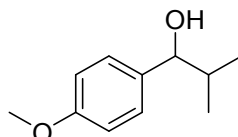
2-methyl-1-(*p*-tolyl)propan-1-ol (37) ^{S17}



¹H NMR (400 MHz, CDCl₃, 298 K) $\delta = 7.20$ (d, 2H, $J = 8.0$ Hz, ArCH), 7.15 (d, 2H, $J = 8.0$ Hz, ArCH), 4.32 (d, 1H, $J = 6.9$ Hz, CH), 2.35 (s, 3H, CH₃), 1.89- 2.01 (m, 1H, CH), 1.71-1.80 (m, 1H, $J = 3.2$ Hz, OH), 1.01 (d, 3H, $J = 6.8$ Hz, CH₃), 0.79 (d, 3H, $J = 6.8$ Hz, CH₃) ppm.

¹³C NMR (101 MHz, CDCl₃, 298 K) $\delta = 140.7, 137.0, 128.9, 126.5, 80.0, 35.2, 21.1, 19.0, 18.3$ ppm.

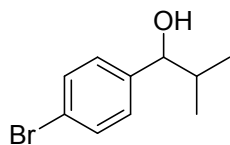
1-(4-methoxyphenyl)-2-methylpropan-1-ol (38) ^{S17}



¹H NMR (400 MHz, CDCl₃, 298 K) $\delta = 7.20$ -7.25 (m, 2H, ArCH), 6.90-6.85 (m, 2H, ArCH), 4.29 (dd, 1H, $J = 7.2$ and 2.8 Hz, CH), 3.80 (s, 3H, OCH₃), 1.87- 2.00 (m, 1H, CH), 1.80 (d, 1H, $J = 3.2$ Hz, OH), 1.01 (d, 3H, $J = 6.8$ Hz, CH₃), 0.77 (d, 3H, $J = 6.8$ Hz, CH₃) ppm.

^{13}C NMR (101 MHz, CDCl_3 , 298 K) δ = 158.9, 135.8, 130.3, 127.7, 113.5, 79.7, 55.2, 35.2, 19.0, 18.5 ppm.

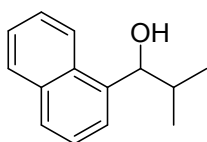
1-(4-bromophenyl)-2-methylpropan-1-ol (39)^{S26}



^1H NMR (400 MHz, CDCl_3 , 298 K) δ = 7.42-7.49 (m, 2H, ArCH), 7.15-7.21 (m, 2H, ArCH), 4.35 (d, 1H, J = 6.6 Hz, CH), 1.82- 1.92 (m, 2H, CH&OH), 0.97 (d, 3H, J = 6.8 Hz, CH_3), 0.80 (d, 3H, J = 6.8 Hz, CH_3) ppm.

^{13}C NMR (101 MHz, CDCl_3 , 298 K) δ = 142.6, 131.3, 128.3, 121.1, 79.3, 35.3, 18.9, 18.0 ppm.

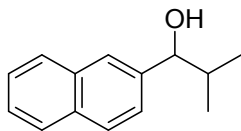
2-methyl-1-(naphthalen-1-yl)propan-1-ol (40)^{S27}



^1H NMR (400 MHz, CDCl_3 , 298 K) δ = 8.10-8.18 (m, 1H, ArCH), 7.85-7.92 (m, 1H, ArCH), 7.79 (d, 1H, J = 8.2 Hz, ArCH), 7.60 (d, 1H, J = 6.0 Hz, ArCH), 7.44-7.56 (m, 3H, ArCH), 5.18 (d, 1H, J = 6.0 Hz, CH), 2.20- 2.34 (m, 1H, CH), 2.05-2.19 (m, 1H, OH), 1.05 (d, 3H, J = 6.8 Hz, CH_3), 0.95 (d, 3H, J = 6.8 Hz, CH_3) ppm.

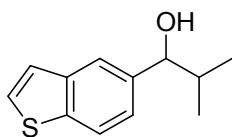
^{13}C NMR (101 MHz, CDCl_3 , 298 K) δ = 139.7, 133.9, 130.8, 128.9, 127.8, 125.8, 125.4, 125.3, 124.0, 123.6, 76.5, 34.5, 20.1, 17.6 ppm.

2-methyl-1-(naphthalen-2-yl)propan-1-ol (41)^{S17}



^1H NMR (400 MHz, CDCl_3 , 298 K) δ = 7.81-7.86 (m, 3H, ArCH), 7.75 (s, 1H, ArCH), 7.43-7.53 (m, 3H, ArCH), 4.53 (dd, 1H, J = 6.8 and 2.7 Hz, CH), 2.02-2.14 (m, 1H, CH), 2.00 (d, 1H, J = 3.2 Hz, OH), 1.05 (d, 3H, J = 6.8 Hz, CH_3), 0.84 (d, 3H, J = 6.8 Hz, CH_3) ppm.

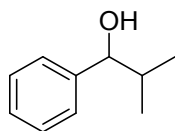
^{13}C NMR (101 MHz, CDCl_3 , 298 K) δ = 141.2, 133.3, 133.1, 128.1, 128.1, 127.8, 126.2, 125.9, 125.5, 124.8, 80.3, 35.3, 19.3, 18.4 ppm.

1-(benzo[b]thiophen-5-yl)-2-methylpropan-1-ol (42)

¹H NMR (400 MHz, CDCl₃, 298 K) δ = 7.84 (d, 1H, J = 8.3 Hz, ArCH), 7.77 (d, 1H, J = 0.8 Hz, ArCH), 7.45 (d, 1H, J = 5.4 Hz, ArCH), 7.28-7.36 (m, 2H, ArCH), 4.49 (dd, 1H, J = 6.8 and 1.5 Hz, CH), 1.97-2.09 (m, 1H, CH), 1.92 (d, 1H, J = 2.5 Hz, OH), 1.04 (d, 3H, J = 6.8 Hz, CH₃), 0.82 (d, 3H, J = 6.8 Hz, CH₃) ppm.

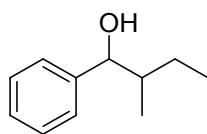
¹³C NMR (101 MHz, CDCl₃, 298 K) δ = 140.1, 139.7, 139.0, 126.9, 124.0, 123.2, 122.4, 121.7, 80.3, 35.6, 19.2, 18.5 ppm.

HRMS (ESI), m/z : [M+H]⁺ calculated for C₁₂H₁₄SO: 206.0765, found: 206.0732.

2-methyl-1-phenylpropan-1-ol (44)^{S17}

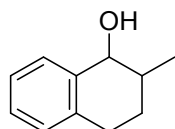
¹H NMR (400 MHz, CDCl₃, 298 K) δ = 7.24-7.38 (m, 5H, ArCH), 4.37 (dd, 1H, J = 6.9 and 3.2 Hz, CH), 1.91-2.02 (m, 1H, CH), 1.82 (d, 1H, J = 3.2 Hz, OH), 1.01 (d, 3H, J = 6.8 Hz, CH₃), 0.80 (d, 3H, J = 6.8 Hz, CH₃) ppm.

¹³C NMR (101 MHz, CDCl₃, 298 K) δ = 143.6, 128.2, 127.4, 126.5, 80.0, 35.2, 19.0, 18.2 ppm.

2-methyl-1-phenylbutan-1-ol (45)^{S28}

¹H NMR (400 MHz, CDCl₃, 298 K) δ = 7.22-7.36 (m, 5H, ArCH), 4.51 (dd, 0.5H, J = 5.9 and 3.5 Hz, CH), 4.42 (dd, 0.5H, J = 7.0 and 3.2 Hz, CH), 1.87-1.92 (m, 0.5H, OH), 1.83-1.86 (m, 0.5H, OH), 1.63-1.80 (m, 1.5H, CH₂), 1.32-1.45 (m, 0.5H, CH₂), 1.14-1.23 (m, 0.5H, CH), 1.02-1.13 (m, 0.5H, CH), 0.82-0.97 (m, 4.5H, CH₃), 0.73 (d, 1.5H, J = 6.8 Hz, CH₃) ppm.

¹³C NMR (101 MHz, CDCl₃, 298 K) δ = 144.0, 143.8, 128.3, 127.5, 127.3, 126.8, 78.9, 78.2, 42.1, 41.8, 26.0, 25.0, 15.2, 14.1, 11.8, 11.4 ppm.

2-methyl-1,2,3,4-tetrahydronaphthalen-1-ol (46)^{S17}

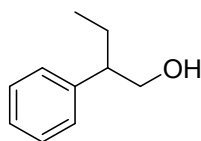
^1H NMR (400 MHz, CDCl_3 , 298 K) $\delta_{(\text{mesitoxylbenzene})} = 6.09$ (s, 3H), $\delta_{(\text{product})} = 4.55$ (1H, CH), 4.32 (1H, CH), 1.12 (d, 3H, $J = 6.7$ Hz, CH_3).

6.6 General procedure for β -alkylation of 2-phenyl ethanol with primary alcohols

To a sealed tube (35 mL) equipped with a stir bar, Ir-NHC catalyst **5d** (0.05 mol%), primary alcohols (1 mL), $t\text{BuONa}$ (3 mmol) and 2-phenyl ethanol (1 mmol) were added under nitrogen atmosphere. The solution was heated at 150 °C for 24 h. After cooling to room temperature, mesitoxylbenzene was added as an internal standard, and sent for NMR measurement.

Pure products were obtained by column chromatography over silica gel using ethyl acetate/petroleum ether mixture as eluent.

2-phenylbutanol (**48**)^{S29}

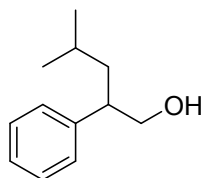


^1H NMR (400 MHz, CDCl_3 , 298 K) $\delta = 7.28$ -7.37 (m, 2H, ArCH), 7.17-7.27 (m, 3H, ArCH), 3.65-3.80 (m, 2H, CH_2), 2.64-2.73 (m, 1H, CH), 1.69-1.84 (m, 1H, CH_2), 1.53-1.65 (m, 1H, CH_2), 0.84 (t,

3H, $J = 8.4$ Hz, CH_3) ppm.

^{13}C NMR (101 MHz, CDCl_3 , 298 K) $\delta = 142.4$, 128.7, 128.2, 126.8, 67.4, 50.6, 25.1, 12.1 ppm.

4-methyl-2-phenylpentan-1-ol (**49**)^{S30}



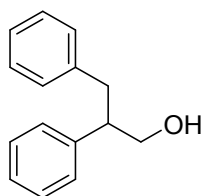
^1H NMR (400 MHz, CDCl_3 , 298 K) $\delta = 7.33$ (t, 2H, ArCH), 7.18-7.27 (m, 3H, ArCH), 3.63-3.77 (m, 2H, CH_2), 2.83-2.94 (m, 1H, CH), 1.51-1.63 (m, 1H, CH), 1.36-1.49 (m, 2H, CH_2), 1.27-1.34

(m, 1H, OH), 0.83-0.89 (m, 6H, CH_3) ppm.

^{13}C NMR (101 MHz, CDCl_3 , 298 K) $\delta = 142.6$, 128.8, 128.2, 126.8, 68.4, 46.6, 41.3, 25.4, 23.7, 22.0 ppm.

2,3-diphenylpropan-1-ol (**50**)^{S20}

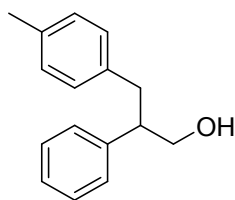
S40



¹H NMR (400 MHz, CDCl₃, 298 K) δ = 7.27-7.34 (m, 2H, ArCH), 7.19-7.26 (m, 1H, ArCH), 7.12-7.18 (m, 1H, ArCH), 7.05-7.11 (m, 2H, CH₂), 3.79 (d, 2H, J = 5.5 Hz, CH₂), 2.98-3.14 (m, 2H, CH₂), 2.91 (dd, 1H, J = 12.8 and 7.4 Hz, CH), 1.24-1.33 (m, 1H, OH) ppm.

¹³C NMR (101 MHz, CDCl₃, 298 K) δ = 142.0, 140.0, 129.2, 128.8, 128.4, 128.2, 127.0, 126.2, 66.5, 50.3, 38.8 ppm.

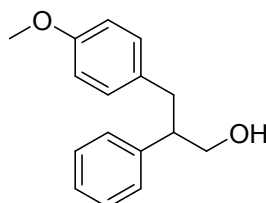
2-phenyl-3-(*p*-tolyl)propan-1-ol (51) ^{S31}



¹H NMR (400 MHz, CDCl₃, 298 K) δ = 7.27-7.33 (m, 2H, ArCH), 7.18-7.25 (m, 3H, ArCH), 6.95-7.05 (m, 4H, ArCH), 3.74-3.82 (m, 2H, CH₂), 3.02-3.11 (m, 1H, CH₂), 2.93-3.01 (m, 1H, CH₂), 2.87 (dd, 1H, J = 13.2 and 7.4 Hz, CH), 2.28 (s, 3H, CH₃), 1.27-1.33 (m, 1H, OH) ppm.

¹³C NMR (101 MHz, CDCl₃, 298 K) δ = 142.2, 136.9, 135.6, 129.1, 129.0, 128.8, 128.2, 126.9, 66.6, 50.4, 38.4, 21.1 ppm.

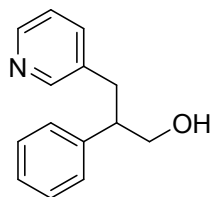
3-(4-methoxyphenyl)-2-phenylpropan-1-ol (52) ^{S31}



¹H NMR (400 MHz, CDCl₃, 298 K) δ = 7.28-7.35 (m, 2H, ArCH), 7.18-7.27 (m, 3H, ArCH), 6.98-7.03 (m, 2H, ArCH), 6.74-6.79 (m, 2H, ArCH), 3.78 (dd, 2H, J = 6.4 and 2.4 Hz, CH₂), 3.76 (s, 3H, OCH₃), 2.94-3.10 (m, 2H, CH₂), 2.86 (dd, 2H, J = 13.6 and 7.5 Hz, CH₂) ppm.

¹³C NMR (101 MHz, CDCl₃, 298 K) δ = 158.0, 142.1, 132.1, 130.1, 128.8, 128.2, 126.9, 113.8, 66.5, 55.3, 50.5, 37.9 ppm.

2-phenyl-3-(pyridin-3-yl)propan-1-ol (53)



¹H NMR (400 MHz, CDCl₃, 298 K) δ = 8.35 (dd, 1H, J = 4.8 and 1.6 Hz, ArCH), 8.29 (d, 1H, J = 2.0 Hz, ArCH), 7.25-7.35 (m, 3H, ArCH), 7.19-7.25 (m, 1H, ArCH), 7.06-7.18 (m, 3H, ArCH), 3.81

(d, 2H, $J = 6.2$ Hz, CH₂), 3.01-3.17 (m, 2H, CH₂), 2.87 (dd, H, $J = 13.1$ and 8.1 Hz, CH) ppm.

¹³C NMR (101 MHz, CDCl₃, 298 K) $\delta = 150.4, 147.4, 141.1, 136.7, 135.6, 128.8, 128.2, 127.2, 123.3, 66.2, 50.2, 35.8$ ppm.

HRMS (ESI), m/z : [M+H]⁺ calculated for C₁₄H₁₆NO: 214.1232, found: 214.1221.

7. Control experiments

7.1 Procedure for β -methylation of 2-arylethanol with TEMPO

To a sealed tube (35 mL) equipped with a stir bar, Ir-NHC catalyst **5d** (0.05 mol%), methanol (1 mL), ^tBuONa (2 mmol), 2-arylethanol (1 mmol) and TEMPO (2,2,6,6-tetramethyl-1-piperidinyloxy) (234 mg, 1.5 mmol) were added under nitrogen atmosphere. The solution was heated at 140 °C for 24 h. After cooling to room temperature, mesitoxybenzene was added as an internal standard, and sent for NMR measurement.

7.2 Procedure for β -methylation of 2-arylethanol with Hg

To a sealed tube (35 mL) equipped with a stir bar, NHC-Ir catalyst **5d** (0.05 mol%), methanol (1 mL), ^tBuONa (2 mmol), 2-arylethanol (1 mmol) and two drops of Hg were added under nitrogen atmosphere. The solution was heated at 140 °C for 24 h. After cooling to room temperature, mesitoxybenzene was added as an internal standard, and sent for NMR measurement.

7.3 Reaction profile for β -methylation of 2-arylethanol

To a sealed tube (35 mL) equipped with a stir bar, Ir-NHC catalyst **5d** (0.05 mol%), methanol (1 mL), ^tBuONa (2 mmol) and 2-arylethanol (1 mmol) were added under nitrogen atmosphere. The solution was heated at 140 °C for different time intervals of 0.25 h, 0.5 h, 1 h, 2 h, 4 h, 6 h, 8 h, and 12 h. After cooling to room temperature, mesitoxybenzene was added as an internal standard, and sent for NMR

measurement to detect the starting material, product and possible intermediate.

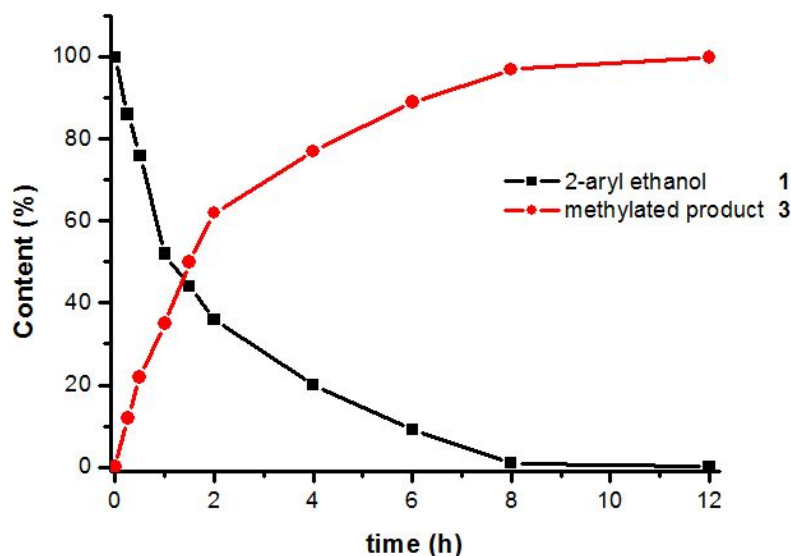
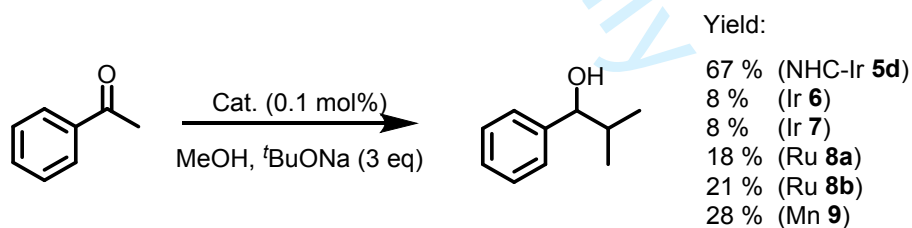


Figure S17. Conversion and yield/time profile for the β -methylation of 2-arylethanol.

7.4 Procedure for β -methylation of acetophenone with methanol

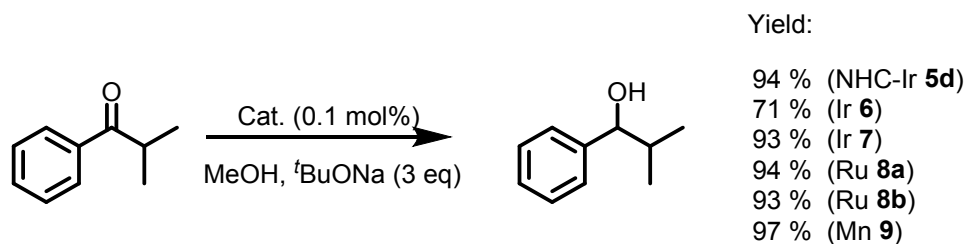
To a sealed tube (35 mL) equipped with a stir bar, catalyst **5d**, **6**, **7**, **8a-b** or **9** (0.1 mol%), methanol (1 mL), t BuONa (3 mmol) and acetophenone (1 mmol) were added under nitrogen atmosphere. The solution was heated at 140 °C for 24 h. After cooling to room temperature, mesitoxylene was added as an internal standard, and sent for NMR measurement.



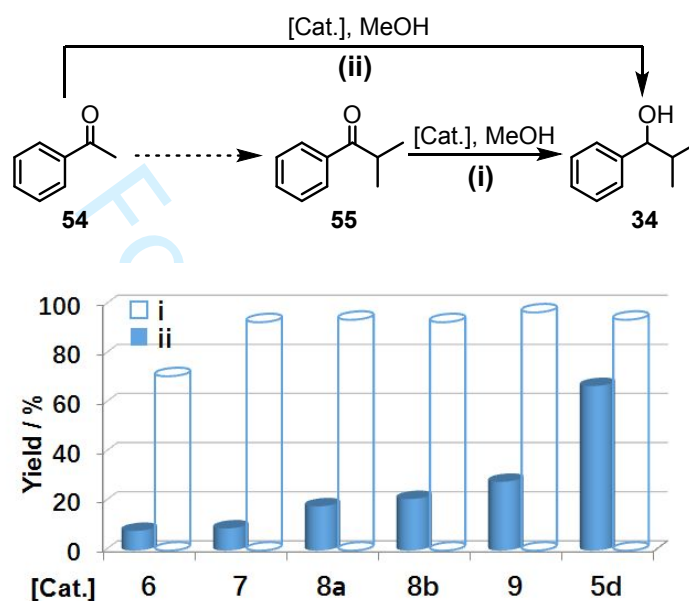
7.5 Procedure for hydrogen transfer of di-methylated-ketone with methanol

To a sealed tube (35 mL) equipped with a stir bar, catalyst **5d**, **6**, **7**, **8a-b** or **9** (0.1 mol%), methanol (1 mL), t BuONa (3 mmol) and di-methylated-ketone (1 mmol) were added under nitrogen atmosphere. The solution was heated at 140 °C for 24 h. After cooling to room temperature, mesitoxylene was added as an internal

standard, and sent for NMR measurement.



Scheme S2 Comparison of catalytic activity of viable complexes **5d** and **6-9**.



7.6 Procedure for β -methylation of acetophenone with CD_3OD

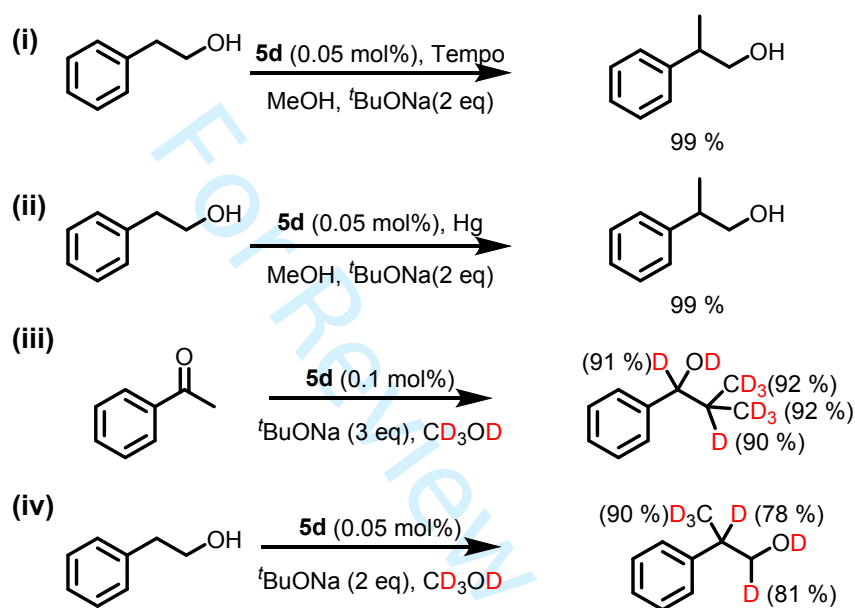
To a sealed tube (35 mL) equipped with a stir bar, NHC-Ir catalyst **5d** (0.1 mol%), deuterated methanol (1 mL), $t\text{BuONa}$ (3 mmol) and acetophenone (1 mmol) were added under nitrogen atmosphere. The solution was heated at 140 °C for 24 h. After cooling to room temperature, the isolation of pure product was carried out using column chromatography over silica gel using ethyl acetate/petroleum ether (1:15) mixture as eluent.

7.7 Procedure for β -methylation of 2-arylethanol with CD_3OD

To a sealed tube (35 mL) equipped with a stir bar, NHC-Ir catalyst **5d** (0.05 mol%) deuterated methanol (1 mL), $t\text{BuONa}$ (2 mmol) and 2-arylethanol (1 mmol)

were added under nitrogen atmosphere. The solution was heated at 140 °C for 24 h. After cooling to room temperature, the isolation of pure product was carried out using column chromatography over silica gel using ethyl acetate/petroleum ether (1:15) mixture as eluent.

Scheme S3 Control experiment of β -methylation of catalyzed by NHC-Iridium complex.



7.8 Procedure for KIE experiment of β -methylation with CH_3OH or CD_3OD .

To a sealed tube (35 mL) equipped with a stir bar, NHC-Ir catalyst **5d** (0.05 mol%), methanol/ deuterated methanol (1 mL), $t\text{BuONa}$ (2 mmol) and 2-arylethanol (1 mmol) were added under nitrogen atmosphere. The solution was heated at 140 °C for different time intervals of 0.25 h, 0.5 h, 1 h, 1.25 h, 1.5 h. After cooling to room temperature, mesitoxybenzene was added as an internal standard, and sent for NMR measurement. Yield was determined by ^1H NMR spectrum. The time-yield profiles were fitting to straight lines. For methanol: $y = 28.51x + 7.14$; for deuterated methanol: $y = 12.61x + 9.26$ and $k_{\text{H}}/k_{\text{D}}$ is 2.26.

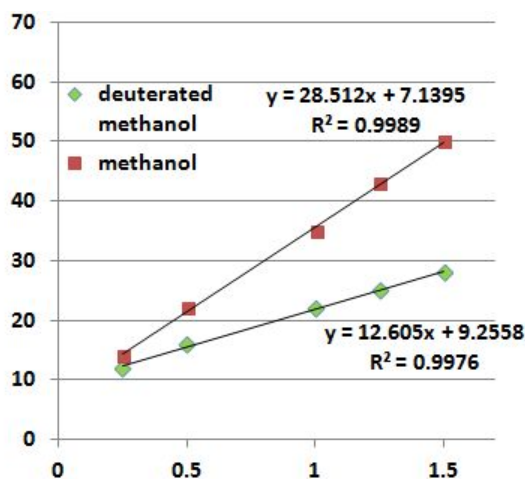


Figure S18. KIE experiment of β -methylation with CH_3OH or CD_3OD .

8. ^1H NMR spectra of reaction mixtures after β -methylation of alcohols

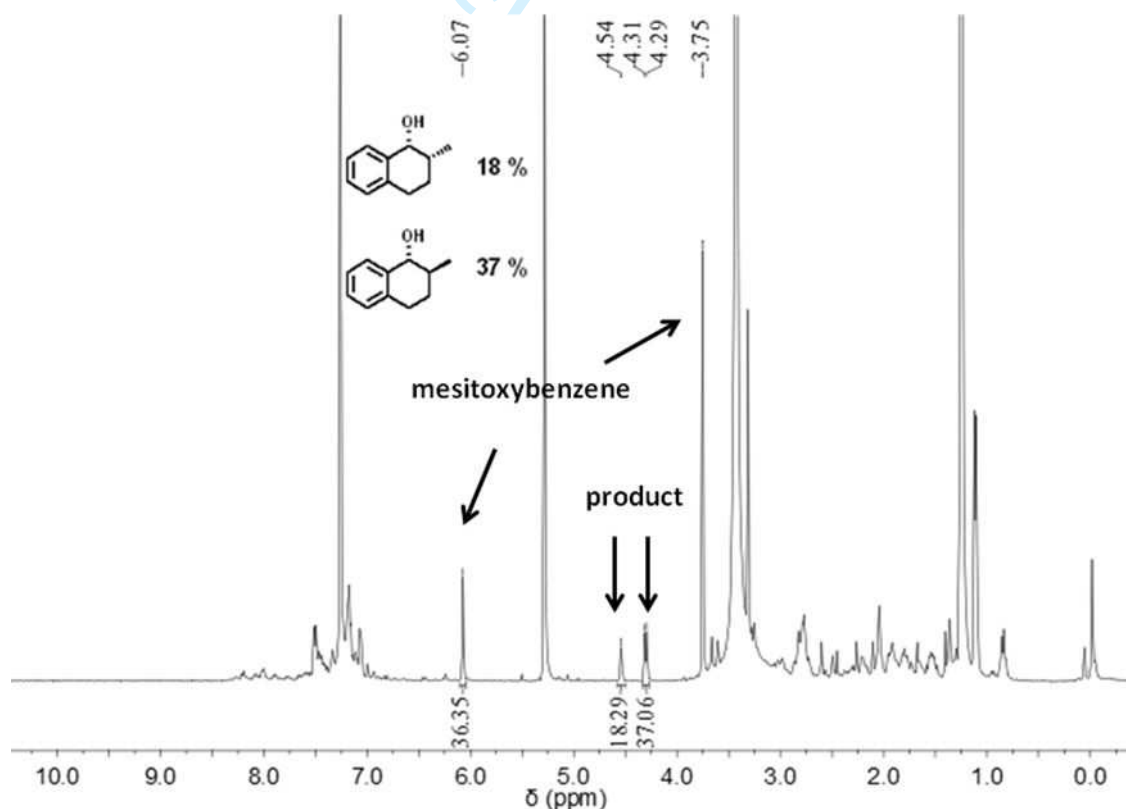


Figure S19. ^1H NMR (400 MHz, CDCl_3 , 298 K) spectrum of the mixtures of **46**.

9. NMR spectra of isolated products

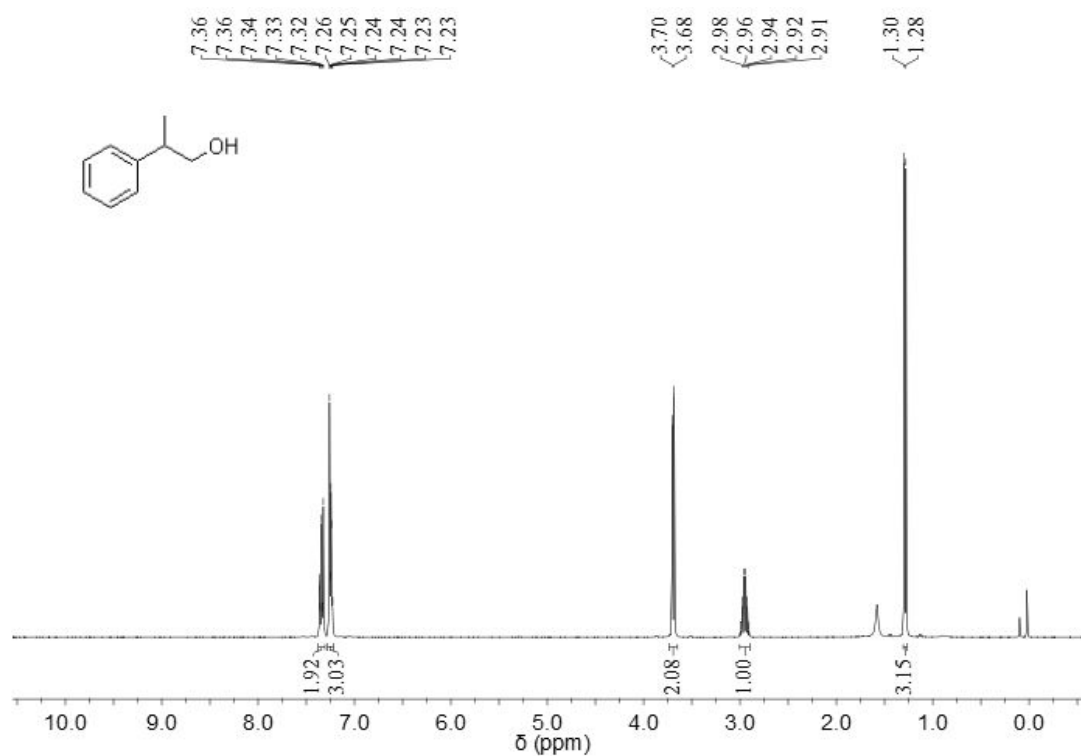


Figure S20. ¹H NMR (400 MHz, CDCl₃, 298 K) spectrum of compound 3.

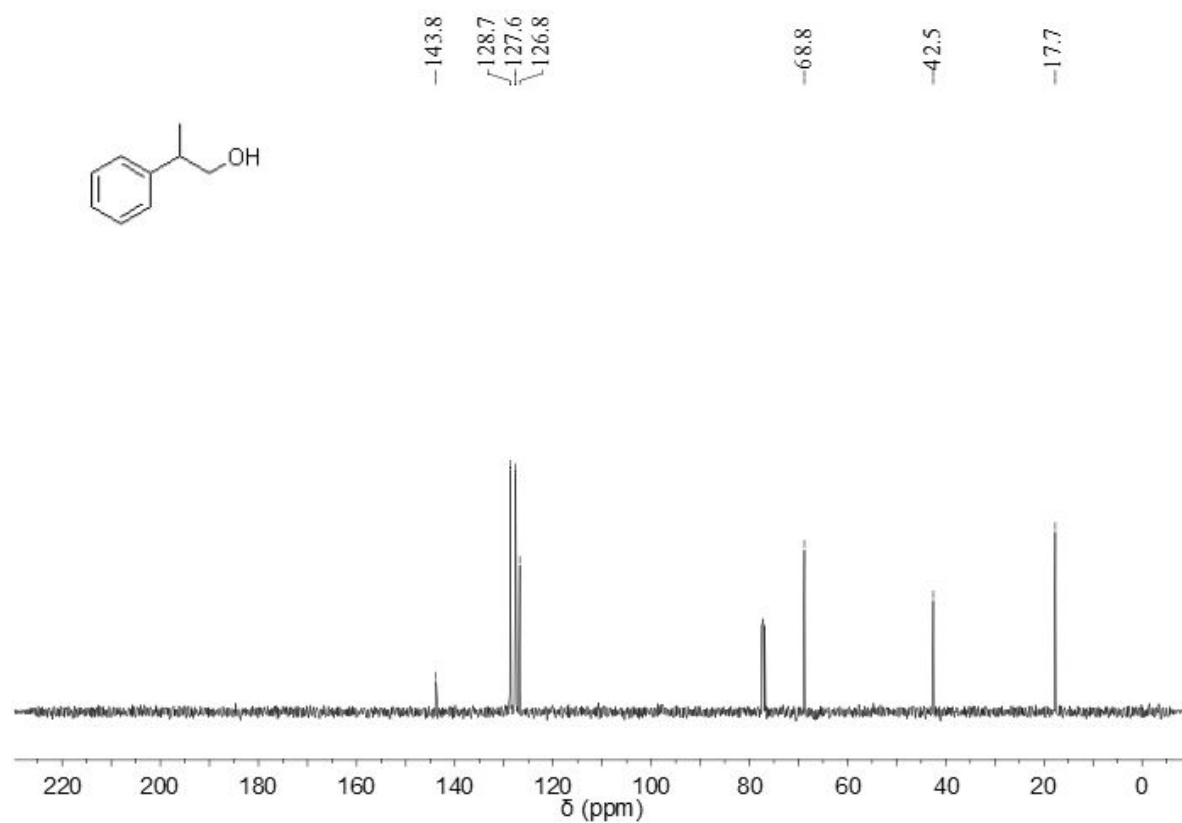


Figure S21. ^{13}C NMR (101 MHz, CDCl_3 , 298 K) spectrum of compound 3.

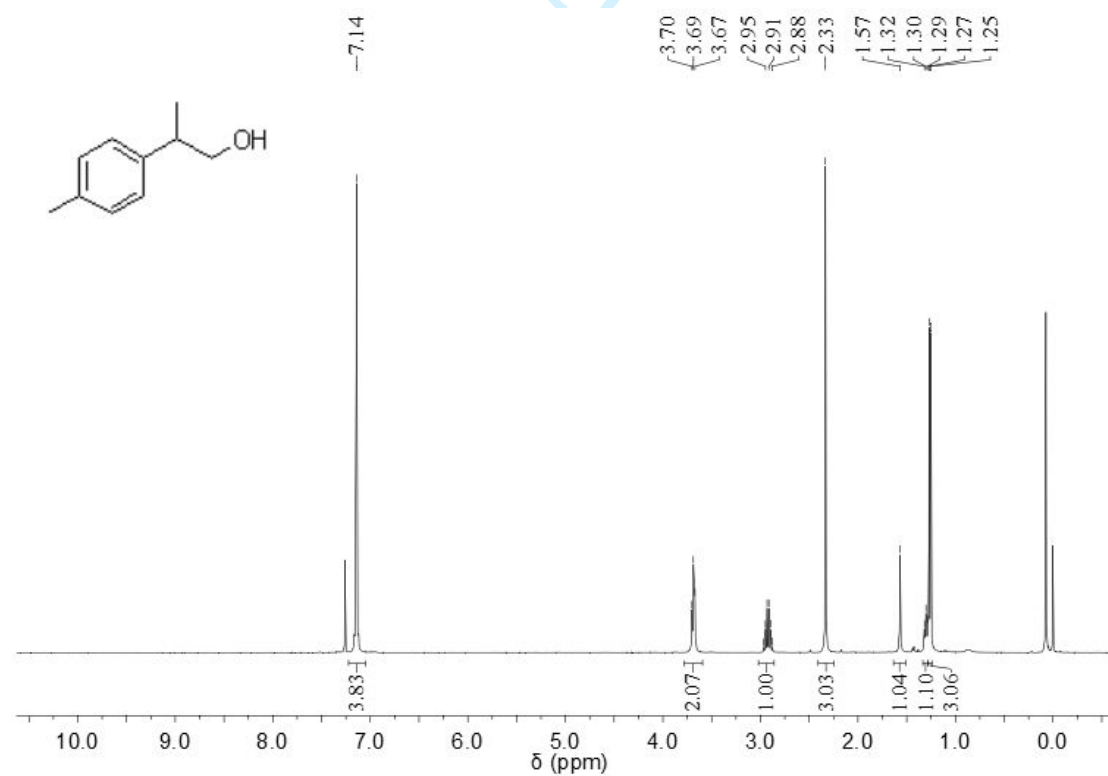


Figure S22. ^1H NMR (400 MHz, CDCl_3 , 298 K) spectrum of 10.

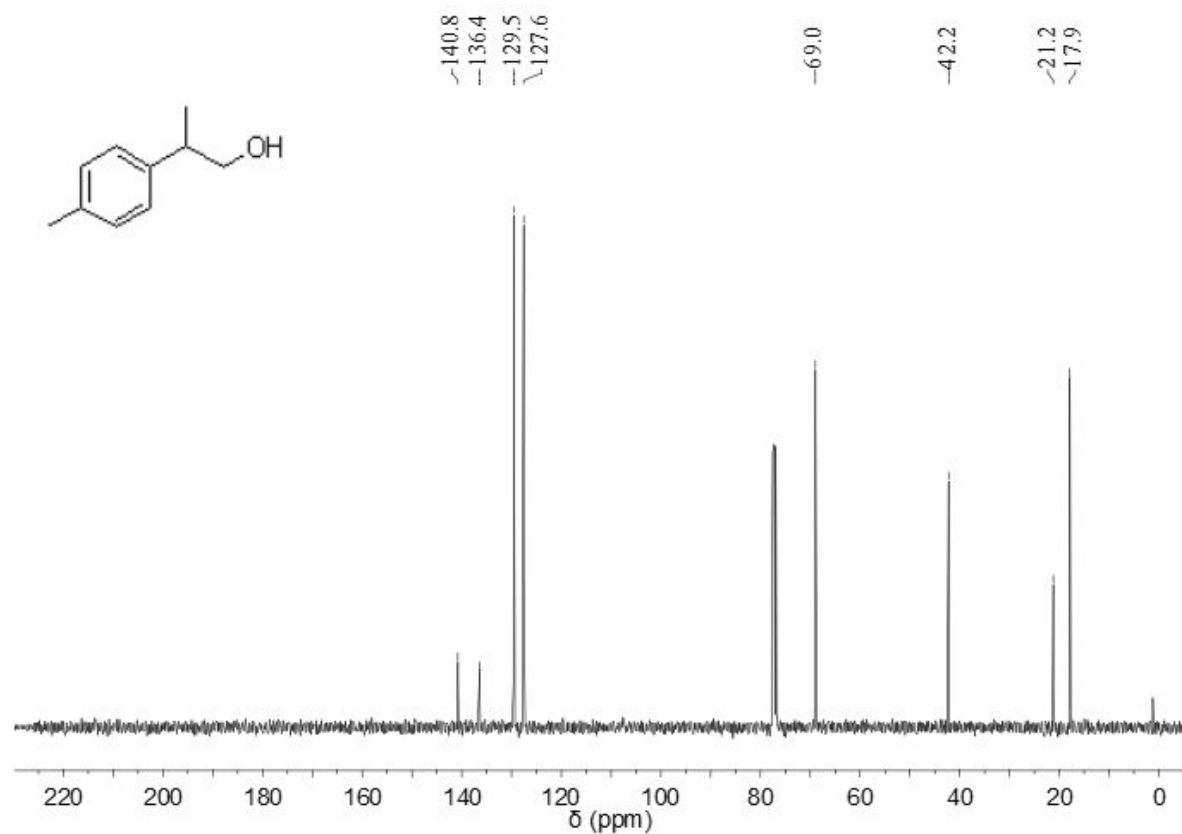


Figure S23. ¹³C NMR (101 MHz, CDCl₃, 298 K) spectrum of **10**.

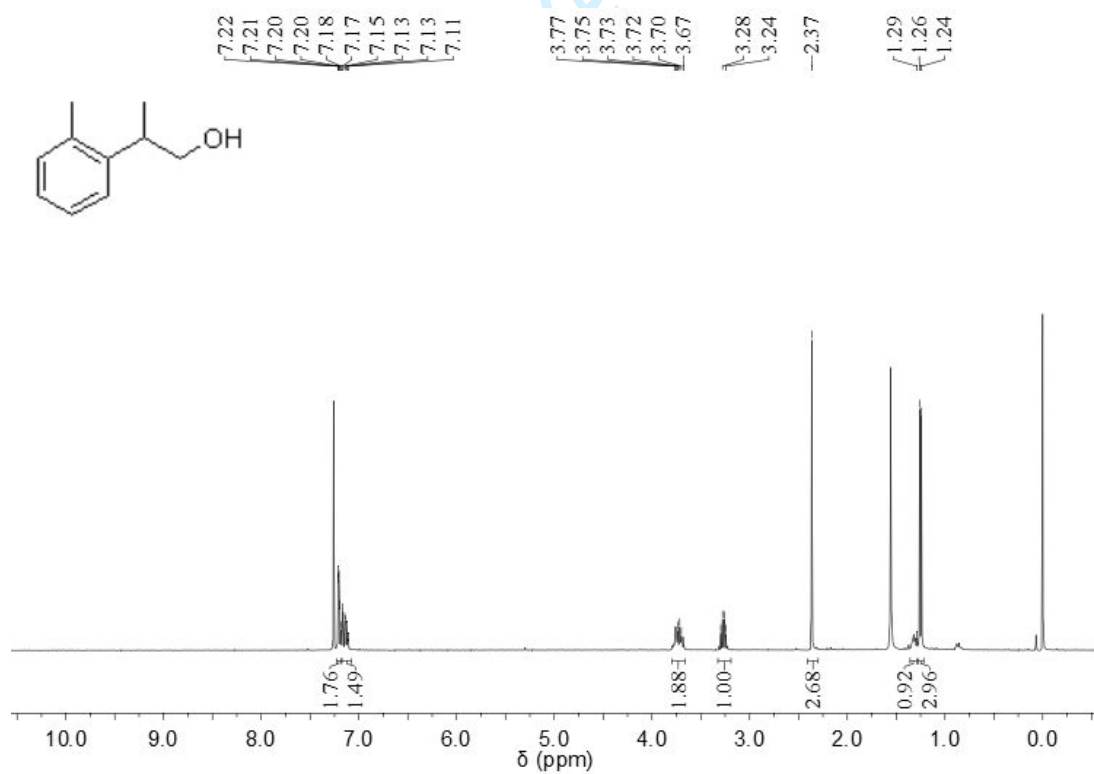


Figure S24. ¹H NMR (400 MHz, CDCl₃, 298 K) spectrum of **11**.

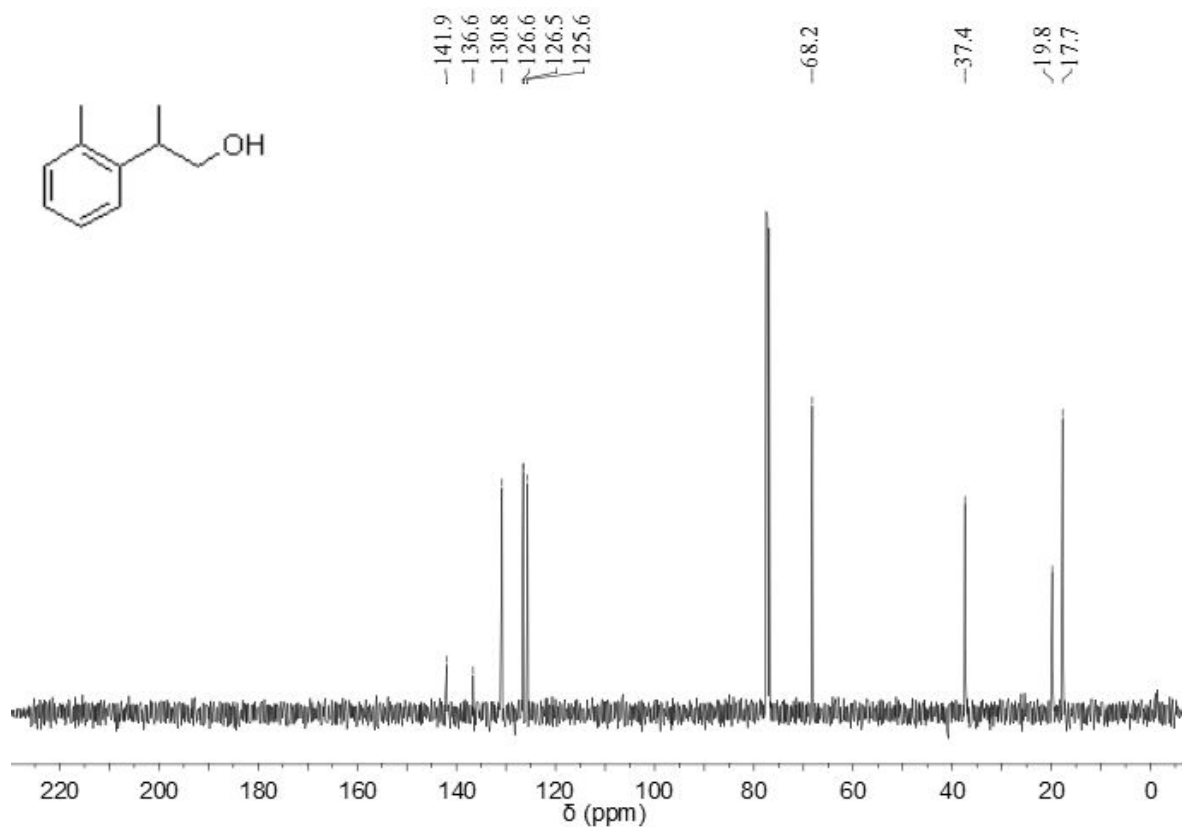


Figure S25. ^{13}C NMR (101 MHz, CDCl_3 , 298 K) spectrum of **11**.

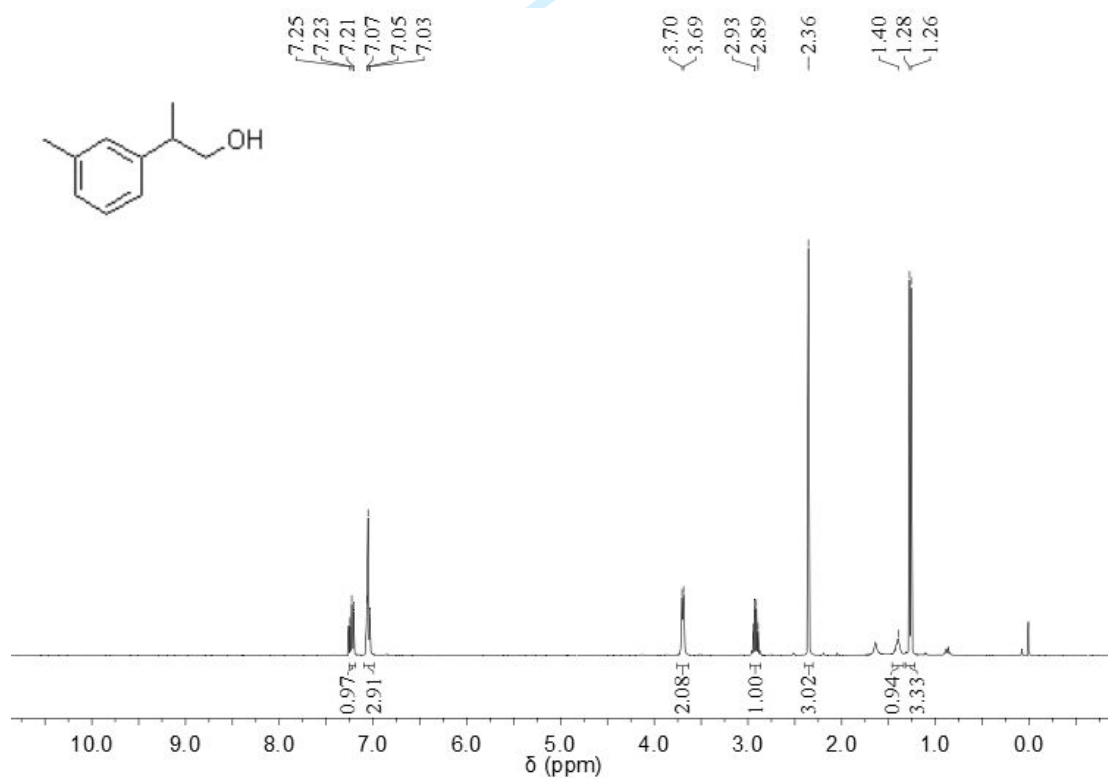


Figure S26. ^1H NMR (400 MHz, CDCl_3 , 298 K) spectrum of **12**.

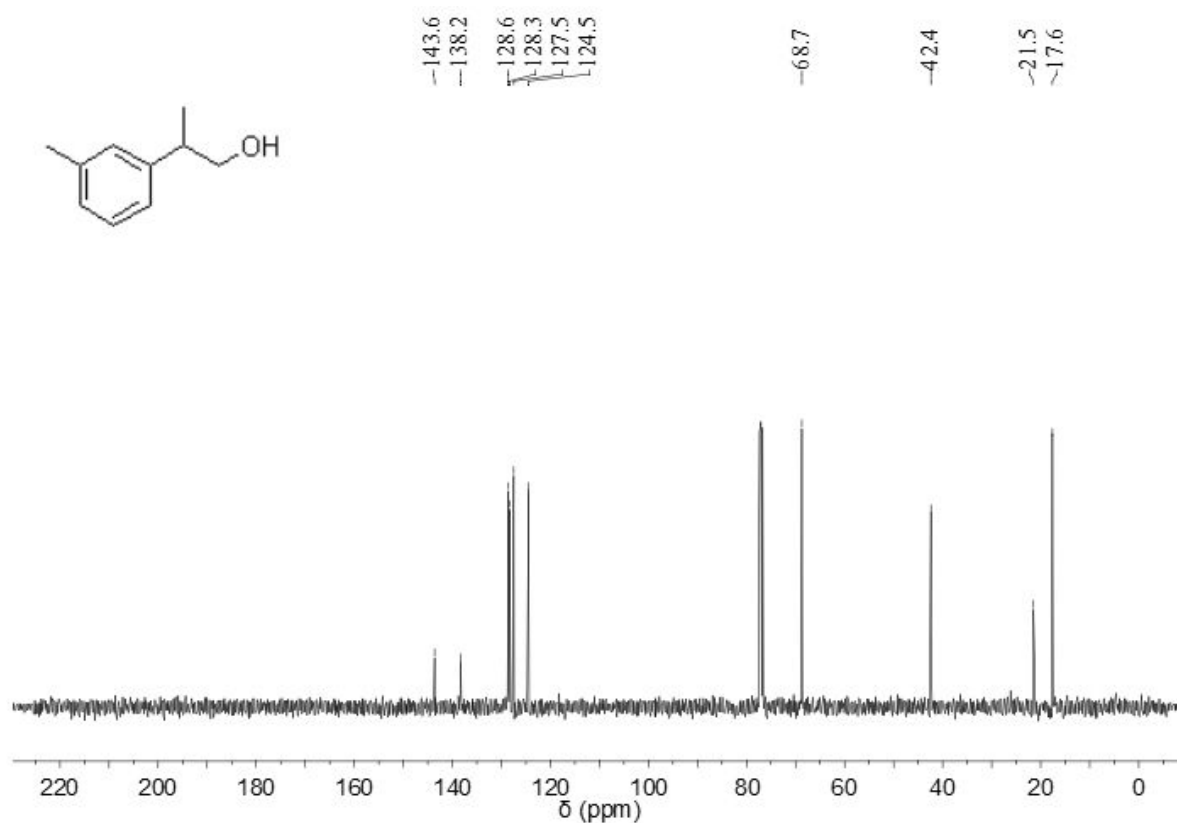


Figure S27. ^{13}C NMR (101 MHz, CDCl_3 , 298 K) spectrum of **12**.

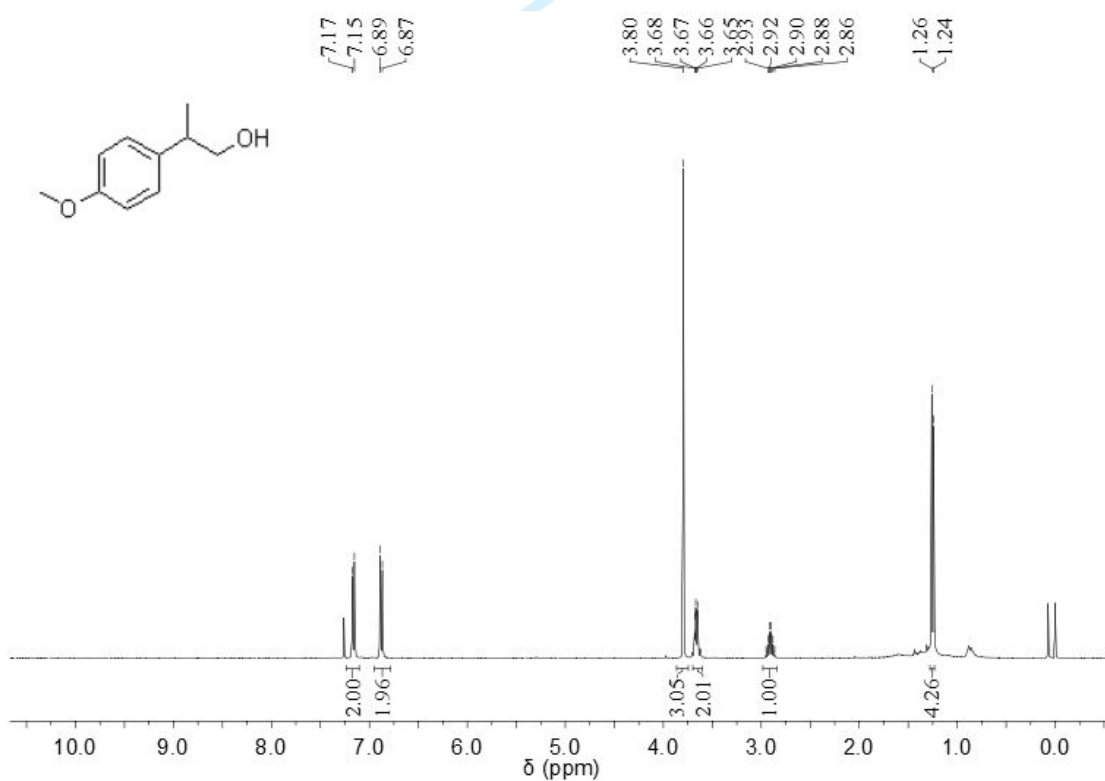


Figure S28. ^1H NMR (400 MHz, CDCl_3 , 298 K) spectrum of **13**.

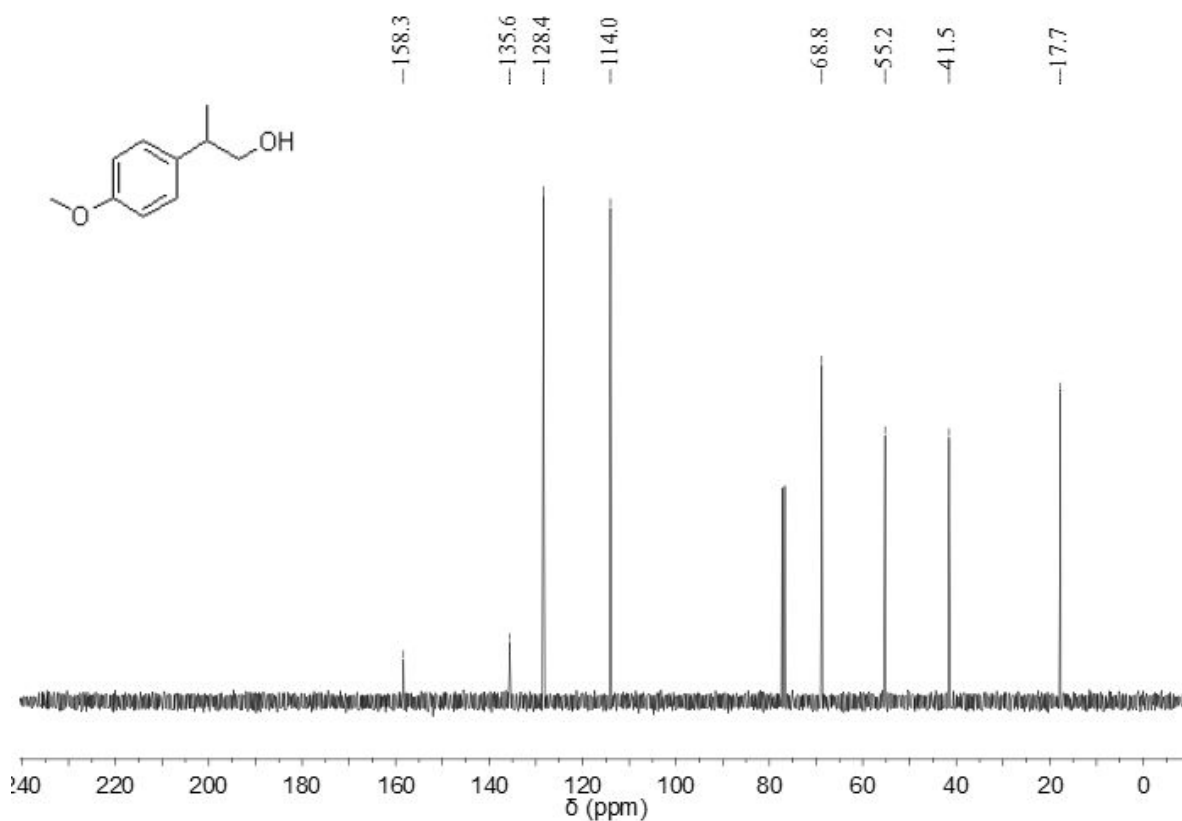


Figure S29. ^{13}C NMR (101 MHz, CDCl_3 , 298 K) spectrum of **13**.

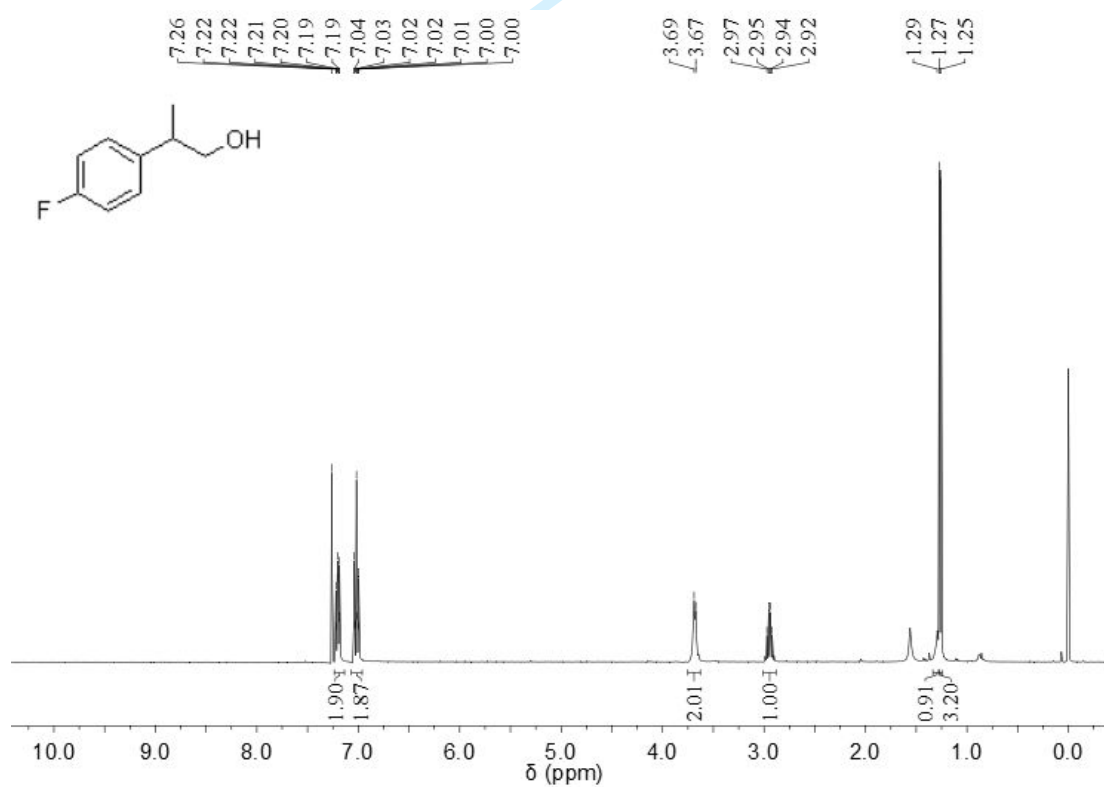


Figure S30. ^1H NMR (400 MHz, CDCl_3 , 298 K) spectrum of **14**.

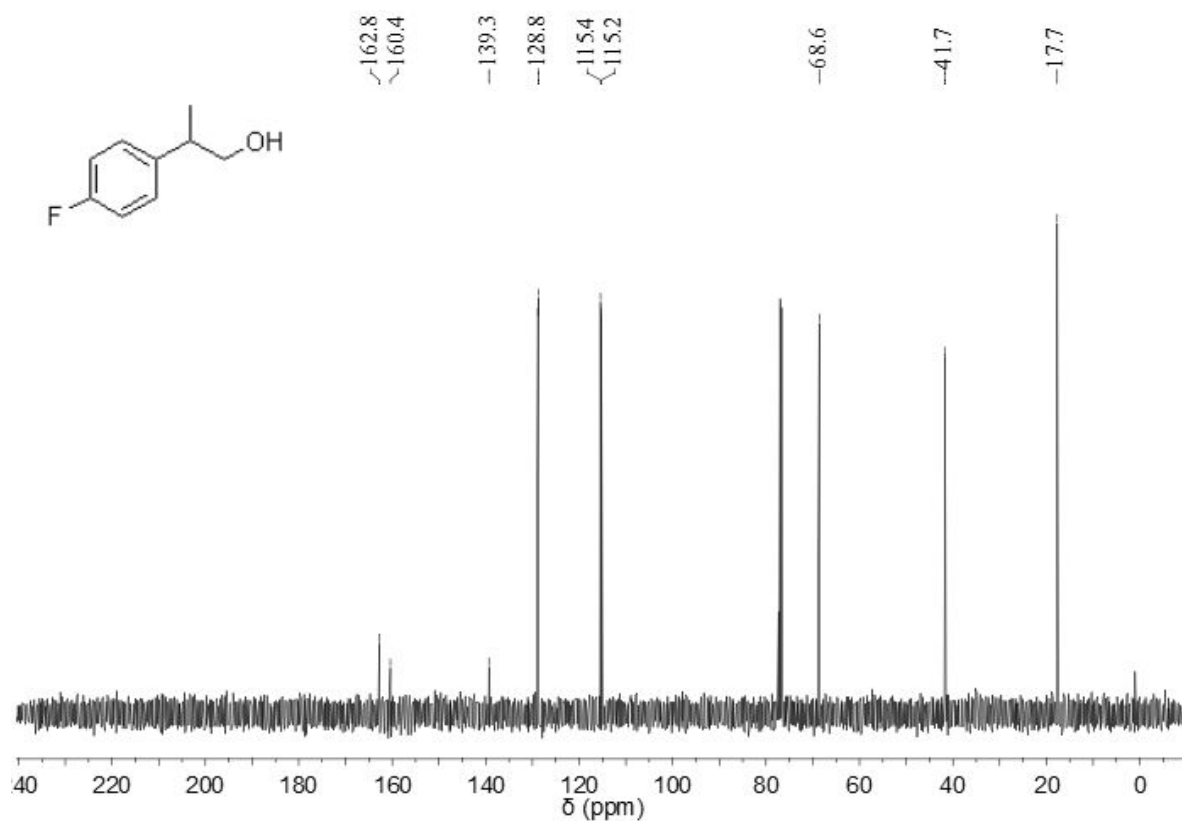


Figure S31. ¹³C NMR (101 MHz, CDCl₃, 298 K) spectrum of **14**.

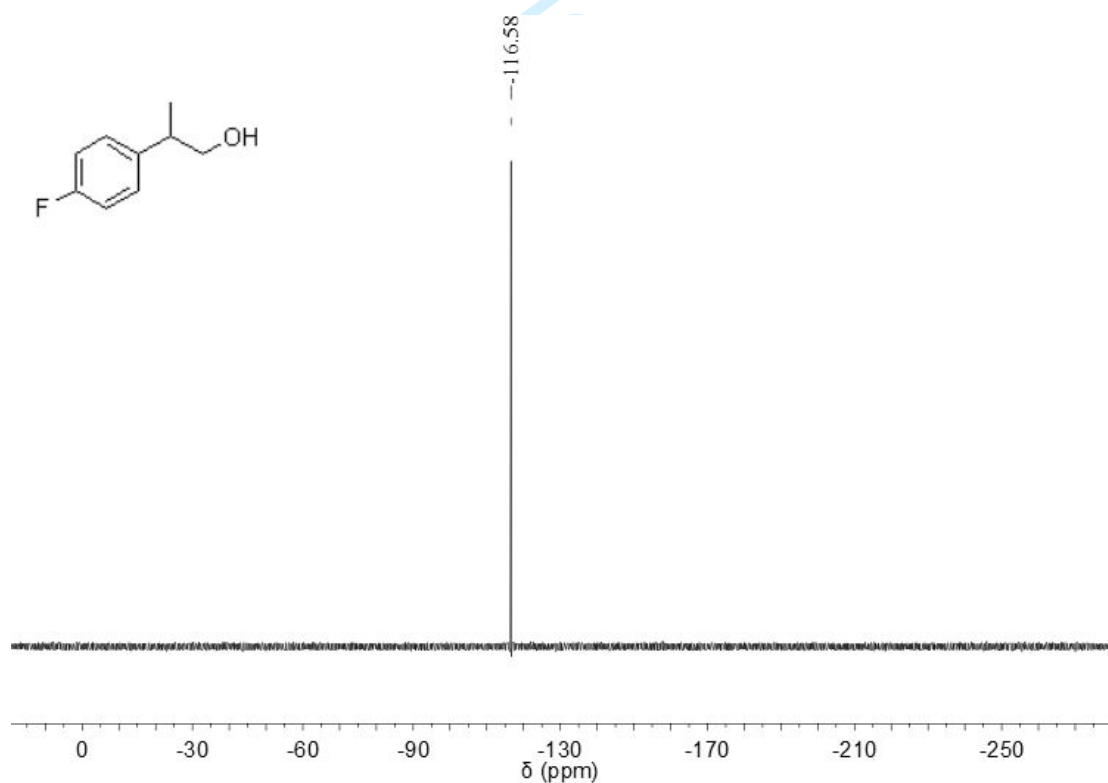


Figure S32. ¹⁹F NMR (376 MHz, CDCl₃, 298 K) spectrum of **14**.

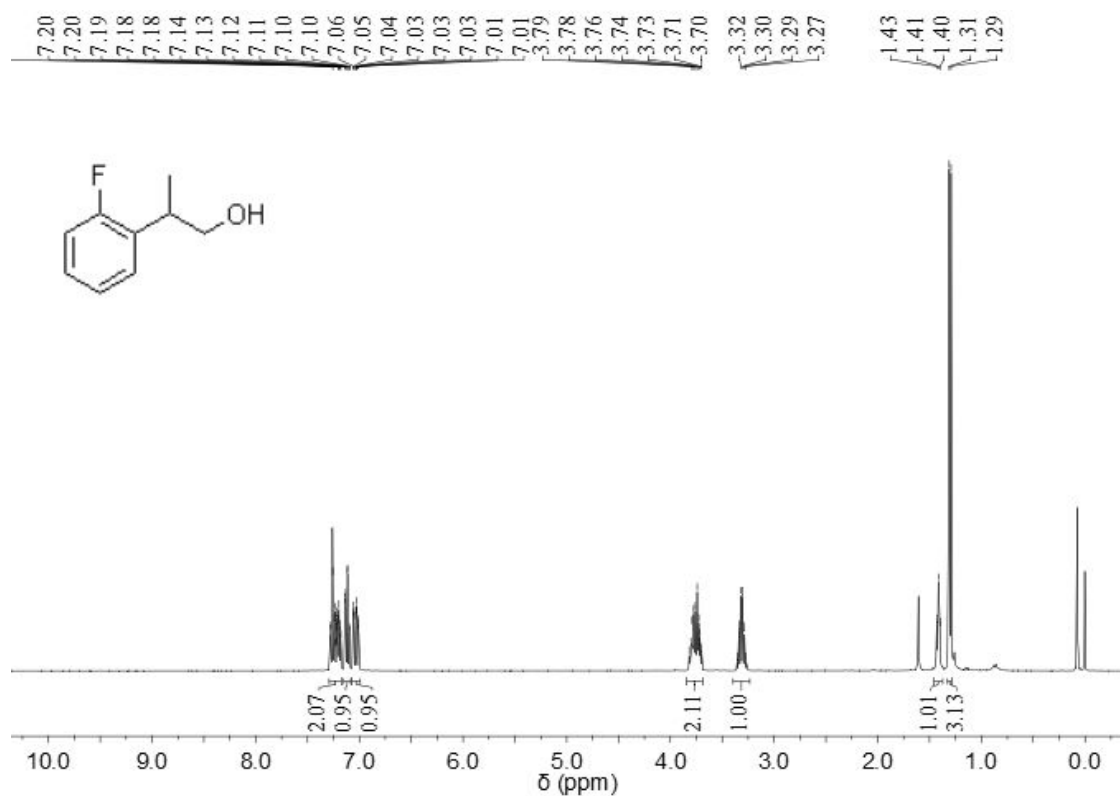


Figure S33. ¹H NMR (400 MHz, CDCl₃, 298 K) spectrum of **15**.

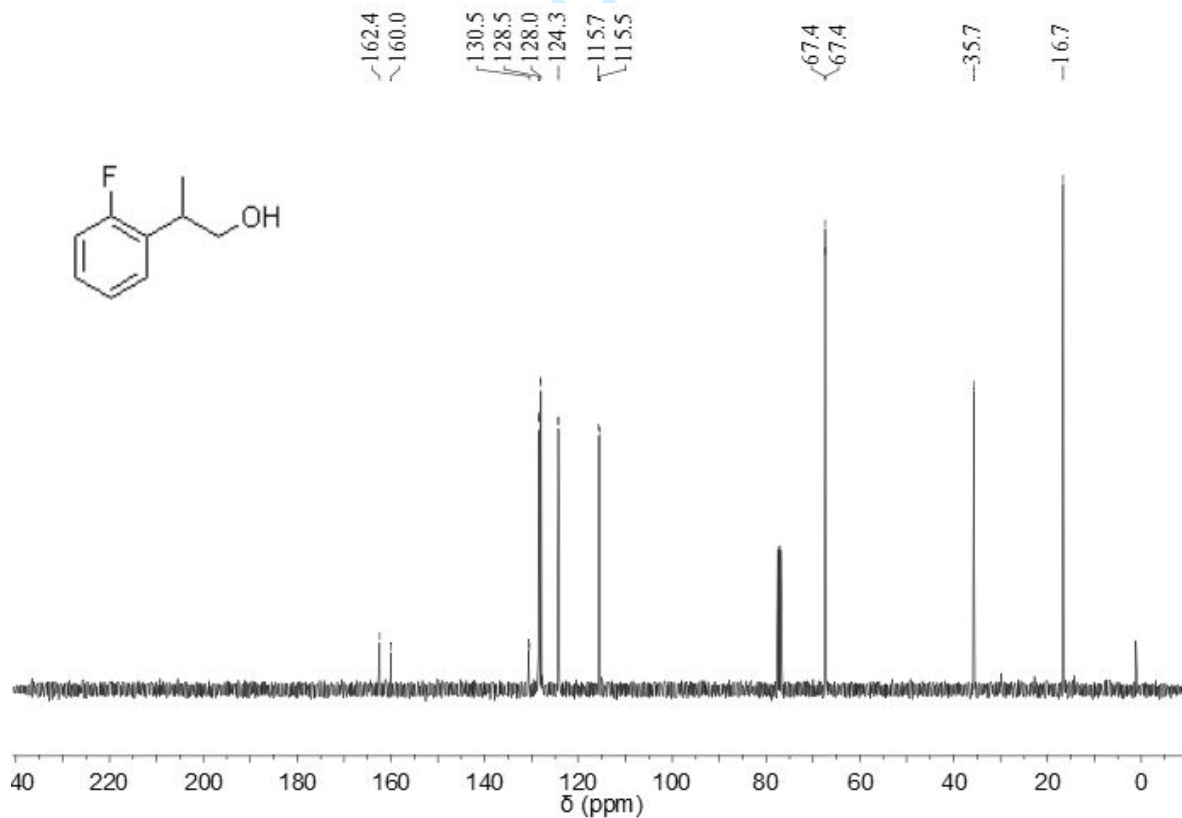


Figure S34. ¹³C NMR (101 MHz, CDCl₃, 298 K) spectrum of **15**.

S54

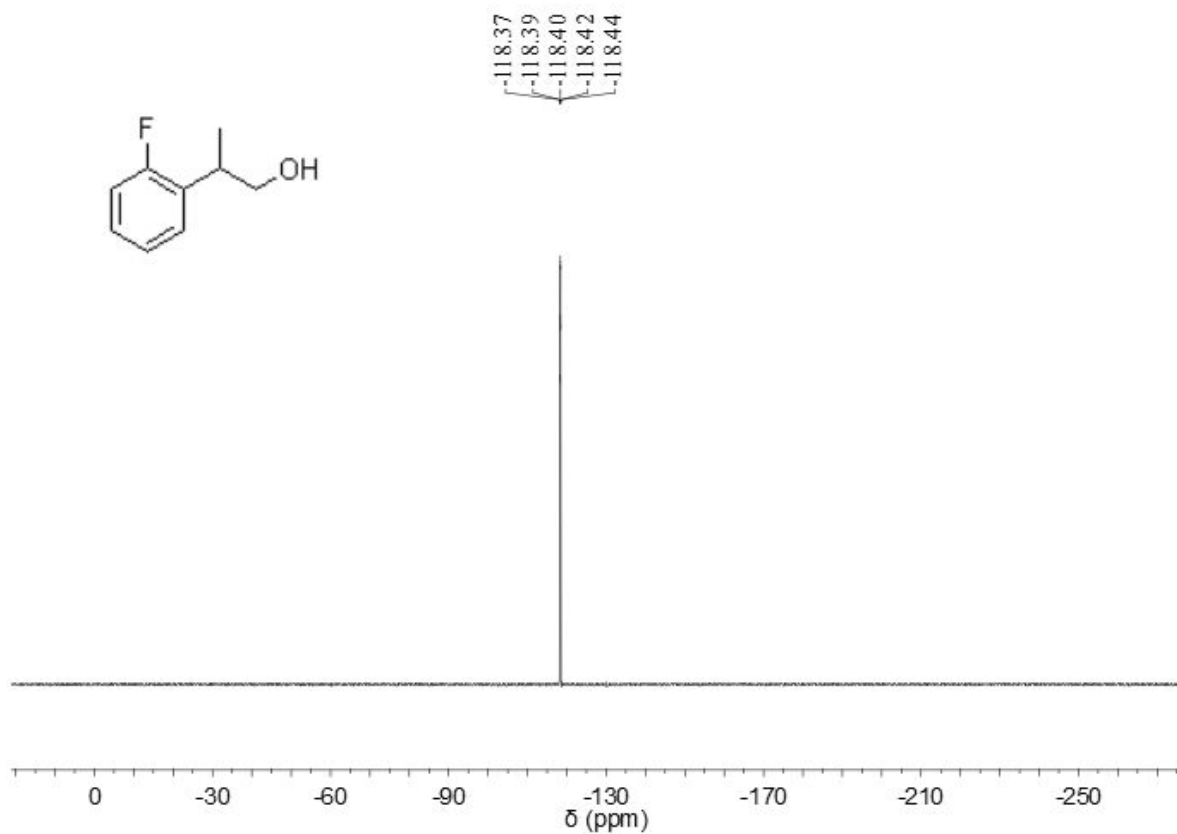


Figure S35. ^{19}F NMR (376 MHz, CDCl_3 , 298 K) spectrum of **15**.

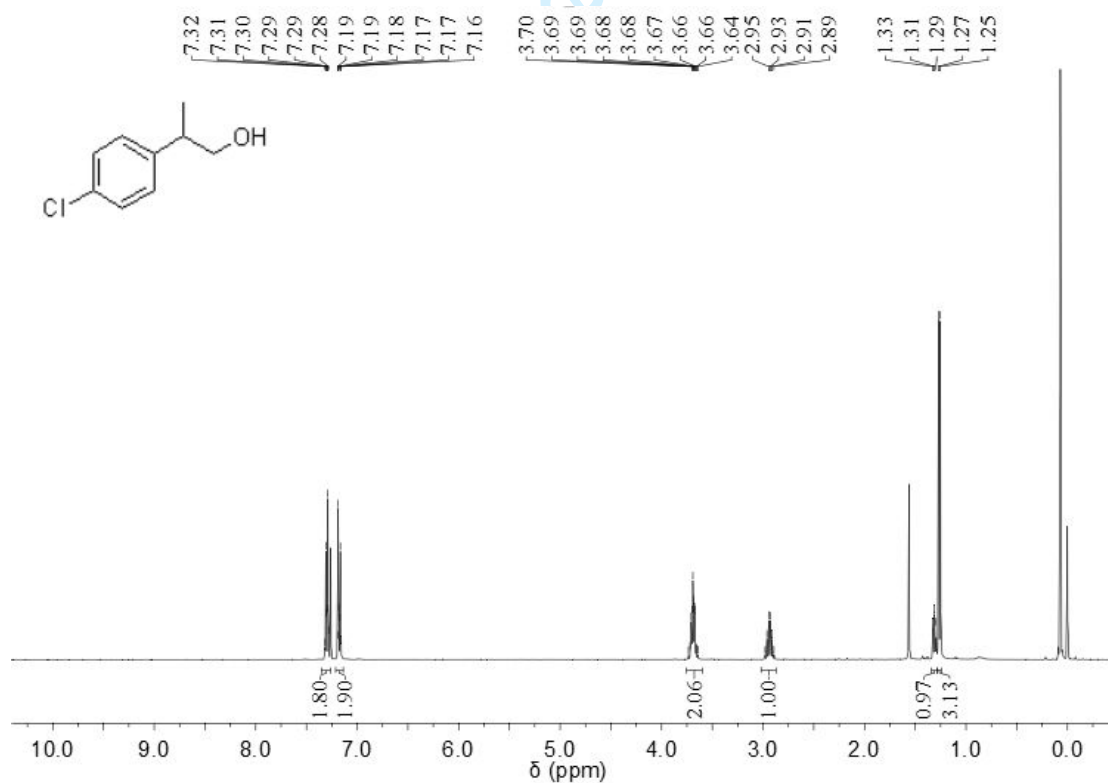


Figure S36. ^1H NMR (400 MHz, CDCl_3 , 298 K) spectrum of **16**.

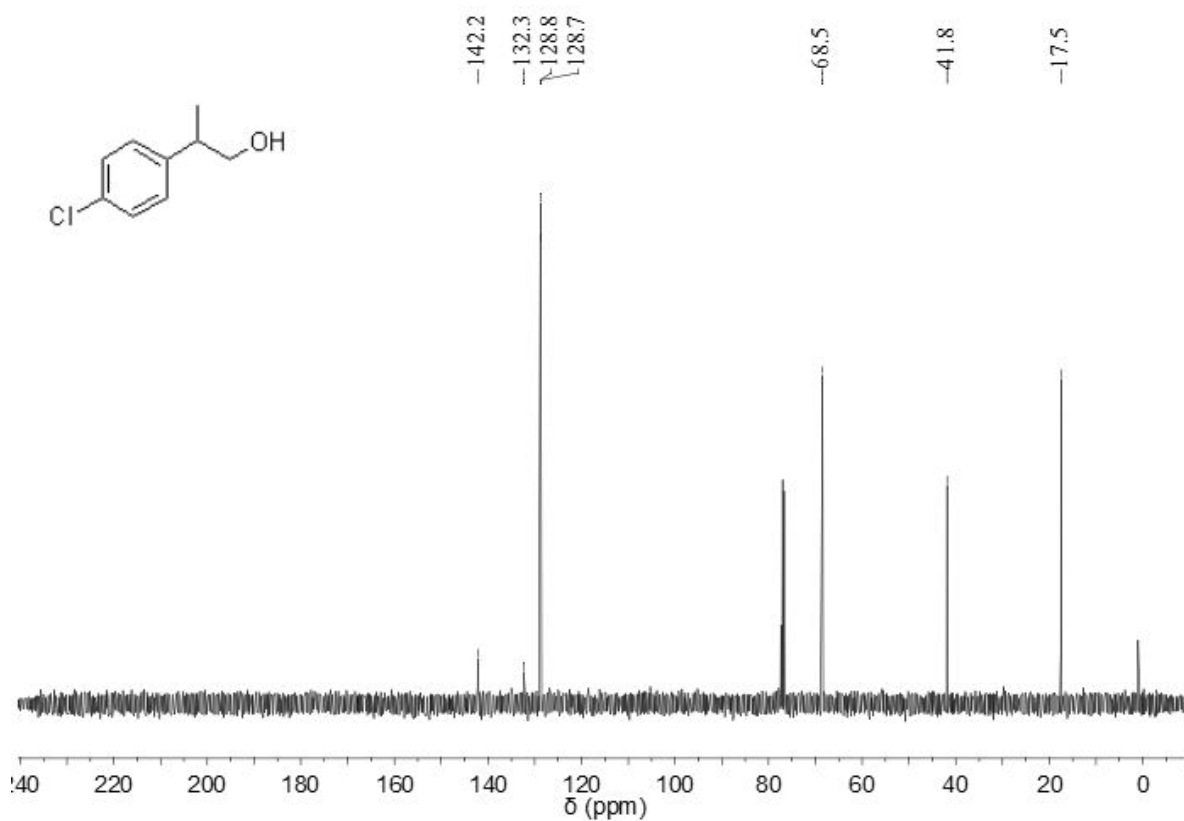


Figure S37. ¹³C NMR (101 MHz, CDCl₃, 298 K) spectrum of **16**.

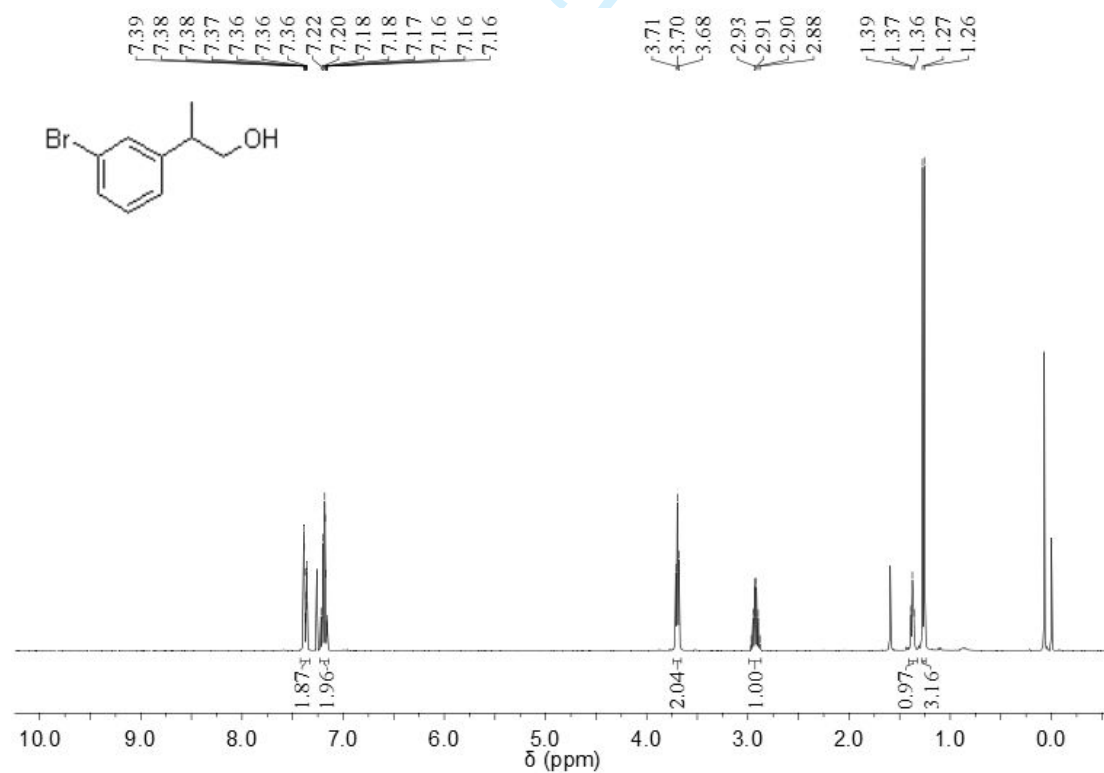


Figure S38. ¹H NMR (400 MHz, CDCl₃, 298 K) spectrum of **17**.

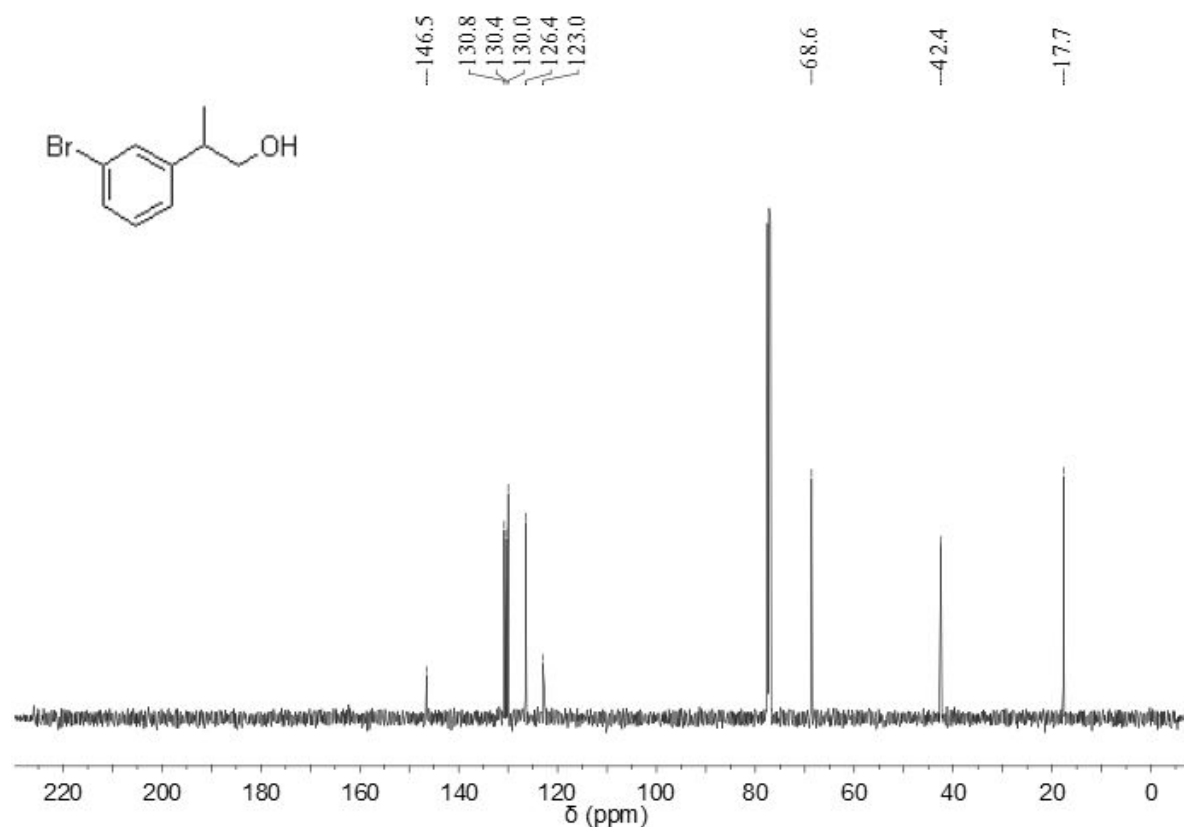


Figure S39. ¹³C NMR (101 MHz, CDCl₃, 298 K) spectrum of **17**.

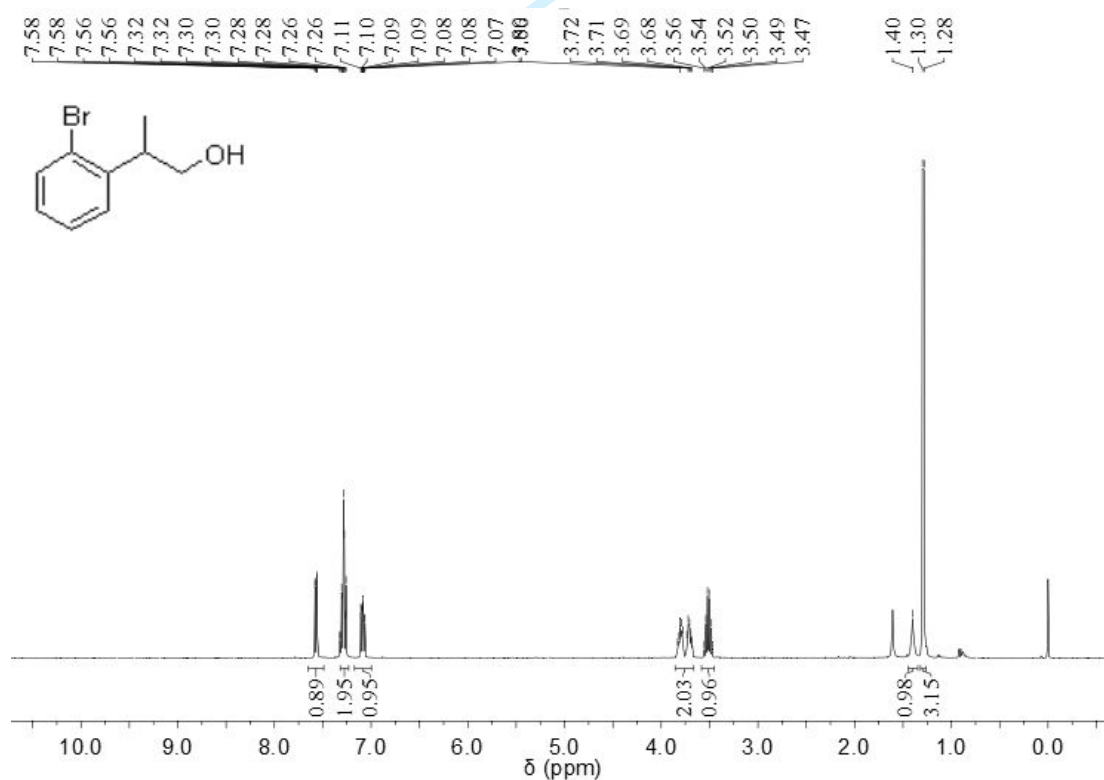


Figure S40. ¹H NMR (400 MHz, CDCl₃, 298 K) spectrum of **18**.

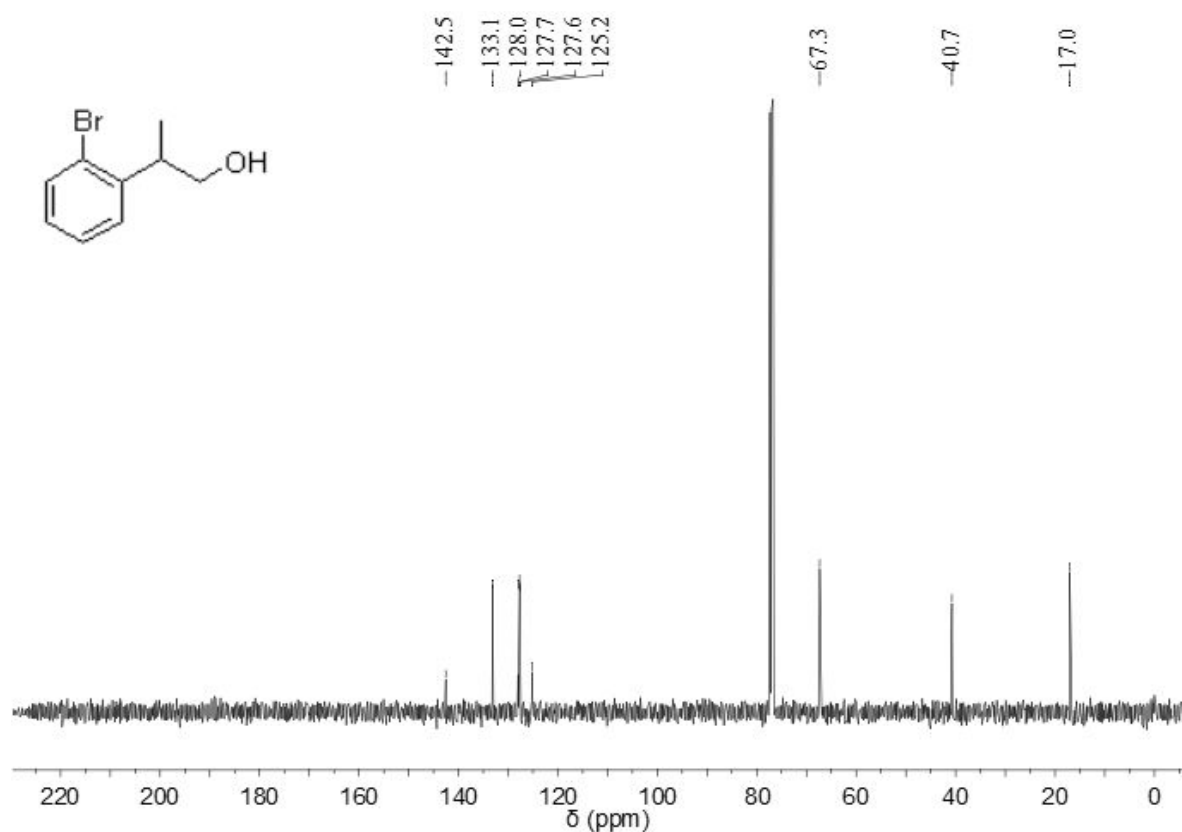


Figure S41. ^{13}C NMR (101 MHz, CDCl_3 , 298 K) spectrum of **18**.

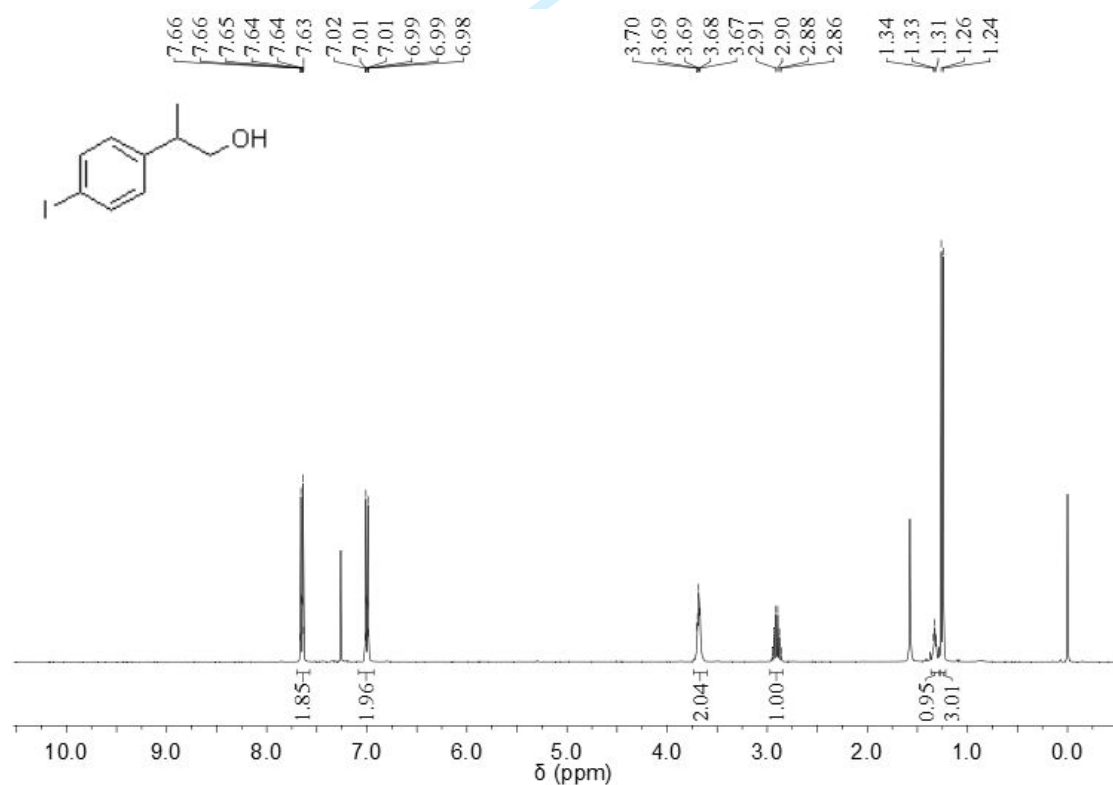


Figure S42. ^1H NMR (400 MHz, CDCl_3 , 298 K) spectrum of **19**.

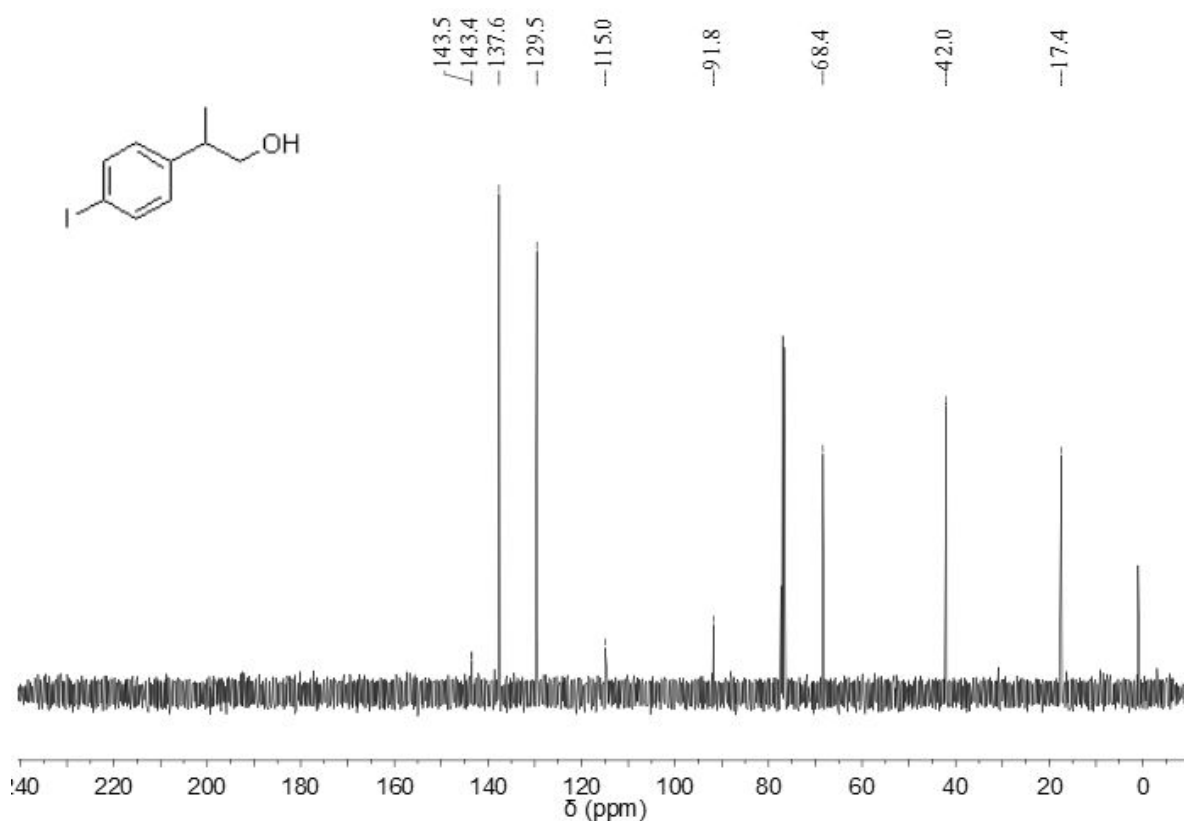


Figure S43. ¹³C NMR (101 MHz, CDCl₃, 298 K) spectrum of **19**.

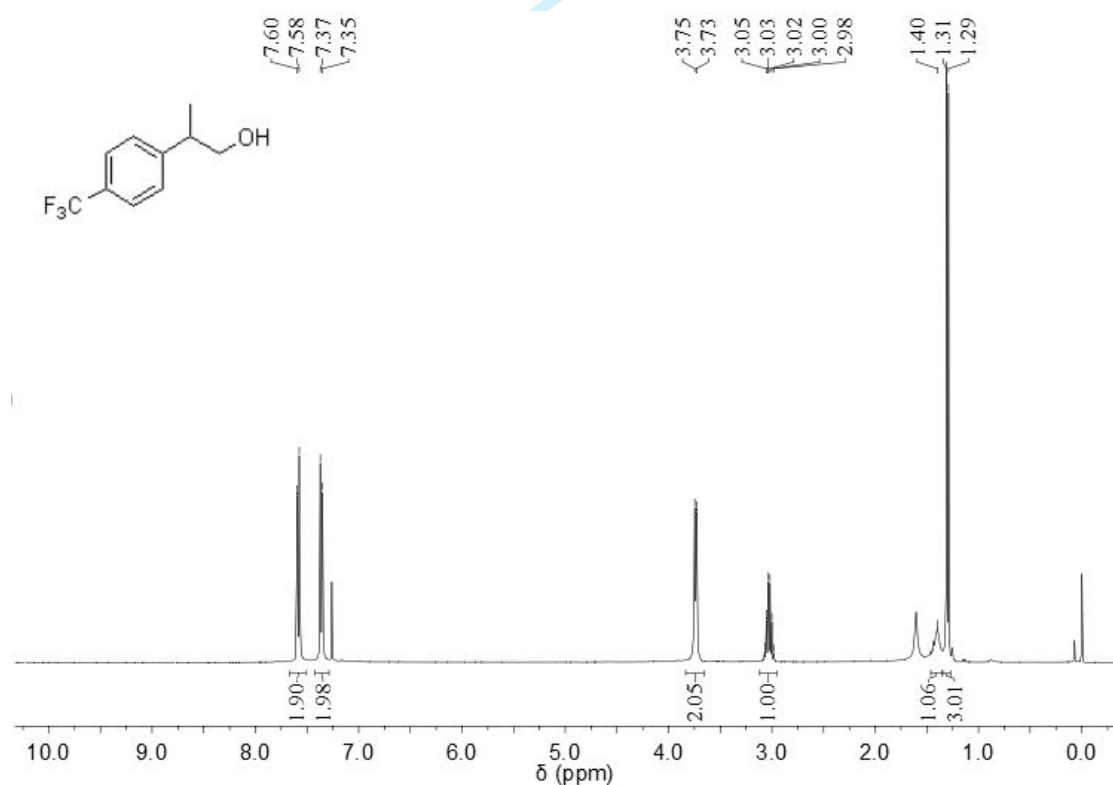


Figure S44. ¹H NMR (400 MHz, CDCl₃, 298 K) spectrum of **20**.

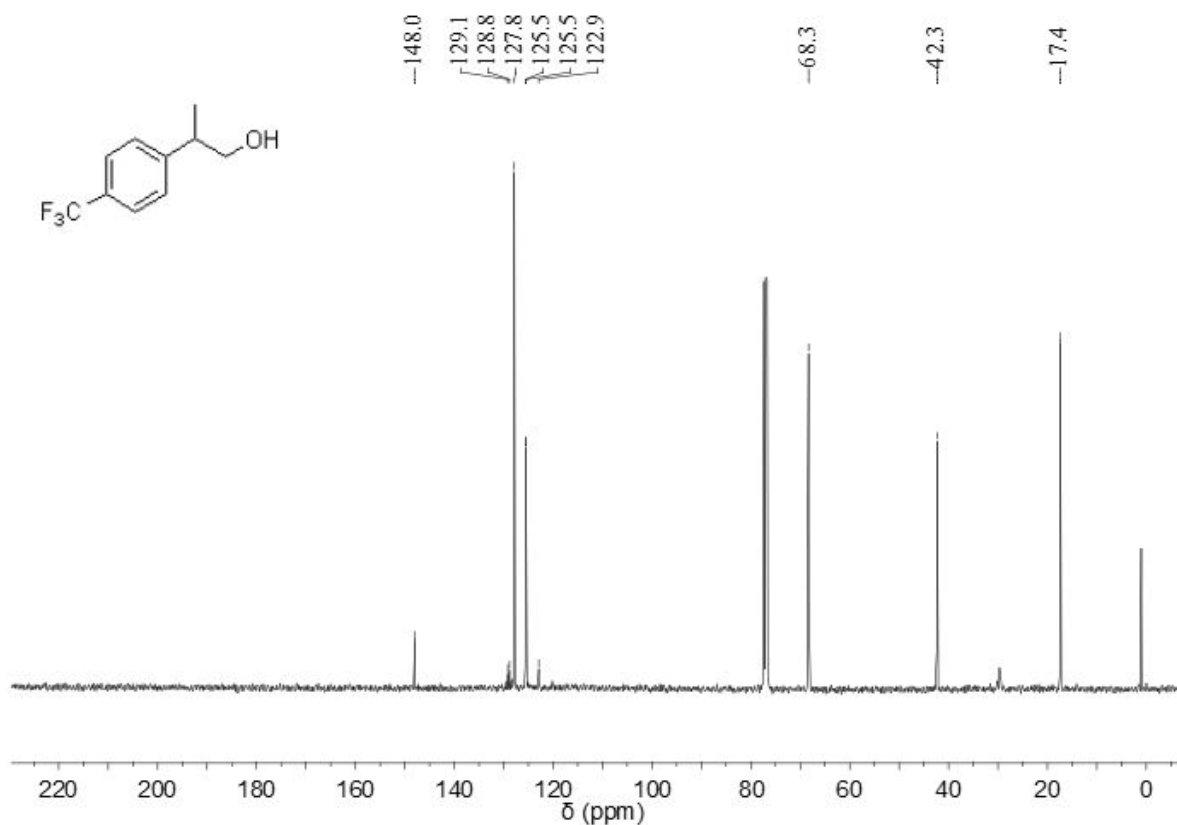


Figure S45. ¹³C NMR (101 MHz, CDCl₃, 298 K) spectrum of **20**.

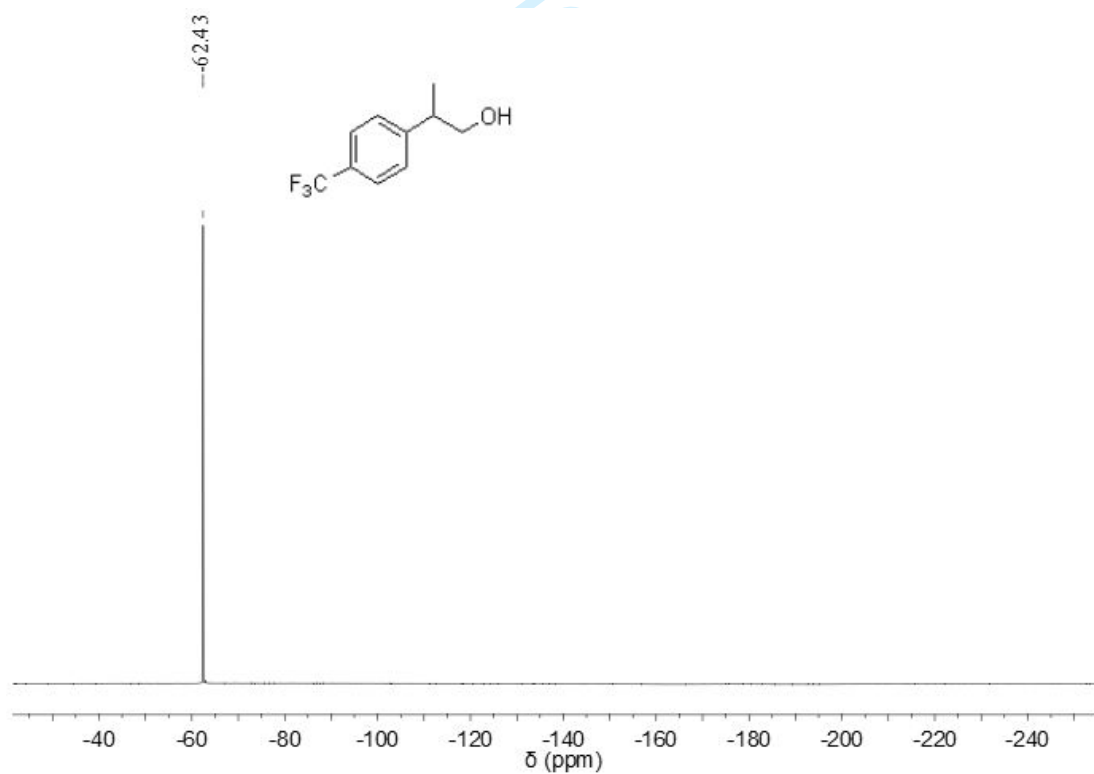


Figure S46. ¹⁹F NMR (376 MHz, CDCl₃, 298 K) spectrum of **20**.

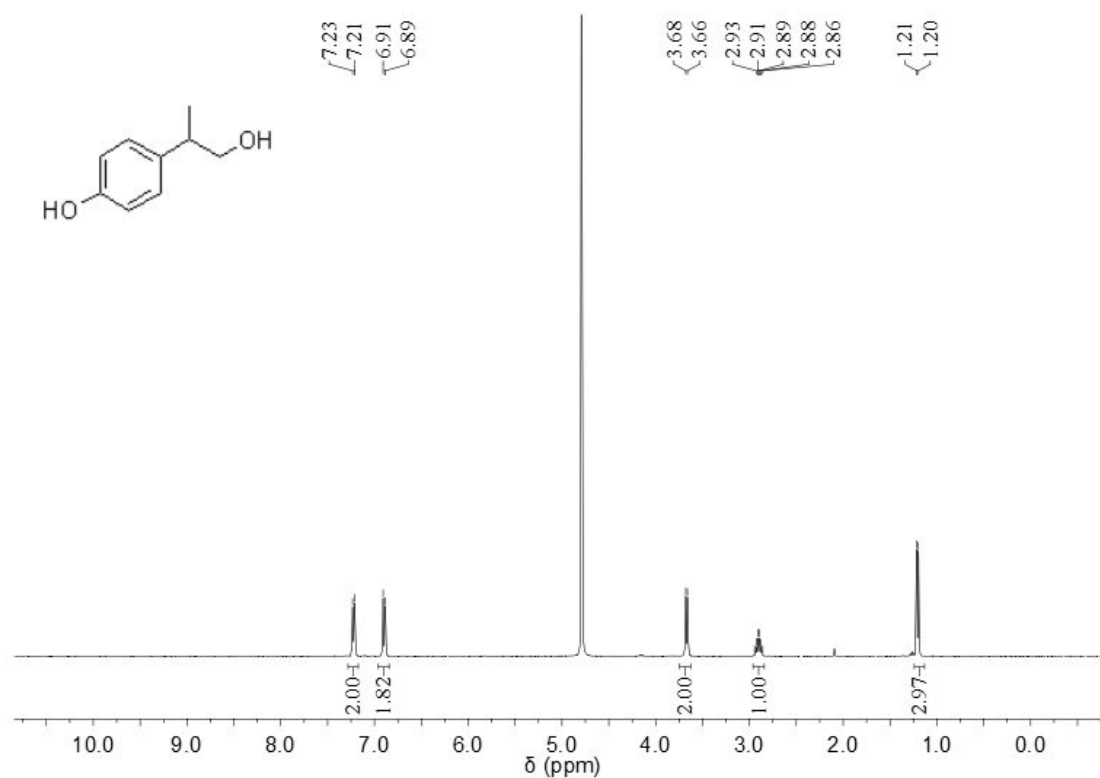


Figure S47. ^1H NMR (400 MHz, D_2O , 298 K) spectrum of **21**.

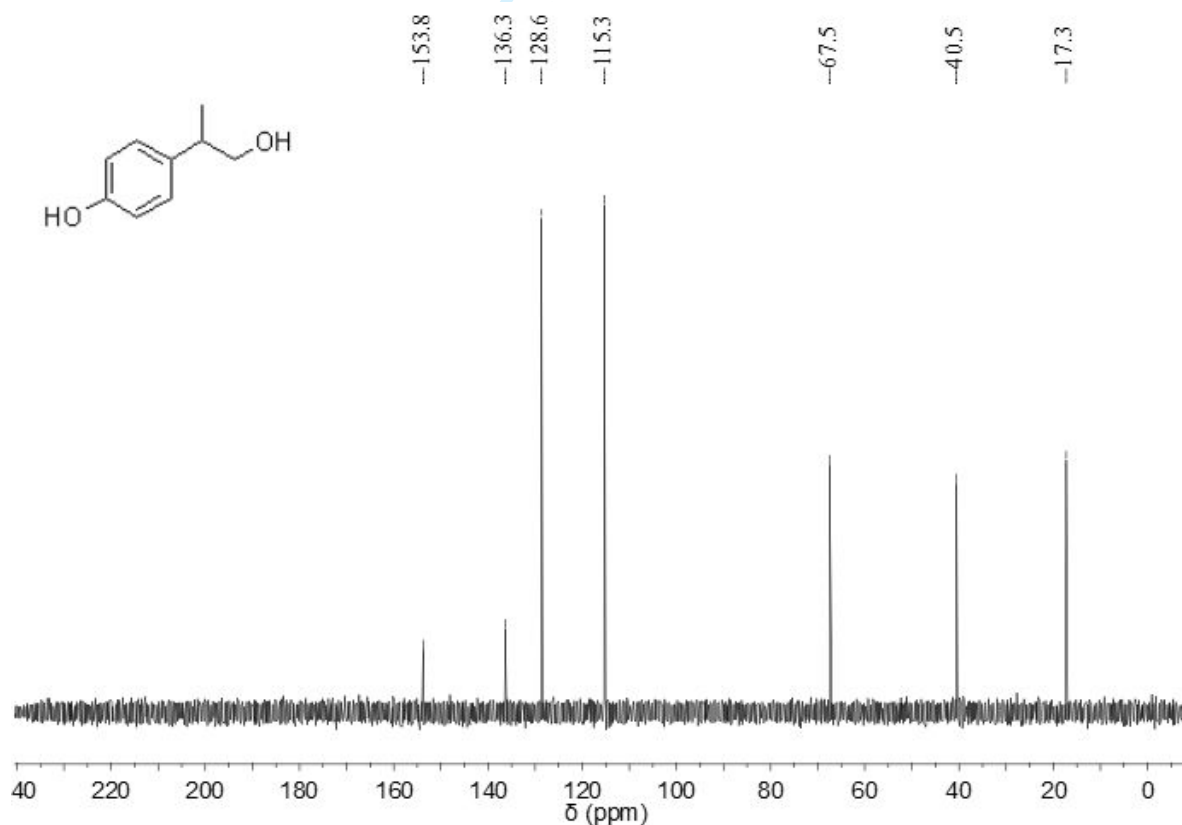


Figure S48. ^{13}C NMR (101 MHz, D_2O , 298 K) spectrum of **21**.

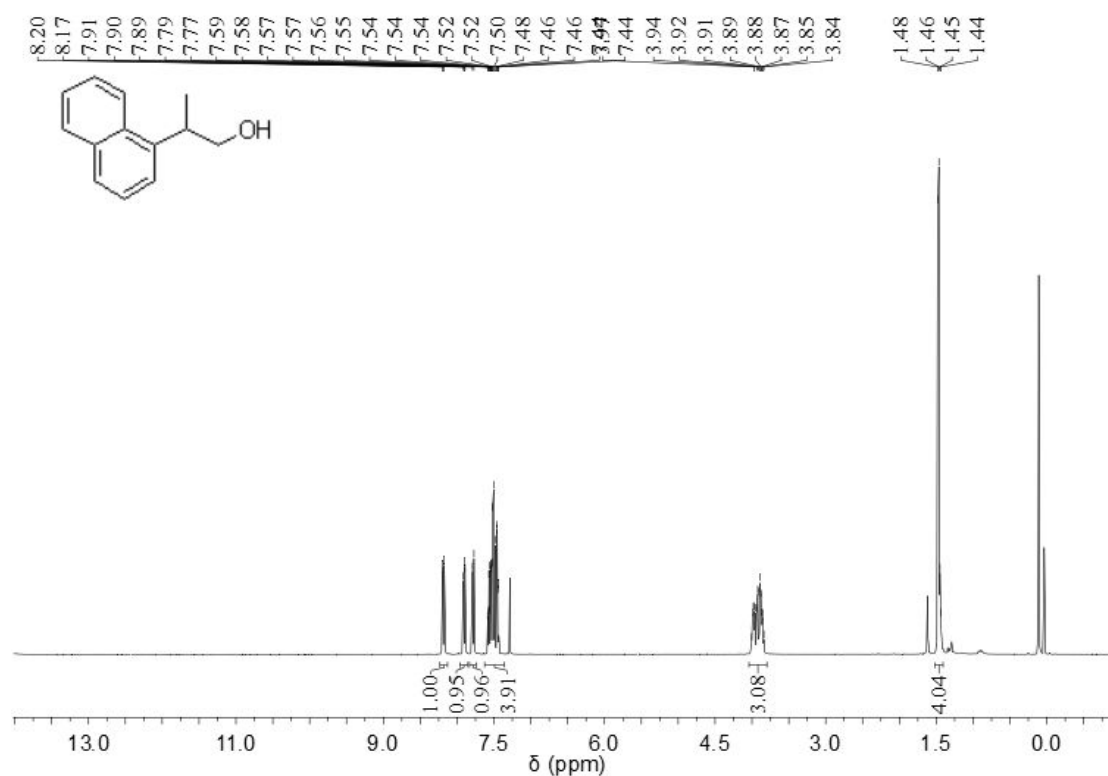


Figure S49. ^1H NMR (400 MHz, CDCl_3 , 298 K) spectrum of **22**.

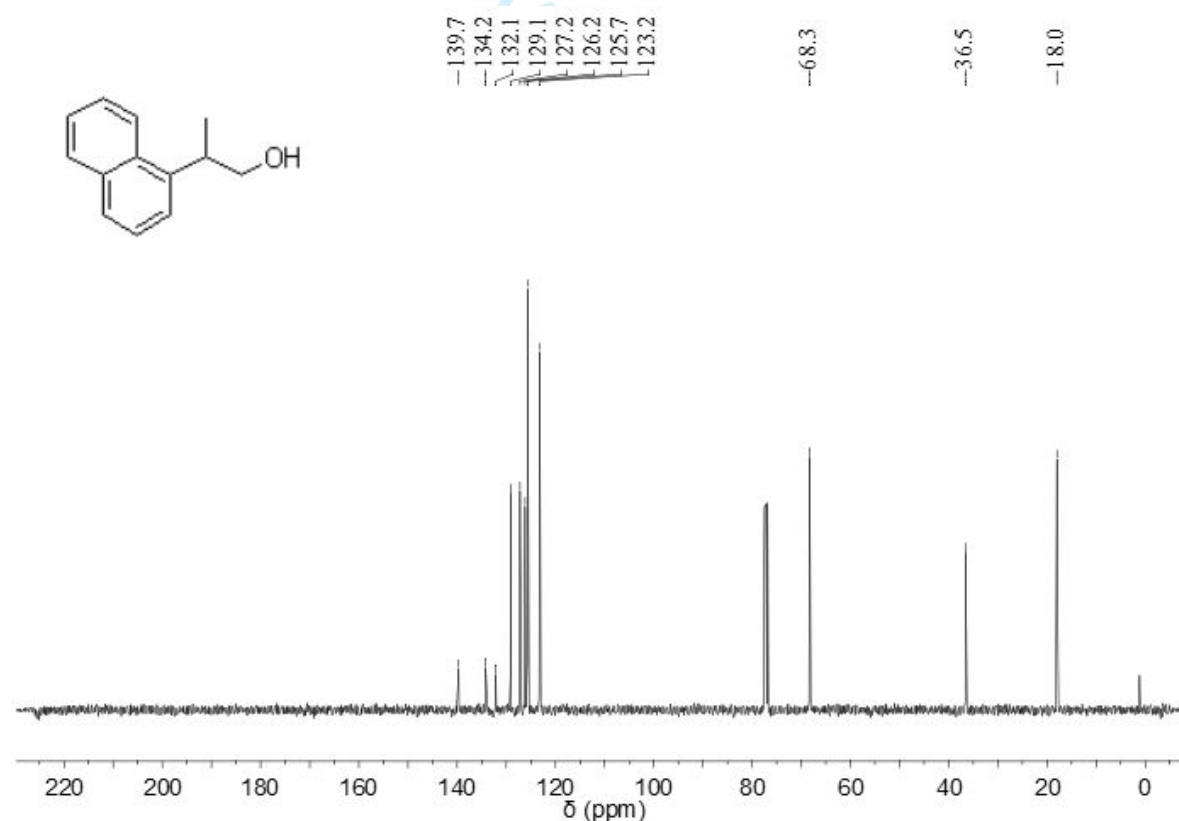


Figure S50. ^{13}C NMR (101 MHz, CDCl_3 , 298 K) spectrum of **22**.

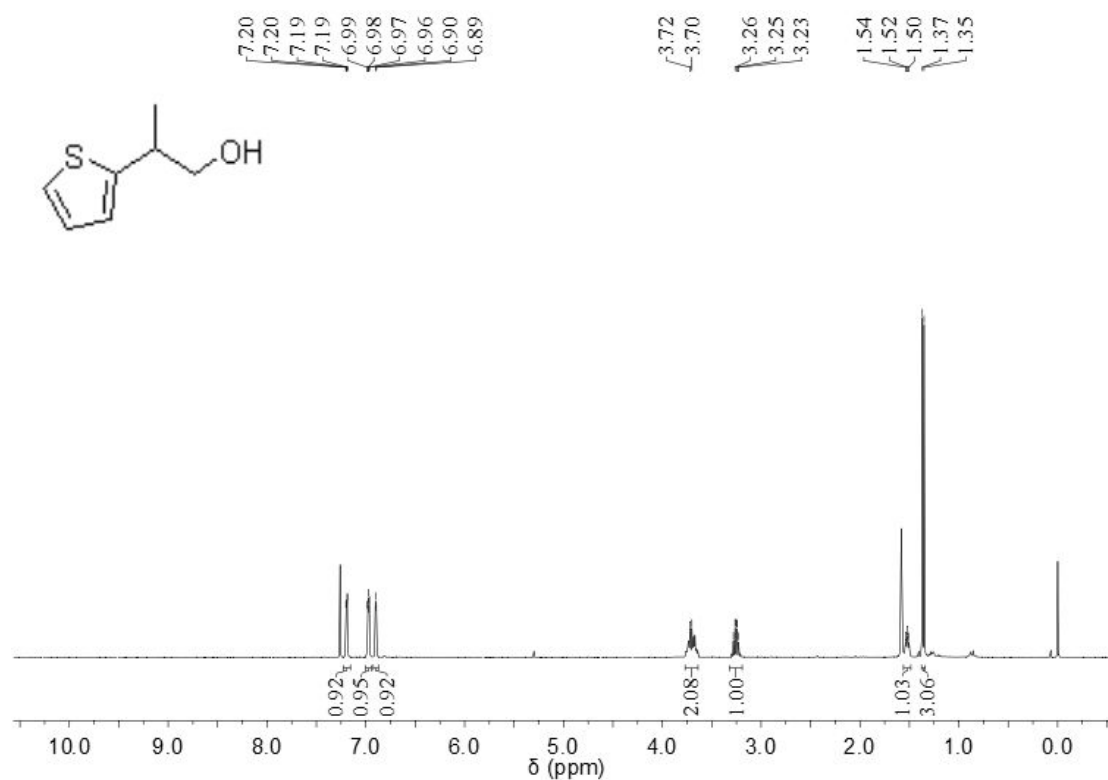


Figure S51. ¹H NMR (400 MHz, CDCl₃, 298 K) spectrum of **23**.

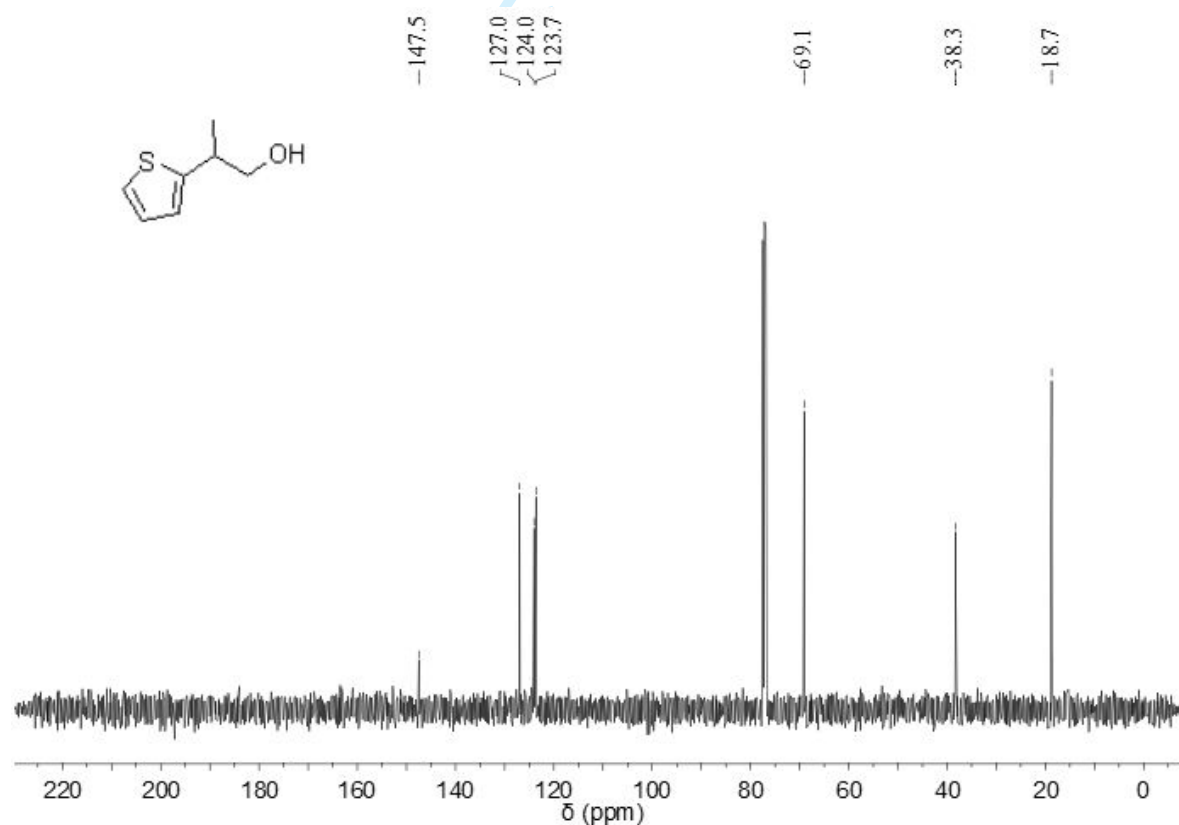


Figure S52. ¹³C NMR (101 MHz, CDCl₃, 298 K) spectrum of **23**.

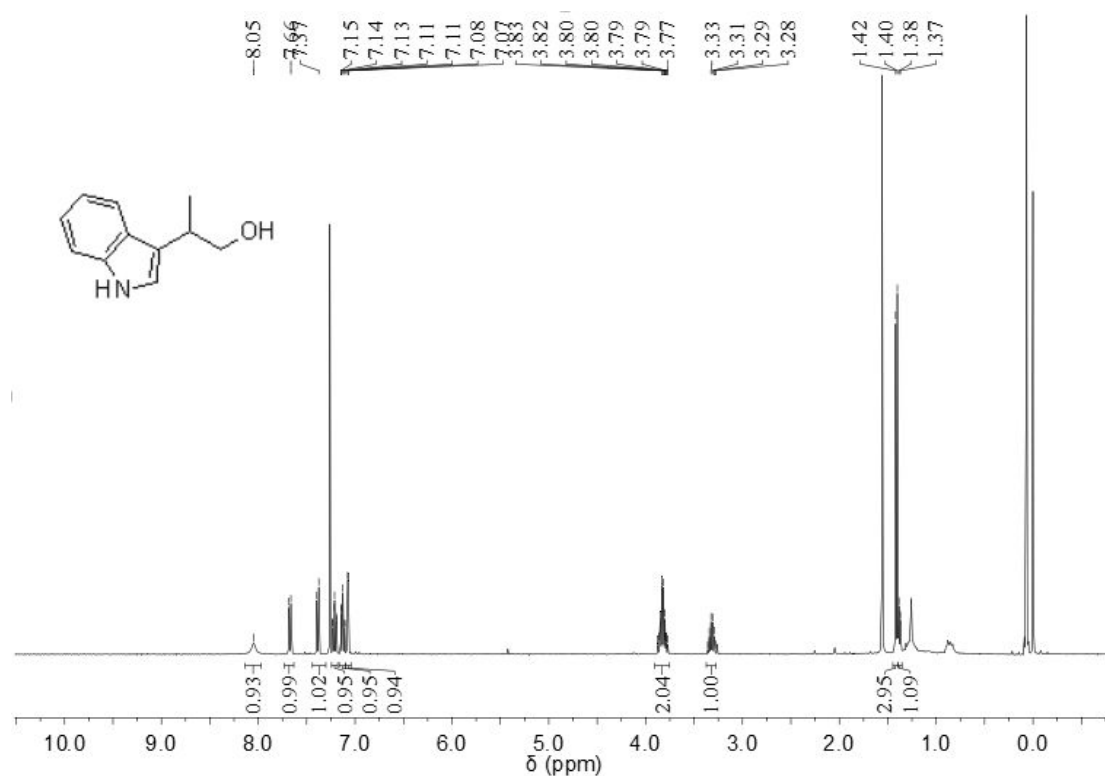


Figure S53. ¹H NMR (400 MHz, CDCl₃, 298 K) spectrum of **24**.

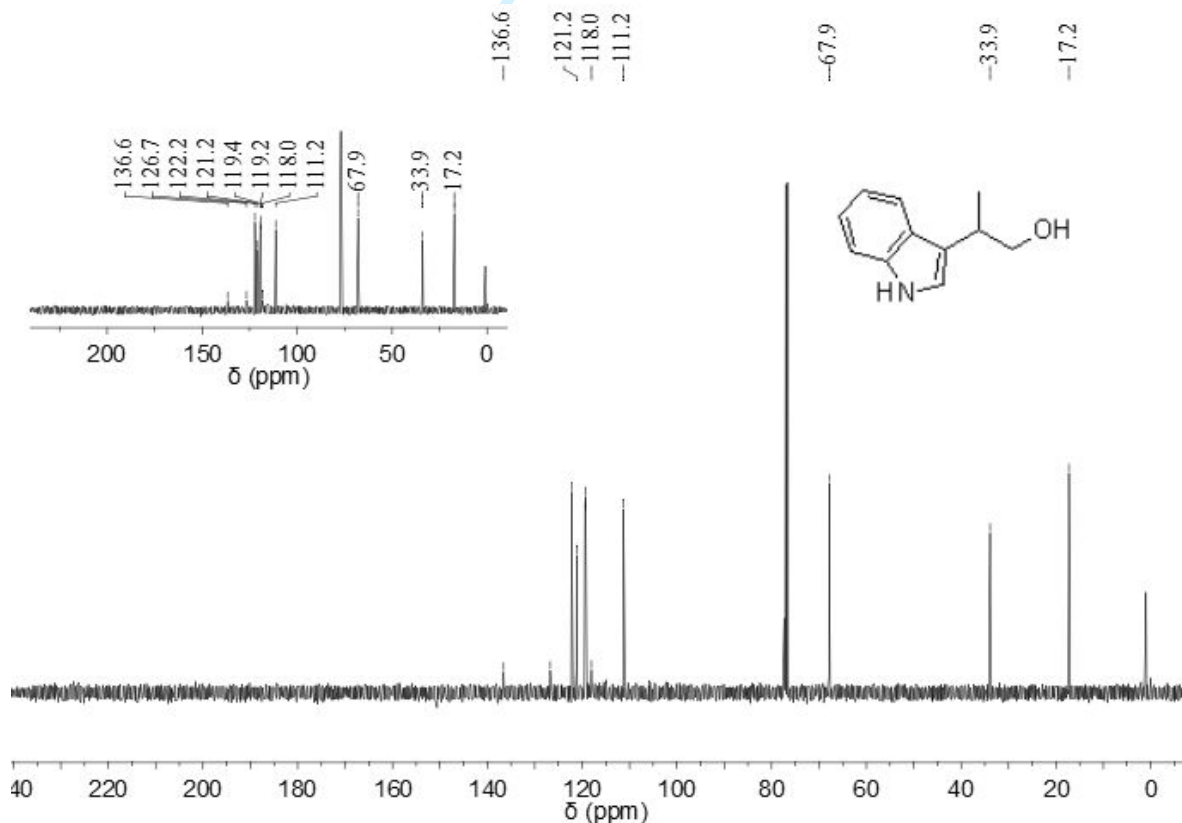


Figure S54. ¹³C NMR (101 MHz, CDCl₃, 298 K) spectrum of **24**.

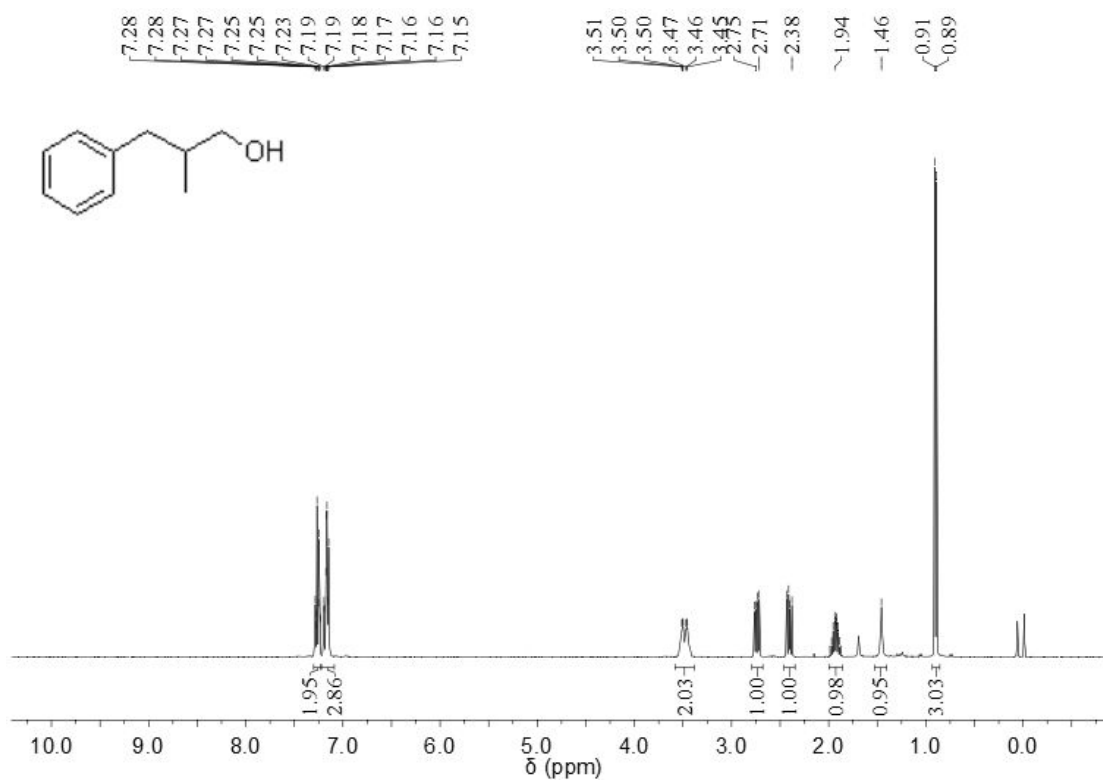


Figure S55. ¹H NMR (400 MHz, CDCl₃, 298 K) spectrum of **25**.

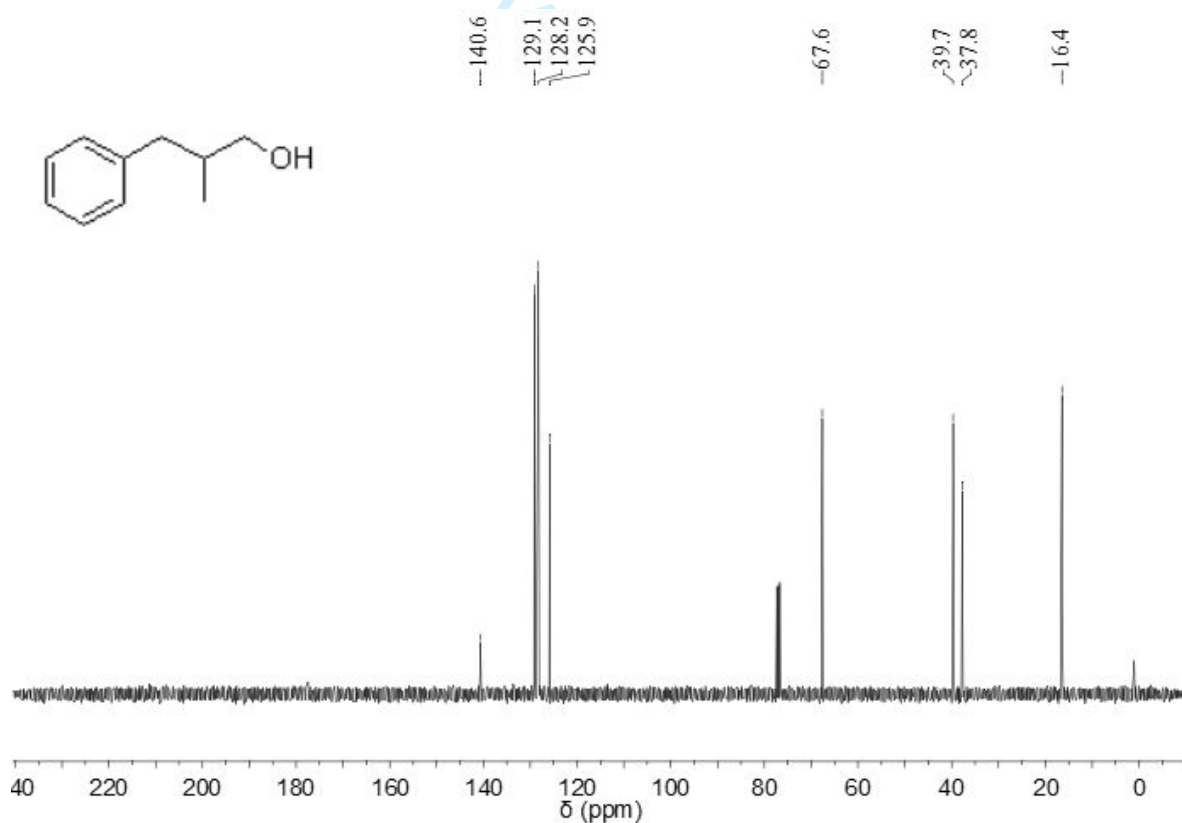


Figure S56. ¹³C NMR (101 MHz, CDCl₃, 298 K) spectrum of **25**.

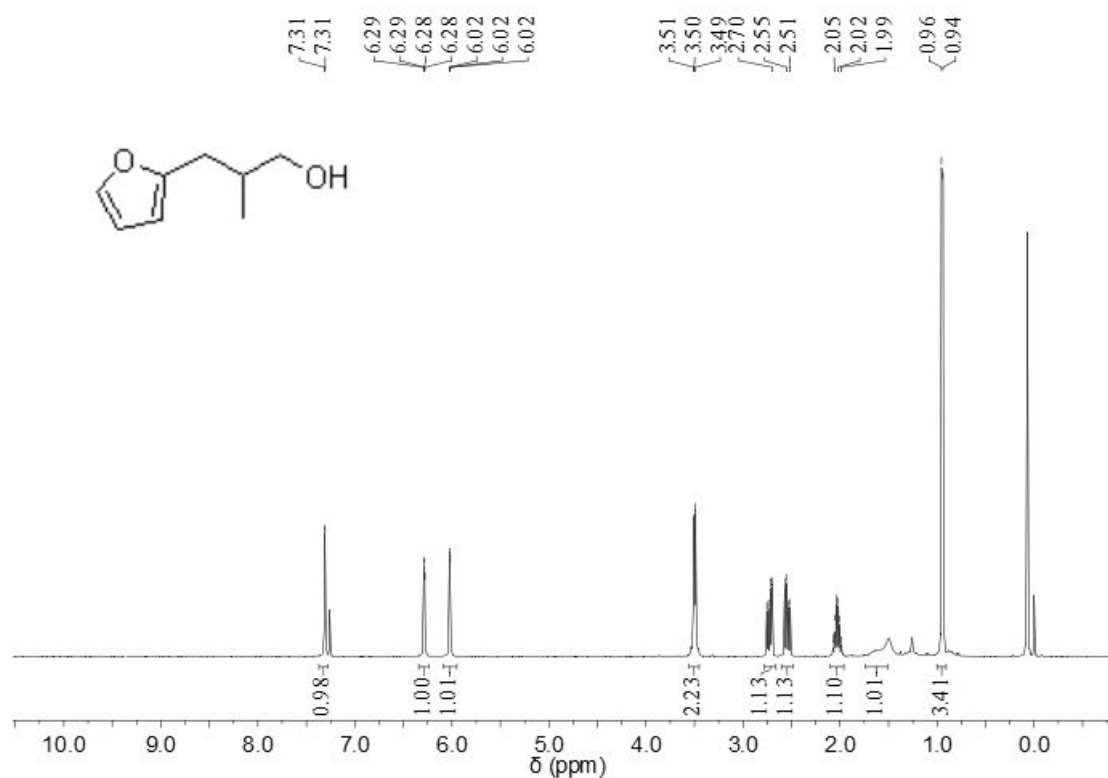


Figure S57. ¹H NMR (400 MHz, CDCl₃, 298 K) spectrum of **26**.

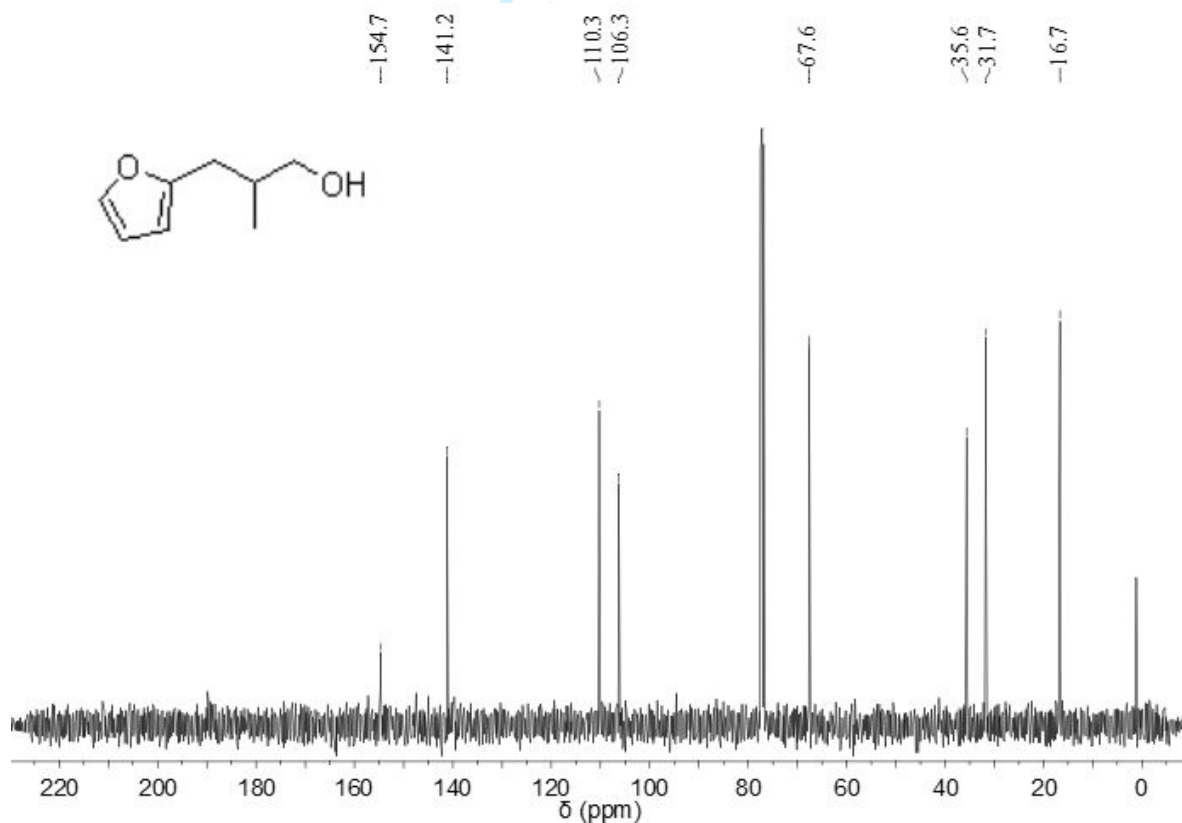


Figure S58. ¹³C NMR (101 MHz, CDCl₃, 298 K) spectrum of **26**.

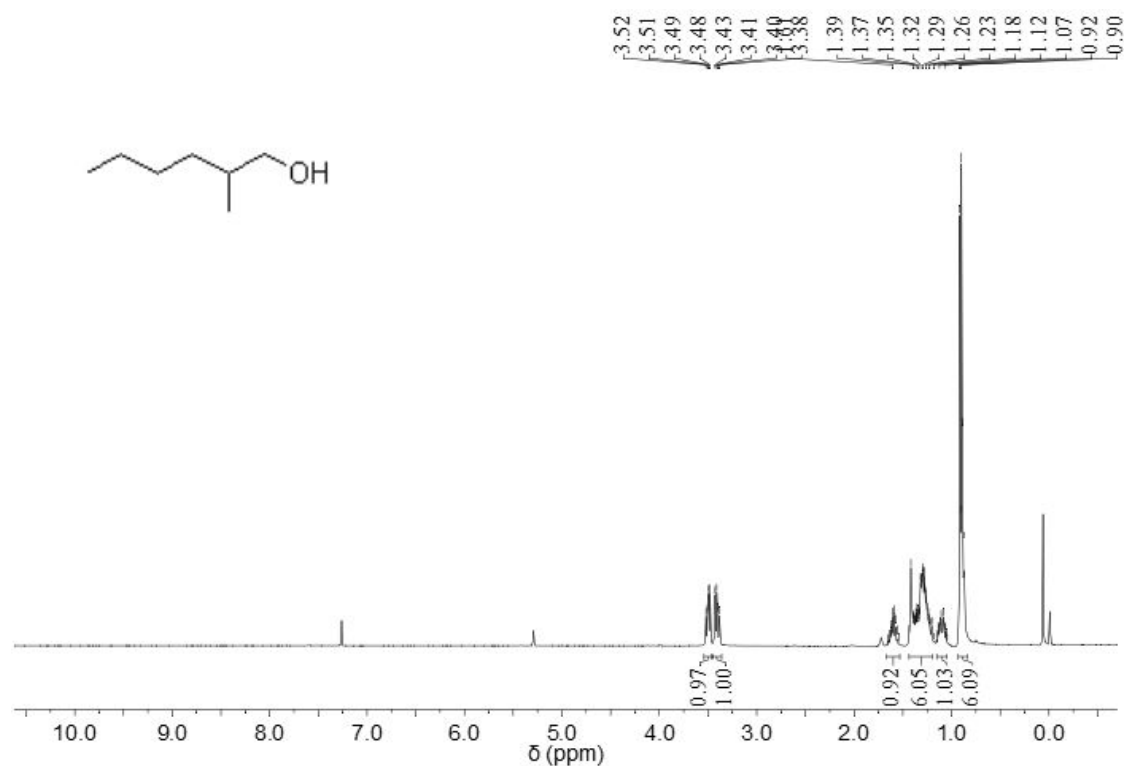


Figure S59. ^1H NMR (400 MHz, CDCl_3 , 298 K) spectrum of **27**.

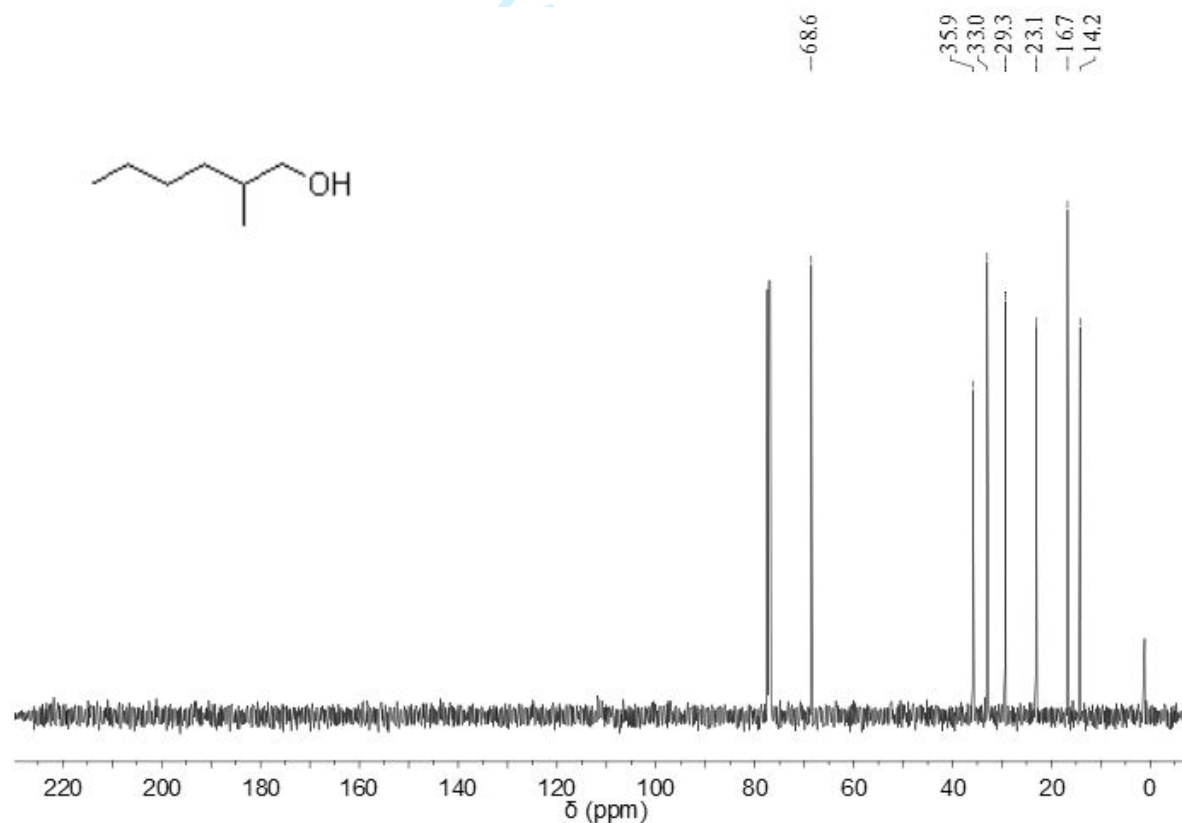
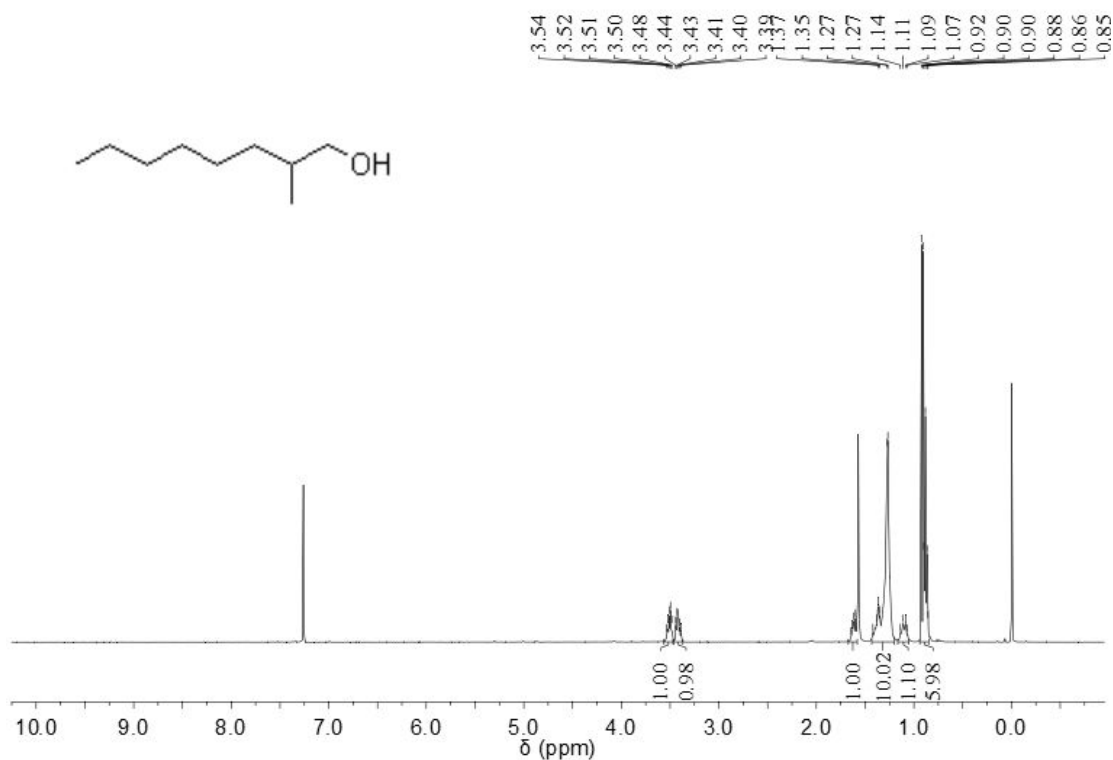


Figure S60. ^{13}C NMR (101 MHz, CDCl_3 , 298 K) spectrum of **27**.



28
29
30
31
32
33
34
35
36
37
38
39
40
41
42
43
44
45
46
47
48
49
50
51
52
53
54
55

Figure S61. ^1H NMR (400 MHz, CDCl_3 , 298 K) spectrum of **28**.

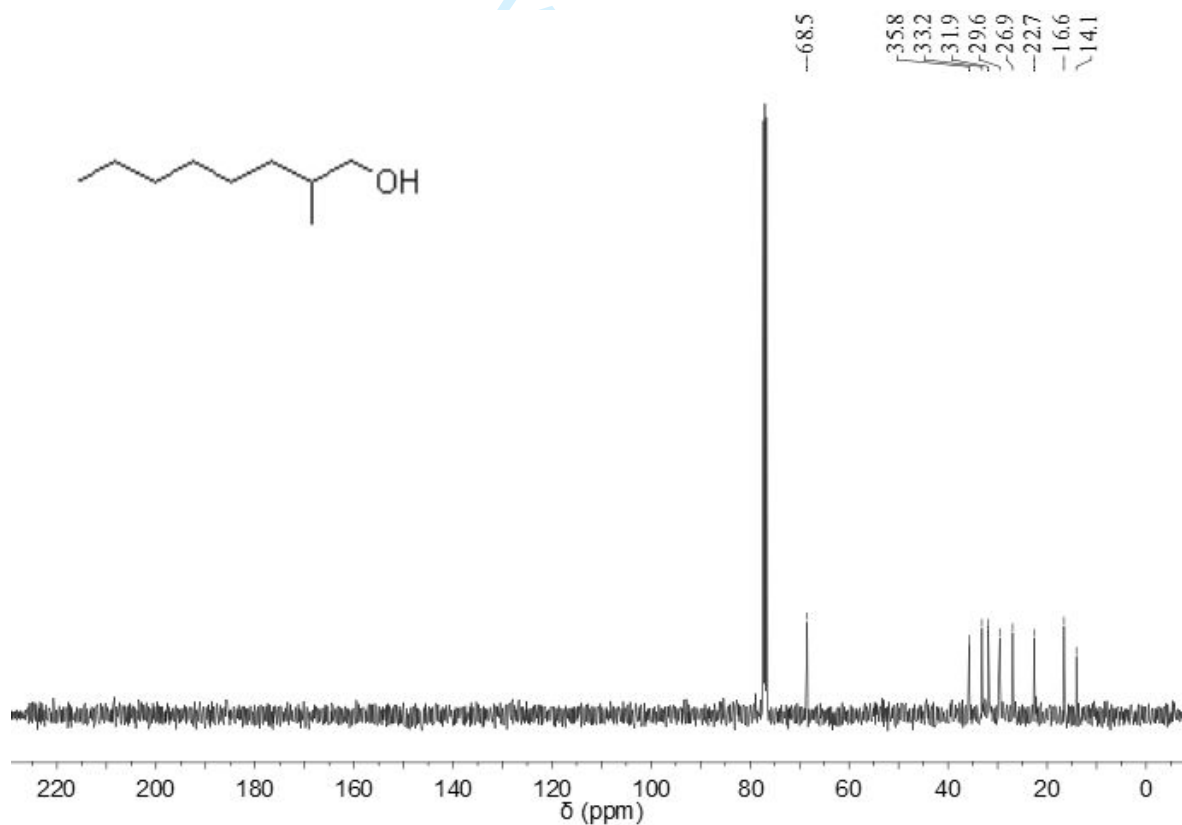


Figure S62. ^{13}C NMR (101 MHz, CDCl_3 , 298 K) spectrum of **28**.

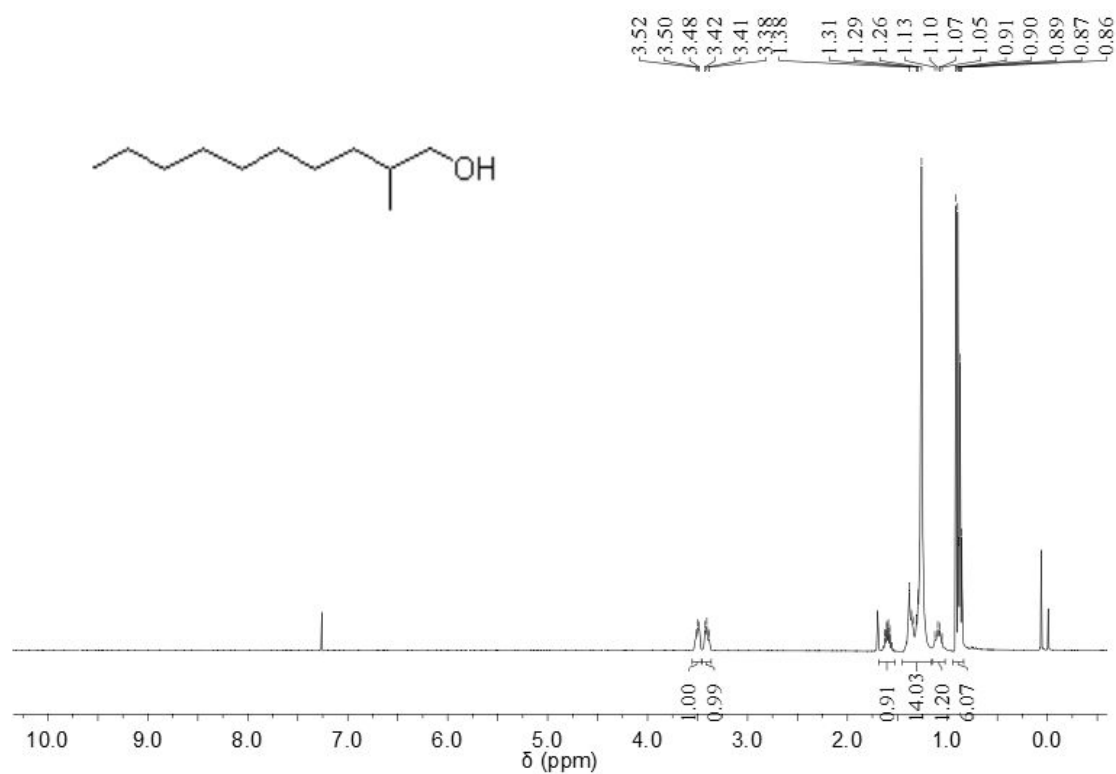


Figure S63. ^1H NMR (400 MHz, CDCl_3 , 298 K) spectrum of **29**.

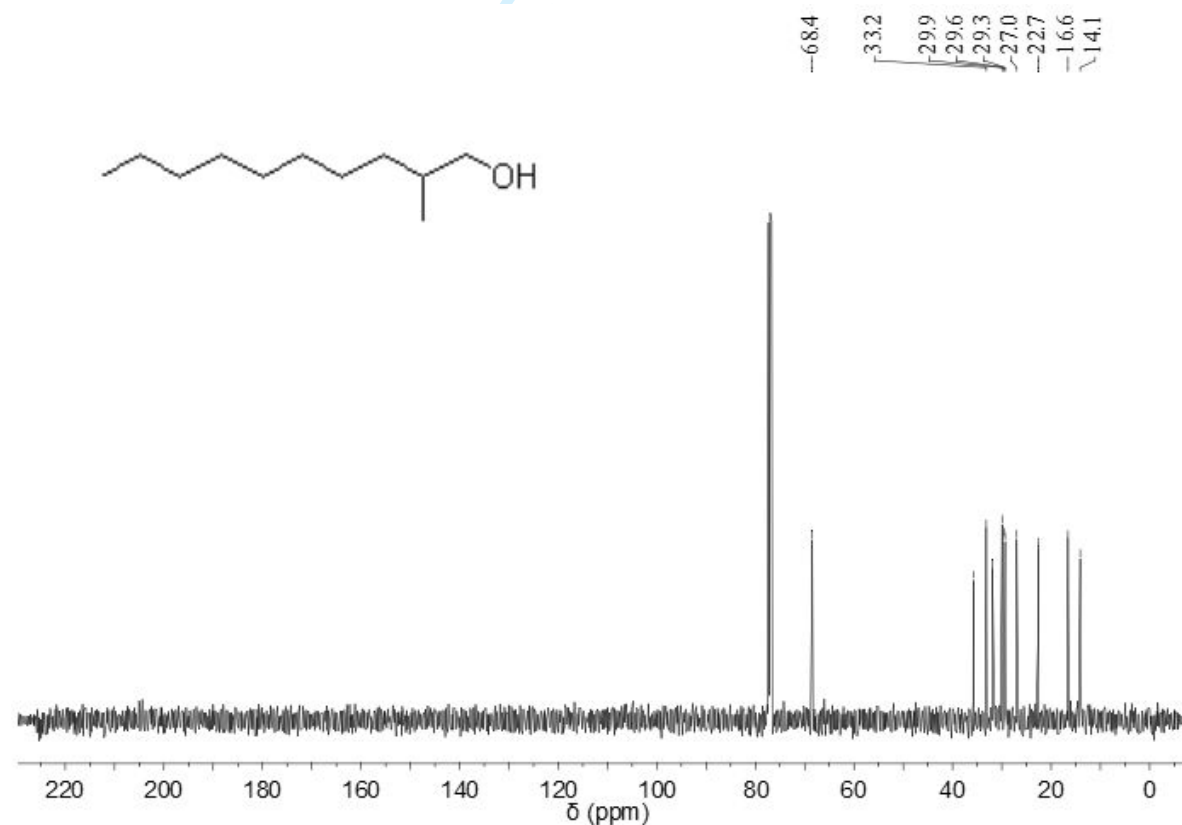


Figure S64. ^{13}C NMR (101 MHz, CDCl_3 , 298 K) spectrum of **29**.

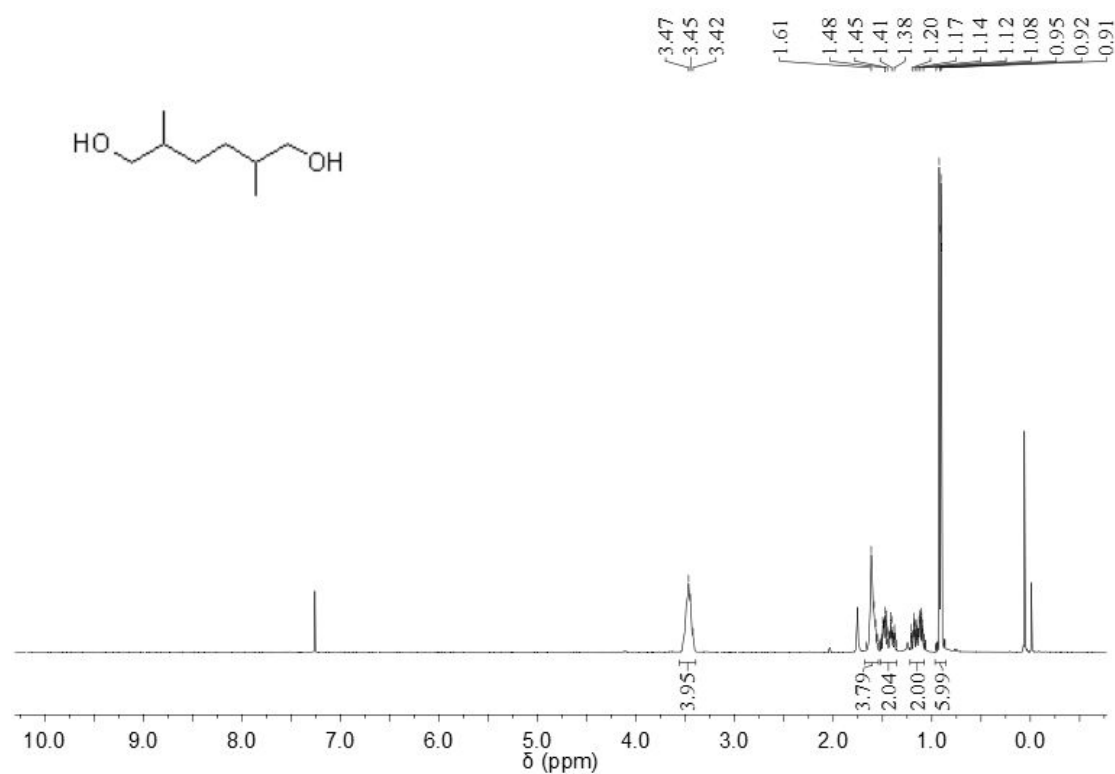


Figure S65. ^1H NMR (400 MHz, CDCl_3 , 298 K) spectrum of **31**.

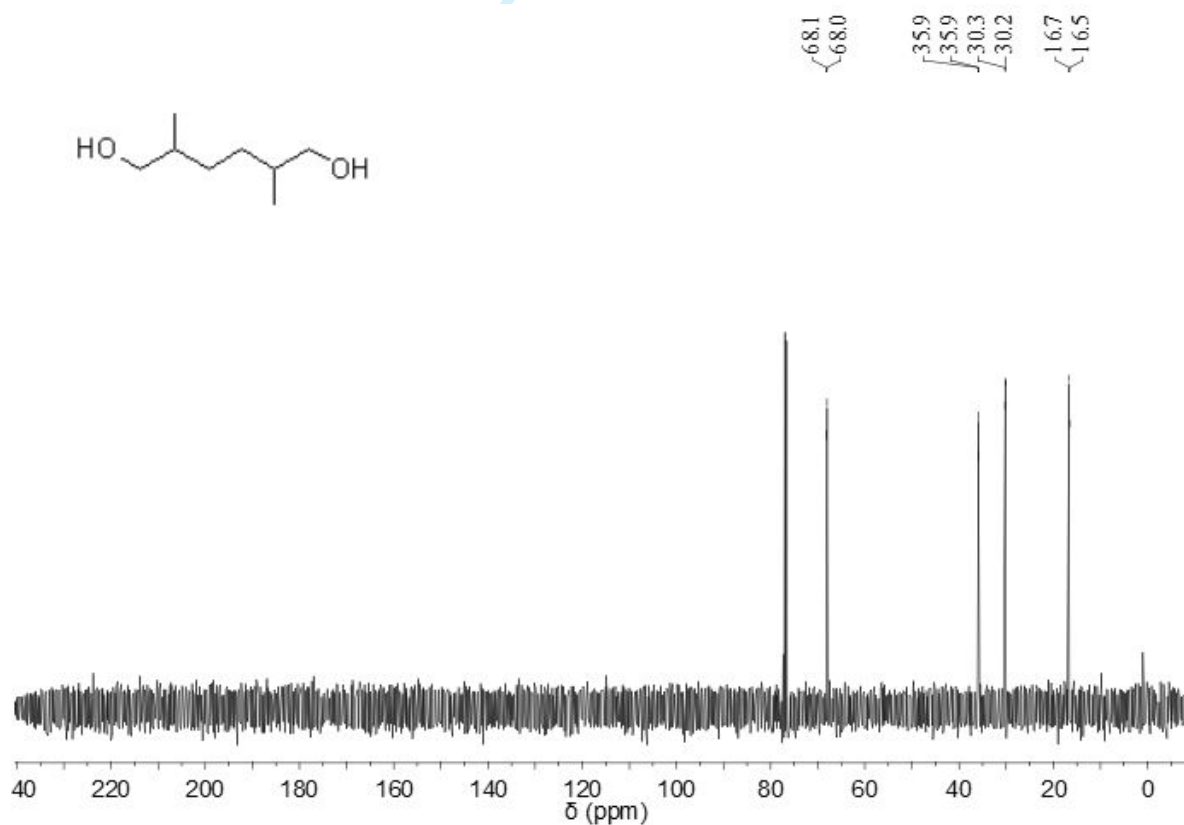


Figure S66. ^{13}C NMR (101 MHz, CDCl_3 , 298 K) spectrum of **31**.

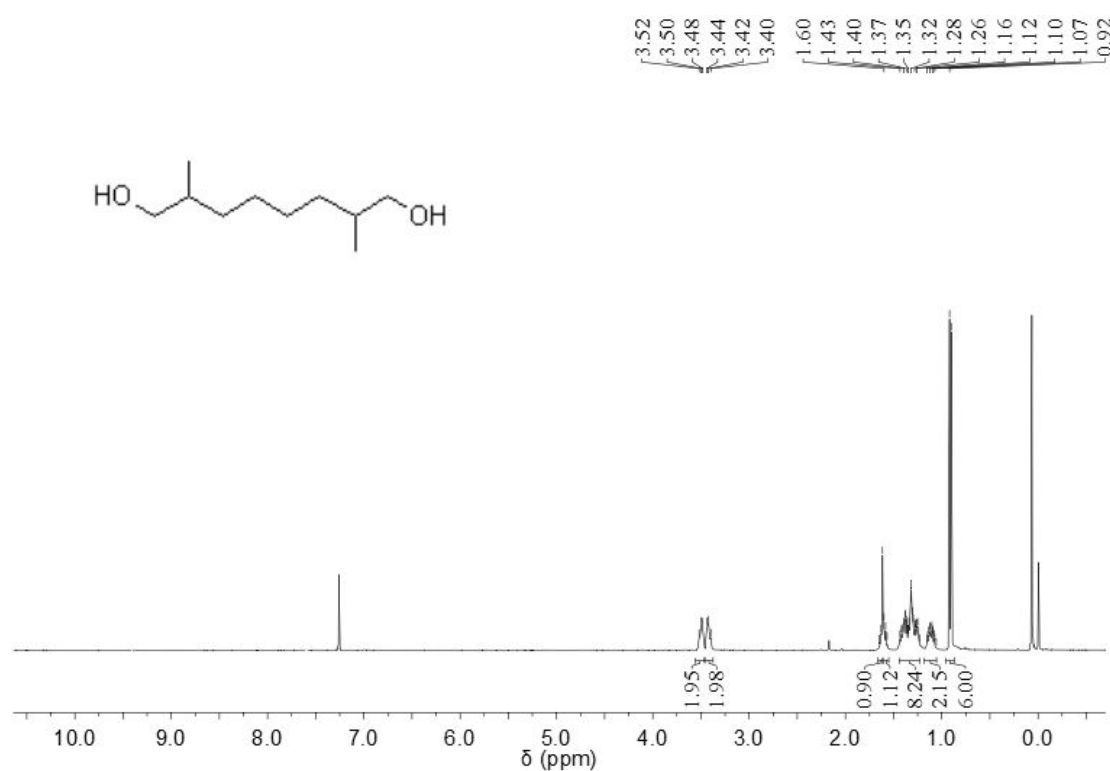


Figure S67. ¹H NMR (400 MHz, CDCl₃, 298 K) spectrum of **32**.

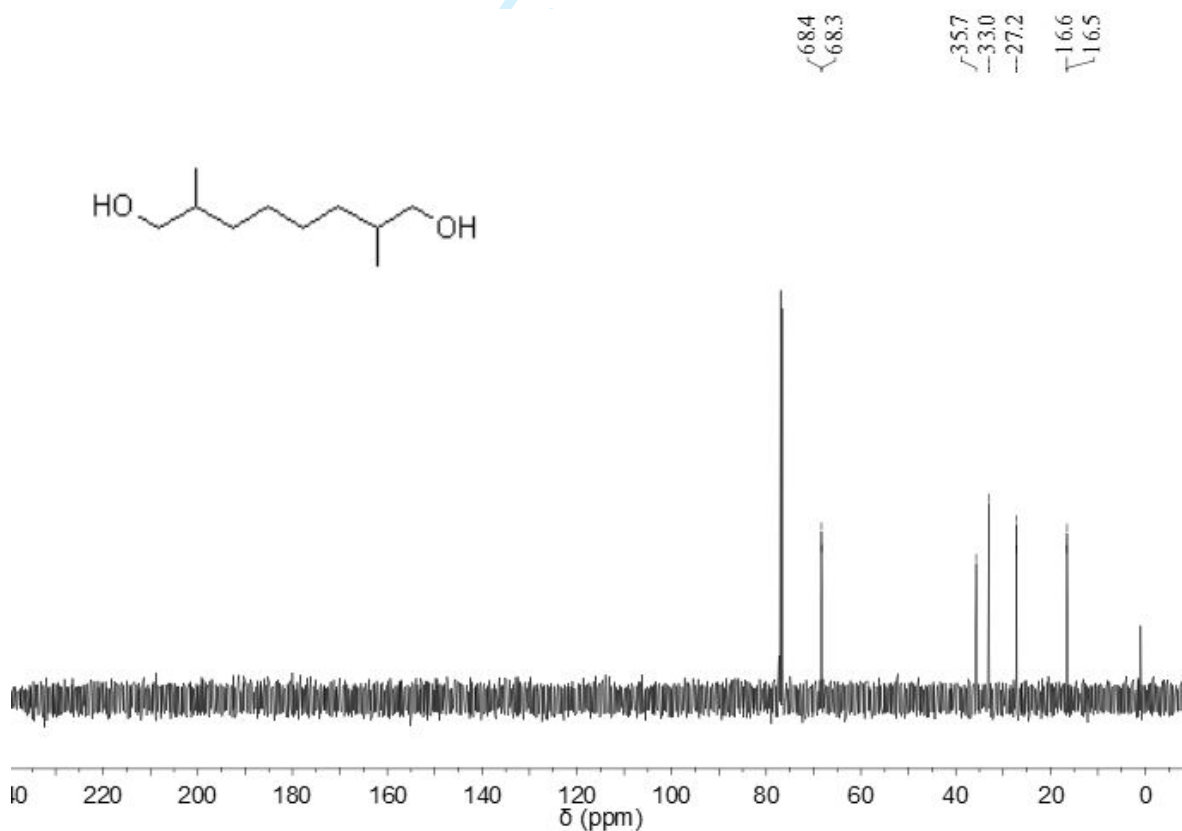


Figure S68. ¹³C NMR (101 MHz, CDCl₃, 298 K) spectrum of **32**.

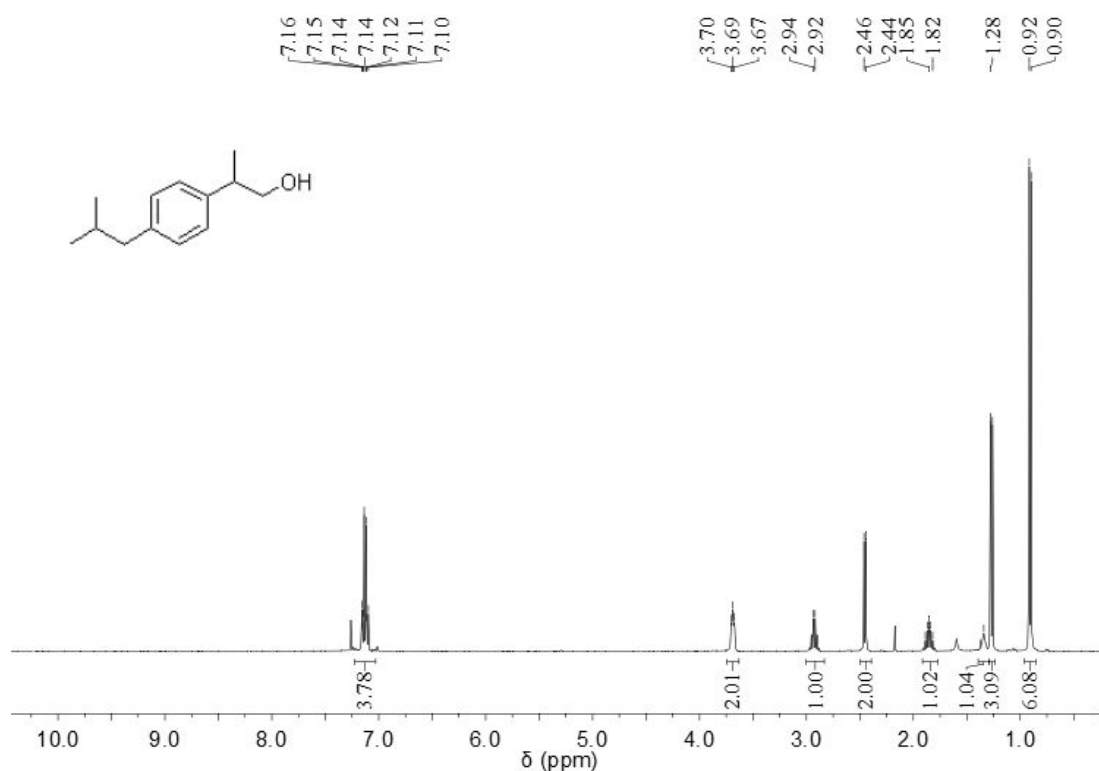


Figure S69. ^1H NMR (400 MHz, CDCl_3 , 298 K) spectrum of **33**.

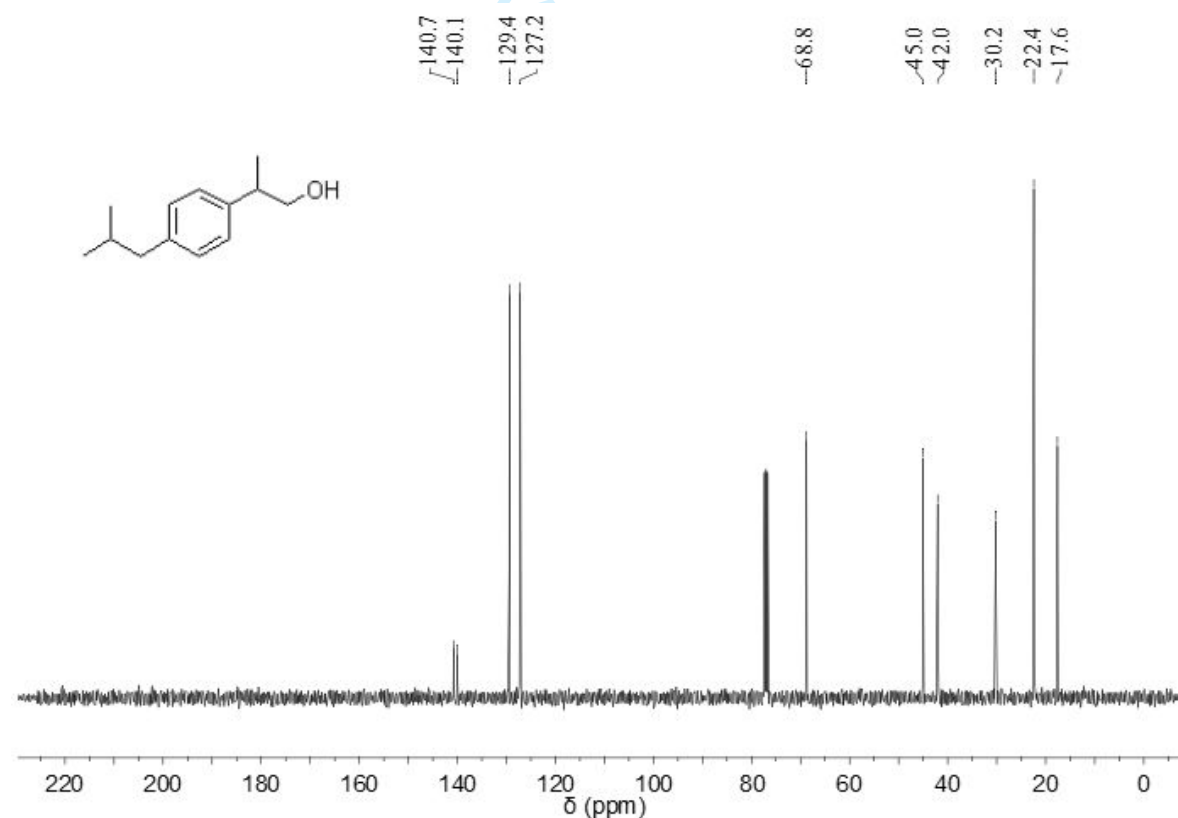


Figure S70. ^{13}C NMR (101 MHz, CDCl_3 , 298 K) spectrum of **33**.

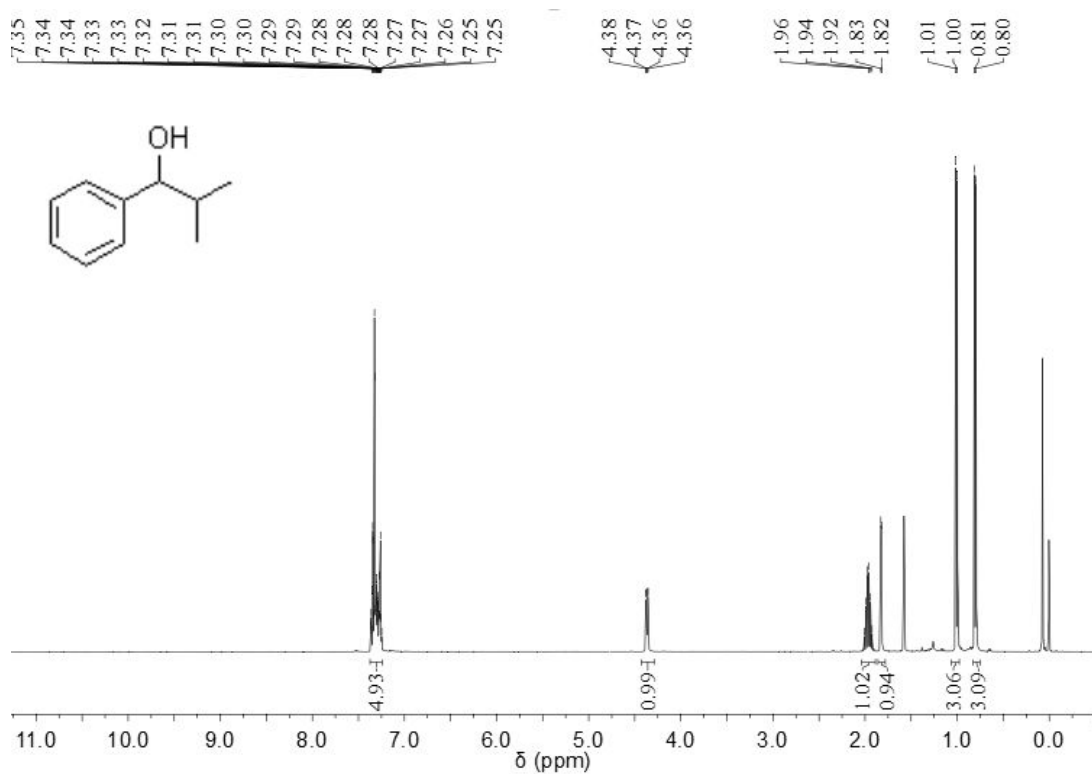


Figure S71. ¹H NMR (400 MHz, CDCl₃, 298 K) spectrum of **34**.

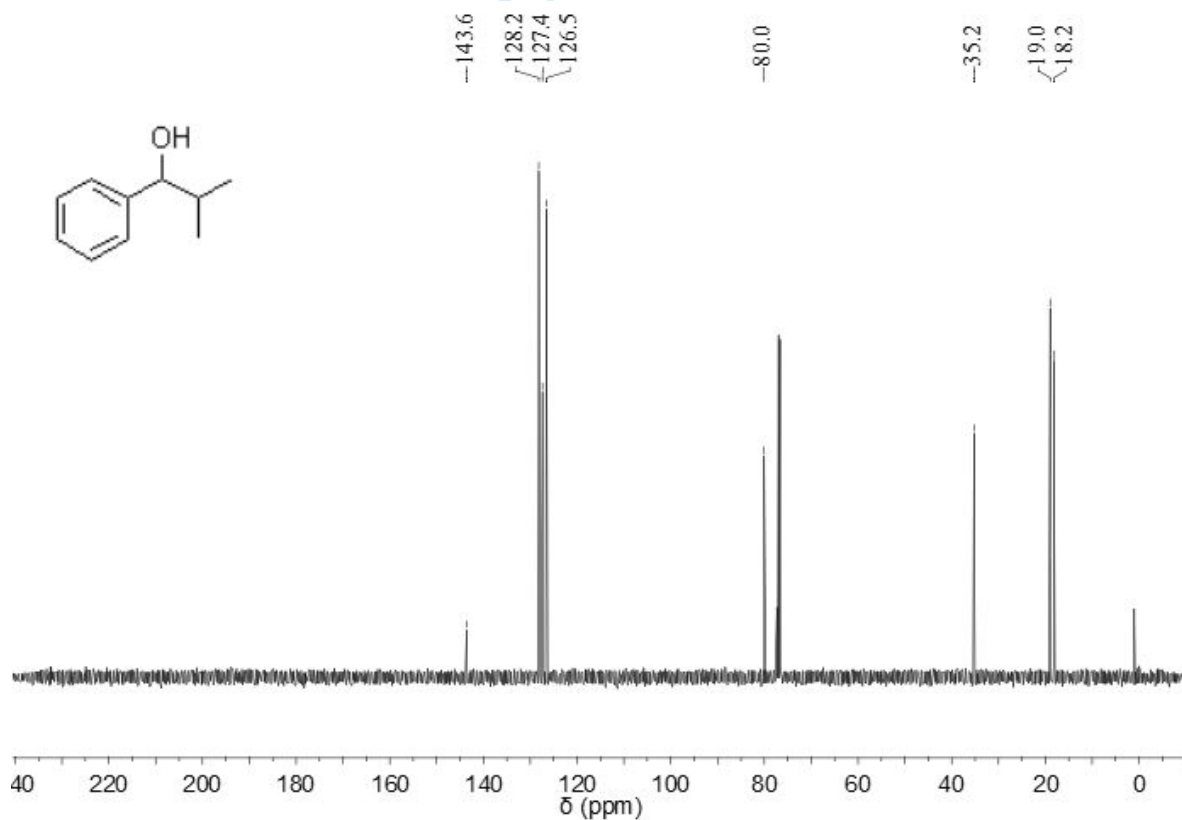


Figure S72. ¹³C NMR (101 MHz, CDCl₃, 298 K) spectrum of **34**.

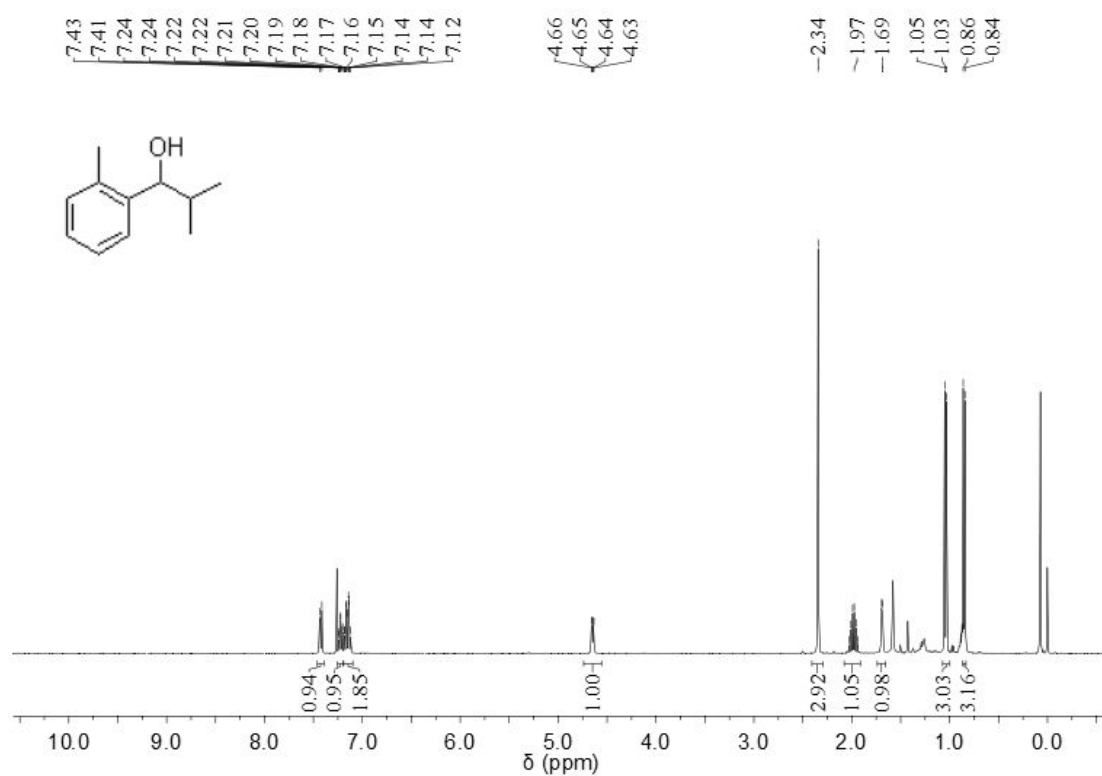


Figure S73. ¹H NMR (400 MHz, CDCl₃, 298 K) spectrum of **35**.

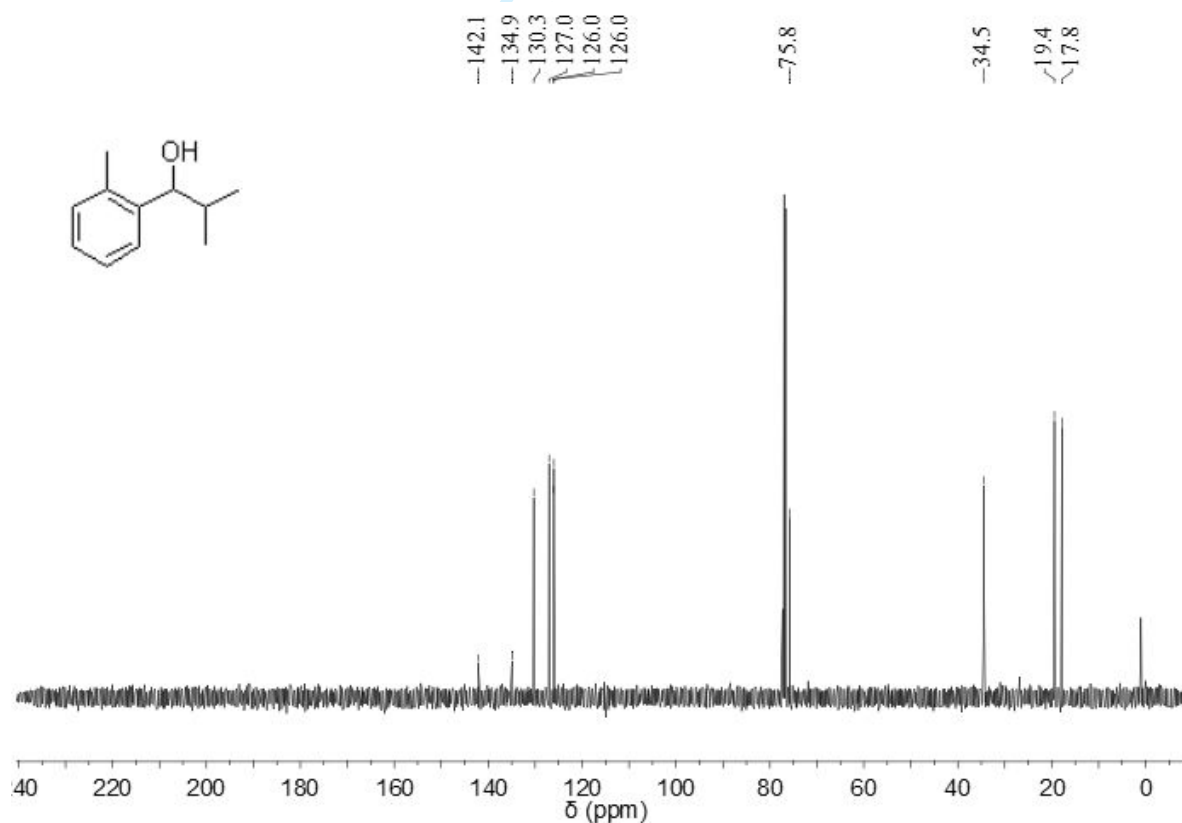


Figure S74. ¹³C NMR (101 MHz, CDCl₃, 298 K) spectrum of **35**.

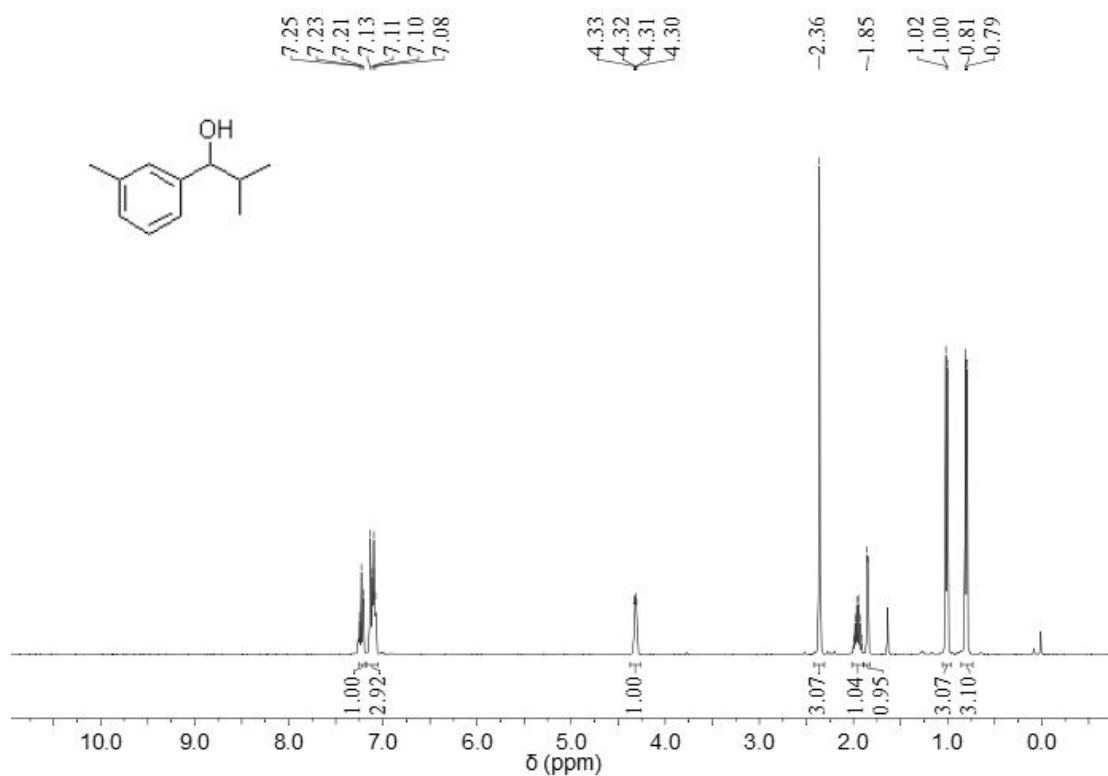


Figure S75. ¹H NMR (400 MHz, CDCl₃, 298 K) spectrum of **36**.

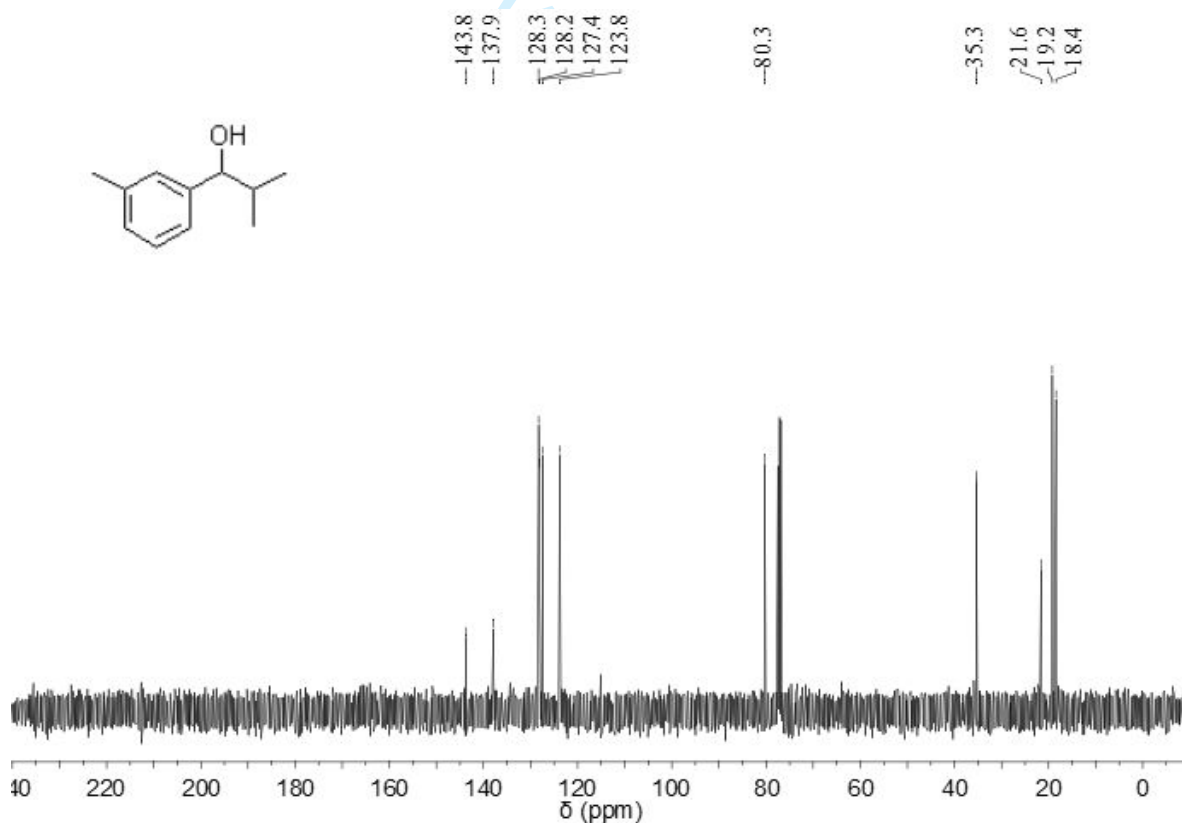


Figure S76. ¹³C NMR (101 MHz, CDCl₃, 298 K) spectrum of **36**.

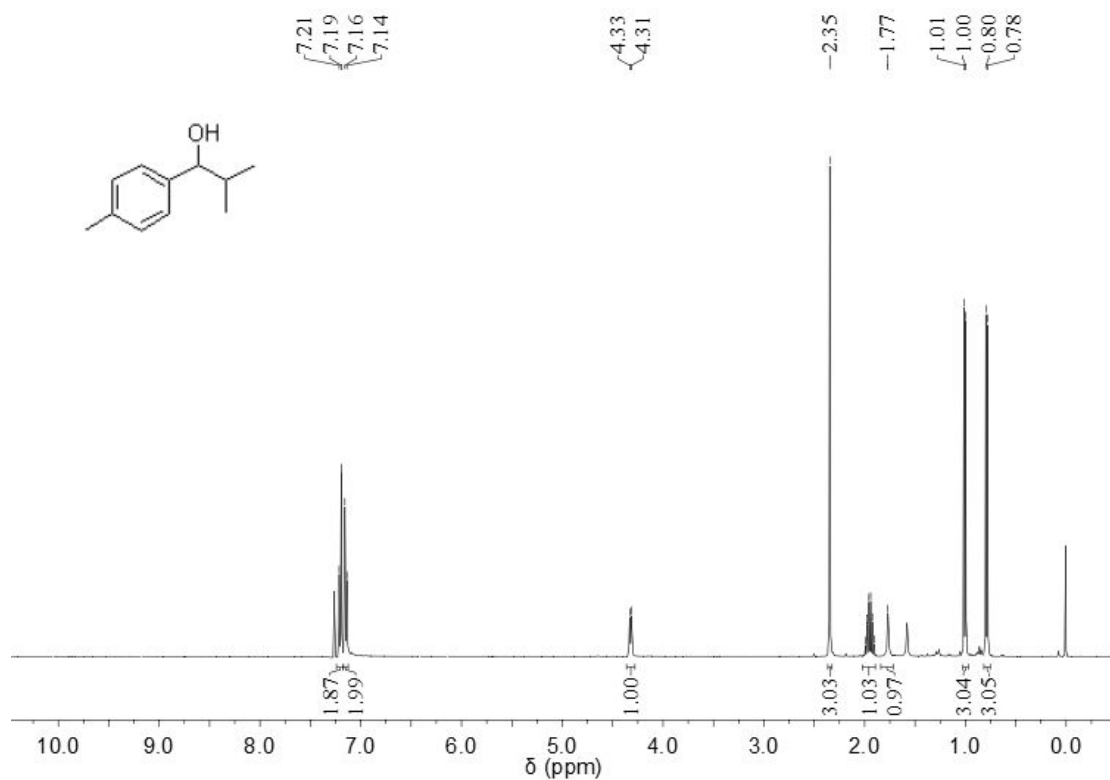


Figure S77. ^1H NMR (400 MHz, CDCl_3 , 298 K) spectrum of **37**.

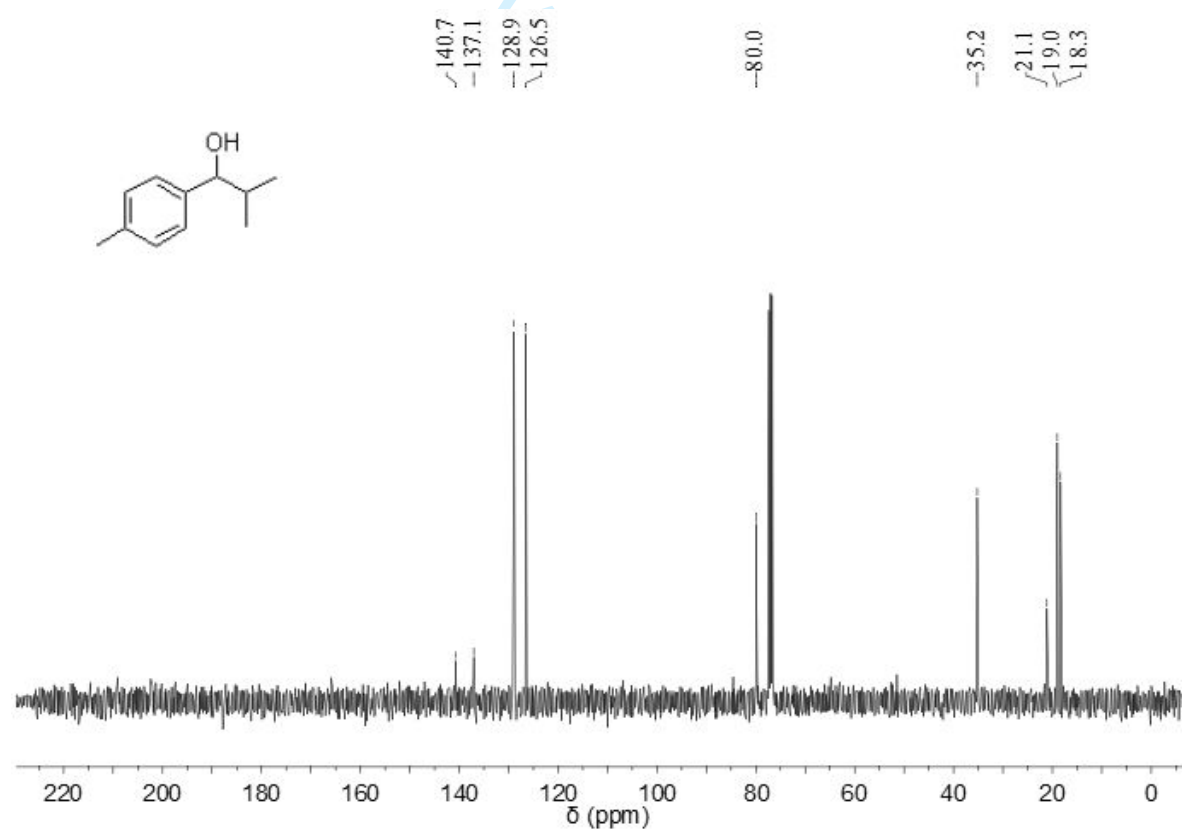


Figure S78. ^{13}C NMR (101 MHz, CDCl_3 , 298 K) spectrum of **37**.

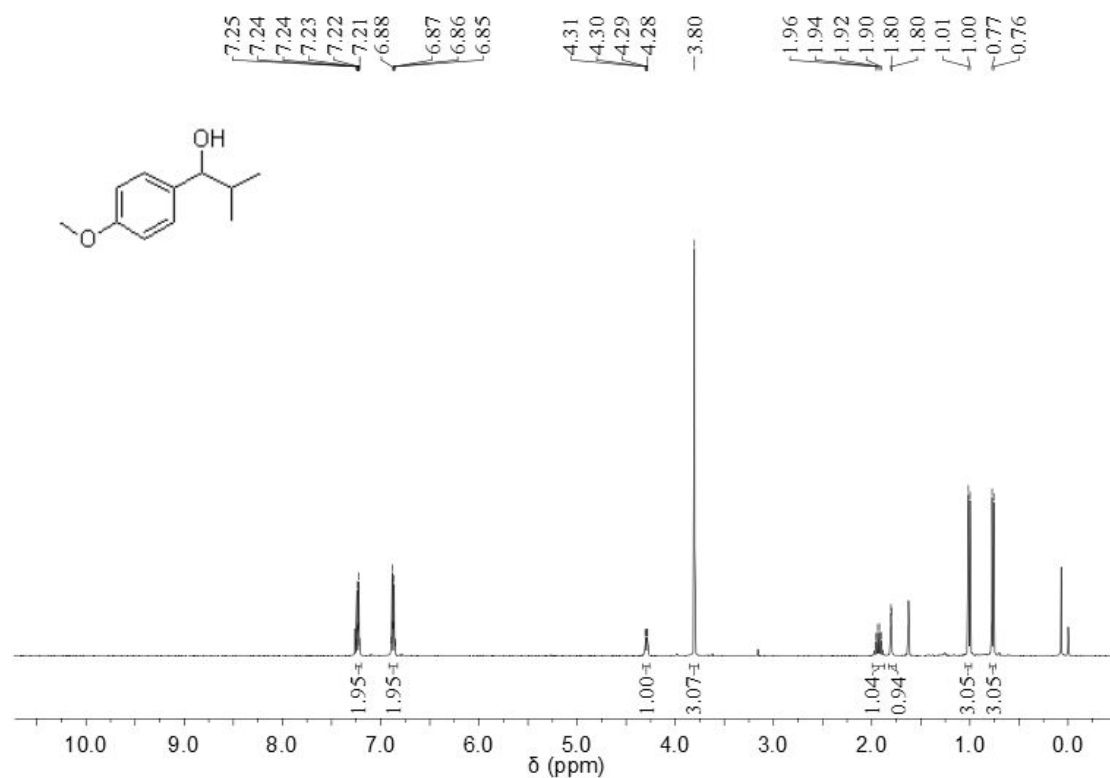


Figure S79. ¹H NMR (400 MHz, CDCl₃, 298 K) spectrum of **38**.

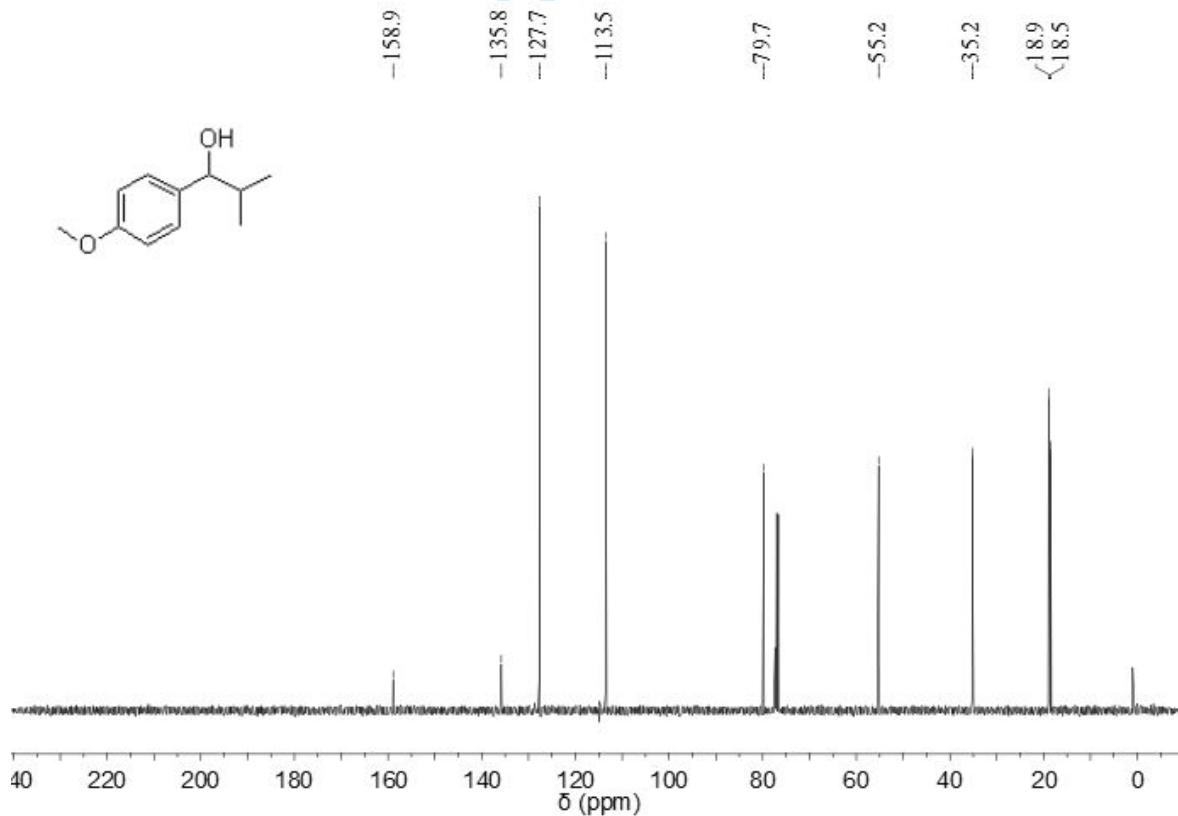
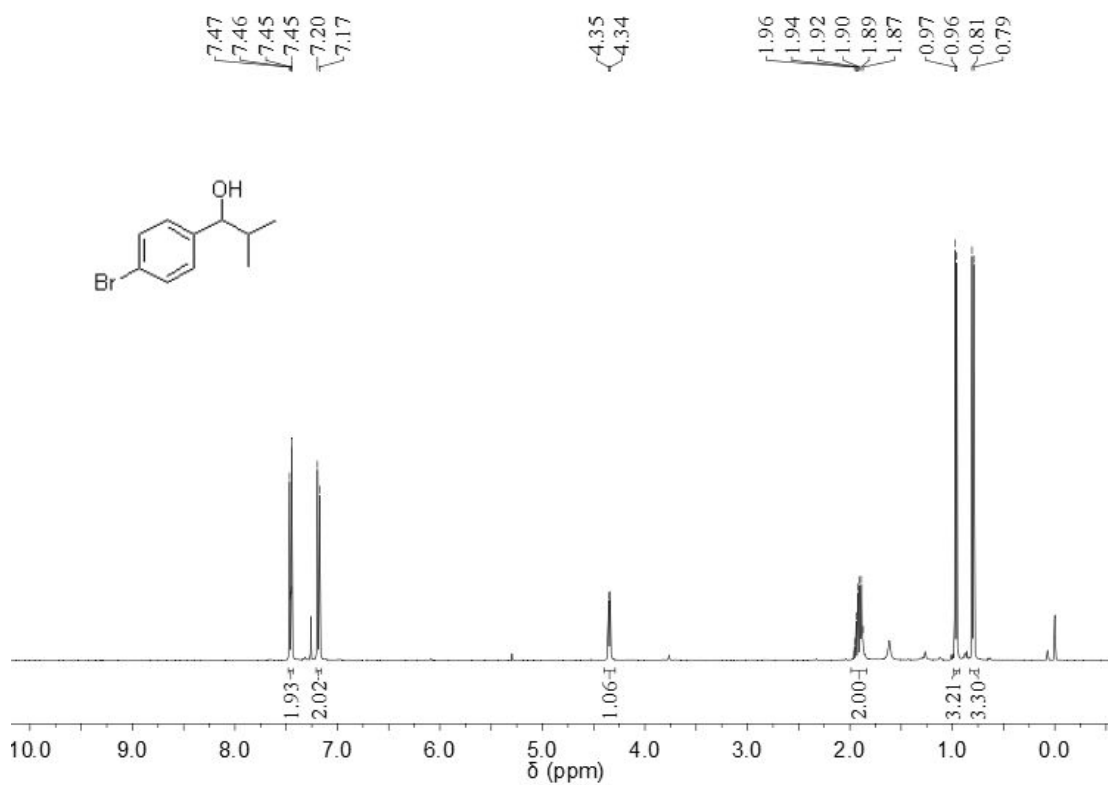


Figure S80. ¹³C NMR (101 MHz, CDCl₃, 298 K) spectrum of **38**.



28
29
30
31
32
33
34
35
36
37
38
39
40
41
42
43
44
45
46
47
48
49
50
51
52
53
54
55
56
57
58
59
60

Figure S81. ^1H NMR (400 MHz, CDCl_3 , 298 K) spectrum of **39**.

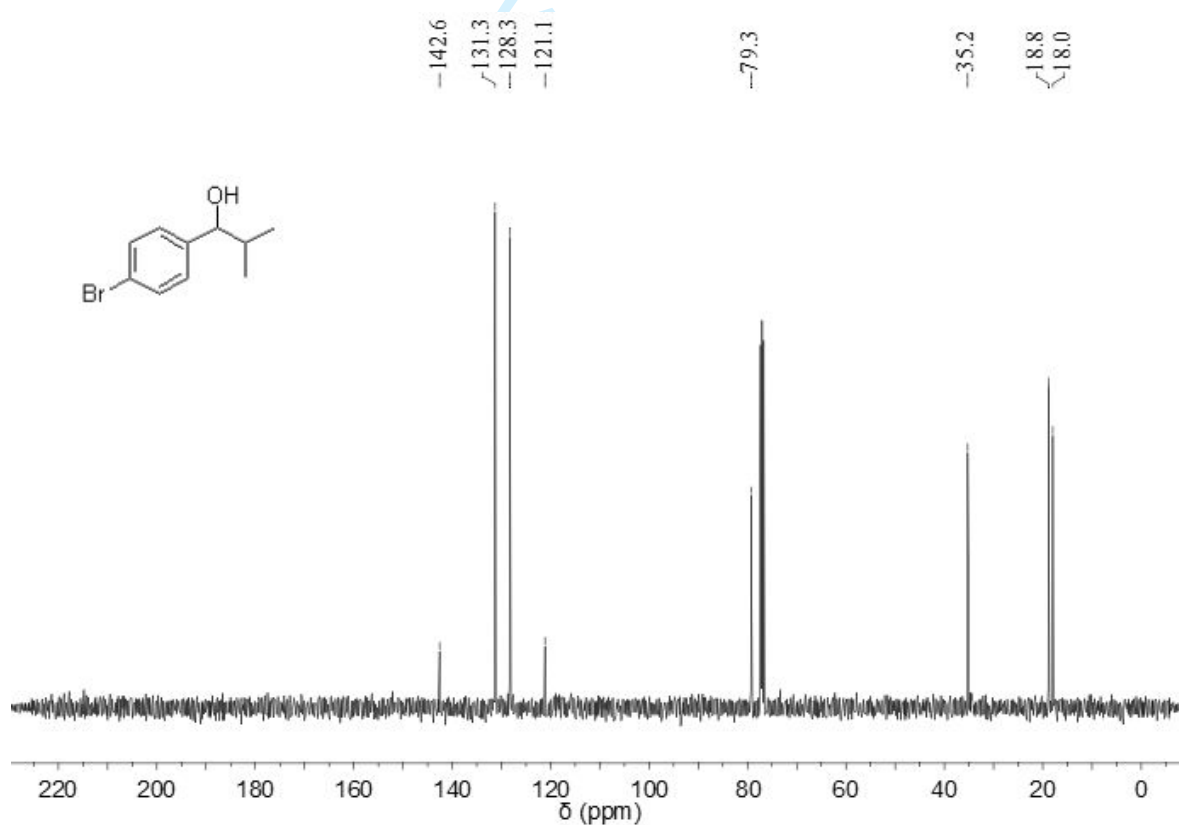


Figure S82. ^{13}C NMR (101 MHz, CDCl_3 , 298 K) spectrum of **39**.

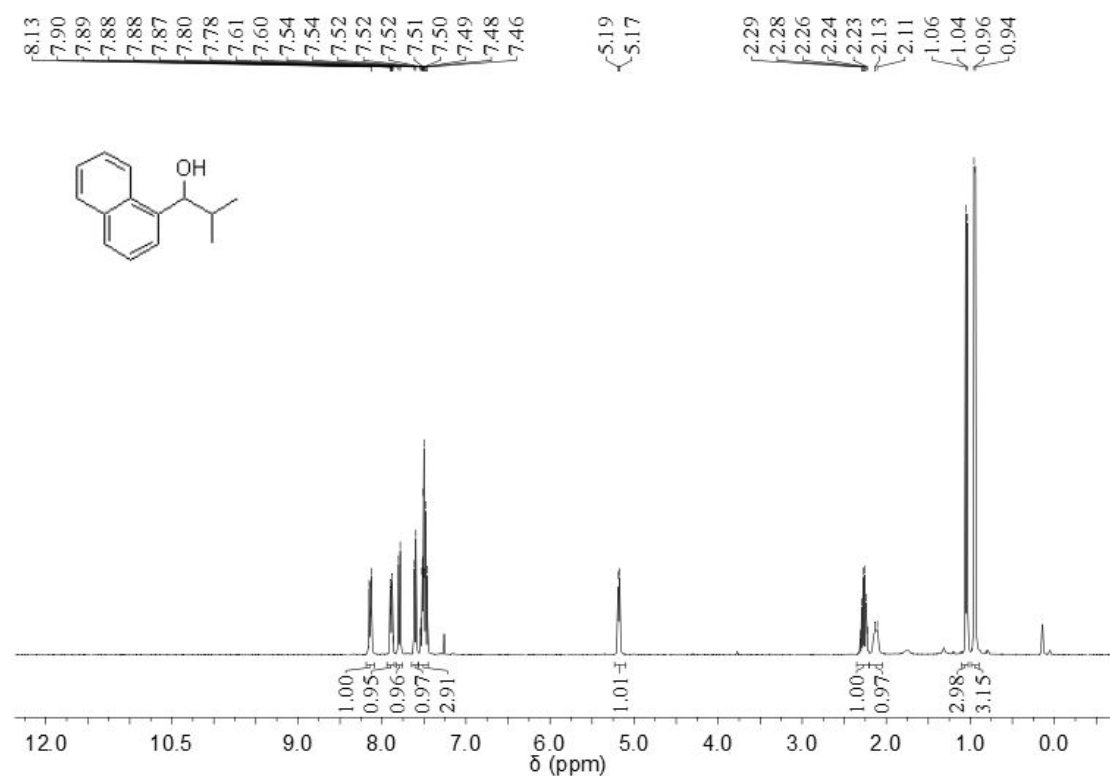


Figure S83. ¹H NMR (400 MHz, CDCl₃, 298 K) spectrum of **40**.

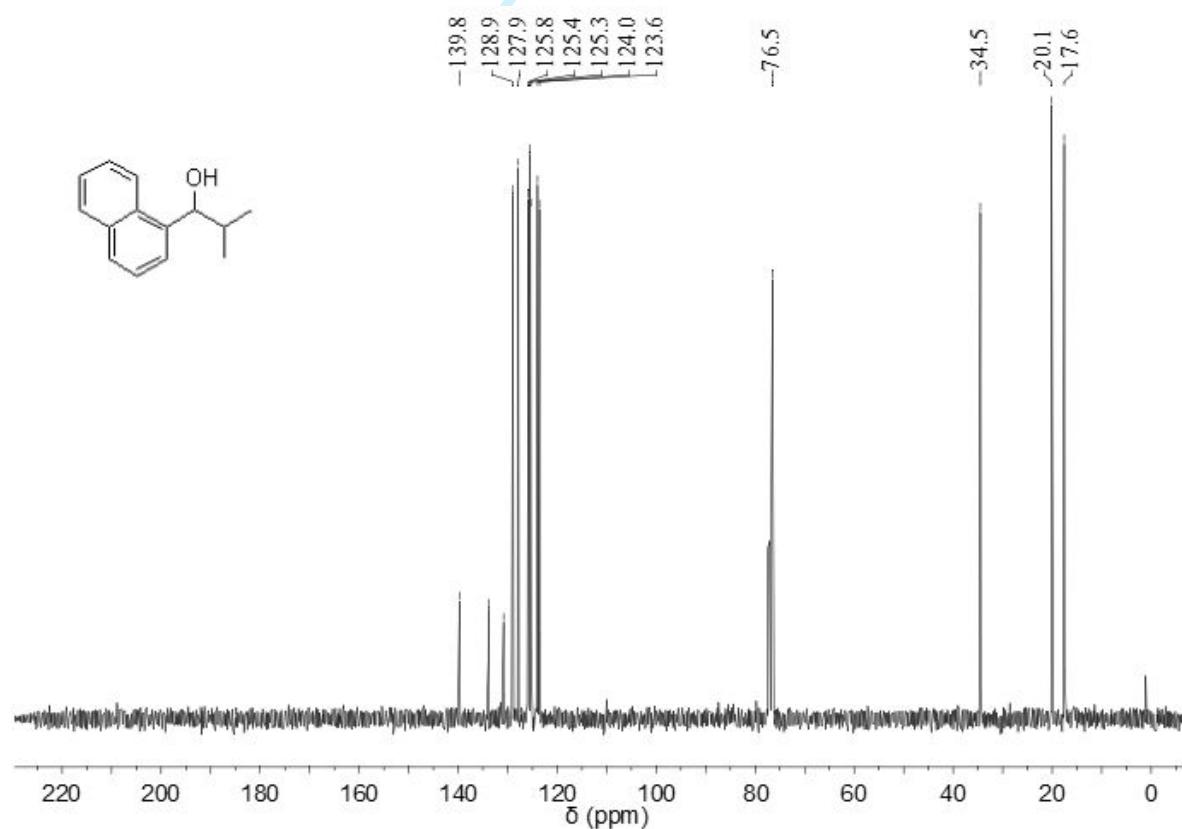


Figure S84. ¹³C NMR (101 MHz, CDCl₃, 298 K) spectrum of **40**.

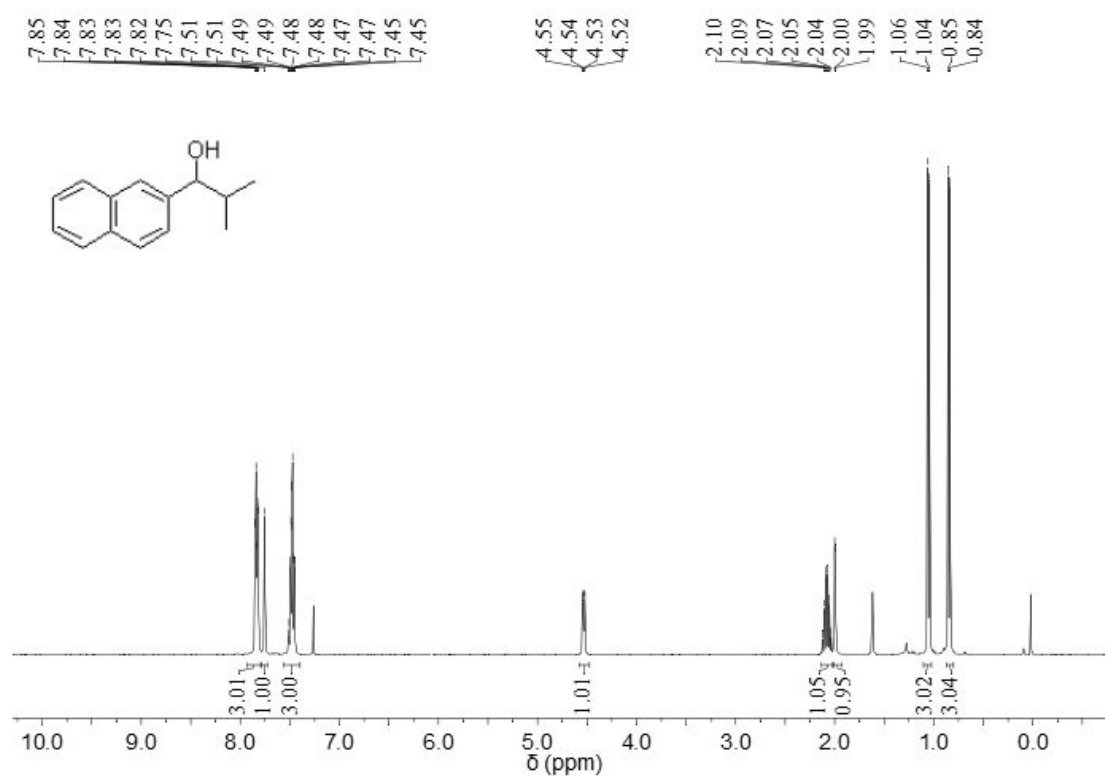


Figure S85. ¹H NMR (400 MHz, CDCl₃, 298 K) spectrum of **41**.

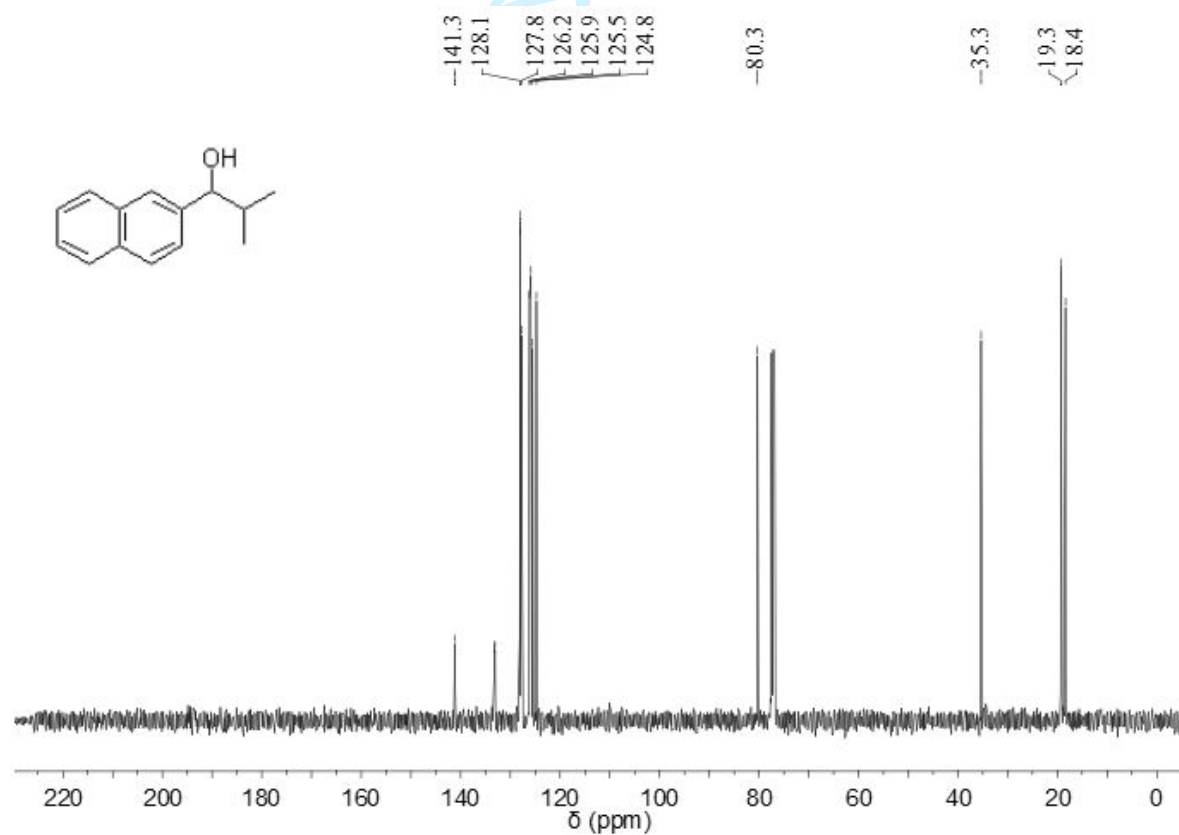


Figure S86. ¹³C NMR (101 MHz, CDCl₃, 298 K) spectrum of **41**.

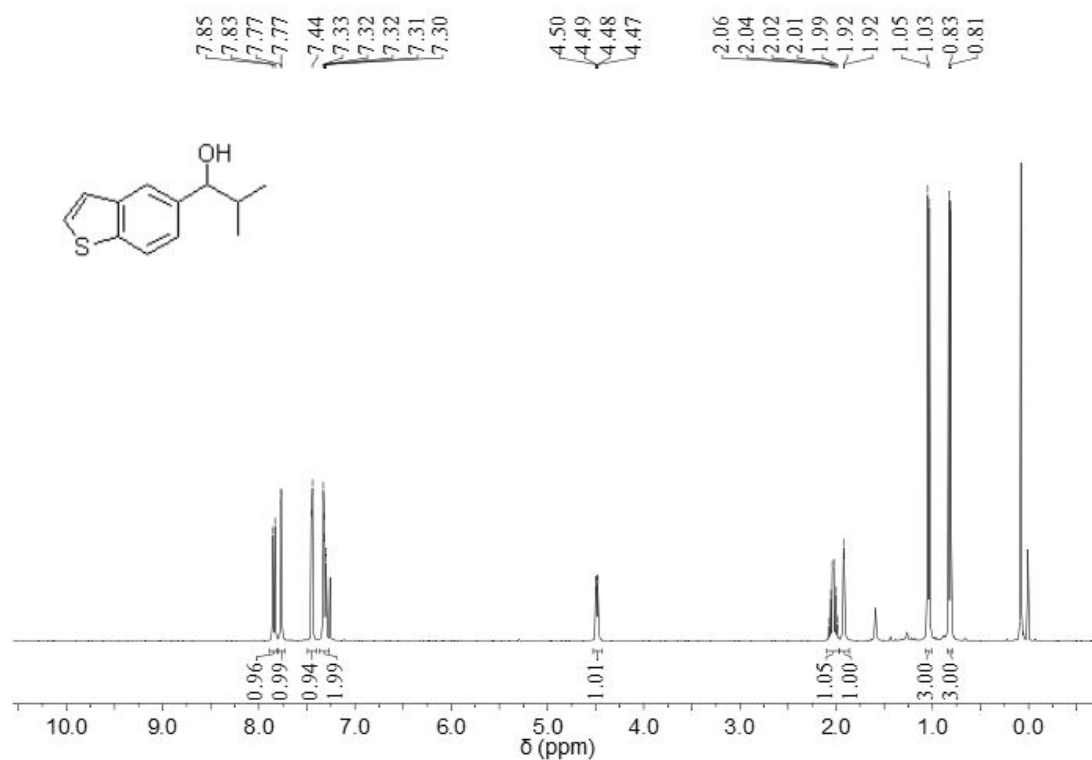


Figure S87. ¹H NMR (400 MHz, CDCl₃, 298 K) spectrum of **42**.

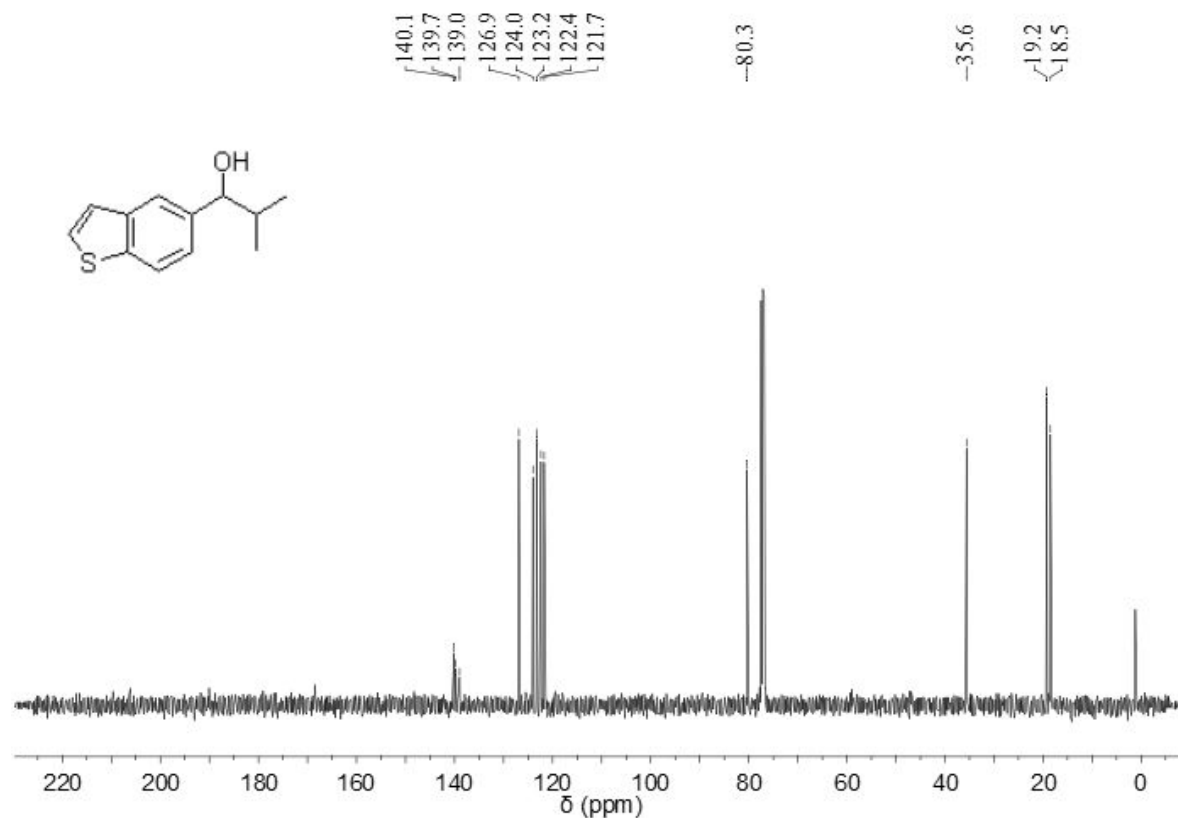


Figure S88. ¹³C NMR (101 MHz, CDCl₃, 298 K) spectrum of **42**.

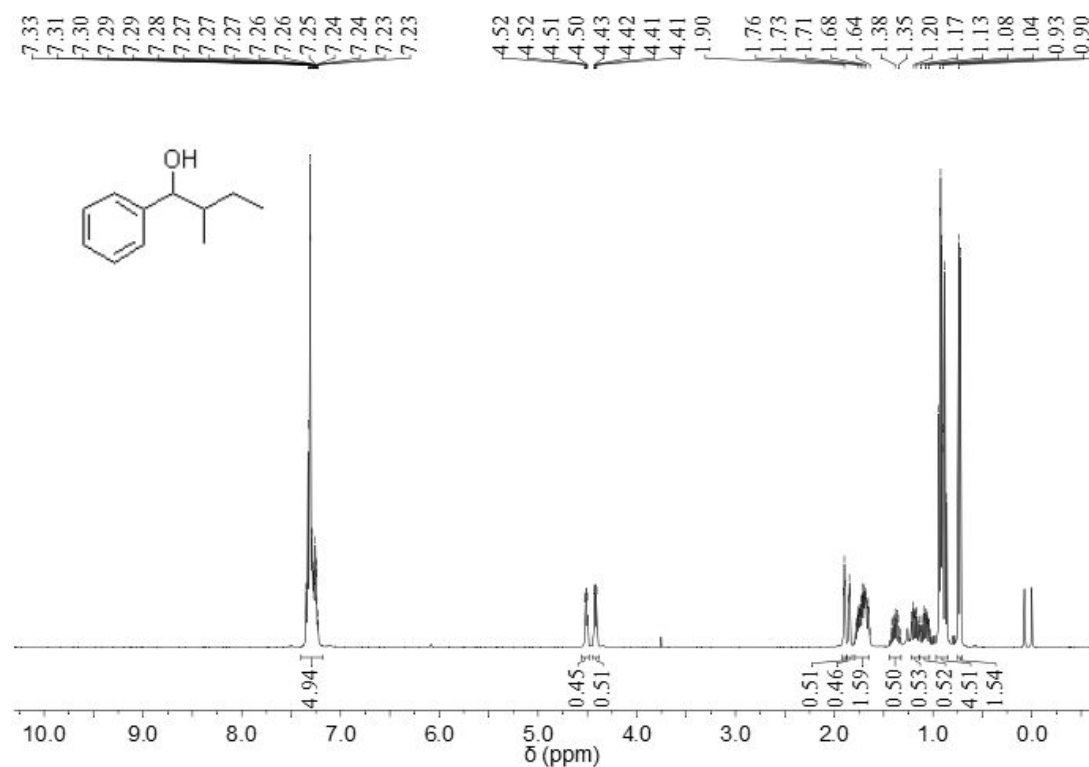


Figure S89. ¹H NMR (400 MHz, CDCl₃, 298 K) spectrum of **45**.

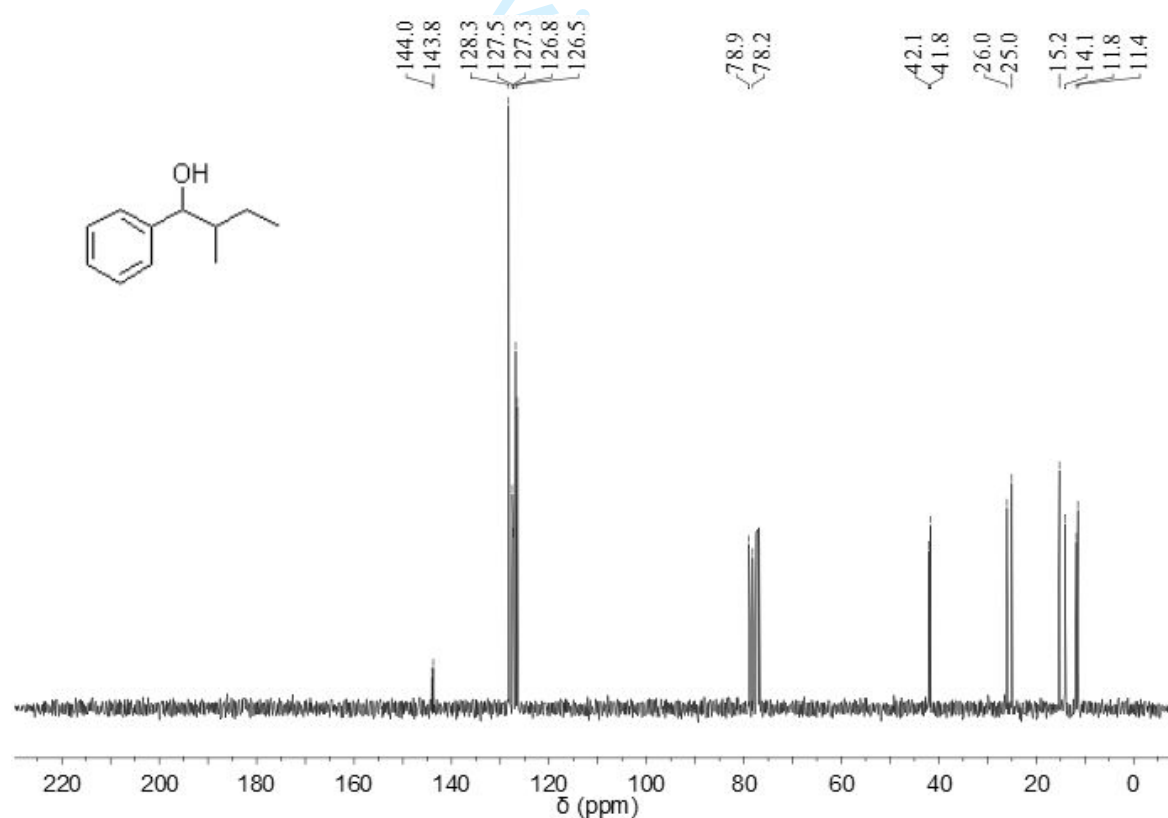


Figure S90. ¹³C NMR (101 MHz, CDCl₃, 298 K) spectrum of **45**.

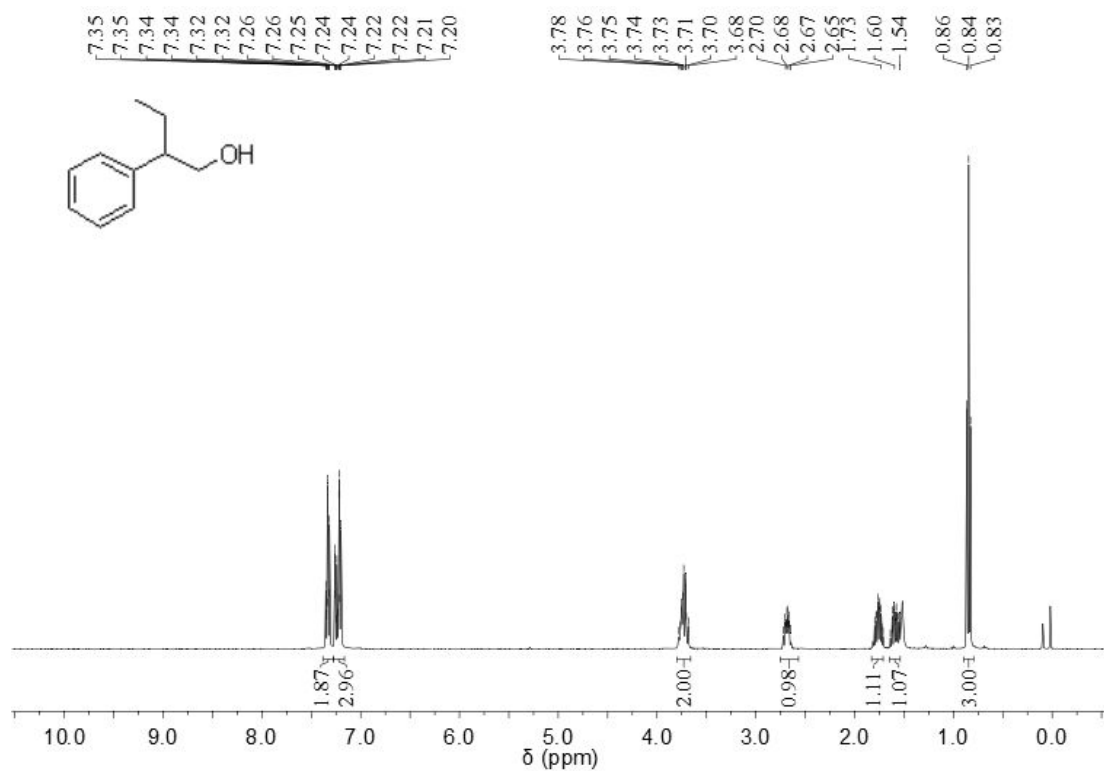


Figure S91. ¹H NMR (400 MHz, CDCl₃, 298 K) spectrum of **48**.

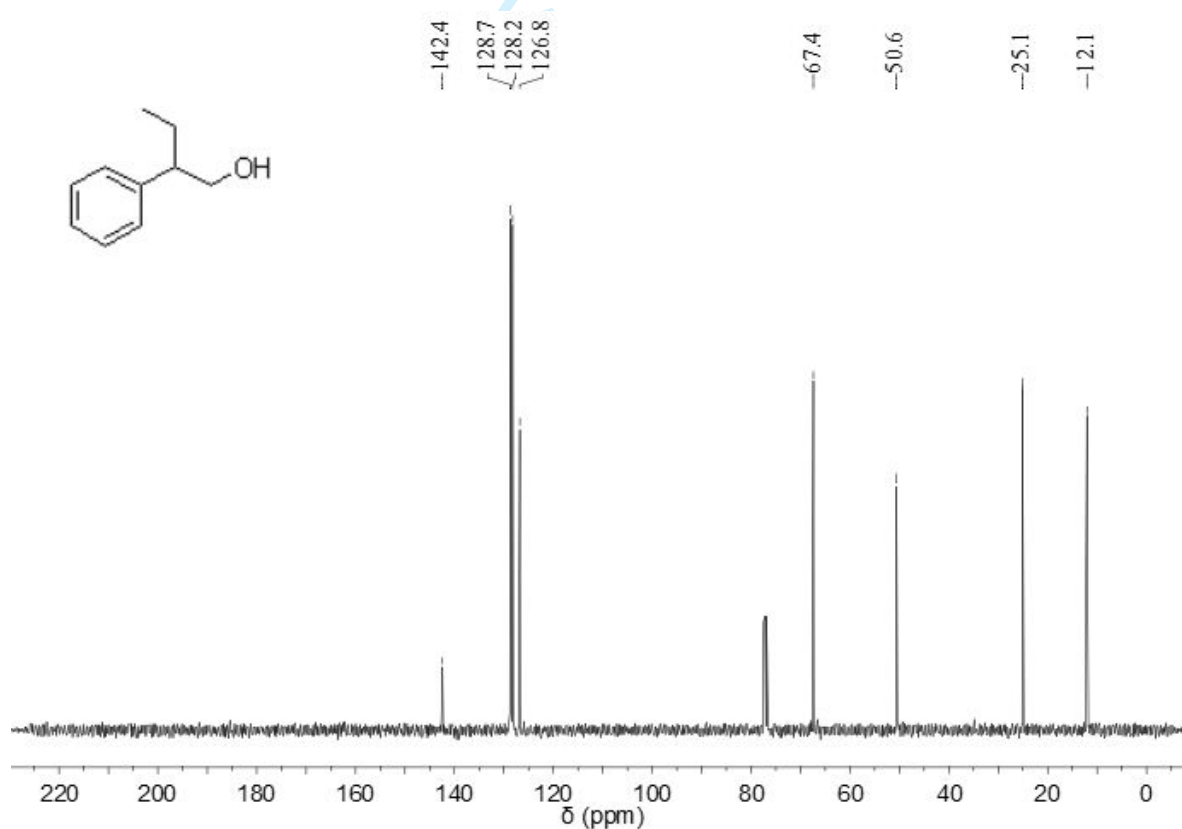


Figure S92. ¹³C NMR (101 MHz, CDCl₃, 298 K) spectrum of **48**.

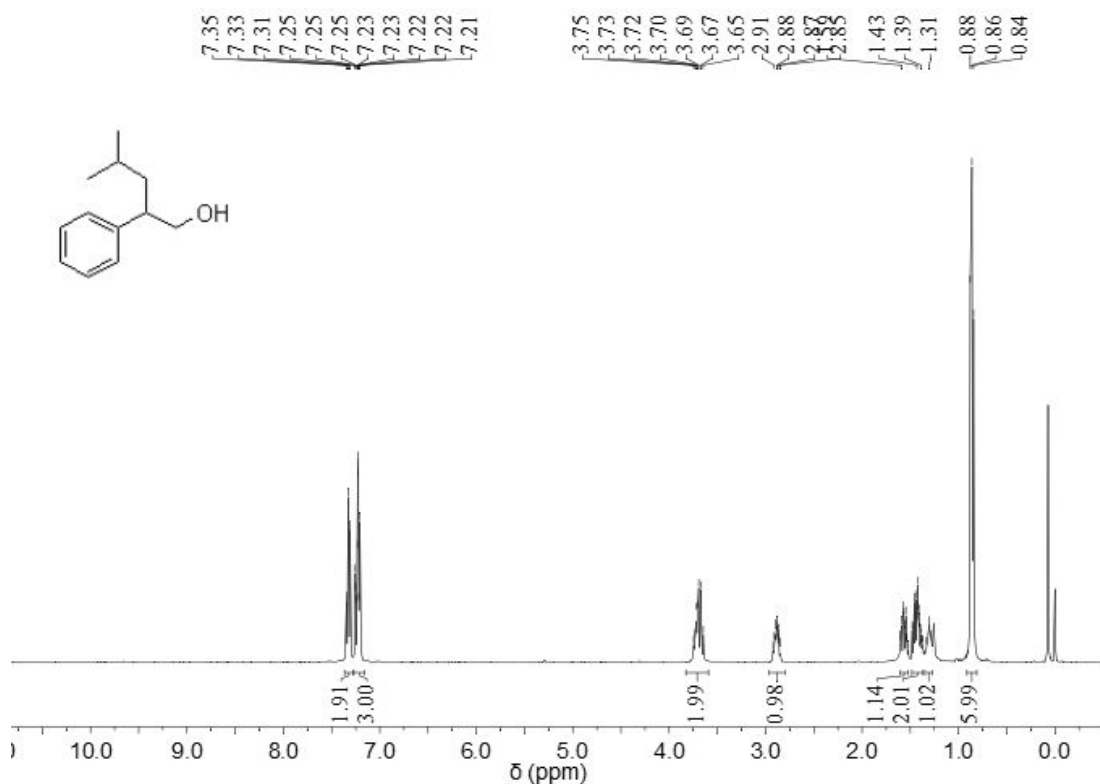


Figure S93. ¹H NMR (400 MHz, CDCl₃, 298 K) spectrum of **49**.

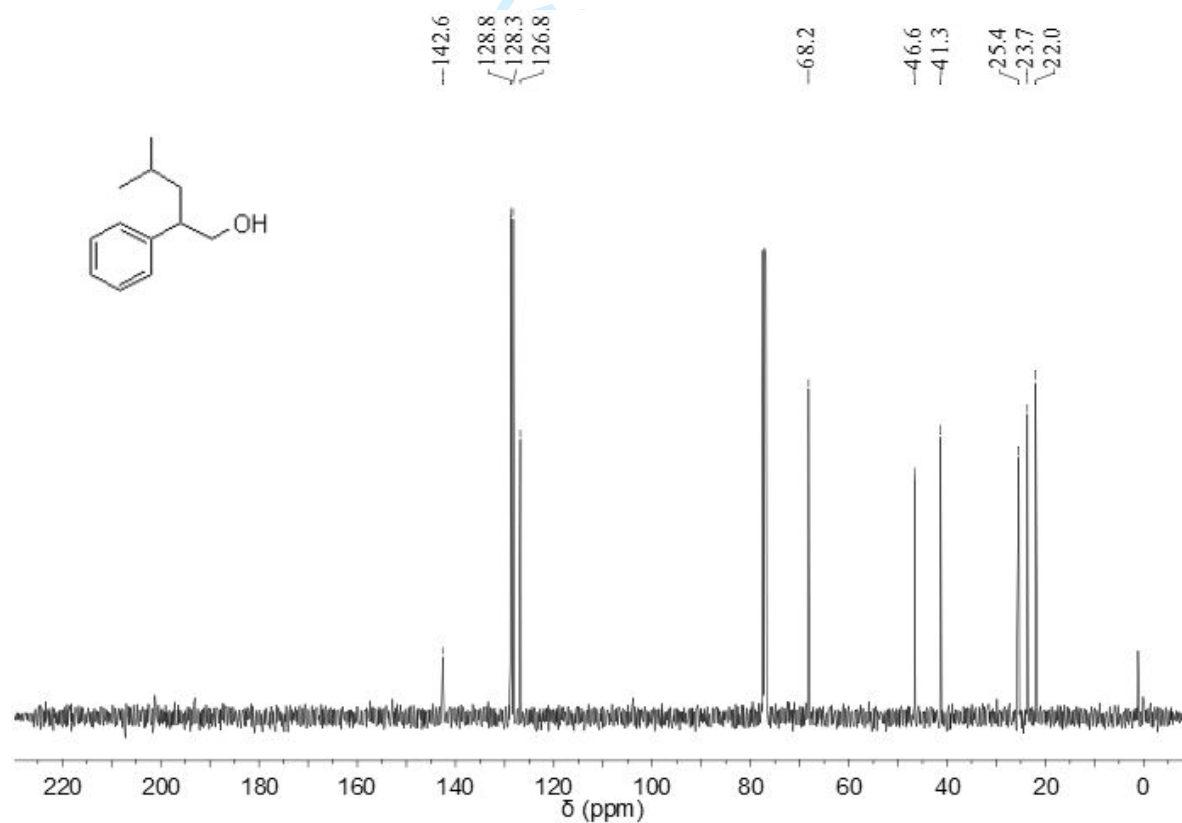


Figure S94. ¹³C NMR (101 MHz, CDCl₃, 298 K) spectrum of **49**.

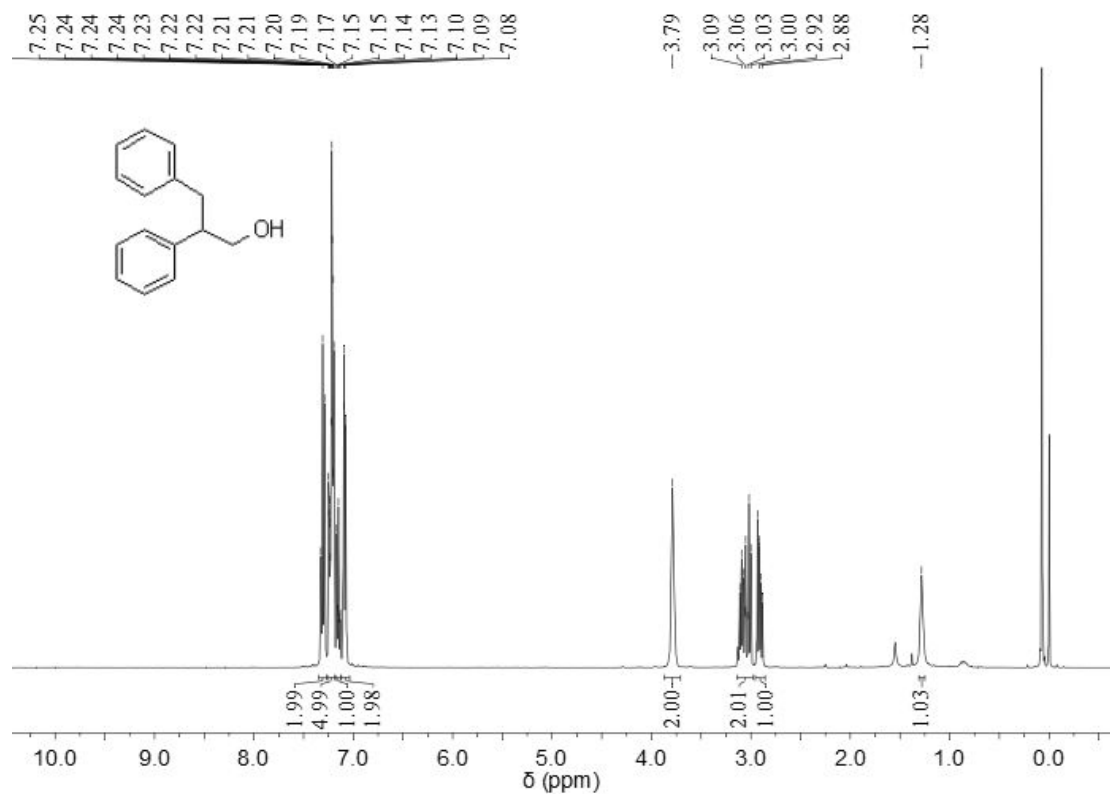


Figure S95. ¹H NMR (400 MHz, CDCl₃, 298 K) spectrum of **50**.

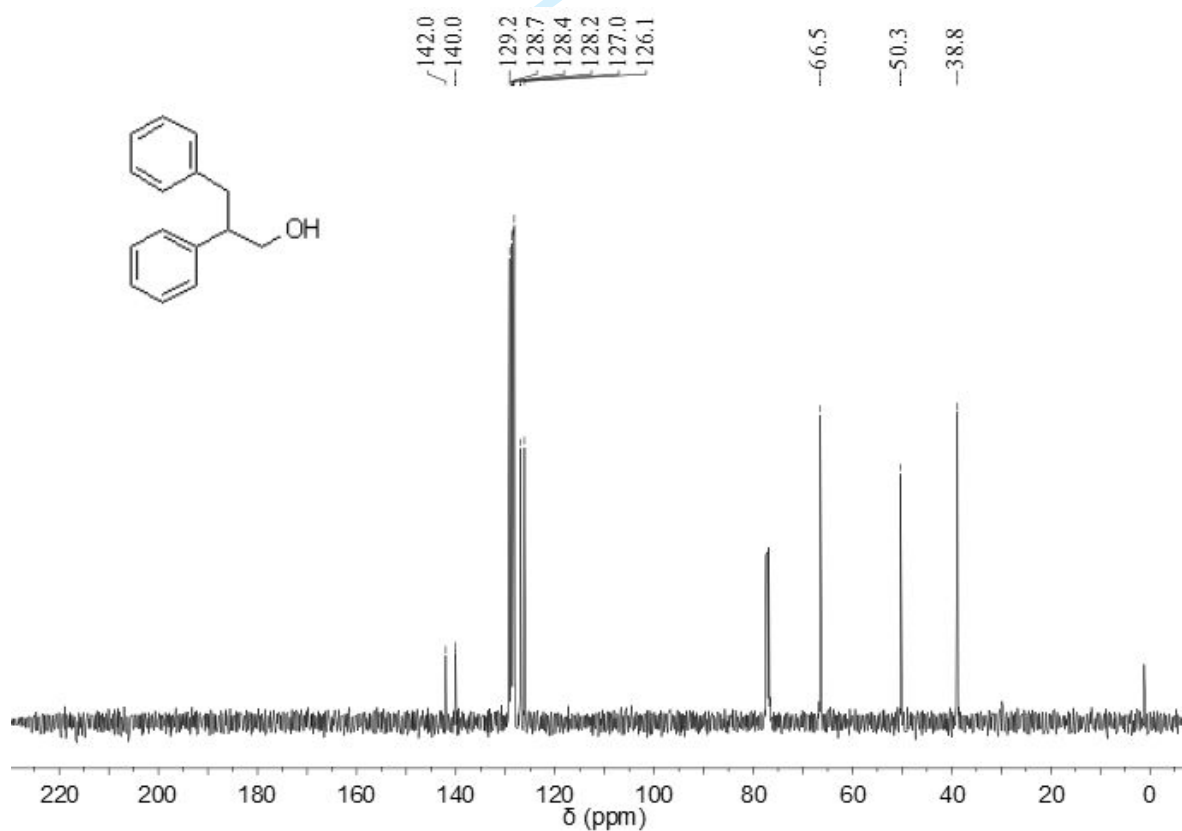


Figure S96. ¹³C NMR (101 MHz, CDCl₃, 298 K) spectrum of **50**.

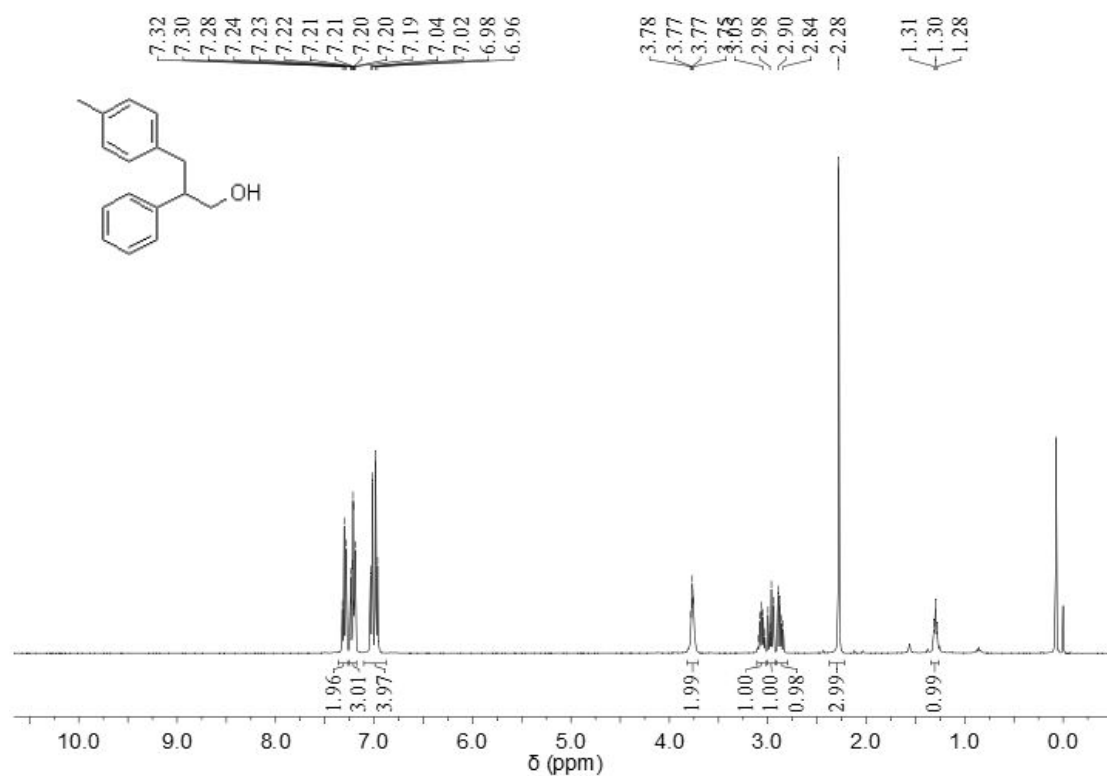


Figure S97. ¹H NMR (400 MHz, CDCl₃, 298 K) spectrum of **51**.

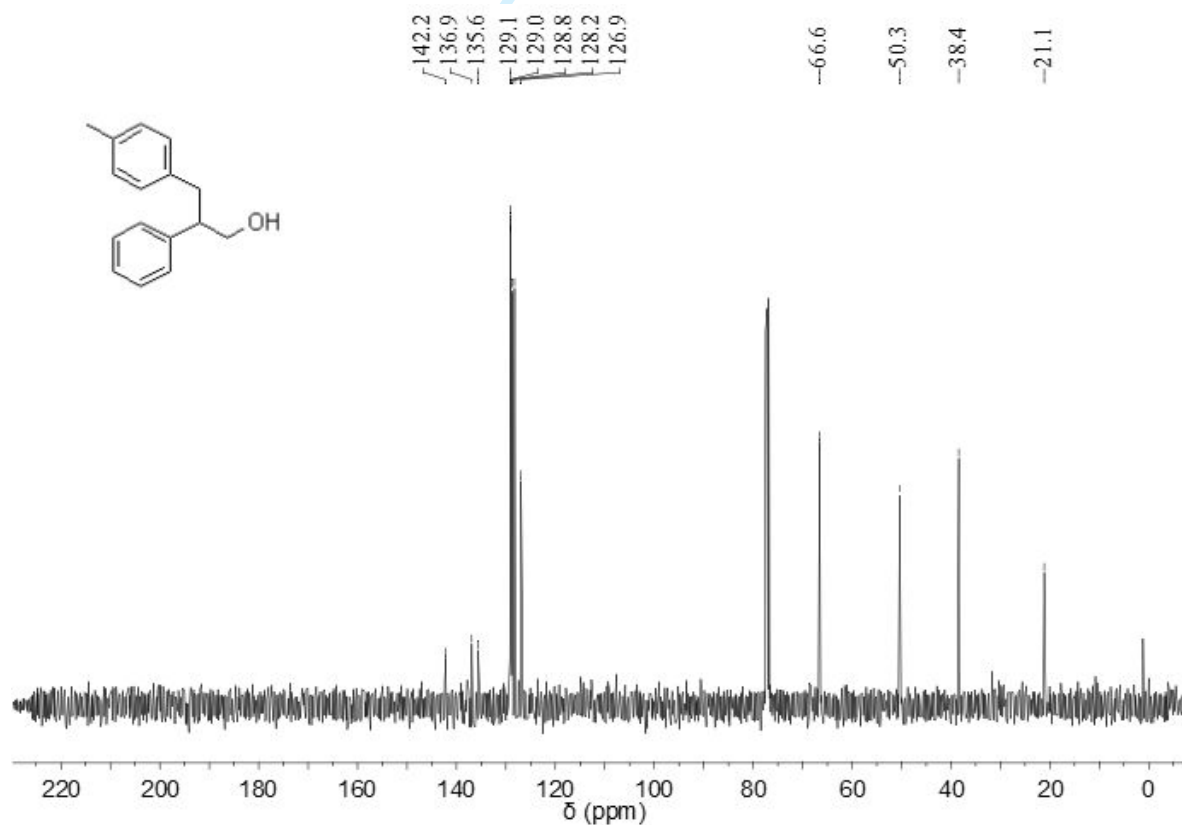


Figure S98. ¹³C NMR (101 MHz, CDCl₃, 298 K) spectrum of **51**.

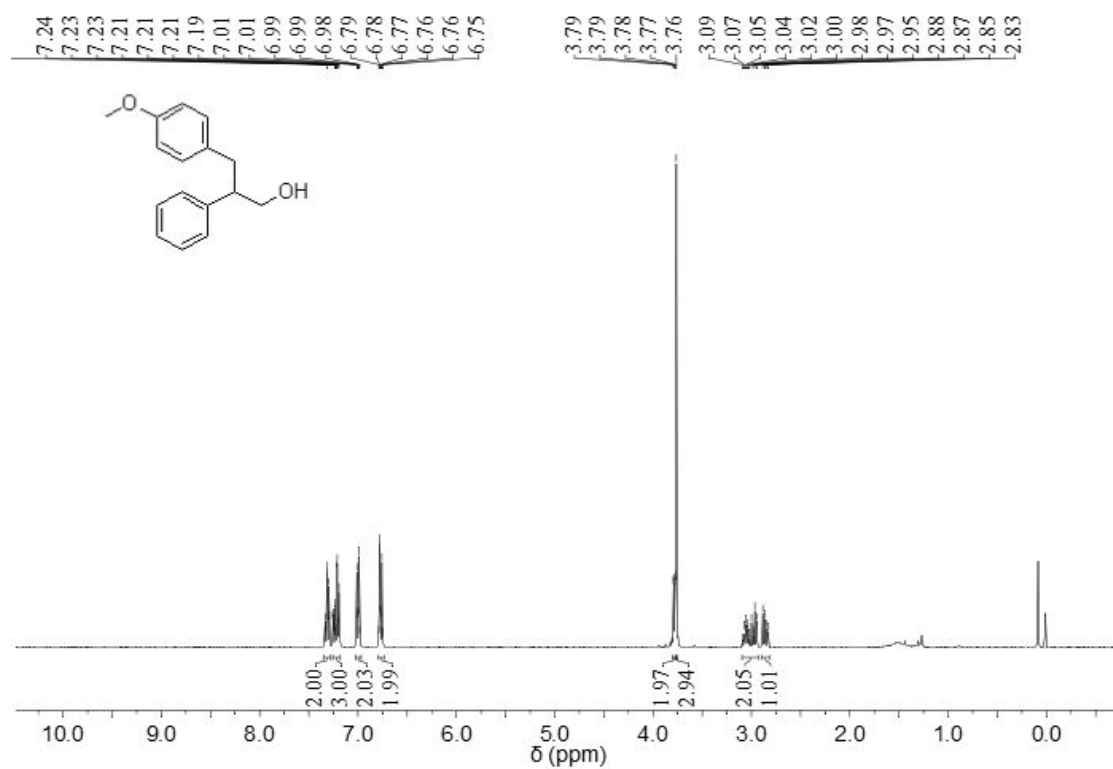


Figure S99. ¹H NMR (400 MHz, CDCl₃, 298 K) spectrum of **52**.

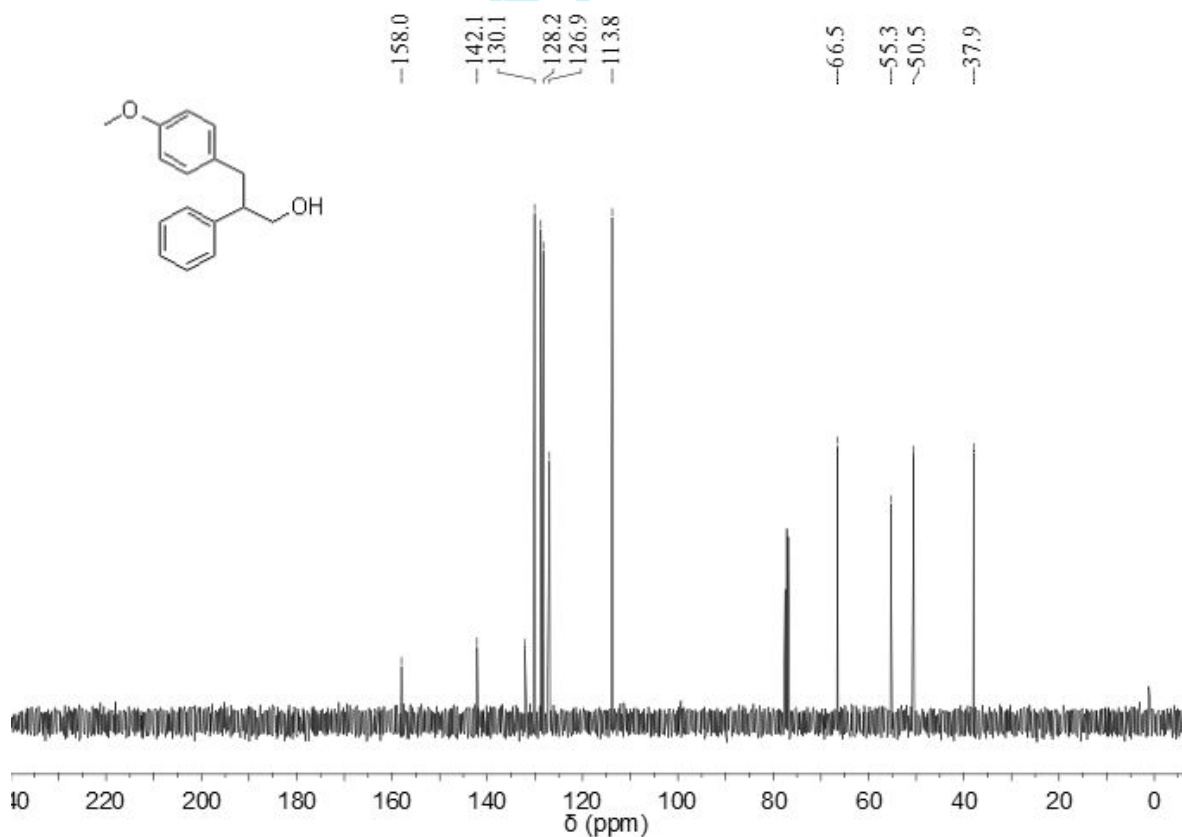


Figure S100. ¹³C NMR (101 MHz, CDCl₃, 298 K) spectrum of **52**.

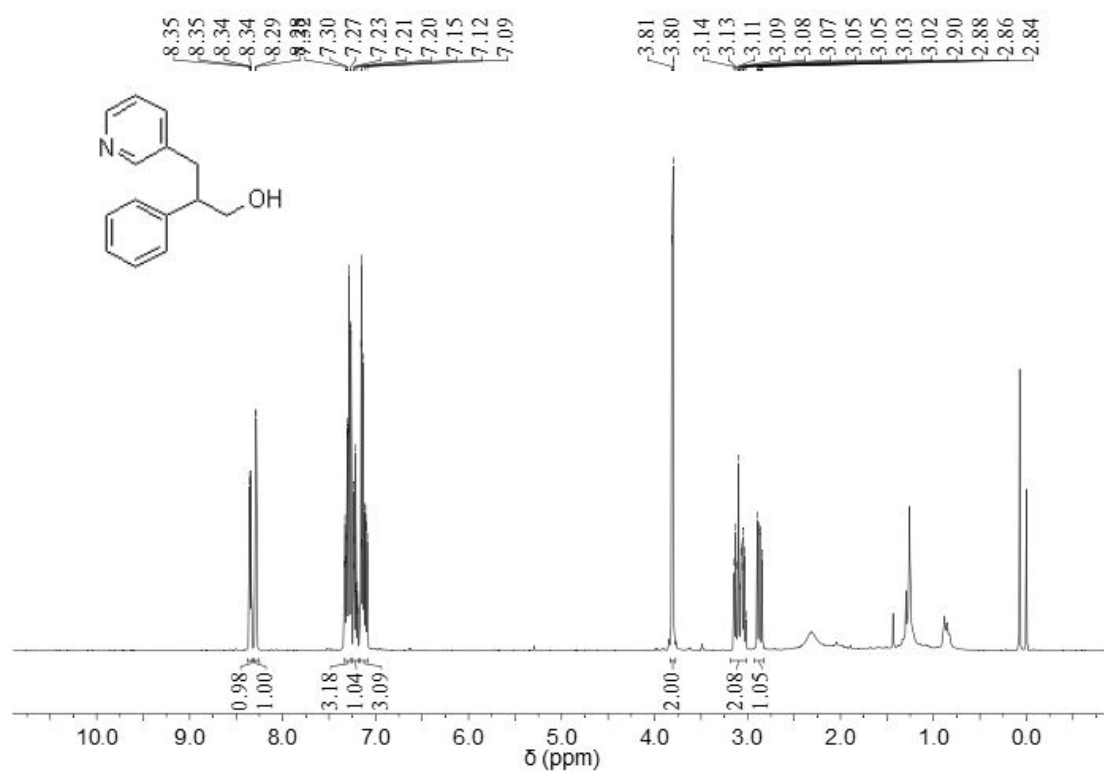


Figure S101. ¹H NMR (400 MHz, CDCl₃, 298 K) spectrum of **53**.

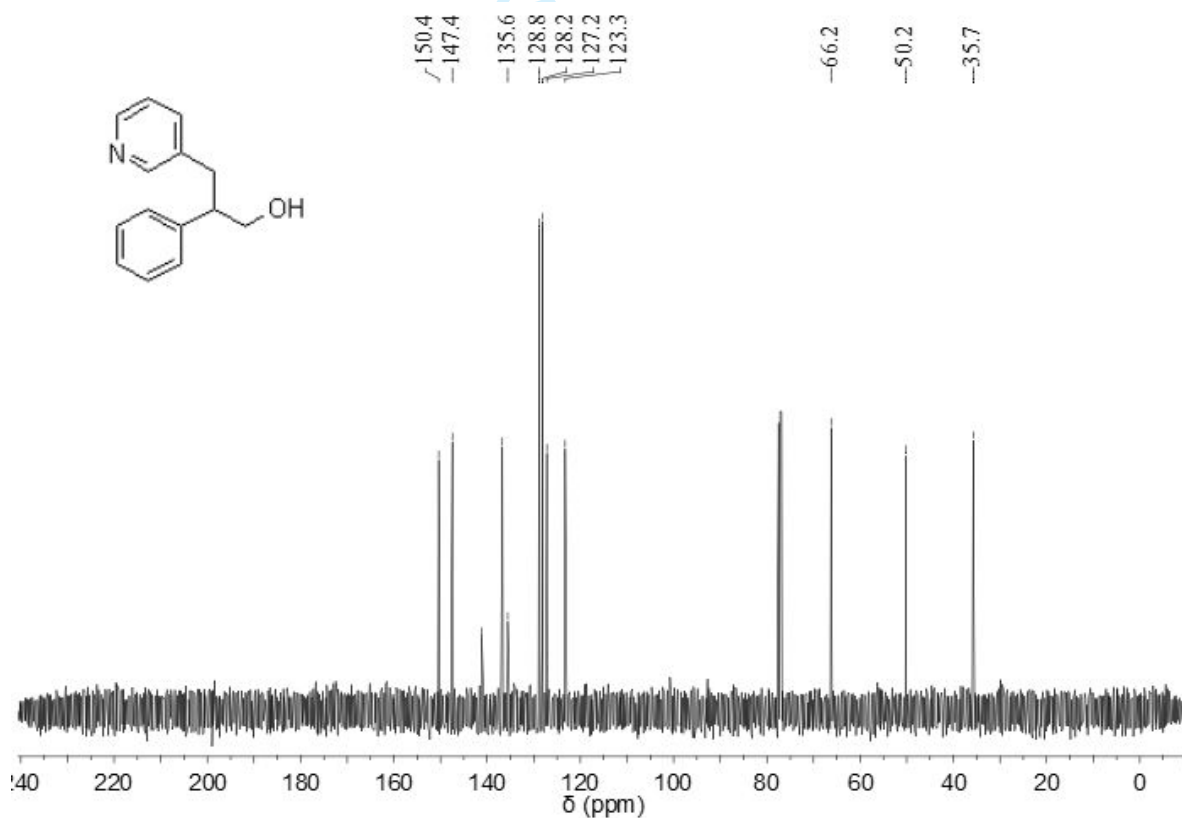


Figure S102. ¹³C NMR (101 MHz, CDCl₃, 298 K) spectrum of **53**.

References

- S1 Falivene L, Cao Z, Petta A, Serra L, Poater A, Oliva R, Scarano V, Cavallo L. *Nat. Chem*, 2019, 11: 872
- S2 Poater A, Cosenza B, Correa A, Giudice S, Ragone F, Scarano V, Cavallo L. *Eur. J. Inorg. Chem*, 2009, 1759-1766
- S3 Perdew JP, Burke K, Ernzerhof M. *Phys. Rev. Lett*, 1996, 77: 3865-3868
- S4 Grimme S, Antony J, Ehrlich S, Krieg H. *J. Chem. Phys*, 2010, 132
- S5 Grimme S, Ehrlich S, Goerigk L. *J. Comput. Chem*, 2011, 32: 1456-1465
- S6 Petersson GA, Bennett A, Tensfeldt TG, Allaham MA, Shirley WA, Mantzaris J. *J. Chem. Phys*, 1988, 89: 2193-2218
- S7 Häussermann U, Dolg M, Stoll H, Preuss H, Schwerdtfeger P, Pitzer RM. *Mol. Phys*, 1993, 78: 1211-1224
- S8 Kuchle W, Dolg M, Stoll H, Preuss H. *J. Chem. Phys*, 1994, 100: 7535-7542
- S9 Leininger T, Nicklass A, Stoll H, Dolg M, Schwerdtfeger P. *J. Chem. Phys*, 1996, 105: 1052-1059
- S10 Cioslowski J. *J. Am. Chem. Soc*, 1989, 111: 8333-8336
- S11 Frisch MJ, Trucks GW, Schlegel HB, Scuseria GE, Robb MA, Cheeseman JR, Scalmani G, Barone V, Mennucci B, Petersson GA, Nakatsuji H, Caricato M, Li X, Hratchian HP, Izmaylov AF, Bloino J, Zheng G, Sonnenberg JL, Hada M, Ehara M, Toyota K, Fukuda R, Hasegawa J, Ishida M, Nakajima T, Honda Y, Kitao O, Nakai H, Vreven T, Montgomery JA, Peralta JJE, Ogliaro F, Bearpark M, Heyd JJ, Brothers E, Kudin KN, Staroverov VN, Kobayashi R, Normand J, Raghavachari K, Rendell A, Burant JC, Iyengar SS, Tomasi J, Cossi M, Rega N, Millam JM, Klene M, Knox JE, Cross JB, Bakken V, Adamo C, Jaramillo J, Gomperts R, Stratmann RE, Yazyev O, Austin AJ, Cammi R, Pomelli C, Ochterski JW, Martin RL, Morokuma K, Zakrzewski VG, Voth GA, Salvador P, Dannenberg JJ, Dapprich S, Daniels AD, Farkas O, Foresman JB, Ortiz JV,

- Cioslowski J, Fox DJ. Gaussian 16, Revision B. 01. Wallingford, CT: Gaussian, Inc.; 2016.
- S12 Wu JJ, Shen LY, Chen ZN, Zheng QS, Xu X, Tu T. *Angew. Chem. Int. Ed*, 2020, 59: 10421-10425
- S13 Sharninghausen LS, Campos J, Manas MG, Crabtree RH. *Nat. Commun*, 2014, 5: 5084
- S14 Dobereiner GE, Nova A, Schley ND, Hazari N, Miller SJ, Eisenstein O, Crabtree RH. *J. Am. Chem. Soc*, 2011, 133: 7547-7562
- S15 Berding J, Paridon JA, Rixel VHS, Bouwman E. *Eur. J. Inorg. Chem*, 2011, 2450-2458
- S16 Li Y, Li HQ, Junge H, Beller M. *Chem. Commun*, 2014, 50: 14991-14994
- S17 Kaithal A, Bonn P, Holscher M, Leitner W. *Angew. Chem. Int. Ed*, 2020, 59: 215-220
- S18 Qu B, Tan R, Herling MR, Haddad N, Grinberg N, Kozlowski MC, Zhang X, Senanayake CH. *J. Org. Chem*, 2019, 84: 4915-4920
- S19 Mazet C, Gerard D. *Chem. Commun*, 2011, 47: 298-300
- S20 Bettoni L, Gaillard S, Renaud JL. *Org. Lett*, 2019, 21: 8404-8408
- S21 Cook MJ, Khan TA, Nasri K. *Tetrahedron*, 1986, 42: 249-258
- S22 Tobiesen HN, Leth LA, Iversen MV, Naeborg L, Bertelsen S, Jorgensen KA. *Angew. Chem. Int. Ed*, 2020, 59: 18490-18494
- S23 Chen Y, Leonardi M, Dingwall P, Labes R, Pasau P, Blakemore DC, Ley SV. *J. Org. Chem*, 2018, 83: 15558-15568
- S24 Sun ZM, Liu YQ, Chen JB, Huang CY, Tu T. *ACS Catal*, 2015, 5: 6573-6578
- S25 Sappino C, Promitativo L, Angelis M, Righi F, Di Pietro F, Iannoni M, Pilloni L, Cipriotti SV, Suber L, Ricelli A, Righi G. *RSC Adv*, 2020, 10: 29688-29695
- S26 Hasegawa M, Endo J, Iwata S, Shimasaki T, Mazaki Y. *Beilstein J. Org. Chem*, 2015, 11: 972-979
- S27 Iuliano A, Barretta GU, Salvadori P. *Tetrahedron: Asymmetry*, 2000, 11: 1555-1563

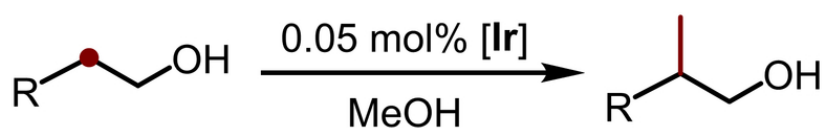
S28 Barker G, Brien PO, Campos KR. *Org. Lett*, 2010, 12: 4176-4179

S29 Magre M, Paffenholz E, Maity B, Cavallo L, Rueping M. *J. Am. Chem. Soc*, 2020, 142: 14286-14294

S30 Guduguntla S, Mastral MF, Feringa BL. *J. Org. Chem*, 2013, 78: 8274-8280

S31 Cano R, Yus M, Ramon DJ. *Chem. Commun*, 2012, 48: 7628-7630

For Review Only



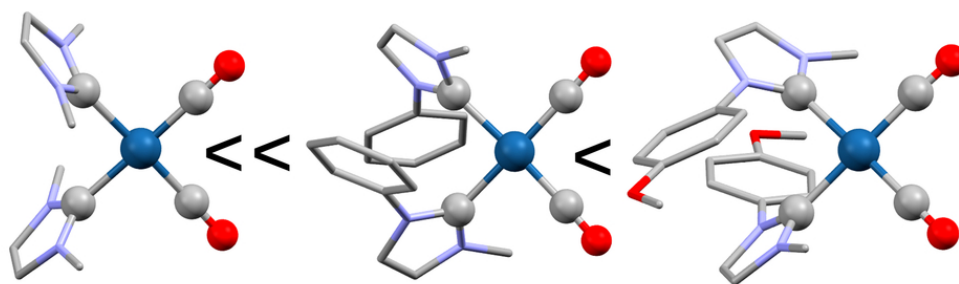
R = Aryl, Alkyl

Up to 99 % yield and selectivity;

Broad substrate scope;

TON: 30800 and TOF: 4640 h⁻¹

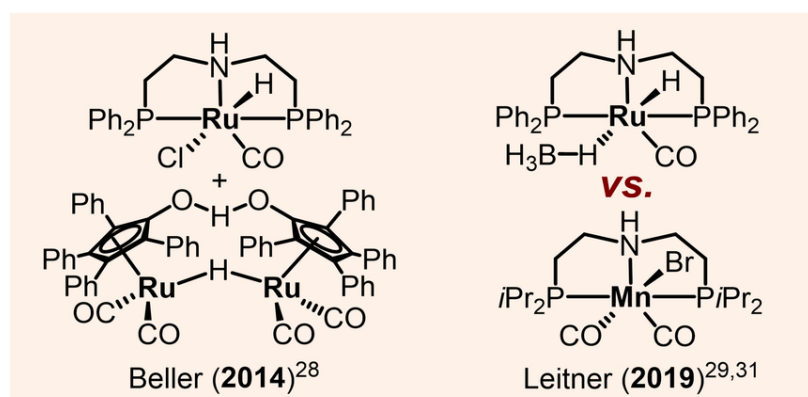
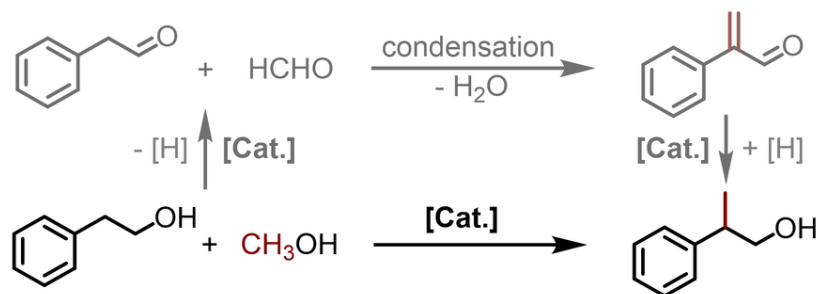
Catalytic activity



TOC

80x56mm (300 x 300 DPI)

a) Previous work: with catalysts bearing phosphine ligands



b) This work: by using bis-NHC-Iridium complexes

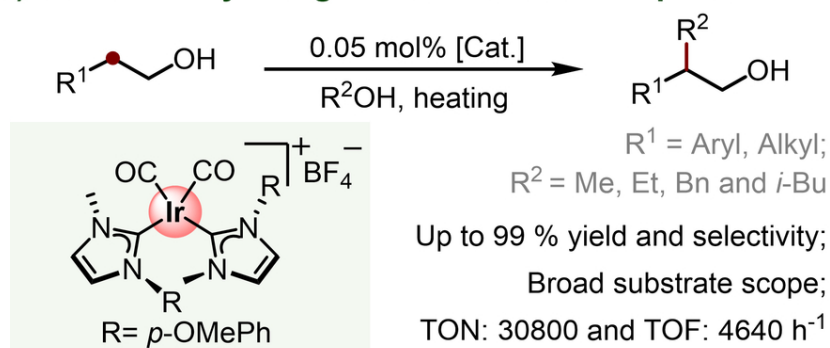


Figure 1 Represented β-methylation of alcohols

83x108mm (300 x 300 DPI)

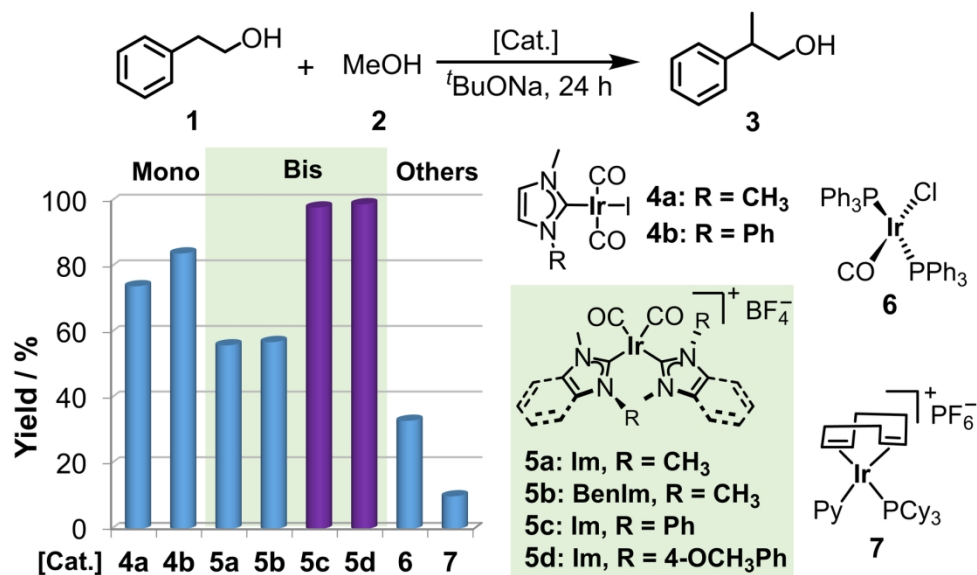


Figure 2 Catalysts screening

164x97mm (300 x 300 DPI)

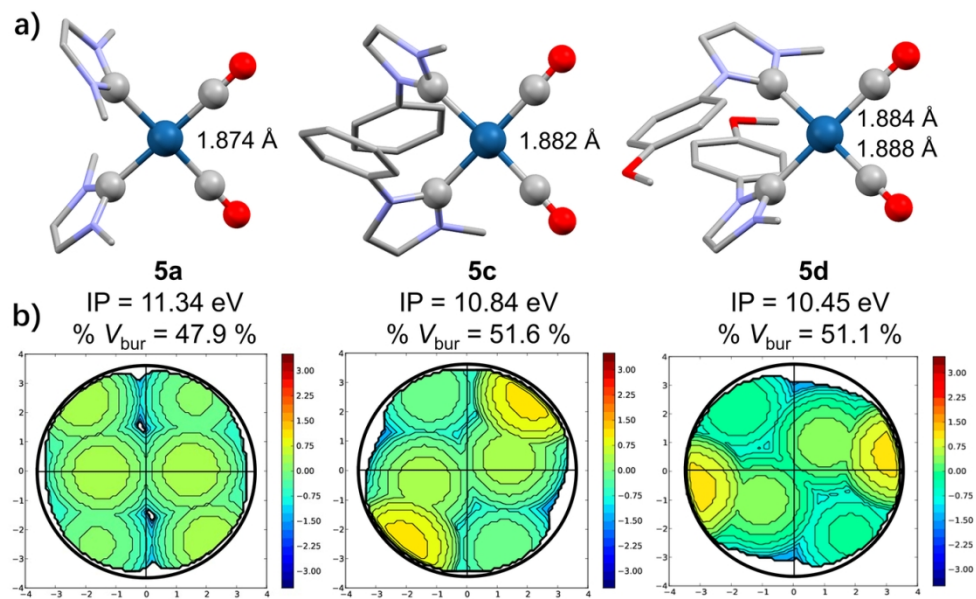


Figure 3 a) Crystal structures of complexes 5a, 5c and 5d, and the corresponding CCO-Ir bond lengths (Colour code: Ir, cyan; O, red; N, blue; C grey. Hydrogens are omitted for clarity). b) Percent buried volumes and steric maps of complexes 5a, 5c and 5d.

120x75mm (300 x 300 DPI)

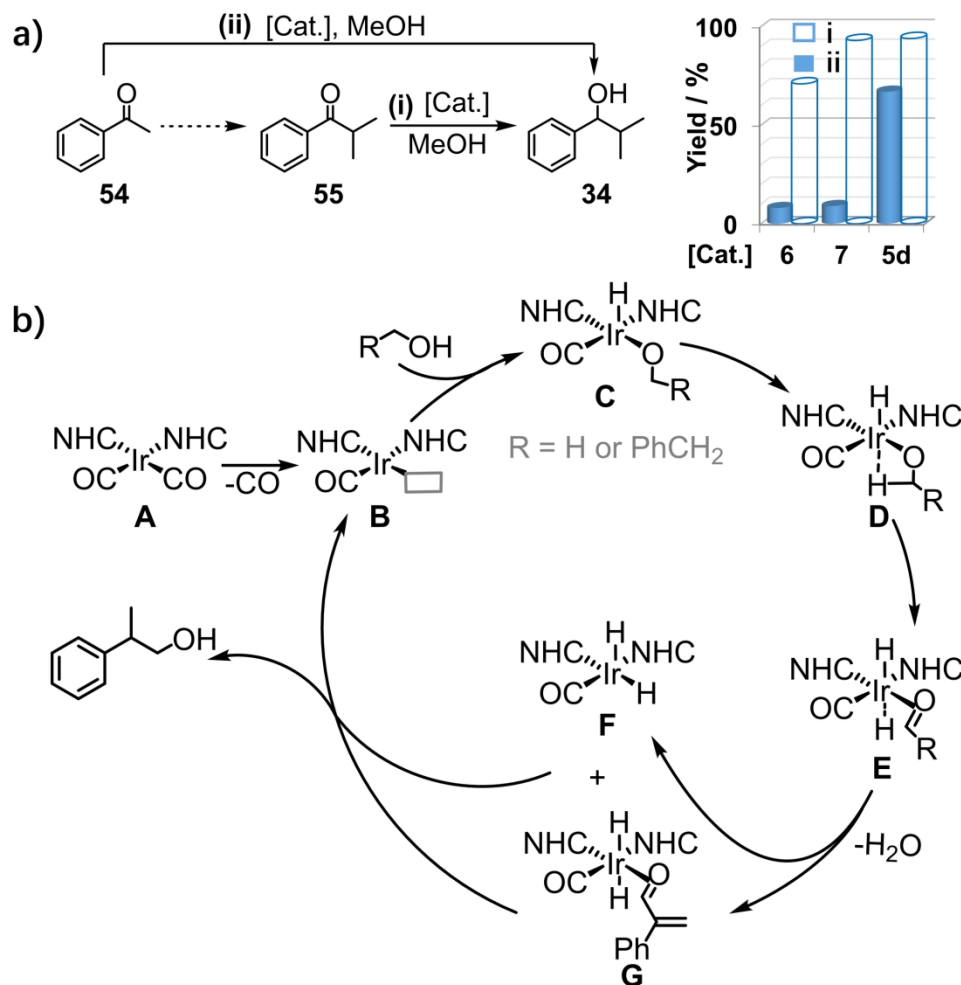


Figure 4 a) Comparison of the catalytic activity of selected viable catalysts in methylation of acetophenone or di-methylated-ketone. b) The plausible mechanism of the β -methylation of alcohols.

191x189mm (300 x 300 DPI)